INFORMATION TO USERS

The most advanced technology has been used to photograph and reproduce this manuscript from the microfilm master. UMI films the text directly from the original or copy submitted. Thus, some thesis and dissertation copies are in typewriter face, while others may be from any type of computer printer.

The quality of this reproduction is dependent upon the quality of the copy submitted. Broken or indistinct print, colored or poor quality illustrations and photographs, print bleedthrough, substandard margins, and improper alignment can adversely affect reproduction.

In the unlikely event that the author did not send UMI a complete manuscript and there are missing pages, these will be noted. Also, if unauthorized copyright material had to be removed, a note will indicate the deletion.

Oversize materials (e.g., maps, drawings, charts) are reproduced by sectioning the original, beginning at the upper left-hand corner and continuing from left to right in equal sections with small overlaps. Each original is also photographed in one exposure and is included in reduced form at the back of the book. These are also available as one exposure on a standard 35mm slide or as a 17" x 23" black and white photographic print for an additional charge.

Photographs included in the original manuscript have been reproduced xerographically in this copy. Higher quality 6" x 9" black and white photographic prints are available for any photographs or illustrations appearing in this copy for an additional charge. Contact UMI directly to order.

U·M·I

University Microfilms International
A Bell & Howell Information Company
300 North Zeeb Road, Ann Arbor, MI 48106-1346 USA
313/761-4700 800/521-0600

Order Number 9005524

A model of vapor-liquid equilibria for acid gas-alkanolamine-water systems

Austgen, David Michael, Jr., Ph.D.

The University of Texas at Austin, 1989

U·M·I
300 N. Zeeb Rd.
Ann Arbor, MI 48106

A MODEL OF VAPOR - LIQUID EQUILIBRIA FOR ACID GAS - ALKANOLAMINE - WATER SYSTEMS

by

DAVID MICHAEL AUSTGEN JR., B.S., M.S.

DISSERTATION
Presented to the Faculty of the Graduate School of
The University of Texas at Austin
in Partial Fulfillment
of the Requirements
for the Degree of

DOCTOR OF PHILOSOPHY

THE UNIVERSITY OF TEXAS AT AUSTIN
August, 1989

A MODEL OF VAPOR - LIQUID EQUILIBRIA FOR ACID GAS - ALKANOLAMINE - WATER SYSTEMS

APPROVED BY
SUPERVISORY COMMITTEE:

Gary Rochelle
Gary T. Rochelle

Robert S. Schechter
Robert S. Schechter

Keith P Johnston
Keith P. Johnston

Joel W. Barlow
Joel W. Barlow

Peter J. Rossky

Copyright

by

David Michael Austgen Jr.

1989

To Tê

ACKNOWLEDGEMENTS

I would like to express my appreciation to all those people who have contributed to my graduate education. Above all, I am indebted to Dr. Gary T. Rochelle who served as my thesis supervisor. He has provided guidance, encouragement, and especially insight. It has been enjoyable working with him.

I would also like to thank the other members of my committee, Professors Robert S. Schechter, Peter J. Rossky, Keith P. Johnston, and Joel W. Barlow for their comments, suggestions, and insights. It has been my good fortune to learn from each of them, either through visits to their offices or through classroom lectures. Thanks also to Professor James R. Fair for encouraging me to work towards a Ph.D. and for his guidance in my job search.

I have greatly appreciated the opportunity to work with Chau-Chyun Chen of Aspen Technology during the past two years. My thanks go to Joe Boston for providing the opportunity to work at Aspen Tech during the summer of 1987. The assistance of Suphat Watanisiri and others at Aspen, who were always willing to answer my questions about ASPEN PLUS, has also been appreciated.

I am grateful to Dr. Alan Mather of the University of Alberta who provided much of the raw experimental data upon which this work is based. In addition, he was always willing to communicate his experiences and insight regarding experimental techniques relevant to this work.

Special thanks go to the Separations Research Program at UT and Texaco Chemical Co. for providing personal financial support and research funding, and to The International Paper Co. for providing a fellowship.

No graduate student works in a vacuum. It has been my privilege to work and study with some very intelligent people and good friends. Jim Critchfield, David Glasscock, Joe Peterson, and the other members of Dr. Rochelle's group, have been great research colleagues. It was Dave who originally coded the chemical equilibrium algorithm used in this work. It has been to my benefit, not to mention enjoyment, to associate with Noel Bell, Walt Witkowski, John Eaton, Mike Liebman, Ashutosh Patwardhan, Jim Bosley, Wayne Bequette, Dave Dalle Molle, Doyle Broom, and Marcia Middleton. Many others, both within and outside the department, too numerous to name, have been good friends making the graduate experience all the more enjoyable.

I would especially like to thank my own parents. The values which they passed on to me are responsible for the joy that I get from learning and for my decision to work towards a Ph.D. Furthermore, their support, moral and financial, and encouragement have helped to make the last four years agreeable. I would also like to thank my wife's parents for their moral and financial support.

Finally, my deepest thanks and gratitude must go to my wife, Teresa, who has been the source of my happiness during the past six years. She has supported me in my every endeavor. And through her own endeavors she has been a true inspiration, showing me that persistence and determination are true virtues.

A MODEL OF VAPOR - LIQUID EQUILIBRIA FOR ACID GAS - ALKANOLAMINE - WATER SYSTEMS

Publication No. ______________

David Michael Austgen Jr., Ph.D.
The University of Texas at Austin, 1989

Supervising Professor: Gary T. Rochelle

A physico-chemical model was developed for representing liquid phase chemical equilibria and vapor-liquid (phase) equilibria of H_2S-CO_2-alkanolamine-water systems. The equilibrium composition of the liquid phase is determined by minimization of the Gibbs free energy. Activity coefficients are represented with the Electrolyte-NRTL equation treating both long-range electrostatic interactions and short-range binary interactions between liquid phase species. Vapor phase fugacity coefficients are calculated using the Redlich-Kwong-Soave Equation of State.

Adjustable parameters of the model, binary interaction parameters and carbamate stability constants, were fitted on published binary system (alkanolamine-water) and ternary system (H_2S-alkanolamine-water, CO_2-alkanolamine-water) VLE data. The Data Regression System of ASPEN PLUS, based upon the Maximum Likelihood Principle, was used to estimate adjustable parameters. Ternary system measurements used in parameter estimation ranged in temperature from 25 to 120°C, in alkanolamine concentration from 1 to 5 M, in acid gas loading from 0 to 1.5 moles per mole alkanolamine, and in acid gas partial pressure from 0.1 to 1000 kPa.

Maximum likelihood estimates of ternary system H_2S or CO_2 equilibrium partial pressures and liquid phase concentrations were found to be in good agreement with measurements for aqueous solutions of monoethanolamine (MEA), diethanolamine (DEA), diglycolamine (DGA), and methyldiethanolamine (MDEA) indicating that the model successfully represents ternary system data. Without fitting additional parameters on quaternary system VLE data (H_2S-CO_2-alkanolamine-water), maximum likelihood estimates of H_2S and CO_2 equilibrium partial pressures and liquid phase concentrations were found to be in satisfactory agreement with quaternary system measurements for all alkanolamine solutions of interest.

The model was extended to represent CO_2 solubility in aqueous mixtures of MDEA with MEA or DEA. In support of this effort, the solubility of CO_2 in aqueous mixtures of MDEA with MEA or DEA was measured at 40 and 80°C over a wide range of CO_2 partial pressures. These measurements were used to estimate additional binary parameters of the mixed solvent systems. Representation of the data by the model was seen to be good, especially at industrially important acid gas loadings.

TABLE OF CONTENTS

Acknowledgements.......... v

Abstract vii

List of Tables xii

List of Figures xiv

Chapter One: Introduction to Gas Treating.......... 1
- 1.1 Acid Gases and Gas Treating.......... 1
- 1.2 Gas Treating by Absorption/Stripping.......... 2
  - 1.2.1 Chemical Solvents: Aqueous Solutions of Alkanolamines..... 2
  - 1.2.2 Physical Solvents.......... 4
  - 1.2.3 Process Flow Sheet.......... 4
  - 1.2.4 Commercially Important Alkanolamines.......... 6
- 1.3 Phase Equilibria in Weak Electrolyte Systems 11
  - 1.3.1 Chemical Equilibria and Phase Equilibria 12
- 1.4 Rate-based Simulation and Design 14
- 1.5 Objectives and Scope of this Work.......... 15

Chapter Two: Thermodynamics of Weak Electrolyte Solutions.......... 18
- 2.1 Concentration Scales.......... 19
- 2.2 Conditions of Equilibrium.......... 22
  - 2.2.1 Application of Phase Equilibria to Electrolyte Systems 23
  - 2.2.2 An Alternate Expression of Phase Equilibrium 23
- 2.3 Expressions for the Chemical Potential 25
  - 2.3.1 Ideal Solutions, Nonideal Solutions, and the Activity Coefficient.......... 25
- 2.4 Standard State Conventions 27
  - 2.4.1 Normalization Convention I.......... 27
  - 2.4.2 Normalization Convention II 28
  - 2.4.3 Normalization Convention III.......... 31
  - 2.4.4 Relation Between Activity Coefficients Based on Mole Fraction and Molality Scales 32
- 2.5 Chemical Equilibrium 33
  - 2.5.1 The Traditional Approach and Equilibrium Constants 33
- 2.6 Applications to the System H2S-CO2-alkanolamine-H2O.......... 38
  - 2.6.1 Acid - Base Buffer Equilibria.......... 38
  - 2.6.2 Formation of Carbamate.......... 39
  - 2.6.3 Relation Between Equilibrium Constants Based on the Mole Fraction and the Molality Scales.......... 40
  - 2.6.4 Relation Between Equilibrium Constants Based on Different Standard States 43
  - 2.6.3 Single Solute Systems.......... 45
  - 2.6.4 Multisolute Solutions 45

2.6.5 Absorption of H_2S and CO_2 with Akanolamine Solutions 47
2.7 Phase Equilibrium 47
2.7.1 Vapor Phase Fugacity 48
2.7.2 Liquid Phase Fugacity 49
2.7.3 The Pressure Dependence of the Liquid Phase Fugacity 52
2.8 Excess Gibbs Energy 55
2.8.1 Relation to Activity Coefficient and Chemical Potential 55
2.8.2 Excess Gibbs Energy of Electrolyte Solutions 58
2.8.3 Unsymmetric Excess Gibbs Free Energy 61
2.9 Conclusions 62

Chapter Three: Modeling VLE of Weak Electrolyte Systems, A Review of the Literature 64
3.1 Excess Gibbs Free Energy Models for Electrolyte Solutions 64
3.2 Vapor-Liquid Equilibria Models for Weak Electrolyte Systems 77

Chapter Four: A VLE Model for H_2S-CO_2-Alkanolamine-H_2O Systems 84
4.1 Thermodynamic Framework 84
4.1.1 Standard States 84
4.1.2 Chemical Equilibria 86
4.1.3 Phase Equilibria 88
4.1.4 Units and Temperature Dependence 91
4.1.5 Partial Molar Volumes of Solute Species 92
4.1.6 Solvent Molar Volumes: Modified Rackett Equation 96
4.2 Liquid Phase Equilibrium Composition 97
4.2.1 Nonstoichiometric Formulation 100
4.2.2 Smith and Missen Algorithm 102
4.2.3 Nonstoichiometric Algorithm for Nonideal Solutions 107
4.2.4 Standard State Chemical Potentials from K's 109
4.3 Thermodynamic Functions 110
4.3.1 Fugacity Coefficient: Redlich - Kwong - Soave EOS 110
4.3.2 Activity Coefficient: Electrolyte - NRTL Equation 114
4.3.3 Debye-Hückel Coefficient 120
4.3.4 Mixed Solvent Dielectric Constant 121
4.3.5 Parameters of the Electrolyte - NRTL Equation 123
4.4 Data Regression 124
4.4.1 Adjustable Parameters: Binary Interaction Parameters 124
4.4.2 Adjustable Parameters: Carbamate Stability Constant 127
4.4.3 Parameter Estimation with ASPEN PLUS 128
4.4.4 Minimization Algorithms - Theoretical Development 129
4.4.5 Application of the Data Regression System 132
4.4.6 Parameter Variance and Correlation 134
4.5 VLE Model Algorithm 136
4.5.1 Stand-Alone Model 136
4.5.2 The Chemical Equilibrium Algorithm 139
4.5.3 Phase Equilibrium Algorithm 141

Chapter Five: Measurement of CO_2 Solubility in Mixtures of MDEA with MEA and DEA 145
- 5.1 Experimental 145
  - 5.1.1 Reagents 145
  - 5.1.2 Apparatus and Procedure 146
  - 5.1.3 Solution Density 152
- 5.2 Solubility Measurement Results 156

Chapter Six: Representation of Equilibria in H_2S-CO_2-Alkanolamine-Water Systems 164
- 6.1 Introduction 164
  - 6.1.1 Adjustable Parameters and Data Regession: A Review 165
- 6.2 Binary (Nonelectrolyte) System VLE Representation 168
  - 6.2.1 Data Sources 169
  - 6.2.2 Parameter Estimation Results 170
  - 6.2.3 Binary System Data Representation 175
  - 6.2.4 Nonideality in the Binary Systems 185
- 6.3 Ternary System VLE Representation 198
  - 6.3.1 Data Sources 198
  - 6.3.2 Parameter Estimation: Electrolyte-NRTL Parameters 200
  - 6.3.3 Parameter Estimation: Carbamate Stability Constants 206
  - 6.3.4 Ternary system data representation 208
- 6.4 Ternary Systems: Interpolation and Extrapolation and VLE Behavior 235
- 6.5 Quaternary Systems: Experimental Data Representation 252
- 6.6 Speciation 265

Chapter Seven: Modeling CO_2 Solubility in Mixtures of MDEA with MEA or DEA 276
- 7.1 Gas Treating with MDEA and Mixtures of MDEA with MEA or DEA 276
- 7.2 Representation of CO_2 Solubility in Mixed Amine Solutions 278
  - 7.2.1 Data Regression 278
  - 7.2.2 Data Representation 281
- 7.3 Speciation 293

Chapter Eight: Summary, Conclusions and Recommendations 297
- 8.1 Summary 297
- 8.2 Conclusions 299
- 8.3 Recommendations 302

Appendix A: Activity coefficients 305
- Pitzer - Debye - Hückel Contribution 305
- Born Contribution 305
- NRTL Contribution 306

Appendix B: Parameter Correlation Matrices 309
- Binary Systems 310
- Ternary Systems 312

Nomenclature 319

References 324

LIST OF TABLES

Table 1.1 Heats of reaction for H_2S and CO_2 reactions with common alkanolamines 9

Table 4.1 Temperature dependence of equilibrium constants 93

Table 4.2 Temperature dependence of H_2S and CO_2 Henry's constants........ 94

Table 4.3 Temperature dependence of pure component vapor pressures for H_2O, MEA, DEA, MDEA, and DGA........ 95

Table 4.4 Pure component properties for acid gases, water, and alkanolamines........ 98

Table 4.5 Dielectric constant of pure MDEA 122

Table 4.6 Temperature dependence of MEA, DEA, and MDEA dielectric constants........ 122

Table 4.7 Thermodynamic variables evaluated during execution of VLE model........ 137

Table 5.1 Density of CO_2 loaded 2.0 M MDEA - 2.0 M MEA and 2.0 M MDEA - 2.0 M DEA solutions at 23 °C. 154

Table 5.2 Solubility of CO_2 in 2.5 M MEA solution at 40 and 80°C........ 157

Table 5.3 Solubility of CO_2 in 2.0 and 4.28 M MDEA solution at 40°C........ 157

Table 5.4 Solubility of CO_2 in 2.0 M MDEA , 2.0 M MEA aqueous mixture at 40 and 80°C. 162

Table 5.5 Solubility of CO_2 in 2.0 M MDEA , 2.0 M DEA Aqueous mixture at 40 and 80°C........ 163

Table 6.1 Summary of literature sources of VLE data used for adjusting amine-water binary interaction parameters........ 171

Table 6.2 Fitted values of NRTL binary interaction parameters for alkanolamine - H_2O systems........ 172

Table 6.3 Summary of VLE data literature sources used for adjusting molecule - ion pair binary interaction parameters........ 201

Table 6.4 Fitted values of molecule-ion pair binary interaction parameters....... 204

Table 6.5 Temperature dependence of the carbamate stability constant.......... 209

Table 6.6 Carbamate Stability Constants at 25°, 40°, and 100° C................ 210

Table 6.7 Comparison of maximum likelihood estimates and experimentally measured values of H_2S and CO_2 equilibrium partial pressures and liquid phase mole fractions (apparent) for the quaternary system H_2S-CO_2-MEA-H_2O............ 255

Table 6.8 Comparison of maximum likelihood estimates and experimentally measured values of H_2S and CO_2 equilibrium partial pressures and liquid phase mole fractions (apparent) for the quaternary system H_2S-CO_2-DEA-H_2O............ 257

Table 6.9 Comparison of maximum likelihood estimates and experimentally measured values of H_2S and CO_2 equilibrium partial pressures and liquid phase mole fractions (apparent) for the quaternary system H_2S-CO_2-MDEA-H_2O.......... 259

Table 6.10 Comparison of maximum likelihood estimates and experimentally measured values of H_2S and CO_2 equilibrium partial pressures and liquid phase mole fractions (apparent)for the quaternary system H_2S-CO_2-DGA-H_2O............. 262

Table 7.1 Fitted values of molecule - ion pair binary interaction parameters for CO_2 - alkanolamine (1) - alkanolamine (2) - H_2O systems......... 281

LIST OF FIGURES

Figure 1.1 Simplified absorption/stripping system for the removal of acid gases. 5

Figure 1.2 Structural formulas of several alkanolamines used in gas treating. 7

Figure 1.3 Chemical and physical equilibria in a closed aqueous weak electrolyte system. 13

Figure 4.1 Block diagram of chemical equilibrium algorithm 143

Figure 4.2. Block diagram of phase equilibrium algorithm 144

Figure 5.1 Experimental apparatus for the determination of CO_2 solubility in aqueous alkanolamine solutions 147

Figure 5.2 Flow schematic for Oceanography International model 525 carbon analyzer 150

Figure 5.3 Density of carbonated 2 M MDEA - 2 M MEA and 2 M MDEA - 2 M DEA aqueous mixtures at 23°C. 155

Figure 5.4 Solubility of CO_2 in 2.5 M MEA aqueous solution at 40 and 80°C... 158

Figure 5.5 Solubility of CO_2 in 2.0 M MDEA aqueous solution at 40°C. 159

Figure 5.6 Solubility of CO_2 in 4.28 M MDEA aqueous solution at 40°C. 160

Figure 6.1 Comparison of maximum likelihood estimates and experimentally measured values of total pressure in MEA-water mixtures 177

Figure 6.2 Comparison of maximum likelihood estimates and experimentally measured values of the liquid phase mole fraction of MEA in MEA-water mixtures. 178

Figure 6.3 Comparison of maximum likelihood estimates and experimentally measured values of the total pressure in DEA-water mixtures. 179

Figure 6.4 Comparison of maximum likelihood estimates and experimentally measured values of the liquid phase mole fraction of DEA in DEA-water mixtures. 180

Figure 6.5 Comparison of maximum likelihood estimates and experimentally measured values of the total pressure in MDEA-water mixtures. 181

Figure 6.6 Comparison of maximum likelihood estimates and experimentally measured values of the liquid phase mole fraction of MDEA in MDEA-water mixtures. 182

Figure 6.7 Comparison of maximum likelihood estimates and experimentally measured values of the total pressure in DGA-water mixtures.......... 183

Figure 6.8 Comparison of maximum likelihood estimates and experimentally measured values of the liquid phase mole fraction of DGA in DGA-water mixtures.......... 184

Figure 6.9 Representation of the excess Gibbs energy of aqueous solutions of MEA, DEA, MDEA, and MDEA at 298.15 °K 186

Figure 6.10 Representation of component activity coefficients in an MEA-water mixture at 298.15 °K with the NRTL equation.......... 191

Figure 6.11 Representation of component activity coefficients in a DEA-water mixture at 298.15 °K with the NRTL equation. 192

Figure 6.12 Representation of component activity coefficients in an MDEA-water mixture at 298.15 °K with the NRTL equation.......... 193

Figure 6.13 Representation of component activity coefficients in a DGA-water mixture at 298.15 °K with the NRTL equation.......... 194

Figure 6.14 Representation of component activity coefficients in an H_2S-water mixture at 298.15 °K with the NRTL equation.......... 195

Figure 6.15 Representation of component activity coefficients in a CO_2-water mixture at 298.15 °K with the NRTL equation.......... 196

Figure 6.16 Representation of H_2S and CO_2 activity coefficients in H_2S-water and CO_2-water mixtures over the temperature range 273 to 373 °K with the NRTL equation 197

Figure 6.17 Comparison of maximum likelihood estimates and experimentally measured values of H_2S equilibrium partial pressures over aqueous MEA solutions 219

Figure 6.18 Comparison of maximum likelihood estimates and experimentally measured values of equilibrium H_2S apparent mole fractions in aqueous MEA solutions 220

Figure 6.19 Comparison of maximum likelihood estimates and experimentally measured values of CO_2 equilibrium partial pressures over aqueous MEA solutions. 221

Figure 6.20 Comparison of maximum likelihood estimates and experimentally measured values of equilibrium CO_2 apparent mole fractions in aqueous MEA solutions 222

Figure 6.21 Comparison of maximum likelihood estimates and experimentally measured values of H_2S equilibrium partial pressures over aqueous DEA solutions 223

Figure 6.22 Comparison of maximum likelihood estimates and experimentally measured values of H_2S equilibrium apparent mole fractions in aqueous DEA solutions. 224

Figure 6.23 Comparison of maximum likelihood estimates and experimentally measured values of CO_2 equilibrium partial pressures over aqueous DEA solutions 225

Figure 6.24 Comparison of maximum likelihood estimates and experimentally measured values of equilibrium CO_2 apparent mole fractions in aqueous DEA solutions 226

Figure 6.25 Comparison of maximum likelihood estimates and experimentally measured values of equilibrium H_2S partial pressures over aqueous MDEA solutions 227

Figure 6.26 Comparison of maximum likelihood estimates and experimentally measured values of the equilibrium H_2S apparent mole fractions in aqueous MDEA solutions 228

Figure 6.27 Comparison of maximum likelihood estimates and experimentally measured values of equilibrium CO_2 partial pressures over aqueous MDEA solutions 229

Figure 6.28 Comparison of maximum likelihood estimates and experimentally measured values of equilibrium CO_2 apparent mole fractions in aqueous MDEA solutions 230

Figure 6.29 Comparison of maximum likelihood estimates and experimentally measured values of equilibrium H_2S partial pressures over aqueous DGA solutions 231

Figure 6.30 Comparison of maximum likelihood estimates and experimentally measured values of equilibrium H_2S apparent mole fractions in aqueous DGA solutions 232

Figure 6.31 Comparison of maximum likelihood estimates and experimentally measured values of equilibrium CO_2 partial pressures over aqueous DGA solutions 233

Figure 6.32 Comparison of maximum likelihood estimates and experimentally measured values of equilibrium CO_2 apparent mole fractions in aqueous DGA solutions....... 234

Figure 6.33 Model representation of H_2S equilibrium partial pressure over 2.5 and 5.0 M MEA solutions from 40 to 120 °C....... 240

Figure 6.34 Model representation of H_2S equilibrium partial pressure over 2.0 and 5.0 M DEA solutions from 40 to 120 °C....... 241

Figure 6.35 Model representation of H_2S equilibrium partial pressure over a 4.0 M MDEA solution from 40 to 120 °C....... 242

Figure 6.36 Model representation of H_2S equilibrium partial pressure over a 2.5 M MEA solution from 40 to 120 °C. 243

Figure 6.37 Model representation of H_2S equilibrium partial pressure over a 2.0 M DEA solution from 40 to 120 °C....... 244

Figure 6.38 Model representation of H_2S equilibrium partial pressure over a 4.0 M MDEA solution from 40 to 120 °C. 245

Figure 6.39 Model representation of CO_2 equilibrium partial pressure over 2.5 and 5.0 M MEA solutions from 40 to 120 °C....... 246

Figure 6.40 Model representation of CO_2 equilibrium partial pressure over 2.0 and 5.0 M DEA solutions from 40 to 120 °C....... 247

Figure 6.41 Model representation of CO_2 equilibrium partial pressure over a 4.0 M MDEA solution from 40 to 120 °C....... 248

Figure 6.42 Model representation of CO_2 equilibrium partial pressure over a 2.5 M MEA solution from 40 to 120 °C. 249

Figure 6.43 Model representation of CO_2 equilibrium partial pressure over a 2.0 M DEA solution from 40 to 120 °C....... 250

Figure 6.44 Model representation of CO_2 equilibrium partial pressure over a 4.0 M MDEA solution from 40 to 120 °C. 251

Figure 6.45 Liquid-phase composition of a 2.5 M MEA solution loaded with H_2S at 40°C....... 269

Figure 6.46 Liquid-phase composition of a 2.5 M MEA solution loaded with H_2S at 120°C....... 270

Figure 6.47 Liquid-phase composition of a 2.5 M MEA solution loaded with CO_2 at 40°C........ 271

Figure 6.48 Liquid-phase composition of a 2.5 M MEA solution loaded with CO_2 at 120°C........ 272

Figure 6.49 Liquid-phase composition of a 2.0 M DEA solution loaded with CO_2 at 40°C........ 273

Figure 6.50 Liquid-phase composition of a 2.0 M DEA solution loaded with CO_2 at 120°C........ 274

Figure 6.51 Liquid-phase composition of a 4.0 M MDEA solution loaded with CO_2 at 40°C........ 275

Figure 7.1 Equilibrium solubility of CO_2 in 4 M MDEA, 4 M MEA, and 2 M MDEA - 2 MEA M aqueous solutions at 40°C........ 285

Figure 7.2 Equilibrium solubility of CO_2 in 4 M MDEA, 4 M MEA, and 2 M MDEA - 2 MEA M aqueous solutions at 80°C........ 286

Figure 7.3 Equilibrium solubility of CO_2 in 4 M MDEA, 4 M DEA, and 2 M MDEA - 2 M DEA aqueous solutions at 40°C........ 287

Figure 7.4 Equilibrium solubility of CO2 in 4 M MDEA, 4 M DEA, and 2 M MDEA - 2 DEA M aqueous solutions at 80°C........ 288

Figure 7.5 CO2 equilibrium partial pressure over 4 M MDEA-MEA aqueous mixtures relative to the CO_2 equilibrium partial pressure over 4 M at 40°C........ 289

Figure 7.6 CO_2 equilibrium partial pressure over 4 M MDEA-MEA aqueous mixtures relative to the CO_2 equilibrium partial pressure over 4 M at 120°C........ 290

Figure 7.7 CO_2 equilibrium partial pressure over 4 M MDEA-DEA aqueous mixtures relative to the CO_2 equilibrium partial pressure over 4 M MDEA at 40°C. 291

Figure 7.8 CO_2 equilibrium partial pressure over 4 M MDEA-DEA aqueous mixtures relative to the CO_2 equilibrium partial pressure over 4 M MDEA at 120°C. 292

Figure 7.9 Liquid phase mole fractions of a CO_2 loaded 3 M MDEA - 1 M MEA aqueous solution at 40°C........ 295

Figure 7.10 Liquid phase mole fractions of a CO_2 loaded 3 M MDEA - 1 M DEA aqueous solution at 40°C 296

Chapter One

Introduction to Gas Treating with Aqueous Alkanolamine Solutions

1.1 Acid Gases and Gas Treating

Acid gases, primarily H_2S and CO_2, are components in a variety of sour gas mixtures including natural gas, synthesis gas, flue gas, and various refinery streams. In addition, CO_2 is a by-product of ammonia and hydrogen manufacture. Normally, H_2S must be nearly completely removed from a gas stream due to its toxicity and corrosiveness, and to avoid catalyst poisoning in refinery operations. For example, the maximum concentration of H_2S permitted by pipeline specifications in natural gas is often 4 ppm by volume (Astarita et al., 1983). CO_2 is removed from natural gas because it acts as a diluent, increasing transportation costs and reducing the energy value per unit volume of gas. CO_2 is separated from reformer product gas in the production of ammonia because it poisons synthesis catalyst in the ammonia converter. More recently, CO_2 has been recovered for use in enhanced oil recovery. The process of separating acid gases from source gases is commonly referred to as *Gas Treating, Acid Gas Removal, or Gas Sweetening.*

H_2S or CO_2 concentrations in the above mentioned gases vary widely, constituting from several parts per million to 50 percent by volume of the host gas stream. Cleanup specifications also vary widely depending on the process and nature of the impurity. Astarita et al. (1983) provide a more complete summary of major industrial processes that require gas treating as well as common cleanup specifications required by these process.

1.2 Gas Treating by Absorption/Stripping

1.2.1 Chemical Solvents: Aqueous Solutions of Alkanolamines

Aqueous solutions of alkanolamines are widely used in absorption/stripping operations to separate H_2S and CO_2 from source gas streams. Absorption/stripping of acid gases with aqueous alkanolamine solvents is characterized as mass transfer enhanced by chemical reaction; following absorption into the aqueous solution the acid gases react either directly or through an acid-base buffer mechanism with the alkanolamines to form nonvolatile ionic species. Mass transfer of acidic gases from the bulk gas to a bulk liquid phase in which chemical reaction occurs, such as an aqueous alkanolamine solution, can be described as follows (Astarita, 1967):

(1) Diffusion of one or more acidic gas components from the bulk gas phase to the gas-liquid interface followed by absorption (dissolution) into the liquid. Physical equilibria is normally assumed for molecular species at the gas - liquid interface.

(2) Diffusion and convection of the reactants from the gas - liquid interface to the bulk liquid phase.

(3) Occuring simultaneously with mass transfer, reaction between the dissolved gas and the liquid reactant in the liquid phase.

(4) Diffusion of the reaction products into the bulk liquid phase due to concentration gradients created by the chemical reactions.

The use of aqueous alkanolamine solutions for gas treating results in two important affects that make these solutions preferable to physical solvents for acid gas absorption. First, the presence of an alkanolamine drastically affects the solubility of an acid gas in water. Acid gases in the vapor phase come to equilibrium (phase) with the *unreacted molecular* form of the same acid gas in water. That is, at equilibrium, the solubility of a unreacted acid gas in an aqueous solution containing a reactive solvent is governed by the partial pressure of that gas above the liquid. If the gas reacts in the aqueous phase to form nonvolatile products, then additional gas can be solubilized at a given acid gas partial pressure. As a result, alkanolamines significantly enhance the solubility of acid gases in the aqueous phase.

Alkanolamines also significantly affect the rates of absorption of acid gases into aqueous solution. When an acid gas is absorbed into aqueous solution it is partially consumed by chemical reaction so that its concentration in the bulk liquid remains low. Since the driving force for mass transfer is the difference between the concentration of the gas in the liquid at the gas-liquid interface and the concentration of unreacted acid gas in the bulk liquid phase, chemical reaction results in a higher driving force for mass transfer than would exist if no chemical reaction occurred. This, of course, results in a greater rate of mass transfer. Moreover, chemical reactions can lead to absorption rate enhancement beyond that due to the increased levels of the driving forces between the bulk gas and bulk liquid phases. Chemical reactions can create very steep gradients in the concentration profiles of the absorbing species in the liquid at the gas-liquid interface. This further enhances the rate of absorption of the acid gases into the aqueous solution.

1.2.2 Physical Solvents

Acid gases are also separated from source gases in absorption/stripping processes using polar organic solvents that do not react with the acid gases. This separation process is often referred to as gas treating by physical absorption. It is based on the ability of certain organic solvents to preferentially solubilize acid gases from a source gas. Kohl and Riesenfeld (1985) provide a thorough discussion of commercial processes employing this technology. Physical absorption processes are generally applied when acid gas partial pressures are high and acid gases constitute a substantial fraction of the host gas, providing large driving forces for mass transfer. The advantage of a physical process is that, unlike processes employing reactive aqueous alkanolamine solutions, the physically dissolved acid gases can be stripped from solution by reducing the acid gas partial pressure without a significant application of heat. While physical organic solvents play an important role in gas treating, this work is concerned with separation of acid gases using aqueous based *chemical* solvents.

1.2.3 Process Flow Sheet

A simplified flow schematic of a typical gas treating operation which employs an aqueous alkanolamine solution in absorption/stripping is shown in Figure 1.1. A sour gas containing H_2S and/or CO_2, among other possible acid gases, is introduced at the bottom of an absorber where it rises and countercurrently contacts an aqueous alkanolamine solution that is introduced at the top of the absorber at approximately 40°C. The pressure of the absorber varies widely depending on the gas stream being

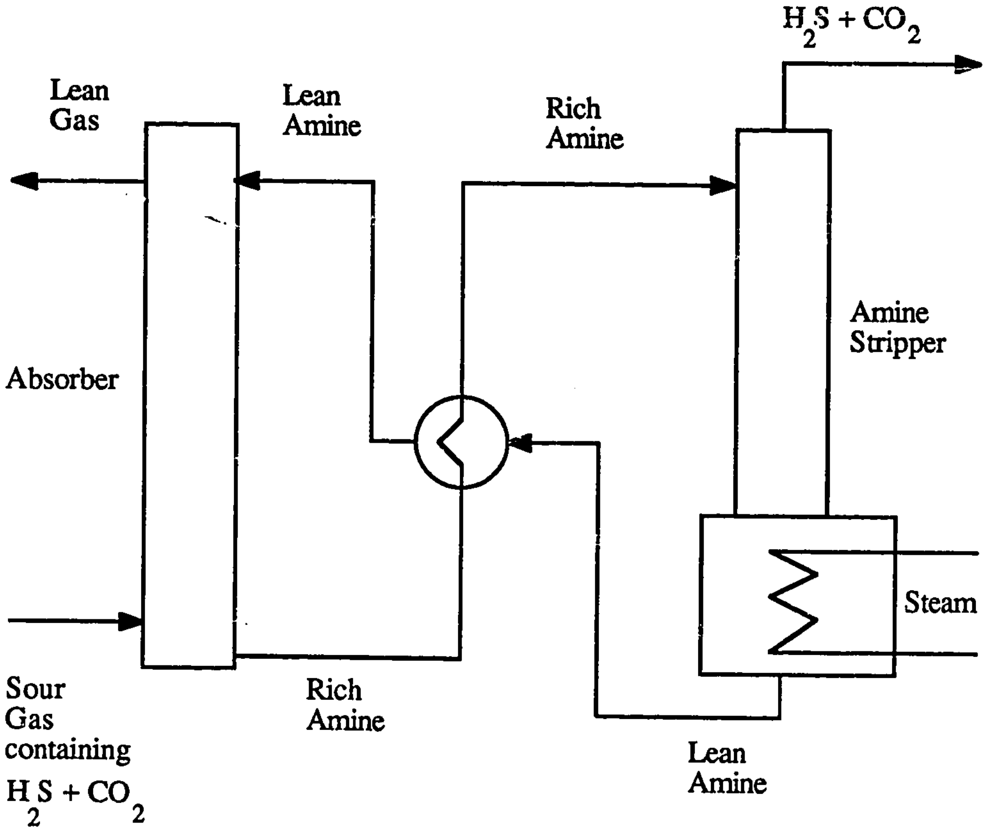
$H_2S + CO_2$
Lean Gas
Lean Amine
Rich Amine
Amine Stripper
Absorber
Steam
Sour Gas containing $H_2S + CO_2$
Rich Amine
Lean Amine

Figure 1. Simplified absorption/stripping system for the removal of acid gases.

treated. The amine solution selectively absorbs the acidic components from the sour gas to produce a *sweet* product gas. The alkanolamine solution rich in absorbed acid gases is pumped through heat exchangers where its temperature is raised. It is then introduced at the top of a stripper where it countercurrently contacts steam at an elevated temperature, approximately 120°C, and reduced pressure. The steam, produced in a reboiler, provides the energy necessary to reverse the reactions of the acid gases with alkanolamine thus increasing acid gas partial pressure. It also simultaneously strips the acid gases from solution. The lean alkanolamine solution is then pumped through the heat exchanger, where it is cooled, and then reintroduced at the top of absorber. Both trayed and packed towers are used in gas treating applications.

1.2.4 Commercially Important Alkanolamines

Alkanolamines are characterized as containing both hydroxyl groups and amino groups. The hydroxyl groups serve to reduce vapor pressure and increase water solubility while the amino provides the necessary alkalinity in aqueous solution to react with acid gases (Kohl and Riesenfeld, 1985). Structural formulas for several commercially important alkanolamines are presented in Figure 1.2.

Monoethanolamine (MEA), a primary amine, and diethanolamine (DEA), a secondary amine, have been the most widely employed gas treating alkanolamine agents during the last several decades (Kohl and Riesenfeld, 1985). Other commercially important alkanolamines include diglycolamine, DGA, and methyldiethanolamine, MDEA.

MEA, DEA, and DGA react rapidly with both H_2S and CO_2 in the aqueous phase. H_2S is a Brönsted acid and alkanolamines are Brönsted bases. Hence, H_2S reacts with all alkanolamines in the aqueous phase through a very fast proton transfer mechanism. This reaction is essentially instantaneous with respect to mass transfer (Astarita et al., 1983). MEA, DEA, and DGA, like other primary and secondary

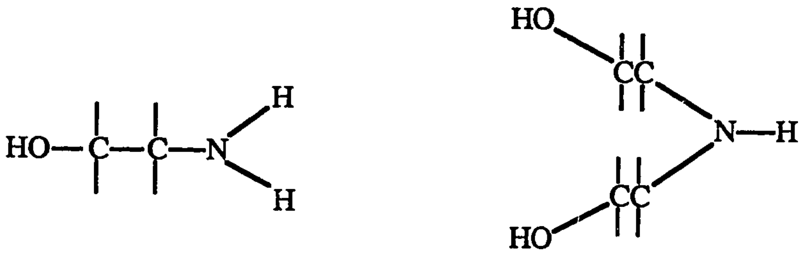

Monoethanolamine

Diethanolamine

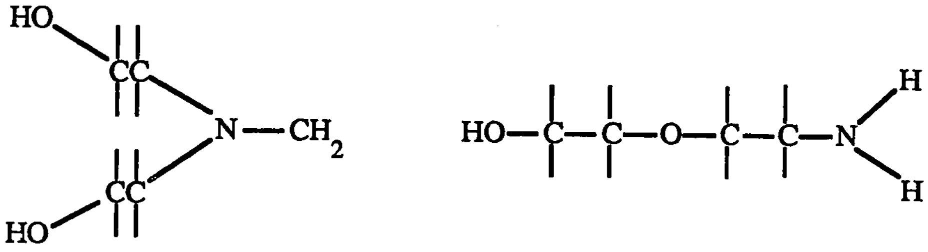

Methyldiethanolamine

B,B'-Hydroxyaminoethyl ether
'Diglycolamine'

Figure 1.2 Structural formulas for several alkanolamines used in gas treating.

amines, react directly with CO_2 primarily to form carbamates of the respective amines. This is a rapid, but finite rate, reaction.

Because of the absorption rate enhancement effected by MEA, DEA, and DGA in aqueous solution, these solvents allow for removal of all but trace quantities of H_2S

and for removal of all but a minor fraction of the CO_2. Therefore, they are used in applications wherein it is necessary to remove the bulk fraction of H_2S and CO_2 from a gas stream to very low levels. The drawback of using either MEA, DEA, or DGA for gas treating is that the reactions between these amines and H_2S or CO_2 are highly exothermic (see Table 1.1). As a result, gas treating applications employing aqueous alkanolamine solvents require a substantial input of energy in the stripper to reverse the reactions and strip the acid gases from solution.

When H_2S and CO_2 are both present in a gas stream, such as natural gas, it may or may not be desirable to remove all or most of the CO_2 together with the H_2S. When it is not necessary to remove the major fraction of CO_2 from a gas stream, a substantial reduction in consumption of reboiler steam for stripping and a reduction in solvent recirculation rates can be realized if H_2S can be selectively absorbed (Astarita et al., 1983). Moreover, selective absorption allows the use of smaller Claus sulfur recovery plants and Claus tail-gas plants because less CO_2 accompanies H_2S into these plants.

In recent years, methyldiethanolamine (MDEA) has come into favor as a gas treating agent (Jou et al., 1982; Kohl and Riesenfeld, 1985). MDEA reacts rapidly with H_2S through the aforementioned proton donor mechanism. However, as a tertiary amine, it cannot react directly with CO_2 to form a carbamate anion. This is the primary mechanism by which MEA, DEA, and DGA react (rapidly) with CO_2. MDEA reacts with CO_2 in an acid-base buffer reaction primarily to produce bicarbonate. However, CO_2, a Lewis base, must first react with water by a slow chemical reaction (hydrolysis) to form carbonic acid which then dissociates to produce bicarbonate ion. This reaction is substantially slower than either the formation of

Table 1.1 Heats of reaction for H_2S and CO_2 reactions with common alkanolamine. (From Kohl and Riesenfeld, 1985).

Acid Gas	Amine	ΔH_{RXN} (kcal/gmol gas)
H_2S	MEA	15.5
H_2S	DEA	9.66
H_2S	DGA	12.7
CO_2	MEA	20.2*
CO_2	DEA	16.0
CO_2	DGA	20.8
CO_2	MDEA	11.6

* Calculated for 0.4 mole of CO_2 per mole of MEA.

carbamate by MEA, DEA, or DGA or the reaction of an amine with H_2S (Astarita et al., 1983).

Because MDEA reacts much faster with H_2S than with CO_2, it is often used for *selective* removal of H_2S from a gas stream containing both acid gases. Selective separation of H_2S in a gas stream that contains both H_2S and CO_2 is achieved by sizing the absorber for a contact area that allows most of the H_2S to be absorbed and reacted, but is insufficient for a significant fraction of the CO_2 to be absorbed and reacted. Indeed, solvents exhibiting *kinetic selectivity* towards H_2S, like MDEA, are capable of reducing H_2S concentrations to as low as 4 ppm by volume in treated gas while allowing the major fraction of CO_2 to *slip* through the absorber with the treated gas (Kohl and Riesenfeld, 1985).

Because MDEA cannot react with CO_2 to form a carbamate species, its heat of reaction with CO_2 is substantially lower than that of MEA, DEA, or DGA as shown in Table 1.1. This also makes it useful for gas treating applications that require absorption of a large quantity of CO_2. That is, the use of an aqueous MDEA solution as an alternative to aqueous MEA, DEA, or DGA solutions for bulk CO_2 removal results in a reduction in energy required for stripping. The drawback of using MDEA for bulk CO_2 removal is that, as noted previously, it reacts relatively slowly with CO_2. To effect the same level of CO_2 removal, an MDEA application requires a greater number of trays, or a greater height of packing, in the absorber or desorber than does an MEA, DEA, or DGA application.

Recent research (Chakravarty et al., 1985; Critchfield and Rochelle 1987, 1988; Katti and Wolcott, 1987) suggests that a small amount of a primary or secondary amine, such as MEA or DEA, can be added to an aqueous MDEA solution to promote or enhance the absorption rate of CO_2 without significantly affecting the steam stripping requirements. Critchfield and Rochelle (1987, 1988) discuss the interactive mass transfer and equilibrium mechanisms by which MEA or DEA can significantly enhance the absorption rate of CO_2 into an MDEA based solvent mixture. The amount of MEA or DEA added to an aqueous MDEA solution must be determined by balancing the capital savings due to the use of smaller absorbers permitted by enhanced rates of absorption, with increased stripping costs due to the greater heats-of-reaction of the promoters with CO_2, and with the relative costs of the amines.

1.3 Phase Equilibria in Weak Electrolyte Systems

Design of gas treating absorption/stripping systems by the traditional equilibrium stage approach requires knowledge of the vapor-liquid equilibria (VLE) behavior of the aqueous acid gas - alkanolamine system. Moreover, the equilibrium solubility of the acid gases in aqueous alkanolamine solutions (ie. the capacity of the solution for acid gases) determines the minimum circulation rate of the solution to treat a given sour gas, and it determines the maximum concentrations of the acid gases which can be left in the regenerated solution in order to meet the product gas specifications.

A large body of experimental vapor - liquid equilibria data for aqueous acid gas - alkanolamine systems has been reported in the literature. The data is generally limited to high acid gas loadings; little VLE is reported in the low acid gas pressure range where it is perhaps most important (it is in this range that VLE determines the limitation of sweet gas purity). Representation of experimental data with a thermodynamically rigorous model is needed so that the design engineer can confidently and systematically interpolate between and extrapolate beyond the available data. In addition, the availability of a thermodynamically rigorous model can result in the reduction of experimental effort required to characterize the VLE behavior of systems for which no data have been reported. This is especially important for mixed amine systems which have an additional degree of freedom (ratio of amine concentrations). Unfortunately, process simulation and design of gas treating systems has been hindered by our inabilility, until recently, to satisfactorily represent the thermodynamic properties of concentrated aqueous electrolyte solutions. As a result, design calculations have often been based upon empirical methods.

Fortunately, several semi-empirical excess Gibbs energy models and/or activity coefficient models for aqueous electrolyte systems, valid to ionic strengths representative of those found in industrial applications have been recently developed. Among them are the models of Pitzer (1973), Meissner and Tester (1972), Bromley (1973), Cruz and Renon (1978), Ball et al. (1985), Chen et al. (1982, 1986), and Christensen et al. (1983). Sander et al. (1986) developed an excess Gibbs energy model to represent the salt effect on the VLE of mixed solvent systems. Mock et al. (1986) extended Chen's model to represent the salt effect on mixed solvent VLE. Chen and coworkers (Scauflaire et al., 1989) completed this extension to represent activity coefficients of both ionic and molecular species in mixed solvent systems.

1.3.1 Chemical Equilibria and Phase Equilibria

Both acid gases and alkanolamines are weak electrolytes. As such they partially dissociate in the aqueous phase to form a complex mixture of nonvolatile or moderately volatile solvent species, highly volatile acid gas (molecular) species, and nonvolatile ionic species. Thermodynamics provides a framework for representing the physical and chemical equilibria of a weak electrolyte system.

The chemical and physical equilibria of a weak electrolyte system such as the acid gas - alkanolamine - water system are illustrated in Figure 1.3, adapted from the work of Edwards et al. (1978). In a closed system at constant temperature and pressure, physical equilibria governs the distribution of molecular species (including

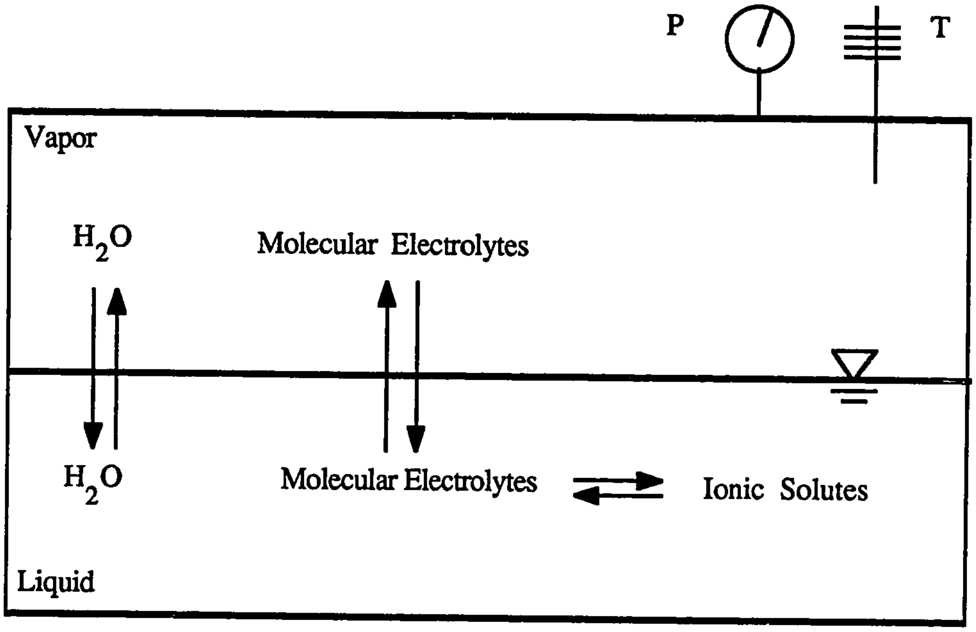
P
T
Vapor
H_2O
Molecular Electrolytes
H_2O
Molecular Electrolytes
Ionic Solutes
Liquid

Figure 1.3 Chemical and Physical Equilibria in a closed aqueous weak electrolyte system.

electrolytes) between the liquid phase and the vapor phase. This is indicated by the vertical arrows. In the liquid phase, basic alkanolamine reacts with acidic CO_2 and H_2S, either through an acid-base buffer mechanism, or through direct reaction of CO_2 with alkanolamine, to produce a number of ionic species. Chemical equilibria between molecular electrolytes and ionic species in the liquid phase is indicated by horizontal arrows. As suggested by Figure 1.3, physical and chemical equilibria are highly coupled in this system. That is, the partial pressure of an acid gas in the vapor phase influences the degree of dissociation of the weak electrolytes in the liquid phase and vice-versa.

Representation of the VLE behavior of acid gas - alkanolamine -water systems is complicated by the large number of chemical reactions which occur in the system. These reactions result in highly nonlinear solubility behavior. Representation of equilibria in the acid gas - alkanolamine - water system, therefore, requires that both *physical* and *chemical* equilibria be accounted for in a thermodynamically rigorous manner. For engineering applications such as design and simulation, this suggests that a useful model of VLE for the acid gas - alkanolamine - water system will be formulated in such a way that the equations governing chemical equilibria can be solved in an efficient and reliable manner. In addition, activity coefficients must be represented with an activity coefficient model (or excess Gibbs energy model) that is valid for electrolyte solutions to high ionic strengths.

1.4 Rate-based Simulation and Design

One of the drawbacks of the conventional equilibrium stage approach to the design and simulation of absorption and stripping is that, in practice, absorbers and strippers often do not approach equilibrium conditions. This is especially true for those applications involving mass transfer with simultaneous chemical reaction, including acid gas treating. The actual separation that is achieved is limited by finite rate mass transfer and kinetic processes that occur on any stage. Stage efficiencies are generally low and difficult to predict *a priori*. For example, Kohl and Riesenfeld (1985) approximate Murphree vapor efficiencies on a given stage at from 5 to 15 percent for the absorption of CO_2 by aqueous DEA solutions.

Recent research (Hermes and Rochelle, 1987; Sivasubramanian et al. 1985; Katti and Langfitt, 1986) suggests that a better approach to simulation of absorber/stripper models for mass transfer operations enhanced by chemical reaction is by the use of mass and heat transfer *rate-based* (nonequilibrium) models. These models account explicitly for finite rates of mass and heat transfer and chemical reaction. However, phase and chemical equilibria continue to play an important role in a rate based model. Generally, physical equilibrium is assumed to exist at the gas-liquid interface and the bulk liquid solution is assumed to be in a state of chemical equilibrium. Indeed, these assumptions define the boundary conditions for the partial differential equations describing mass transfer with chemical reaction. Physical and chemical equilibria models are, therefore, necessary and important components of a *rate-based* model.

1.5 Objectives and Scope of this Work

The objective of this work was to develop a VLE model that represents H_2S and/or CO_2 solubility data reported in the literature for aqueous solutions of MEA, DEA, DGA, and MDEA in the industrially relevant ranges of temperature, 25 - 120°C, alkanolamine concentration, 1.0 - 5.0 kmol m^{-3}, acid gas loadings, 0 - 1.0 moles acid gas per mole of alkanolamine, and acid gas partial pressures, 0.1 to 1000 kPa. In light of recent efforts to employ mixtures of MDEA with MEA or DEA for bulk CO_2 removal, extension of the VLE model to represent the solubility of CO_2 in these mixtures was also included within the scope of this work. Unfortunately, no data have been published in the literature reporting the solubility of CO_2 in mixed amine solutions. This made it impossible to either validate the model for mixed amine systems and/or to estimate unique adjustable parameters of model for mixed amine systems from experimental data. Therefore, in support of the modeling effort, a second objective of this work was to measure the solubility of CO_2 in mixtures of MDEA with MEA and DEA over a wide range of temperatures and acid gas loadings to provide data for estimating adjustable parameters specific to mixed amine systems and for validation of the extended model.

Finally, an implicit objective of this work was to make the model thermodynamically rigorous so that it could be used with confidence to calculate the equilibrium distribution of species, molecular and ionic, in the highly nonideal liquid phase. This, it was felt, would make the equilibrium model useful in the context of a rate-based model for speciation of the bulk liquid phase. Moreover, the application of thermodynamically rigorous relations and thermodynamic functions valid for electrolyte solutions to high ionic strengths will facilitate extension of the model to represent the solubility of CO_2 and H_2S in new alkanolamine mixtures with a minimum expenditure of experimental effort.

The main contribution of the model is improved representation of activity coefficients in the liquid phase using Chen's Electrolyte-NRTL model (Scauflaire et al., 1989). This is a generalized excess Gibbs energy model that treats both long-range electrostatic interactions between ions and short-range interactions between all liquid phase species, molecular and ionic. It has been validated to ionic strengths representative of those found in industrial applications of acid gas - alkanolamine systems (Chen et al., 1982; Chen and Evans, 1986). Adjustable parameters of the Electrolyte-NRTL equation were estimated from experimental VLE solubility data reported in the literature and from measurements of CO_2 solubility in mixtures of MDEA with MEA or DEA made in this work.

Chapter Two

Thermodynamics of Weak Electrolyte Solutions with Applications to the H_2S-CO_2-alkanolamine-H_2O System

The present chapter is included to introduce the reader to some of the thermodynamic concepts that have been applied in this work to model the vapor-liquid equilibria of the weak electrolyte system - H_2S-CO_2-alkanolamine-H_2O. It is not intended to be a thorough review of the thermodynamic principles of weak electrolyte systems. It simply provides the reader with a brief review of relations between chemical potential, fugacity, activity coefficients, and excess Gibbs energy functions especially as they relate to weak electrolyte systems. An understanding of these chemical thermodynamic variables and the relationships between them, as well as an understanding of the concept of reference state or standard state in relation to these variables, is essential for research involving chemically reacting, multicomponent, multiphase systems. All of the information contained herein can be found in various thermodynamics textbooks (see for example, Prausnitz et al., 1986; Denbigh 1981; Smith and Van Ness, 1975; Prausnitz and Chueh, 1968). It is hoped that the chapter will provide a convenient reference for use with the Chapters Three and Four which are a review of the literature and summarize the modeling approach and thermodynamic functions adopted in this work respectively.

Perhaps most importantly, this chapter is included to facilitate reproduction of the model in the event that such a task is ever undertaken. Much of the thermodynamic data reported in the literature for the systems of interest in this work are based on the molality scale. Because the mole fraction scale was adopted for expressing concentrations in this work, it was necessary to convert thermodynamic data based on the molality scale to equivalent data based on the mole fraction scale. The equations necessary for making these conversions are developed within this chapter. In addition, equilibrium constants governing the dissociation of protonated alkanolamines that are reported in the literature are based on different standard states than those adopted here. Hence, it was necessary to adjust the pertinent equilibrium constants to the adopted standard states. The equations necessary to convert the equilibrium constants to the adopted standard state are also discussed herein.

2.1 Concentration Scales

For solutions of nonelectrolytes composed of substances which are liquid at room temperature, the mole fraction is the measure of concentration most often applied. However, the amount of a solid (including salts) or gas that is dissolved in a liquid is often expressed in terms of moles per unit volume, typically as moles per liter, molarity, or in terms of moles per kilogram solvent, molality. The use of molarity or molality is generally a matter of convenience; for solutions with electrolyte concentrations on the order of 1 molal, mole fractions are significantly smaller than unity making calculations cumbersome.

However, with the extensive application of digital computers in engineering practice today, the use of the mole fraction scale is no longer inconvenient. Moreover, because concentrations of the components of nonelectrolyte solvent mixtures are normally expressed in terms of mole fractions in engineering practice, as in the use of process simulators for example, it is practical to adopt the mole fraction scale for use with solutions of electrolytes and highly volatile gases as well.

Finally, the mole fraction scale embodies a theoretical significance not possessed by the other concentration scales; the entropy of mixing of an ideal solution is proportional to sum of the products of the component mole fractions and the logarithms of the component mole fractions. Also, for ideal solutions obeying Raoult's law or Henry's law, the equilibrium partial pressure of any component above the solution is directly proportional to its mole fraction in the solution, but is not directly proportional to its molality or molarity, except for very dilute solutions.

In the VLE model to be described in Chapter Four, the mole fraction scale was adopted for expressing concentrations. Because a significant amount of thermodynamic data related to weak electrolyte systems, including for example, equilibrium constants and Henry's constants, have been reported in the literature based on other concentration scales, it was necessary to convert much of the data taken from the literature to the mole fraction scale. To show how this was done, it is first necessary to develop relationships between the concentration scales.

It is a simple matter to convert between mole fraction and molality. However, conversion between either of these measures of concentration and a volume based concentration scale, such as molarity, is more difficult because the latter varies as a function of solution density, and therefore, as a function of temperature. Consider a solution containing n_i moles of solute and n_o moles of solvent with a molecular weight of M_s. The mole fraction of the solute is given by

$$x_i = \frac{n_i}{n_o + \sum n_i} \qquad (2.1)$$

and its molality is expressed as

$$m_i = \frac{n_i * 1000}{M_s * n_o} \qquad (2.2)$$

where the summation is over all solutes. Dividing equation (2.1) by equation (2.2) we obtain the following relationship between mole fraction and molality:

$$\frac{x_i}{m_i} = \frac{M_s * n_o}{1000 * (n_o + \sum n_i)} \qquad (2.3)$$

Therefore, for a dilute solution in which $\sum n_i << n_o$

$$x_i \approx m_i * \frac{M_s}{1000} \qquad (2.4)$$

For a solution with density ρ (gram cm^{-3}), the concentration of a solute (in gmol cm^{-3}) is given by

$$c_i = \frac{1000 * \rho * n_i}{M_s * n_o + \sum M_i * n_i} \qquad (2.5)$$

where M_i is the molecular weight of solute i. Dividing equation (2.5) by equation (2.1) yields the following relation between concentration and mole fraction:

$$\frac{c_i}{x_i} = \frac{1000 * \rho * (n_o + \sum n_i)}{M_s * n_o + \sum M_i * n_i} \qquad (2.6)$$

Therefore, for a dilute solution in which $\sum n_i << n_o$

$$c_i \approx x_i * \frac{1000 * \rho}{M_s} \qquad (2.7)$$

2.2 Conditions of Equilibrium

Consider a heterogeneous, closed system made up of two or more phases. Each phase is treated as an open system within the larger closed system allowing mass and heat transfer between the various phases. Neglecting surface effects and gravitational, electric, and magnetic fields, at thermal and mechanical equilibrium we expect the temperature and pressure to be uniform throughout the entire heterogeneous closed system. Gibbs (1961) showed that at chemical equilibrium each species must have a uniform value of chemical potential in all phases between which it can pass. These conditions of phase equilibrium for the closed heterogeneous system can be summarized as:

$$\begin{aligned} T^1 &= T^2 = \dots = T^n \\ P^1 &= P^2 = \dots = P^n \\ \mu_i^1 &= \mu_i^2 = \dots = \mu_i^n \qquad i = 1, 2, \dots, m \end{aligned} \tag{2.8}$$

where n is the number of phases and m is the number of species present in the closed system. μ_i is defined by the equation

$$\mu_i = \left(\frac{\partial G}{\partial n_i} \right)_{T,P,n_{j \neq i}} \tag{2.9}$$

G is the total Gibbs free energy of the open system (phase) and n_i is the number of moles of component i.

2.2.1 Application of Phase Equilibria to Electrolyte Systems

In a closed vapor - liquid system containing both electrolytes and nonelectrolytes, the electrolyte species will partially or wholly dissociate in the liquid phase to form ionic species. However, unless the system temperature is very high, vapor phase dissociation of the electrolyte components will be negligible. This suggests that, in practice, it is necessary to apply equations (2.8) only to neutral molecular species to determine the equilibrium distribution of components between the vapor and liquid phases. Because ions will be present only in the liquid phase for applications of interest in this work, equations (2.8) can be neglected for ionic species. This is not to suggest that ionic species do not play an important role in phase equilibrium calculations. Chemical equilibria, to be discussed later in this chapter, governs the distribution of an electrolyte in the liquid phase between its molecular and ionic forms. Since it is the molecular form of the electrolyte that comes to equilibrium with the same component in the vapor phase, chemical equilibria significantly affects phase equilibria and vice-versa. In addition, the presence of ionic species in the liquid phase results in highly nonideal thermodynamic behavior that is manifest in activity coefficients which depart significantly from unity.

2.2.2 An Alternate Expression of Phase Equilibrium

Chemical potential is a difficult thermodynamic variable to use in practice, partly because only relative values of this variable can be computed. Moreover, as the mole fraction of a component approaches infinite dilution, its chemical potential approaches negative infinity. To overcome these difficulties, G. N. Lewis (Lewis and Randall, 1961) defined a new thermodynamic variable called fugacity, f_i, which he related to the chemical potential as

$$\mu_i - \mu_i^o = RT \ln \frac{\hat{f}_i}{f_i^o} \tag{2.10}$$

where μ_i^o and f_i^o are arbitrary, but not independent, values of the chemical potential and fugacity of component i for some chosen reference state. $\hat{f}_i$ is the value of the fugacity for component i in a mixture. The difference in chemical potentials, $\mu_i - \mu_i^o$, is written for an isothermal change between the arbitrary reference state and the actual state for any component in the system. The ratio, $\frac{\hat{f}_i}{f_i^o}$, is defined as the activity of species i, a_i. Lewis was able to show from equations (2.10) and (2.8) that an equivalent, and more conveniently applicable, expression of phase equilibrium at constant and uniform values of the system temperature and pressure is

$$\hat{f}_i^1 = \hat{f}_i^2 = \ldots = \hat{f}_i^n \qquad i = 1, 2, \ldots, m \tag{2.11}$$

for all species of a system. Equation (2.11) has been widely adopted for phase equilibrium calculations. However, the concept of chemical potential continues to be used in the chemical literature, especially as it relates to chemically reactive systems including electrolyte systems. Indeed, because of its relation to the Gibbs free energy, chemical potential is the thermodynamic variable generally manipulated to determine the equilibrium distribution of species in a chemically reacting system at constant temperature and pressure (Gautam and Seider, 1979a,b; Smith and Missen, 1982).

In Chapter One, it was postulated that for weak electrolyte systems, both phase equilibrium and chemical equilibrium must be considered in determining the equilibrium distribution of species between a vapor and liquid phase. Fugacity and chemical potential are important thermodynamic variables in phase and chemical equilibrium calculations. Both will be discussed further in the sections to follow, especially insofar as they relate to other commonly employed **liquid** phase (solution) thermodynamic variables including the activity, activity coefficient, and equilibrium constant. It is liquid phase behavior that poses the most difficult challenge to representation of VLE in weak electrolyte systems. Relationships between these variables based on different concentration scales and based on different standard states will also be explored.

2.3 Expressions for the Chemical Potential

2.3.1 *Ideal Solutions, Nonideal Solutions, and the Activity Coefficient*

A solution is *defined* to be ideal if the chemical potential of every species in the solution is a linear function of the logarithm of its mole fraction. That is, a solution is ideal if, for every component, the following relation holds:

$$\mu_i = \mu_i^o + RT \ln x_i \tag{2.12}$$

where μ_i^o is known as the standard state or reference state chemical potential of component i. μ_i^o depends on temperature and pressure only (ie. reference state temperature and pressure). Both Raoult's and Henry's laws can be derived from equations (2.10) and (2.12) assuming that the vapor phase behaves as an ideal gas. For a real solution, the chemical potential is not a linear function of the logarithm of the mole fraction. In order to preserve the form of equation (2.12) for real solutions, the activity coefficient, γ_i, is *defined* such that

$$\mu_i = \mu_i^o + RT \ln x_i \gamma_i \tag{2.13}$$

where γ_i is a function of temperature, pressure, and composition of the solution. It is emphasized that equation (2.13) should be viewed as a definition for the activity coefficient. Comparing equations (2.10) and (2.13), it can be seen that

$$\gamma_i = \frac{\hat{f}_i}{x_i f_i^o} = \frac{a_i}{x_i} \tag{2.14}$$

The definition of the activity coefficient from equation (2.14) is incomplete until a reference state is specified and thus a value of μ_i^o. This can be accomplished by identifying the conditions of temperature, pressure, and composition at which γ_i becomes equal to unity. μ_i^o, then, is the chemical potential of component i at the conditions at which γ_i is taken, by convention, to be unity.

To specify the conditions at which the activity coefficient of component i becomes equal to unity, it is customary to adopt one of three primary conventions. The first two of these are based on the fact that in a real solution, component i behaves ideally both as its mole fraction, x_i, approaches unity, leading to Raoult's law, and as x_i approaches zero, leading to Henry's law. The process of identifying reference states at which the activity coefficients of all species in a solution become unity is referred to as normalization. In the discussion to follow concerning normalization of activity coefficients, a formalism has been adopted which is similar to that used by Denbigh (1981).

2.4 Standard State Conventions

2.4.1 Normalization Convention I

This convention leads to Raoult's law and is normally applied when all components of the solution are liquid at the system temperature and pressure. For such a system, all components are called solvents. The reference state for each solvent of the solution is the state of the pure component at the system temperature and an arbitrary reference pressure, often the system pressure or the vapor pressure of the component at the system temperature. By Normalization Convention I, the activity coefficient of each component approaches unity as its mole fraction approaches unity at the system temperature and the system reference pressure. That is, for all components

$$\mu_s = \mu_i^o + RT \ln x_i \gamma_s \tag{2.15}$$

$$\gamma_s \rightarrow 1 \quad \text{as} \quad x_s \rightarrow 1 \tag{2.16}$$

Since this normalization convention holds for all components of a solution, it is known as the *symmetric* normalization convention; activity coefficients normalized in this manner are said to be symmetrically normalized.

At the reference state implied by Convention I, the pure component, the logarithm term in equation (2.15) vanishes. Therefore, μ_i^o is the chemical potential of pure component i at the system temperature and the reference pressure. μ_i^o is also the molar Gibbs free energy of pure component i at the system temperature and reference pressure.

2.4.2 Normalization Convention II

This normalization convention leads to Henry's law and is usually applied when some components of the solution are solids or gases at the system temperature and pressure. For solutions of gases, Convention II is often adopted when the system temperature approaches or exceeds the critical temperature of one or more of the gaseous components of the solution but is well below the critical temperature of the solvent (Prausnitz and Chueh, 1968). Systems of interest in this work (i.e. aqueous solutions of H_2S or CO_2) can be characterized in this way.

The reference state for the solvent is different from the reference state for the solutes adopted under Convention II. For the solvent, the reference state is the same as that adopted under Normalization Convention I. That is, the reference state is taken to be the state of the pure solvent at the system temperature and an arbitrary pressure, usually the system pressure or the vapor pressure of the pure solvent. The reference state for a solute is taken to be the hypothetical state of pure solute found by extrapolating its chemical potential from infinite dilution in the solvent to the pure solute (Denbigh, 1981) at the solution temperature and the reference pressure. It is sometimes referred to as the ideal dilute reference state. For a binary solution, Convention II leads to the following expressions for chemical potentials and activity coefficients

$$\mu_s = \mu_s^o + RT \ln x_s \gamma_s \qquad \gamma_s \rightarrow 1 \quad \text{as} \quad x_s \rightarrow 1 \tag{2.17}$$

$$\mu_i = \mu_i^o + RT \ln x_i \gamma_i^* \qquad \gamma_i^* \rightarrow 1 \quad \text{as} \quad x_i \rightarrow 0 \tag{2.18}$$

where the subscripts s and i refer to solvent and solute respectively. Following the symmetric normalization convention, μ_s^o is the chemical potential of pure solvent at the system temperature and reference pressure. However, μ_i^o is the chemical potential of the pure solute in a hypothetically ideal solution corresponding to extrapolation of the chemical potential from infinite dilution to the pure solute. Since solvent and solute activity coefficients are not normalized in the same way, Convention II is known as the *unsymmetric* normalization convention. The superscript, *, on the activity coefficient for the solute is used to indicate that the activity coefficient of this solute approaches unity as its mole fraction approaches zero. Activity coefficients which are normalized unsymmetrically are related to the corresponding symmetrically normalized activity coefficients in a binary solution in the following way (Prausnitz et al., 1986; also see Van Ness and Abbott, 1979):

$$\gamma_i = \frac{\hat{f}_i}{x_i f_{\text{pure } i}} \tag{2.19}$$

and

$$\gamma_i^* = \frac{\hat{f}_i}{x_i H_{i,s}} \tag{2.20}$$

where $H_{i,s}$ is, by definition

$$H_{i,s} = \lim_{x_i \to 0} \frac{\hat{f}_i}{x_i} \tag{2.21}$$

Comparison of equation (2.21) with equation (2.14) reveals that $H_{i,s}$ is the reference state fugacity of the solute. It is called the Henry's constant of solute i in solvent s. Dividing equation (2.20) by (2.21) gives

$$\frac{\gamma_i}{\gamma_i^*} = \frac{H_{i,s}}{f_{\text{pure } i}} \tag{2.22}$$

Recalling that

$$\lim_{x_i \to 0} \gamma_i^* = 1$$

then, in the limit as x_i approaches zero

$$\lim_{x_i \to 0} \gamma_i = \frac{H_{i.s}}{f_{\text{pure } i}} \tag{2.23}$$

Substituting equation (2.23) into (2.22) gives

$$\frac{\gamma_i}{\gamma_i^*} = \lim_{x_i \to 0} \gamma_i \tag{2.24}$$

or

$$\frac{\gamma_i}{\gamma_i^*} = \gamma_i^\infty \tag{2.25}$$

and

$$\ln \gamma_i^* = \ln \gamma_i - \ln \gamma_i^\infty \tag{2.26}$$

where γ_i^∞ is the symmetrically normalized activity coefficient of solute i at infinite dilution in the solvent. That is

$$\gamma_i^\infty = \lim_{x_i \to 0} \gamma_i \tag{2.27}$$

For a multicomponent solution, consisting of a single solvent and multiple solutes, equations (2.17) and (2.18) can be written as

$$\mu_s = \mu_s^o + RT \ln x_s \gamma_s \qquad \gamma_s \to 1 \quad \text{as} \quad x_s \to 1 \tag{2.17}$$

$$\mu_i = \mu_i^o + RT \ln x_i \gamma_i \qquad \gamma_i^* \to 1 \quad \text{as} \quad \begin{array}{l} x_i \to 0 \\ \& \; x_k = 0 \end{array} \tag{2.28}$$

where k refers to all other solute components (Prausnitz and Chueh, 1968). An unsymmetrically normalized activity coefficient is then related to its symmetric counterpart through following equation

$$\ln \gamma_i^* = \ln \gamma_i - \ln \gamma_i^\infty \tag{2.29}$$

where

$$\gamma_i^\infty = \lim_{\substack{x_i \to 0 \\ x_k = 0}} \gamma_i \tag{2.30}$$

2.4.3 Normalization Convention III

As was mentioned earlier, the concentrations of solids, including salts, and gases are often measured on the molality scale. Accordingly, activity coefficients of these species are also often defined with reference to the molality scale. Again, for the solvent, the reference state is taken to be the state of the pure solvent at the system temperature and an arbitrary pressure, usually the system pressure or the vapor pressure of the pure solvent. The activity coefficient of the solvent is then defined on the mole fraction scale. Like Normalization Convention II, the reference state for a solute is taken to be the hypothetical state of pure solute found by extrapolating the chemical potential of the solute from infinite dilution in the solvent to the pure solute state at the solution temperature and the reference pressure. However, the reference state chemical potential for the solute, μ_i^Δ, is specified differently under Normalization Convention III. For a binary solution the activity coefficients of solvent and solute are defined as

$$\mu_s = \mu_i^o + RT \ln x_s \gamma_s \qquad \gamma_s \rightarrow 1 \quad \text{as} \quad x_s \rightarrow 1 \qquad (2.17)$$

$$\mu_i = \mu_i^\Delta + RT \ln m_i \gamma_i^\Delta \qquad \gamma_i^\Delta \rightarrow 1 \quad \text{as} \quad m_i \rightarrow 0 \qquad (2.31)$$

Again, μ_s^o is the chemical potential of pure solvent at the system temperature and reference pressure. μ_i^Δ is loosely referred to as the chemical potential of the solute in a hypothetical solution of unit molality (Denbigh, 1981). That is, μ_i^Δ is the chemical potential of the solute in a hypothetically ideal solution when m_i and γ_i^Δ are both equal to unity. Equation (2.31) can be generalized for multiple solute solutions in the same way that this was done for activity coefficient normalized by Convention II leading to equation (2.28).

2.4.4 Relation Between Activity Coefficients Based on Mole Fraction and Molality Scales

The relationship between the activity coefficients for solutes defined in terms of Normalization Conventions II and III can be determined by equating chemical potentials as expressed by equations (2.18) and (2.31) and using equation (2.3) to relate mole fraction to molality. This can be done because the actual chemical potential must be independent of the concentration scale used. It is then easy to show that

$$\ln \gamma_i^\Delta = \ln \gamma_i^* + \ln \frac{(1000 * x_i)}{M_s m_i} \qquad (2.32)$$

2.5 Chemical Equilibrium

2.5.1 *The Traditional Approach and Equilibrium Constants*

In a chemically reacting system, the mole numbers, n_i, are related to the extents of R independent reactions, ξ_j, by

$$n_i = n_i^o + \sum_{j=1}^{R} \upsilon_{ij}\,\xi_j \qquad i = 1, 2, ..., N \qquad (2.33)$$

where υ_{ij} is the stoichiometric coefficient of species i in reaction j, and n_i^o is some reference amount of species i. Equation (2.33) serves as a definition for ξ_j which has units of moles. Therefore, the Gibbs free energy, G, of the system can be transformed from a function of temperature, pressure, and N mole numbers to a function of temperature, pressure and R extents of reaction:

$$G = G(T, P, \xi_1, \xi_2, ..., \xi_R) \qquad (2.34)$$

The condition of chemical equilibria is found by minimizing G at constant temperature and pressure with respect to the R independent extents of reaction. The first order necessary conditions for a minimum in G are

$$\left(\frac{\partial G}{\partial \xi_j}\right)_{T, P, \xi_{j\neq k}} = 0 \qquad j = 1, 2, ..., R \qquad (2.35)$$

Using the chain rule for differentiation, $\left(\frac{\partial G}{\partial \xi_j}\right)_{T, P, \xi_{j\neq k}}$ can be expressed as

$$\left(\frac{\partial G}{\partial \xi_j}\right)_{T, P, \xi_{j\neq k}} = \sum_{i=1}^{N} \left(\frac{\partial G}{\partial n_i}\right)_{T,P,n_{k\neq i}} \left(\frac{\partial n_i}{\partial \xi_j}\right)_{\xi_{j\neq k}} \quad j = 1, 2, ..., R \quad (2.36)$$

From equation (2.33)

$$\left(\frac{\partial n_i}{\partial \xi_j}\right)_{\xi_{j \neq k}} = \nu_{ij} \tag{2.37}$$

Combining equations (2.35), (2.36), (2.37), and (2.9) finally gives

$$\sum_{i=1}^{N} \nu_{ij}\,\mu_i = 0 \qquad j = 1, 2, \ldots\ldots, R \tag{2.38}$$

Equations (2.38) are the classical forms of the equilibrium conditions (Smith and Missen, 1982). When appropriate expressions are introduced for the chemical potential in terms of mole numbers, the nonlinear equations (2.38) can be solved, together with N minus R independent linear mass balance equations, for the composition of the system at equilibrium. If appropriate expressions are introduced for the chemical potential in terms of extent of reaction variables, equations (2.38) can be solved for the R extents of reaction at equilibrium. The composition of the system at equilibrium can then be determined using equations (2.33).

For electrolyte solutions, chemical potentials are often written in terms of mole fractions and unsymmmetrically normalized activity coefficients (Convention II, equations (2.17) and (2.18)). For a system in which a single chemical reaction takes place, substitution of equations (2.17) and (2.18) for μ_i in equation (2.38) for any reaction j yields

$$\sum_{i=1}^{N} \nu_i\,\mu_i^{o} + RT\sum_{i=1}^{N} \nu_i \ln \gamma_i\, x_i = 0 \tag{2.39}$$

where the summations are over all N components of the system. The activity coefficients of solvent species are symmetrically normalized in equation (2.39) while the solute activity coefficients are unsymmetrically normalized. For generality, the asterisk above the activity coefficient denoting unsymmetrically normalized activity coefficients has been omitted from equation (2.39). Rearranging equation (2.39) gives

$$\ln \Pi (\gamma_i x_i)^{\upsilon_i} = -\frac{1}{RT}\sum_{i=1}^{N} \upsilon_i \mu_i^o \tag{2.40}$$

The right hand side is a function of temperature only at specified reference states for all components. A thermodynamic equilibrium constant, based on the mole fraction scale - K_x, can then be defined in the following way

$$RT \ln K_x = -\sum_{i=1}^{N} \upsilon_i \mu_i^o = \Delta G_T^o \tag{2.41}$$

Equation (2.41) relates K to the N values of the reference state chemical potentials, μ_i^o. ΔG_T^o is known as the standard Gibbs free energy change of reaction at the specified temperature T. Equation (2.41) indicates that for any reaction K_x is a function of temperature only at the specified standard states for the participating components. Combining equations (2.40) and (2.41) yields

$$K_x = \Pi (\gamma_i x_i)^{\upsilon_i} \tag{2.42}$$

Using $\gamma_i x_i = a_i$, equation (2.42) can also be expressed as

$$K_x = \Pi (a_i)^{\upsilon_i} \tag{2.43}$$

Equations (2.42) and (2.43) represent the *traditional* approach to solving for the composition of a system at chemical equilibrium. Each is a nonlinear algebraic equation relating the standard state Gibbs free energy change of reaction to the activities of the various species participating in the chemical reaction under consideration. One equation of this type is written for each reaction occurring in the system. For a system composed of N species and for which R independent chemical reactions can be written, R equations of the form (2.42) or (2.43) and N minus R independent linear algebraic equations, representing mass balances, must be solved simultaneously for the composition of the system at equilibrium.

This traditional approach to solving for the equilibrium composition of a reactive system was not used in this work. The approach adopted here, however, is completely equivalent to the use of equations (2.42) and (2.43), and will be discussed at length in Chapter Four. Of note at this time is that equilibrium constants defined by equation (2.41) and taken from the literature play a central role in the adopted approach. The purpose of the above discussion was to establish a definition for the equilibrium constant, K_X, and to show how it is related to other thermodynamic variables, in particular, the mole fraction and activity coefficient. Later in Chapter Two, this will aid in the development of relationships between equilibrium constants based on different concentration scales and on different standard states. Such relationships are important because equilibrium constants reported in the literature for any given reaction may be based on a different concentration scale than that adopted, or based on different reference states for the participating components than those adopted.

As noted earlier, concentrations and activity coefficients of solutes in electrolyte solutions are also often based on the molality scale. Like activity coefficients normalized under Convention II, the activity coefficients of solute species normalized by Convention III approach unity at infinite dilution. However, as noted previously, the values of reference state chemical potentials of solute species calculated by the Conventions II and III are different. If the molality based activity coefficient convention is adopted, then equations (2.41) and (2.42) must be rewritten as

$$RT \ln K_m = - \sum_{i=1}^{N} \upsilon_i \, \mu_i^{\Delta} = \Delta G_T^{\Delta} \tag{2.44}$$

$$K_m = \Pi \, (\gamma_i \, m_i)^{\upsilon_i} \tag{2.45}$$

where the superscript to the activity coefficient for solute species denoting unsymmetrically normalized activity coefficients expressed on the molality scale has been omitted for generality.

The equilibrium constant is often the only available thermodynamic data related to the standard states of components in a reaction. If the traditional approach to solving for the composition of a reacting system is adopted using equation (2.42) or (2.43), then equilibrium constants reported in the literature can be used directly. However, other approaches to solving for the equilibrium composition of a reacting system do not employ equilibrium constants directly (Smith and Missen, 1982). As a result, it may be necessary to determine a set of consistent standard state chemical potentials from reported equilibrium constants. Such a procedure is necessary for the approach adopted in this work. The details of the procedure will be described in Chapter Four.

2.6 Applications to the System H_2S-CO_2-alkanolamine-H_2O

In aqueous solution, the extent of electrolyte dissociation is governed by chemical equilibrium. Electrolytes that dissociate completely are referred to as strong electrolytes. Electrolyte species which only partially dissociate in water are commonly referred to as weak electrolytes.

2.6.1 Acid - Base Buffer Equilibria

The compounds of interest in this work are characterized as weak electrolytes: H_2S and CO_2 are weak acid electrolytes and alkanolamines are weak organic base electrolytes. These weak acids and weak bases partially ionize, or partially dissociate, in aqueous solution. For the species of interest in this work, dissociation can be expressed as

Water: $2\,H_2O \leftrightarrow H_3O^+ + OH^-$ (2a)

Hydrogen Sulfide: $H_2O + H_2S \leftrightarrow H_3O^+ + HS^-$ (2b)

Hydrogen Bisulfide: $H_2O + HS^- \leftrightarrow H_3O^+ + S^=$ (2c)

Carbon Dioxide: $2\,H_2O + CO_2 \leftrightarrow H_3O^+ + HCO_3^-$ (2d)

Bicarbonate: $H_2O + HCO_3^- \leftrightarrow H_3O^+ + CO_3^=$ (2e)

Protonated
Alkanolamine $H_2O + RR'R''NH^+ \leftrightarrow H_3O^+ + RR'R''N$ (2f)

In these equations RR'R"N is the chemical formula for the alkanolamine. R represents an alkyl group, alkanol group, or hydrogen. Note that reactions (2a), (2b), (2c), (2e), and (2f) are proton transfer reactions. As such, they occur very rapidly and are often assumed to be instantaneous with respect to mass transfer. Reaction (2d), representing dissociation of CO_2 proceeds by one of two alternate mechanisms (Astarita et al., 1983). The first is a two step mechanism. CO_2 reacts with water to form carbonic acid (H_2CO_3). This is a slow reaction. Carbonic acid then dissociates to bicarbonate by donating a proton to water. This is a fast reaction. The overall reaction rate is slow relative to a simple proton transfer reaction. CO_2 is also capable of reacting directly with hydroxide ion, OH^-, to form bicarbonate ion. This mechanism is believed to be dominant at pH values greater than 8 (Astarita et al., 1983). The rate of this reaction is also slow relative to proton transfer reactions.

2.6.2 Formation of Carbamate

In addition to its reaction with amines through an acid-base buffer mechanism, CO_2 may also react directly with many primary and secondary amines to form stable carbamate species. Caplow (1968) first proposed a two-step zwitterion mechanism for this reaction. This mechanism is reproduced here:

$$CO_2 + RR'NH \leftrightarrow RR'NH^{+}COO^{-}$$

$$RR'NH^{+}COO^{-} + RR'NH \leftrightarrow RR'NH^{+} + RR'NCOO^{-} \qquad (2g)$$

Blauhoff et al. (1984) were able to satisfactorily interpret absorption rate data for the absorption of CO_2 into DEA solutions in terms of this mechanism. Tertiary amines, having no hydrogen on the amino nitrogen available for extraction, are unable to react with CO_2 to form carbamates. Sterically hindered primary and secondary amines, possessing a secondary or tertiary carbon atom attached to the amino group, form weakly stable carbamates (Sartori and Savage, 1983). Of the alkanolamines of interest in this work, monoethanolamine (MEA), diethanolamine (DEA), diglycolamine (DGA), and methyldiethanolamine (MDEA), the first three are known to form stable carbamates.

While the equilibrium constants for reactions (2a) through (2f) have been measured in the temperature range of interest, true equilibrium constants for the formation of the carbamate of MEA, DEA, or DGA have not been accurately measured.

2.6.3 Relation Between Equilibrium Constants Based on the Mole Fraction Scale and the Molality Scale

Equilibrium constants governing the dissociation of weak electrolytes in aqueous solution are customarily reported on the molality scale. Since Convention II was adopted for use in this work, concentrations and activity coefficients are expressed in terms of the mole fraction scale. Hence it was necessary to relate values of the equilibrium constants reported on the molality scale to corresponding values of the equilibrium constants expressed on the mole fraction scale. Using equations (2.42) and (2.45), and the relation between molality and mole fraction, equation (2.3), the relation between K_x and K_m can be developed.

Consider, for example, the dissociation of hydrogen sulfide in water as expressed by reaction (2b). If concentrations and activity coefficients are based on the mole fraction scale in accordance with Convention II, then equation (2.42) can be used to determine the composition of the aqueous phase at equilibrium:

$$K_{x,\,H_2S} = \frac{x_{H_3O}\, x_{HS^-}\, \gamma^*_{H_3O}\, \gamma^*_{HS^-}}{x_{H_2S}\, x_{H_2O}\, \gamma^*_{H_2S}\, \gamma_{H_2O}} \tag{2.46}$$

Again, the superscript, *, on the activity coefficients of the solutes HS^-, H_3O^+, and H_2S, indicate that they are based on the mole fraction scale and that they approach unity as the corresponding mole fraction of each solute approaches zero. The activity coefficient of water approaches unity as its mole fraction approaches unity.

Similarly, if concentrations and activity coefficients are based on the molality scale in accordance with Convention III, then equation (2.43) can be used to determine the composition of the aqueous phase at equilibrium:

$$K_{m,\,H_2S} = \frac{m_{H_3O}\, m_{HS^-}\, \gamma^\Delta_{H_3O}\, \gamma^\Delta_{HS^-}}{m_{H_2S}\, x_{H_2O}\, \gamma^\Delta_{H_2S}\, \gamma_{H_2O}} \tag{2.47}$$

The superscript, Δ, on the activity coefficients of the solutes HS^-, H_3O^+, and H_2S, indicate that they are based on the molality scale and that they approach unity as the corresponding mole fraction of each solute approaches zero. The negative logarithm of $K_{m,\,H_2S}$ is commonly known as the pKa of H_2S.

The relation between K_x and K_m for reaction (2b) can be found most easily at the infinitely dilute state where all activity coefficients in equation (2.46) and (2.47) are *defined* to be unity. Using equation (2.4) for the relation between mole fraction and molality for dilute solutions, it can be shown that

$$K_x = K_m \left(\frac{M_s}{1000}\right) \tag{2.48}$$

In terms of the logarithms of K_x and K_m, equation (2.48) can be written as

$$\ln K_x = \ln K_m - \ln\left(\frac{1000}{M_s}\right) \tag{2.49}$$

Equation (2.49) reveals that the difference between ln K_x and ln K_m is the same at all temperatures. While equations (2.48) and (2.49) were derived for an infinitely dilute aqueous solution of H_2S, they hold for all finite H_2S concentrations. Similar expressions can be derived for all other reactions (2a) through (2g).

In general, to convert the logarithm of an equilibrium constant for the dissociation of an electrolyte in water from the molality scale to the mole fraction scale, it is necessary to subtract $\ln\left(\frac{1000}{M_s}\right)$ for each non-water component on the right hand side of a stoichiometric expression and to add $\ln\left(\frac{1000}{M_s}\right)$ for each non water component on the left hand side of a stoichiometric expression.

The temperature dependence of logarithm of the equilibrium constant is often reported as

$$\ln K = C_1 + C_2/T + C_3 \ln T + C_4 T \tag{2.50}$$

Edwards et al. (1975) show how this general expression is derived from fundamental thermodynamic relationships. To convert a value of K_m, reported in the form of equation (2.50), to K_x, it is necessary only to adjust the value of C_1, using an equation equivalent to (2.49). The same is true for the reverse process, converting K_x to K_m.

2.6.4 Relation Between Equilibrium Constants Based on Different Standard States

Dissociation equilibrium constants for organic bases reported in the literature are normally expressed on the molality scale. Hence, dissociation equilibria of protonated weak organic bases such as alkanolamines, illustrated by reaction (2f), can be expressed in terms of equation (2.47) as

$$K_{m,AmH} = \frac{m_{Am}\, m_{H_3O^+}}{m_{AmH^+}\, x_{H_2O}} \frac{\gamma^{\Delta}_{Am}\, \gamma^{\Delta}_{H_3O^+}}{\gamma^{\Delta}_{AmH^+}\, \gamma_{H_2O}} \tag{2.51}$$

where Am and AmH^+ refer to the amine and protonated amine species respectively. The superscript, Δ, on the activity coefficients of the solutes indicate that they are based on the molality scale and that they approach unity as the corresponding mole fraction of each solute approaches zero. The negative logarithm (base 10) of $K_{m,AmH}$ is known as the pKa of the organic base alkanolamine. If concentrations and activity coefficients are to be expressed on the mole fraction scale, $K_{m,AmH}$ can be converted to $K_{x,AmH}$ using equation (2.49) so that

$$K_{x,AmH} = \frac{x_{Am}\, x_{H_3O^+}}{x_{AmH^+}\, x_{H_2O}} \frac{\gamma^{*}_{Am}\, \gamma^{*}_{H_3O^+}}{\gamma^{*}_{AmH^+}\, \gamma_{H_2O}} \tag{2.52}$$

where the asterisk superscript on the solute activity coefficients identifies that they are unsymmetrically normalized in accordance with Convention II.

In the context of a vapor - liquid equilibria model, it is most convenient to treat an alkanolamine as a solvent, rather than as a solute, because it exists as a liquid at relevant temperatures and pressures. That is, it is useful to normalize the activity coefficient of an alkanolamine in the same way that the activity coefficient of water in is normalized so that

$$\gamma_{Am} \rightarrow 1 \quad \text{as} \quad x_{Am} \rightarrow 1 \tag{2.53}$$

This is the normalization convention adopted for alkanolamines in this work. By adopting this normalization convention, a new dissociation constant can be defined as

$$K'_{x\,AmH} = \frac{x_{Am}\, x_{H_3O^+}}{x_{AmH^+}\, x_{H_2O}} \frac{\gamma_{Am}\, \gamma^*_{H_3O^+}}{\gamma^*_{AmH^+}\, \gamma_{H_2O}} \tag{2.54}$$

K'_x can be related to K_x by dividing equation (2.54) by equation (2.52) so that

$$K'_x = K_x \frac{\gamma_{Am}}{\gamma^*_{Am}} \tag{2.55}$$

Using equation (2.25) to relate γ_{Am} to γ^*_{Am} yields

$$K'_x = K_x\, \gamma^{\infty}_{Am} \tag{2.56}$$

where γ^{∞}_{Am} is the symmetrically normalized activity coefficient of alkanolamine at infinite dilution in water. The value of γ^{∞}_{Am} can then be obtained from VLE data (TPx or TPxy) for the binary amine-water mixture by extrapolation of the alkanolamine activity coefficient to infinite dilution.

2.6.3 Single Solute Systems

Water is both a weak acid and a weak base. When a proton donating weak acid like H_2S is present in water, the water acts as a weak base and accepts a proton from the acid to form a hydronium ion. However, the value of the equilibrium constant for this reaction is very small. As a result, when a single weak acid electrolyte is present in solution, the extent of dissociation is appreciable only at high dilutions of the solute. At higher concentrations only a small fraction of the weak acid will exist in ionized form, the major fraction of the acid remains in its molecular form. Similarly, when a weak proton accepting base is present in water, the hydronium ion, formed by self-ionization of water, acts as a weak acid and donates a proton to the base. Once again, the value of the equilibrium constant for this reaction is very small. As a result, when a single weak base electrolyte is present in solution, the extent of protonation is appreciable only at high dilutions of the base. At higher concentrations only a small fraction of the weak base will exist in protonated form, the major fraction of the base remains in its molecular form.

2.6.4 Multisolute Solutions

Aqueous mixtures of weak acid and weak base electrolytes behave drastically different than single solute systems. When a weak acid and a weak base, like H_2S and alkanolamine, are present together in aqueous solution, the extents of the respective dissociation reactions increase greatly. That this is true can be clearly seen in light of the principle of mass action. Consider, for example, an aqueous solution of H_2S and monoethanolamine (MEA). The primary dissociation/protonation reactions that occur in this solution include

K_w $$2\,H_2O \leftrightarrow H_3O^+ + OH^- \tag{2a}$$

$K_{a\text{-}H_2S}$ $$H_2O + H_2S \leftrightarrow H_3O^+ + HS^- \tag{2b}$$

$K_{b\text{-}MEA}$ $$H_3O^+ + HOC_2H_4NH_2 \leftrightarrow H_2O + HOC_2H_4NH_3^+ \tag{2h}$$

Equilibrium phenomena for this system, and others like it, can then be viewed in the following way. Reaction (2a) represents a restriction on the amount of hydronium ion that may exist at equilibrium in aqueous solution. Because K_w is very much less than unity, water self-ionizes only to an extremely limited extent. Thus, in an aqueous solution of a single *weak* acid or a single *weak* base (characterized by equilibrium constants $K_a << 1$ and $K_b << 1$ respectively) very little of the acid or base dissociates. However, when both the weak acid H_2S and weak base MEA are present in solution, hydronium ion produced by dissociation of H_2S in reaction (2b) is consumed in reaction (2h) for protonation of MEA. In this way, the weak acid electrolyte dissociates in water to far greater extent in the presence of the weak base electrolyte, and the fractions of the weak electrolytes existing in ionic form are substantially increased.

It should also be noted that this shift to the ionic forms reduces the concentrations of the molecular or unreacted forms of the weak electrolytes in solution. Since it is the molecular forms of the weak electrolytes that come to equilibrium with the same species in the vapor phase, the equilibrium partial pressures of the weak electrolytes in the vapor phase can be greatly reduced.

2.6.5 Absorption of H2S and CO2 with Akanolamine Solutions

When an aqueous solution of alkanolamine is used to absorb H_2S or CO_2 from a gas mixture, the absorbed acid gases exist primarily as ionic species in the aqueous solution due to the resulting acid-base buffer reactions and the formation of carbamates. This is true provided that the total acid gas concentrations do not substantially exceed the amine concentration. As mentioned previously, it is the unreacted (molecular) H_2S and CO_2 in the liquid phase which come to equilibrium with the same components in the vapor phase. Therefore, at a given acid gas partial pressure, the solubilities of H_2S and CO_2 in all forms, molecular and ionic, are greatly increased in an aqueous alkanolamine solution relative to the solubilities of these solutes in pure water owing to the dissociation of acid gases and protonation of the alkanolamines. This phenomena may also be viewed from the reverse point-of-view. At a given apparent acid gas concentration (the composition assuming the electrolytes do not dissociate) in an aqueous alkanolamine solution, the acid gas partial pressure in equilibrium with the solution will be greatly reduced relative to the acid gas partial pressure in equilibrium with pure water at the same liquid phase loading of acid gas.

2.7 Phase Equilibrium

The condition of phase equilibrium in a multiphase system at constant and uniform values of pressure and temperature is given by equation (2.11). This is sometimes referred to as the *isofugacity* condition. For a two-phase vapor-liquid multicomponent system, equation (2.11) may be expressed as

$$\hat{f}_i^v\,(T, P, \underline{y}) = \hat{f}_i^l\,(T, P, \underline{x}) \qquad i = 1, 2, \ldots, N \qquad (2.57)$$

where $\hat{f}_i^v$ and $\hat{f}_i^l$ are the fugacities of component i in the vapor mixture and liquid mixture respectively, and $\underline{y}$ and $\underline{x}$ represent the mole fractions of all components in the vapor and liquid phases respectively.

Equation (2.57) is of little value in practice unless the fugacities can be related to experimentally accessible state variables including T, P, x, y. The desired relation between vapor phase fugacity and accessible vapor phase state variables is provided by the fugacity coefficient, φ. A similar relation for the liquid phase fugacity is provided by the activity coefficient, γ. Both of these relationships will be reviewed in the discussions which follow.

2.7.1 Vapor Phase Fugacity

The vapor phase fugacity of each species in a mixture is related to its concentration, y_i, and the system pressure, P, through the fugacity coefficient $\hat{\varphi}_i(T, P, \underline{y})$:

$$\hat{f}_i^v\,(T, P, \underline{y}) = \hat{\varphi}_i(T, P, \underline{y})\,y_i\,P \qquad i = \text{molecules} \qquad (2.58)$$

where $\hat{\varphi}_i$ is defined as

$$\hat{\varphi}_i = \frac{\hat{f}_i^v}{y_i\,P} \qquad (2.59)$$

At constant temperature and vapor phase composition, the fugacity coefficient of component i, $\hat{\varphi}_i(T, P, \underline{y})$, can be calculated using the following exact relation:

$$\ln \hat{\varphi}_i = \frac{-1}{RT} \int_0^P \left(\frac{RT}{P} - \bar{v}_i\right) dP \qquad (2.60)$$

where $\bar{v}_i$ is the partial molar volume of species i in the gas mixture and R is the gas constant. In the context of a vapor-liquid equilibrium model, it is most convenient to calculate vapor phase fugacities using equations (2.58) and (2.60) and an equation of state that adequately describes the volumetric behavior of the vapor phase over the whole concentration range of interest. The equation of state would be used to represent the pressure dependence of $\bar{v}_i$ in equation (2.60).

2.7.2 Liquid Phase Fugacity

The liquid phase fugacity can also be calculated using an equation-of-state approach. However, equations-of-state often do not satisfactorily describe the volumetric properties of condensed phases. In addition, volumetric data are usually not available over the entire density range from zero pressure to the system pressure. Therefore, an alternative method is usually adopted by which deviations from ideal behavior are described in terms of excess functions (Prausnitz et al., 1986). The activity coefficient, $\gamma_i(T,P,\underline{x})$, which is related to the fugacity as shown by equation (2.14) is the corresponding mole number derivative of the excess Gibbs energy. Using the activity coefficient, the fugacity of an component of a liquid solution can be expressed as

$$\hat{f}_i^{l}\ (T, P, \underline{x}) \;=\; \gamma_i(T, P, \underline{x})\, x_i\, f_i^{oL}(T) \qquad i = \text{molecule} \qquad (2.61)$$

where $f_i^{oL}(T)$ is some (arbitrary) reference fugacity. As discussed previously, for a solvent, $f_s^{oL}(T)$ is usually taken to be the fugacity of the pure liquid at the solution temperature and at the specified reference pressure, often its vapor pressure at the solution temperature, so that

$$f_s^{oL}(T) \;=\; \lim_{x_s \to 1} \frac{\hat{f}_s(T,\underline{x})}{x_s} \;=\; f_s(T) \qquad s = \text{solvent} \qquad (2.62)$$

where $f_s(T)$ is the pure component fugacity. If the reference pressure is specified to be the saturation pressure of the solvent then $f_s^{oL}(T)$ can be expressed in terms of the fugacity coefficient as

$$f_s^{oL}(T) \;=\; P_s^{o}(T)\, \overset{o}{\varphi}_s(T) \qquad s = \text{solvent} \qquad (2.63)$$

where $P_s^{o}(T)$ is the saturation (vapor) pressure at the system temperature and $\overset{o}{\varphi}_s(T)$ is the fugacity coefficient of *pure* saturated vapor s (at equilibrium $\overset{l}{\varphi}_s(T) = \overset{v}{\varphi}_s(T)$) at the system temperature and pressure $P_s^{o}(T)$. For many solvents $\overset{o}{\varphi}_s(T)$ is approximately unity at temperatures of interest. Using equation (2.63) for the reference state fugacity, the fugacity of a solvent in a liquid mixture is given by

$$\hat{f}^{l}_{s}\,(T, P, \underline{x}) \;=\; \gamma_i(T, P, \underline{x})\, x_i\, P^{o}_{s}(T)\, \varphi^{o}_{s}(T) \qquad s = \text{solvent} \qquad (2.64)$$

where $\gamma_s(T, P, \underline{x})$ is symmetrically normalized so that $\gamma_s \rightarrow 1$ as $x_s \rightarrow 1$ at the system temperature and the reference pressure.

A similar reference state fugacity is not convenient for a gaseous solute if the system temperature exceeds the critical temperature for that solute as this requires extrapolating the vapor pressure of the pure liquid i beyond its critical temperature. A more convenient standard state for near critical or supercritical components was suggested earlier by activity coefficient Normalization Convention II (or III). For gaseous solutes it is common to adopt a reference state such that

$$f^{oL}_{i}(T) \;=\; \lim_{x_i \to 0} \frac{\hat{f}_i(T,\underline{X})}{x_i} \;=\; H^{pref}_{i.s}(T) \qquad (2.65)$$

Equation (2.65) is equivalent to equation (2.21). The reference fugacity defined here is known as the Henry's law constant for component i in the solvent s. The advantage gained by this reference state fugacity is that $H^{pref}_{i.s}(T)$ can be determined, unambiguously, from experimental solubility data. The superscript ^{pref} is meant to indicate that $H_{i,s}$ is to be evaluated at the reference pressure. Often, the reference pressure for molecular solutes is chosen to be the vapor pressure of the solvent, P^{o}_{s}, at the system temperature. Using equation (2.65) for the reference state fugacity, the fugacity of a gaseous component in a liquid mixture can be expressed as

$$\hat{f}^{l}_{i}\,(T, P, \underline{x}) \;=\; \gamma^{*}_{i}(T, P, \underline{x})\, x_i\, H^{pref}_{i.s}(T) \qquad \begin{matrix} i = \text{solute} \\ s = \text{solvent} \end{matrix} \qquad (2.66)$$

where $\gamma_i^*(T, P, \underline{x})$ is unsymmetrically normalized so that $\gamma_i^* \rightarrow 1$ as $x_i \rightarrow 0$ and all $x_{k \neq i} = 0$.

2.7.3 The Pressure Dependence of the Liquid Phase Fugacity

The activity coefficient is a strong function of temperature and liquid phase composition, but a weak function of pressure. At low and moderate pressures, the effect of pressure on the activity coefficient can usually be neglected. However, at high pressures, characteristic of some sour gas systems, the effect can be large and the activity coefficient must corrected for pressure effects. If the reference state is defined at a fixed pressure, P^{ref}, this correction is given by the exact thermodynamic relationship

$$\left(\frac{\partial \ln \gamma_i}{\partial p}\right)_{x,T} = \frac{\bar{v}_i(T,P,\underline{x})}{RT} \qquad (2.67)$$

where $\bar{v}_i(T,P,\underline{x})$ is the partial molar volume of component i at the system temperature and liquid phase composition, $\underline{x}$. Integrating this equation from the reference state pressure to the system pressure gives

$$\ln \gamma_i(T, P, \underline{x}) = \ln \gamma_i(T, P^{ref}, \underline{x}) + \int_{P^{ref}}^{P} \frac{\bar{v}_i(T,P,\underline{x})}{RT}\, dP \qquad (2.68)$$

The integral on the right hand side is known as the Poynting correction (Prausnitz et al., 1986) and accounts for the effect of pressure on the activity coefficient. Hereafter,

$\ln \gamma_i(T, P^o, \underline{x})$ will be denoted as $\ln \gamma_i(T, \underline{x})$ for simplicity. Combining equations (2.61) and (2.68) yields the following equation for liquid phase fugacity

$$\hat{f}_i^l\ (T, P, \underline{x}) = \gamma_i(T, \underline{x})\, x_i\, f_i^{oL}(T) \exp \int_{P^{ref}}^{P} \frac{\bar{v}_i(T,P,\underline{x})}{RT}\, dP \qquad (2.69)$$

If the reference pressure is specified to be the *saturation pressure* of the solvent at the system temperature in a single solvent - single or multiple solute mixture, then $f_i^{oL}(T)$ is $P_s^o(T)\varphi_s^o(T)$ for the solvent and $H_{i,s}^{P^o}(T)$ for each gaseous solute i.

$\bar{v}_i$ is often an unknown and complex function of composition and pressure. When the system pressure is low and mixture conditions are far from critical, it is common practice to equate the partial molar volume of a solvent component to its molar volume, v_s (Prausnitz et al., 1980). Furthermore, because the concentration of a gaseous component does not generally exceed a few percent in the liquid, it is also common practice to equate the partial molar volume of a volatile gaseous component to its partial molar volume at infinite dilution, v_i^∞, at the system temperature and reference pressure. Partial molar volumes at infinite dilution are convenient in this context because they can be estimated from experimental solubility data or from semi-empirical methods (Wilhelm, 1986). If v_s and v_i^∞ are assumed to be independent of pressure and composition over the pressure and composition ranges of interest, then equation (2.69) then becomes

$$\hat{f}_s^l\ (T, P, \underline{x}) = \gamma_s(T, \underline{x})\, x_s\, P_s^o(T)\, \varphi_s^o(T)\ \exp \frac{v_s\,(P - P^{ref})}{RT} \qquad (2.70)$$

for a solvent, and

$$\hat{f}_i^{l}(T, P, \underline{x}) = \overset{*}{\gamma}_i(T, \underline{x})\, x_i\, H_{i.s}^{pref}(T)\, \exp\frac{\bar{v}_i^{\infty}(P - pref)}{RT} \qquad (2.71)$$

for a solute.

Alternatively, the *system pressure* can be adopted as the reference pressure for all components of a solution. The standard state fugacities of the solvents and solutes in a multicomponent mixture can then be expressed as

$$f_s^{oL}(T, P^{ref}) = P_s^{o}(T)\, \varphi_s^{o}(T)\, \exp\int_{P^o}^{pref}\frac{v_s(T,P)}{RT}\,dP \qquad (2.72)$$

for a solvent, and

$$H_{i.s}^{pref} = H_{i.s}^{P^o}(T)\, \exp\int_{P^o}^{pref}\frac{\bar{v}_i^{\infty}(T,P)}{RT}\,dP \qquad (2.73)$$

for the solute. If the reference pressure is taken to be the system pressure and equations (2.72) and (2.73) are used to express standard state fugacities, then the pressure dependence of the activity coefficient is given by

$$\left(\frac{\partial \ln\gamma_s}{\partial p}\right)_{x,T} = \frac{\bar{v}_s(T,P,\underline{x}) - v_s(T,P)}{RT} \qquad (2.74)$$

for solvents, and

$$\left(\frac{\partial \ln\gamma_i}{\partial p}\right)_{x,T} = \frac{\bar{v}_i(T,P,\underline{x}) - \bar{v}_i^{\infty}(T,P)}{RT} \qquad (2.75)$$

for solutes. Often the pressure corrections to the activity coefficients given by equations (2.74) and (2.75) are very small, so that the activity coefficients can be treated as independent of pressure. If the system pressure is adopted as the reference pressure, v_s and v_i^{∞} are assumed to be independent of pressure, and if all activity coefficients are assumed to be independent of pressure, then equation (2.61) can be combined with equations (2.72) and (2.73) to yield the following equations for the liquid phase fugacity

$$\hat{f}^{l}_{s}(T, P, \underline{x}) = \gamma_s(T, \underline{x})\, x_s\, P^{o}_{s}(T)\, \varphi^{o}_{s}(T)\, \exp\frac{v_s\,(P^{ref} - P^{o})}{RT} \tag{2.76}$$

for a solvent, and

$$\hat{f}^{l}_{i}(T, P, \underline{x}) = \gamma^{*}_{i}(T, \underline{x})\, x_i\, H^{pref}_{i,s}(T)\, \exp\frac{\bar{v}^{\infty}_{i}\,(P^{ref} - P^{o})}{RT} \tag{2.77}$$

for a solute. P^{ref} is the system pressure and P^{o} is the saturation pressure of the solvent at the system temperature. Note that equations (2.76) and (2.77) are almost identical to equations (2.70) and (2.71).

2.8 Excess Gibbs Energy

2.8.1 Relation to Activity Coefficient and Chemical Potential

The excess Gibbs energy is defined as the Gibbs energy of a real solution which is in excess of the Gibbs energy of an ideal solution at the same conditions of temperature, pressure, and composition (Prausnitz et al., 1986):

$$G^{ex} = G - G^{id} \tag{2.78}$$

where G is the total Gibbs energy of the solution at the temperature, pressure, and composition of the real solution, and G^{id} is the Gibbs energy of an ideal solution at the same conditions of temperature, pressure, and composition. The excess Gibbs energy, G^{ex}, is a useful property in fluid phase thermodynamics because the partial molar excess Gibbs energy of any species is directly related to the activity coefficient of the same species.

The partial molar Gibbs free energy of component i, $\bar{g}_i$, is defined as

$$\bar{g}_i = \left(\frac{\partial G}{\partial n_i}\right)_{T,P,n_{j\neq i}} \tag{2.79}$$

Likewise, the partial molar *excess* Gibbs free energy of component i, $\bar{g}_i^{ex}$, is defined as

$$\bar{g}_i^{ex} = \left(\frac{\partial G^{ex}}{\partial n_i}\right)_{T,P,n_j} \tag{2.80}$$

Comparison of equations (2.9) and (2.79) shows that the partial molar Gibbs free energy is also the chemical potential of any component in solution. Using equations (2.78), (2.79) and (2.80), the partial molar excess Gibbs free energy can be related to the partial molar Gibbs free energy by

$$\bar{g}_i^{ex} = \bar{g}_i - \bar{g}_i^{id} \tag{2.81}$$

where $\bar{g}_i^{id}$ is the partial molar Gibbs free energy of species i in an ideal solution. Since the excess Gibbs free energy is a homogeneous function of the first degree in mole numbers, Euler's theorem provides for the following relation:

$$g^{ex} = \sum_i x_i \bar{g}_i^{ex} \tag{2.82}$$

Using equations (2.9), (2.12), (2.13), (2.79), and (2.81) it can be shown that

$$\bar{g}_i^{ex} = \mu_i - \mu_i^{id} = RT \ln \gamma_i \tag{2.83}$$

where μ_i^{id} is given by equation (2.12). Furthermore, combining equation (2.82) and (2.83) yields

$$g^{ex} = RT \sum_i x_i \ln \gamma_i \tag{2.84}$$

Finally, from equations (2.80) and (2.83) it can be shown that

$$RT \ln \gamma_i = \bar{g}_i^{ex} = \left(\frac{\partial n_T g^{ex}}{\partial n_i}\right)_{T,P,n_j} \tag{2.85}$$

Therefore, activity coefficients of all species in a solution can be obtained by differentiating the total Gibbs energy of the solution with respect to the corresponding mole numbers.

For representation of liquid phase equilibrium behavior of fluid phase systems it is advantageous to calculate activity coefficients from an expression for the molar excess Gibbs free energy using equation (2.85). This approach assures that the activity coefficients of all species obey the Gibbs-Duhem equation and are, therefore, thermodynamically consistent. Expressions for the excess Gibbs energy usually contain a number of empirical parameters related to interactions between constituent species in the solution. Activity coefficients obtained by equation (2.85) will contain the same empirical parameters. Often, these parameters can be evaluated from binary system VLE data. Thus, for a multicomponent system, it may be possible to obtain all necessary parameters by analyzing VLE data for the constituent binary systems. Application of excess Gibbs energy models which allow this approach, that of building multicomponent solution parameters from the constituent binary systems, results in a significant reduction in the experimental effort necessary to characterize the thermodynamic behavior of a solution containing a large number of components.

The excess Gibbs energy is normally a strong function of temperature and liquid phase composition and a weak function of pressure. At low to moderate pressures it is common to treat the excess Gibbs energy as independent of pressure. Indeed, most of the common algebraic expressions for the excess Gibbs energy include no pressure dependent terms. In this case, the excess Gibbs energy reflects the excess Gibbs energy at the system reference pressure as do the activity coefficients calculated from it. The pressure dependence of the fugacity of any component is then treated by equations (2.67) or (2.74) and (2.75).

2.8.2 Excess Gibbs Energy of Electrolyte Solutions

It is often assumed that the chemical potential of a molecule or ion in an electrolyte solution can be expressed as the sum of different contributions. Dickerson (1969) adopts this formalism in deriving the Debye-Hückel (1923) limiting law activity coefficient equation for electrolytes. In the simplest formulation, for example, the chemical potential of any component in solution could be expressed as

$$\mu_i = \mu_i^{\text{ideal}} + \mu_i^{\text{nonideal}} \tag{2.86}$$

where μ_i^{ideal} includes the reference state chemical, μ_i^o, plus an entropic contribution due to ideal mixing of the solution components, RT ln x_i, as given by equation (2.12). The value of μ_i^o would depend, of course, on the convention selected for normalizing activity coefficients. The nonideal component of the chemical potential includes contributions from the nonideal effects of mixing, an entropic contribution, as well as a enthalpic contribution resulting from interactions between components of the solution. Equation (2.86) can be viewed as a *definition* of μ_i^{nonideal}. Comparing equation (2.86) with equation (2.83) shows that

$$\mu_i^{\text{nonideal}} = \bar{g}_i^{ex} = RT \ln \gamma_i \tag{2.87}$$

Separation of the chemical potential into distinct contributions can be further extended so that the nonideal contribution can, in turn, be written as the sum of separate contributions related to different types of molecular interactions. For example, it may be assumed that both long-range electrostatic forces between ions and short-range forces between various ionic, polar, and nonpolar neutral species contribute to the chemical potential in such a way that

$$\mu_i = \mu_i^{\text{ideal}} + \mu_i^{\text{lr}} + \mu_i^{\text{sr}} \tag{2.88}$$

where the superscripts lr and sr refer to long-range and short-range contributions to the chemical potential. Comparison of equations (2.83), (2.87), and (2.88) reveals that for the assumed arbitrary splitting of the chemical potential

$$\bar{g}_i^{ex} = \mu_i^{\text{lr}} + \mu_i^{\text{sr}} \tag{2.89}$$

This suggests that the partial molar excess Gibbs energy can also be written as the sum of separate contributions:

$$\bar{g}_i^{ex} = \bar{g}_i^{ex\ lr} + \bar{g}_i^{ex\ sr} \tag{2.90}$$

where $\bar{g}_i^{ex\ lr}$ and $\bar{g}_i^{ex\ sr}$ are *defined* as long-range and short-range contributions to the partial molar excess Gibbs free energy of species i respectively. Using equations (2.82) and (2.90) the molar excess Gibbs energy may be written as

$$g^{ex} = \sum_i x_i\, \bar{g}_i^{ex\ lr} + \sum_i x_i\, \bar{g}_i^{ex\ sr} \tag{2.91}$$

Equation (2.91), in turn, suggests that the molar excess Gibbs energy may be written as the sum of separate contributions. In terms of the formulation presented here for an electrolyte solution, g^{ex} would be expressed as

$$g^{ex} = g^{ex\ lr} + g^{ex\ sr} \tag{2.92}$$

where $g^{ex\ lr}$ and $g^{ex\ sr}$ are long-range and short-range contributions to the molar excess Gibbs free energy respectively. Furthermore, since the partial molar excess Gibbs energy is proportional to the logarithm of the activity coefficient, as expressed by equation (2.83), the logarithm of the activity coefficient can also be expressed as the sum of separate contributions

$$\ln \gamma_i = \ln \gamma_i^{lr} + \ln \gamma_i^{sr} \tag{2.93}$$

where $\ln \gamma_i^{lr}$ and $\ln \gamma_i^{sr}$ are defined as the long-range and short-range contributions to the logarithm of the activity coefficient of species i.

Equations (2.92) and (2.93) have been adopted by a number of researchers in recent years as a starting point for the development of semi-empirical expressions for the excess Gibbs energy and/or activity coefficients of the components of an electrolyte solution. Many such developments are discussed in Chapter Three, so references are omitted from this chapter.

2.8.3 Unsymmetric Excess Gibbs Free Energy

Expressions for the excess Gibbs energy are generally developed with respect to symmetrically normalized activity coefficients. If the ideal dilute state is to be used as the reference state for solutes leading to unsymmetrically normalized activity coefficients, the excess Gibbs energy must also be normalized to reflect the standard states of both solvent and solutes. The unsymmetric molar excess Gibbs energy, $g^{ex\,*}$ (Prausnitz and Chueh, 1968), is defined by

$$\frac{g^{ex\,*}}{RT} = \sum_{\substack{\text{all solvent}\\ \text{components}}} x_i \ln \gamma_i + \sum_{\substack{\text{all solute}\\ \text{components}}} x_i \ln \gamma_i^* \qquad (2.94)$$

If the unsymmetrically normalized activity coefficients are expressed in terms of the respective symmetrically normalized activity coefficients as given by equation (2.26), then $g^{ex\,*}$ can be rewritten as

$$\frac{g^{ex\,*}}{RT} = \sum_{\substack{\text{all solvent}\\ \text{components}}} x_i \ln \gamma_i + \sum_{\substack{\text{all solute}\\ \text{components}}} x_i (\ln \gamma_i - \ln \gamma_i^{\infty}) \qquad (2.95)$$

Using equation (2.84), the unsymmetrically normalized molar excess Gibbs energy can be related to its symmetrically normalized counterpart:

$$\frac{g^{ex\,*}}{RT} = \frac{g^{ex}}{RT} - \sum_{\substack{\text{all solute}\\ \text{components}}} x_i \ln \gamma_i^{\infty} \qquad (2.96)$$

Note that when the activity coefficients are unsymmetrically normalized

$$g^{ex\,*} \rightarrow 0 \text{ as } x_s \rightarrow 1 \qquad (2.97)$$

where s refers to solvents. Equation (2.97) does not hold for solute components.

2.9 Conclusions

At the outset of this chapter, it was stated that its purpose is to introduce the reader to some of the thermodynamic concepts that have been applied in this work to model the vapor-liquid equilibria of the weak electrolyte system - H_2S-CO_2-alkanolamine-H_2O. To that end, it has been written primarily for those who follow in this work or who might wish to apply the results of this work in practice. No attempt has been made to provide a thorough review of the thermodynamic principles of weak electrolyte systems. The chapter simply provides the reader with a brief review of relations between chemical potential, fugacity, activity coefficients, and excess Gibbs energy functions especially as they relate to weak electrolyte systems. As noted earlier, an understanding of these chemical thermodynamic variables and the relationships between them, as well as an understanding of the concept of reference state or standard state in relation to these variables, is essential for research involving chemically reacting, multicomponent, multiphase systems. Chapter Two may be viewed as a reference guide of sorts to be used with Chapters Three and Four which are a review of the literature and summarize the modeling approach and thermodynamic functions adopted in this work respectively.

As alluded to above, this chapter was included to facilitate reproduction of the model in the event that such a task is ever undertaken. Because the mole fraction scale has been adopted for expressing concentrations in this work, it was necessary to convert thermodynamic data based on the molality scale that was taken from the literature to equivalent data based on the mole fraction scale. The equations necessary for making these conversions have been reviewed. In addition, equilibrium constants governing the dissociation of protonated alkanolamines that are reported in the literature are based on different standard states than those adopted here. Hence, it was necessary to adjust the relevant equilibrium constants to the adopted standard states. The equations necessary to convert the equilibrium constants to the adopted standard state have also been reviewed.

Finally, it has been postulated that the chemical potential of any component in solution can be arbitrarily divided into *ideal* and *nonideal* contributions. Furthermore, for an electrolyte solution, the *nonideal* contribution can be arbitrarily divided into separate contributions resulting from long-range electrostatic interactions between ions and short-range van der Waals type interactions between various liquid phase species. It has been shown that this arbitrary division of chemical potential into separate contributions leads to a similar separation of contributions to the molar excess Gibbs energy of an electrolyte solution. This discussion was pursued because such a division of excess Gibbs free energy has been a common practice in recent years. Indeed, the excess Gibbs energy function adopted in this work is based upon such a postulate.

Chapter Three

Modeling VLE of Weak Electrolyte Systems
A Review of the Literature

3.1 Excess Gibbs Free Energy Models for Electrolyte Solutions

Classical thermodynamics provides a framework for calculating the equilibrium distribution of species between a vapor and liquid phase in a closed system through equations (2.8) and through exact relationships relating the chemical potential to accessible thermodynamic state variables. As discussed in Chapter Two for example, thermodynamics provides a method for deriving consistent activity coefficients according to the Gibbs-Duhem equation by appropriate differentiation of the excess Gibbs energy function of a solution. The main difficulty has been to develop a valid excess Gibbs energy function, taking into consideration interactions between all species (molecular and ionic) in the system.

Empirical and semi-empirical excess Gibbs functions have been developed and applied to nonelectrolyte solutions for many years with a high degree of success. Prausnitz et al. (1986) discuss a number of the more popular excess Gibbs energy functions valid for nonelectrolyte systems. However, because of the highly nonideal behavior of electrolyte solutions, it has, until recently, been impractical in engineering applications to either predict, or to represent with an empirical correlation, activity coefficients at electrolyte concentrations typical of industrial applications. The purpose of section 3.1 is to review some of the most important developments in representation of the excess Gibbs energy of an electrolyte solution during this century.

The difficulty in representing the excess Gibbs energy of an electrolyte solution stems from the very long-range interactions between charged species in solution. At a microscopic level, the potential energy of ion-ion interaction varies as the inverse distance between ions. The potential energy of dipole-dipole interactions (typical of nonelectrolyte solutions with polar constituents) varies as the inverse distance to the sixth power (Prausnitz et al., 1986). As a result, well established excess Gibbs energy models for nonelectrolyte systems cannot be applied in a straight forward manner to electrolyte solutions. McQuarrie (1976) shows that this is due to the fact that the coulomb potential is so long ranged that the true many-body problem cannot be decomposed into a series of two-body, three-body, etc., problems as is often done with nonionic solutions.

The first significant advance in calculating activity coefficients in electrolyte solutions was achieved by Debye and Hückel (1923). By considering interionic forces between point charges they developed a *limiting law* for expressing, in a predictive manner, the excess Gibbs energy of a dilute electrolyte solution. Unfortunately, the Debye-Hückel limiting law is valid only to ionic strengths approaching 0.005 mol kg^{-1} (Horvath, 1985). An extended limiting law was also developed by Debye and Hückel by taking the finite sizes of the ions in solution into consideration. The extended Debye-Hückel equation was simplified by Guntelberg (1926), who assumed a common ion radius of approximately 3 Å, to yield the following expression for the excess Gibbs energy of an electrolyte solution:

$$\frac{G^{ex}}{n_w RT} = -\frac{4}{3} A_\gamma \, I^{3/2} \, \tau(I^{1/2}) \tag{3.1}$$

with

$$\tau(x) = (3/x^3) \, [\ln (1+x) - x + (x^2/2)]$$

$$I = \sum_i m_i \, z_i^2$$

where G^{ex} is the excess Gibbs energy for a solution containing n_w kilograms of solvent. A_γ is the Debye-Hückel slope; it is a function of solvent density, solvent dielectric constant, and temperature. I is the ionic strength (mol kg^{-1}), z_i is charge of ionic species i, and m_i is the concentration (mol kg^{-1}) of ionic species i. Both the extended Debye-Hückel and Guntelberg equations provide fair estimates of the mean activity coefficient up to ionic strengths of 0.1 mol kg^{-1} (Horvath, 1985).

The Debye-Hückel equation is based on fundamental equations of electrostatics and thermodynamics. The limiting law and its various extensions have severely limited ranges of applicability because of the simplifying assumptions that were adopted to allow the derivation of analytical expressions for the activity coefficient. The adopted assumptions are realistic only for extremely dilute solutions. Hence, the Debye-Hückel equation yields the correct activity coefficient behavior only for very dilute solutions of electrolytes. Other attempts have been made to develop excess Gibbs energy functions and/or activity coefficient equations based on more realistic assumptions (Gronwall et al., 1929; LaMer et al, 1931; Bjerrum, 1926). Still other researchers have made significant advances in recent years towards representing the equilibrium properties of electrolyte solutions by application of developing *statistical mechanical* methods (see for example Blum, 1975; Triolo et al, 1976; Planche and Renon, 1981; Kondo and Eckert, 1983; Ball et al., 1985a; Cabezas and O'Connell, 1986). However, these developments are difficult, as yet, to apply in engineering practice because of the complexities embodied by the respective approaches and resulting representations.

For engineering applications, the most successful developments in representation of activity coefficients of components in electrolyte solutions have come from semi-empirical methods. The most popular practice in this direction has been to combine the electrostatic theory of Debye-Hückel with modifications or reformulations of well-known equations for nonelectrolyte systems. Implicit in this approach is the assumption that the thermodynamic properties of electrolyte solutions can be written as the sum of two independent contributions, a long-range contribution due to electrostatic or coulombic interactions between ions and a contribution representing various types of short-range interactions between various (true) liquid phase species. This approach also implies that at low electrolyte concentrations, the major contribution to solution nonideality is from long-range electrostatic interactions while short-range interactions between neutral molecules (including undissociated electrolytes) or between ions and neutral molecules contribute most to solution nonideality in concentrated electrolyte solutions (Cruz and Renon, 1978).

Guggenheim (1935) was one of the first to adopt this approach. He proposed a model, based on the combination of an extended Debye-Hückel equation, to account for long-range ion-ion interactions, with a second order virial expansion term, to account for various short-range forces between ions of opposite charge. Guggenheim's equation for the excess Gibbs energy can be expressed as

$$\frac{G^{ex}}{n_w RT} = -\frac{4}{3} A_\gamma I^{3/2} \tau(I^{1/2}) + \sum_c \sum_a B_{ca} m_c m_a \tag{3.2}$$

where m is ionic concentration in mol kg^{-1}, and the subscripts C and A refer to cations and anions respectively. The quantities B_{ca} are constants (at a given temperature), analogous to second virial coefficients; they represent the net effect of various short-range forces between the C cations and A anions (Pitzer, 1973). Guggenheim adopted Brönsted's principal of specific interaction assuming that cations (anions) do not closely approach other cations (anions) so that short-range interactions between ions of like sign are negligible. Guggenheim and Turgeon (1955) determined values of B_{ca} for a large number of electrolytes by regression of experimental data. They showed that equation (3.2) could be used to represent, within experimental error, data for 1-1 electrolytes in water at 0°C and at room temperature at concentrations up to 0.1 mol kg^{-1}.

Scatchard (1939) extended the validity of Guggenheim's equation to higher electrolyte concentrations by recognizing that the binary interaction coefficient, or second virial coefficient, is a weak function of ionic strength. Lietzke and Stoughton (1962) extended Guggenheim's equation by adding third and fourth virial coefficients to the equation. They applied this extended equation to single electrolyte aqueous solutions to salt concentrations as high as 6.0 mol kg^{-1}. Scatchard (1961) and coworkers (1970) further extended Guggenheim's equations in several ways. First, the Debye-Hückel term was subdivided into a series of terms with different coefficients in $I^{1/2}$ corresponding to different distances of closest approach for the solute components. Secondly, the Brönsted principle of specific interaction was abandoned and third and fourth virial coefficients were added. While these equations include enough terms to represent experimental data accurately to high concentrations, they are very complicated and not practical for engineering applications.

Bromley (1972) developed a *predictive* formulation of Guggenheim's equation. He showed that individual values of B could be assigned to ions rather than ion pairs (by arbitrarily specifying the value of B for a reference ion) and that for ion pairs

$$B_{ca} = B_c + B_a \tag{3.3}$$

Bromley then showed that there is a strong correlation between the individual ionic values of B_i and values of $z_i s_i^o$ where z_i is the ionic charge and s_i^o is the value of the standard state entropy of the ion at 298.15°K.

Bromley (1973) also developed a semi-empirical equation, similar to Guggenheim's, for representing the mean activity coefficient of a single electrolyte or mixed electrolytes in water. For a single salt solution, he proposed the following equation for the mean molal activity coefficient:

$$\ln \gamma_{ca} = \frac{-A_\gamma \, |z_c \, z_a| \, I^{1/2}}{1 + I^{1/2}} + \frac{(0.06 + 0.60B)\, |z_c z_a| \, I}{(1 + 1.5\, I / |z_c z_a|)^2} + BI \tag{3.4}$$

This is an empirical extension of the Debye-Hückel equation. Here B again represents an ion-ion binary interaction parameter. Bromley approximated values of B by the method he earlier developed for use with Guggenheim's equation (Bromley, 1972). Bromley used equation (3.4) to represent experimentally measured activity coefficients of 180 strong salts to ionic strengths of 6 mol kg^{-1} with an average maximum error of 5.1%.

Stokes and Robinson (1948, 1973) studied the effects of ionic solvation and hydration in concentrated electrolyte solutions. They developed a hydration-equilibrium model that combined the Debye-Hückel treatment of ion-ion interactions with the idea that the species in solution are hydrated ions. In this treatment, they related the mean ionic activity coefficient to average ionic hydration number and to molar volume. Stokes and Robinson (1972) demonstrated that the model provides good quantitative representation of osmotic coefficients of strong, highly soluble electrolytes up to concentrations of 20 to 30 mol kg^{-1}.

In a series of papers Pitzer (1973; 1977; 1980) proposed an excess Gibbs energy model that is based on a reformulation and extension of Guggenheim's equation. From an improved analysis of the Debye-Hückel model in the context of the *pressure* equation of statistical mechanics (which yields the osmotic pressure of a solution), Pitzer showed that there is a theoretically sound basis for the ionic strength dependence of the short-range forces in binary interactions. In addition, he developed an improved expression for the Debye-Hückel term representing long-range ion-ion interactions. Pitzer made two additional changes to Guggenheim's equation. He included a third order virial term to account for short-range ternary interactions, and he allowed for short-range like-ion interactions. Pitzer's general expression for excess Gibbs energy is

$$\frac{G^{ex}}{RT} = n_w f(I) + \left(\frac{1}{n_w}\right) \sum_i \sum_j \lambda_{ij}(I) n_i n_j + \left(\frac{1}{n_w^2}\right) \sum_i \sum_k \sum_j \mu_{ijk} n_i n_j n_k \tag{3.5}$$

where n_w is the number of kilograms of solvent and n_i, n_j etc., are the numbers of moles of the ionic species i, j, etc. The function f(I) depends only on the ionic strength, I, and represents, in essentially the Debye-Hückel manner, the long-range effects of Coulomb forces. The $\lambda_{ij}(I)$ and μ_{ijk} parameters are the effective second and third order virial coefficients which represent, respectively, the effects of short-range forces between ions considered two and three at a time; these coefficients were treated by Pitzer as adjustable parameters to be fitted on experimental osmotic coefficient or activity coefficient data. The μ_{ijk} are functions of temperature but are independent of ionic strength.

Pitzer's model has proven to be highly successful for representing equilibrium behavior of aqueous strong electrolyte solutions. Pitzer and Mayorga (1973) used this equation to represent experimental data, mostly osmotic coefficients, of 227 strong aqueous electrolytes with one or both ions univalent. They were able to represent experimental data, within experimental error, from dilute solutions to an ionic strength of 6 mol kg^{-1} in many cases. Pitzer and coworkers also successfully used the equation to represent experimental osmotic coefficient and activity coefficient data for aqueous solutions of 2-2 electrolytes (Pitzer and Mayorga, 1974) and mixed electrolyte solutions (Pitzer and Kim, 1974).

Chen et al. (1979) extended the Pitzer equation to represent the thermodynamic properties of weak electrolyte solutions by introducing molecular solute - ion and molecular solute - molecular solute virial interaction terms in a consistent way. This extended Pitzer equation reduces to the original Pitzer equation when no molecular solutes are present. In addition, the new equation was formulated to be consistent with the Setschenow equation for the salting out effect of salts on molecular solutes (Gordon, 1975). Chen and coworkers established the validity of this extended Pitzer equation by successfully representing vapor-liquid equilibrium data for three systems: the hydrochloric acid aqueous solution to concentrations of 18 mol kg^{-1}; the aqueous ammonia-carbon dioxide solution; and the aqueous potassium carbonate-carbon dioxide system to 40 weight percent potassium carbonate.

Cruz and Renon (1978) developed a new function for the excess Gibbs energy of a binary electrolyte solution (single electrolyte in water) by combining the thermodynamic formalisms of both Debye-Hückel theory and nonelectrolyte local composition theory. Like Pitzer, they assumed that the excess Gibbs energy could be written as the sum of separate contributions arising from the long-range ion-ion electrostatic interactions and short-range interactions between ions and molecules:

$$G^{ex} = G^{ex}_{LR} + G^{ex}_{SR} \tag{3.6}$$

For the long-range electrostatic contribution to the excess Gibbs energy they adopted the extended Debye-Hückel equation. To this they added a Born equation type term (Harned and Owen, 1958) to account for the change in free energy associated with the decrease in average dielectric constant of the solution due to increasing electrolyte concentration. For the contribution of short-range interactions to the excess Gibbs energy, Cruz and Renon modified the Nonrandom - Two Liquid (NRTL) equation (Renon and Prausnitz, 1968) that was originally developed to represent excess Gibbs energies of nonelectrolyte liquid mixtures. In this modified NRTL model, Cruz and coworkers made the assumption that cations and anions are completely solvated in solution so that the true local mole fraction of solvent molecules around ions is always unity. Additionally, they assumed that undissociated electrolyte molecules are surrounded by other undissociated electrolyte molecules and solvent molecules. Inserting the long-range and short-range functions adopted by Cruz, equation (3.6) can be rewritten as

$$G^{ex} = G^{ex}_{\text{Debye-Huckel}} + G^{ex}_{\text{Born}} + G^{ex}_{\text{NRTL}} \tag{3.7}$$

This excess Gibbs energy function allows for the computation of the equilibrium properties of both strong and weak electrolyte solutions wherein total or partial dissociation of the electrolyte occurs. The final equations for the excess Gibbs energy are complicated and are, therefore, not reproduced here. Ball et al. (1985) modified the Cruz model to yield equations which had fewer adjustable binary parameters and which could be used to represent thermodynamic properties of mixed electrolyte solutions. They applied the revised model to represent the osmotic coefficients of strong electrolyte solutions up to a maximum concentration of 6 mol kg^{-1}. The average root mean square deviation in osmotic coefficient was less than 0.006 for 27 1-1 salts.

Chen et al. (1982) and Chen and Evans (1986) also proposed an excess Gibbs energy model based on a combination of the Debye-Hückel and local composition formalisms. Chen assumed that the excess Gibbs energy of an electrolyte solution could be written as the sum of contributions from long-range ion-ion electrostatic interactions and from short-range interactions between all true species: ion-ion, ion-molecule, and molecule-molecule. The Pitzer-Debye-Hückel equation (mole-fraction based (Pitzer, 1980)) was adopted to represent the long-range electrostatic interactions. The NRTL equation was reformulated to represent all short-range interactions.

The primary difference between the excess Gibbs energy formulations developed by Cruz and Renon (1978) and by Chen and coworkers is in the different liquid phase models or structures adopted by each. As mentioned previously, Cruz and Renon assumed that all ions in solution are completely solvated so that the local composition of solvent molecules around ions is unity. In a straightforward extension of the original NRTL theory (Renon and Prausnitz, 1968), Chen adopted an electrolyte solution structure consisting of three types of cells. One type consists of a central *neutral* molecule surrounded by other molecules and by anions and cations. To this type of cell Chen applied the assumption of *local electroneutrality*. That is, he assumed that the distribution of cations and anions around a central solvent molecule is such that the net local ionic charge is zero. The other two types of cells have either a cation or an anion at the center. Chen assumed that ions are surrounded by molecules and oppositely charged ions, but not by ions of the same charge type. This assumption, *like-ion repulsion*, implies that the local concentration of cations (anions) around cations (anions) is zero.

Chen and coworkers have applied the 'Electrolyte-NRTL' equation to a wide variety of electrolyte solutions. The excess Gibbs energy function has been used to satisfactorily represent the mean molal activity coefficients of single completely dissociated electrolyte solutions to ionic strengths of 6 mol kg^{-1} or higher (Chen et al., 1982), osmotic coefficients in aqueous solutions of salt mixtures and ionic equilibria in aqueous solutions of weak electrolytes including molecular solutes (Chen and Evans, 1986), and the salt affect on vapor-liquid and liquid-liquid equilibria of mixed solvent electrolyte solutions to the salt saturation point (Mock et al., 1986).

Most recently, Scauflaire et al. (1989), added a term, the Born equation (Harned and Owen, 1958), to the Electrolyte-NRTL excess Gibbs energy function so that it could be used to calculate equilibrium properties of both ionic and nonionic species in aqueous-nonaqueous solvent mixtures. The Born term allows the ideal infinitely dilute aqueous phase to be adopted as the reference state for ionic species in a mixed solvent solution. This choice of reference state is convenient because it is the state for which most thermodynamic data pertaining to electrolyte solutions have been reported in the literature. The Born term accounts for the Gibbs energy of transferring an ion from infinite dilution in the mixed solvent to infinite dilution in water. This contribution arises because of the difference in bulk solution dielectric constants between an aqueous-nonaqueous solvent mixture and pure water. The most recent formulation of the Chen's Electrolyte - NRTL equation given by Scauflaire et al. is represented by the following equation:

$$G^{ex} = G^{ex}_{\text{Debye-Huckel}} + G^{ex}_{\text{Born}} + G^{ex}_{\text{NRTL}} \tag{3.8}$$

It should be noted that the Born terms used by Cruz and Renon (1978) and Scauflaire et al. (1989) are applied in different contexts. Cruz and Renon assumed that the Debye-Hückel coefficient, A_γ, a function of dielectric constant, does not change as a function of ionic strength, although it is well know that the dielectric constant of water decreases as the ionic strength increases (Hasted et al., 1948). The Born equation was used to attenuate the error introduced by the Debye-Hückel contribution due to neglect of the variation of the dielectric constant with ionic concentration. Scauflaire and coworkers included a Born term to allow the thermodynamic properties of mixed solvent solutions to be represented. In Chen's model, the Debye-Hückel coefficient is treated as a function of the mixed solvent dielectric constant, but no account is taken of the decrease in dielectric constant as ionic strength increases. The Born term is included to allow the ionic reference state to be the ideal infinitely dilute state in pure water (rather than mixed solvent). Note also that the model of Cruz and Renon (1978) and the modified version of Ball et al. (1985b) appear to have been developed for calculating thermodynamic properties of systems that are primarily aqueous in nature.

Still another electrolyte excess Gibbs energy model was recently introduced based on the local composition concept. Following Cruz and Renon (1978) and Chen et al. (1982, 1986), Christensen et al. (1983) and Sander et al. (1986) formulated an excess Gibbs energy model for strong, completely dissociated electrolytes in pure and mixed solvents as the sum of separate contributions due to long-range electrostatic interactions and short-range interactions. A Debye-Hückel term was adopted to describe electrostatic interactions and a modified UNIQUAC equation (Abrams and Prausnitz, 1975; Maurer and Prausnitz, 1978) was adopted to describe Short-range ion-ion, ion-molecule, and molecule-molecule interactions. Christensen added a Guggenheim (1935) type term, generalized for mixed solvent systems, to the Debye-Hückel term to improve representation of experimental mean activity coefficient data. This term was apparently not included in the work by Sander et al. (1986) presumably because they were attempting only to represent the salt affect on vapor-liquid equilibria data for mixed solvent solutions. Christensen and coworkers expressed the total excess Gibbs energy as

$$G^{ex} = G^{ex}_{\text{Debye-Huckel}} + G^{ex}_{\text{Guggenheim}} + G^{ex}_{\text{UNIQUAC}} \tag{3.9}$$

In reformulating the UNIQUAC equation for electrolyte solutions, Christensen and coworkers adopted Chen's *like-ion repulsion* assumption, but chose not to adopt the concept of *local electroneutrality*. This formulation results in adjustable energy parameters of the model that are ion-specific unlike the parameters of Chen's Electrolyte-NRTL model or the model of Cruz and Renon. The latter models have ion pair-specific parameters. In addition, the parameters of the extended UNIQUAC equation are concentration dependent. And the UNIQUAC equation requires volumes and surface areas for all components of the solution. For anions, Sander and coworkers (1986) based volume and area parameters on molecular sizes of the respective ions. However, they found that it was necessary to treat cation volume and area parameters as adjustable in order to satisfactorily represent experimental data.

The extension of the UNIQUAC equation was intended primarily to determine the 'salt-effect' of strong, completely dissociated electrolytes on the VLE of pure or mixed solvents. In the original formulation including the Guggenheim term, Christensen et al. (1983) found that mean ionic activities and water activities could be satisfactorily represented in single electrolyte solutions and water activities could be well represented in mixed electrolyte solutions. Without the Guggenheim contribution, Sander and coworkers (1986) found that in applications to alcohol-water/salt mixtures, the model satisfactorily represented changes in vapor phase composition on the addition of a salt to the liquid phase. However, they also reported large deviations in calculated pressures or temperatures, especially at high salt concentrations.

3.2 Vapor-Liquid Equilibria Models for Weak Electrolyte Systems

Because of the difficulty in representing activity coefficients in concentrated electrolyte solutions, early VLE models for weak electrolyte models were based on empirical approaches that did not account for molecular interactions. For example, Van Krevelen et al. (1949) proposed a method for representing H_2S, CO_2, and NH_3 partial pressures over aqueous solutions. In equations governing chemical equilibria they used *apparent* equilibrium constants based on component concentrations rather than activities. They essentially set activity coefficients of all species to unity. In the general case, an *apparent* equilibrium constant approaches its *true* value (ie. the thermodynamic equilibrium constant) at infinite dilution where activity coefficients of all species, solutes and solvent, are taken, by convention, to be unity. *Apparent* equilibrium constants were fitted by Van Krevelen and coworkers on experimental data to functions of ionic strength and temperature. Henry's constants for NH_3, H_2S, and CO_2 were also correlated as functions of ionic strength and temperature. The study was successful in representing the ammonia-rich region but was not useful for the complete range of concentrations. Dankwerts and M^{c}Neil (1967) used this method to calculate vapor and liquid phase compositions in amine-CO_2-H_2O systems.

Kent and Eisenberg (1976) used a similar approach to represent H_2S and CO_2 equilibrium solubility in aqueous solutions of MEA and DEA. They also employed *apparent* equilibrium constants in the equations of chemical equilibria. They used the thermodynamic or infinite dilution values (related to component activities), reported in the literature, as *apparent* equilibrium constants for all reactions in the system except amine protonation and carbamate reversion. For these reactions, equilibrium constants were fitted to functions of temperature (but not ionic strength) on published equilibrium solubility data for the amine-H_2S-H_2O and amine-CO_2-H_2O ternary systems. Lee et al. (1976a,b) found that the acid gas partial pressures calculated by the Kent and Eisenberg method can be in error by as much as 100%.

Atwood et al. (1957) proposed a method for calculating equilibrium partial pressures of H_2S over aqueous alkanolamine solutions using a 'mean ionic' activity coefficient. They employed thermodynamically rigorous equations of chemical equilibria relating equilibrium constants to component activities. However, they assumed the activity coefficients of all ionic species to be equal. This single 'mean ionic' activity coefficient was correlated with ionic strength. This method is essentially equivalent to the apparent equilibrium constant approach of Van Krevelen et al. (1949). Instead of lumping the effects of solution nonideality directly into equilibrium constants they lumped nonideal effects into an empirical parameter which was used to adjust equilibrium constants for the affect of ionic strength.

Klyamer and Kolesnikova (1972) adapted Atwood's approach to represent equilibria in the CO_2-amine-H_2O system. The method was further generalized by Klyamer et al. (1973) to represent equilibria in the H_2S-CO_2-amine-H_2O system If the activity coefficients in the model by Klyamer et al. are set to unity, the model is equivalent to the Kent and Eisenberg approach (Deshmukh and Mather, 1981).

While the use of *apparent* equilibrium constants allows fair representation of experimental acid gas solubility data, it has two significant drawbacks. First, the method cannot be easily extended to solution compositions outside the range over which apparent equilibrium constants have been adjusted. For example, good representation of VLE data for the acid gas - amine - water system would dictate that the *apparent* equilibrium constants be fitted to functions of amine concentration as well as functions of acid gas loading (or ionic strength). Secondly, speciation, or calculation of the equilibrium distribution of liquid phase species, ionic and molecular, requires accurate representation of activity coefficients for use in equations of chemical equilibria. Speciation using *apparent* equilibria equations should be treated as only an approximation to the true liquid phase composition.

The capability to calculate accurate values of all liquid phase species is important for design and simulation based upon rates of mass transfer and chemical reaction (Hermes and Rochelle, 1987; Sivasubramanian, 1985). In the rate modeling approach, true liquid phase concentrations enter into mass transfer and reaction rate expressions.

For example, it is generally assumed that the bulk liquid phase is in a state of chemical equilibrium and that physical equilibria exists at the gas-liquid interface. Indeed, the liquid phase concentrations at the gas-liquid interface and in the bulk solution serve as boundary conditions for equations of mass transfer.

Edwards et al. (1975) developed a molecular thermodynamic framework to calculate equilibrium vapor and liquid phase compositions for dilute aqueous solutions of volatile weak electrolytes (sour water systems) including NH_3, CO_2, H_2S, SO_2, and HCN. They treated chemical equilibria in a thermodynamically rigorous manner by employing component activities rather than concentrations. Activity coefficients were represented with an extended Guggenheim equation (1935) by treating long-range ion-ion interactions and short-range ion-ion, ion-molecular solute, and molecular solute-molecular solute interactions. Molecule-molecule binary parameters of the model were determined by data regression. Ion-ion and molecule-ion binary parameters were approximated using the procedure of Bromley (1972). Because Guggenheim's equation is valid only to ionic strengths of approximately 0.1 molal, the method is limited to weak electrolyte concentrations of less than 1 or 2 molal.

Deshmukh and Mather (1981) used a similar approach to calculate the solubility of H_2S and CO_2 in MEA solutions. They also used Guggenheim's equation to represent activity coefficients. The adjustable binary interaction parameters of the model were fitted on H_2S-MEA-H_2O and CO_2-MEA-H_2O ternary system VLE data. They also adjusted the temperature dependence of two equilibrium constants - carbamate formation and MEA protonation - on experimental data. Two binary interaction terms and the pKa of MEA were adjusted on the H_2S-MEA-H_2O experimental VLE data of Lee et al. (1976b). The carbamate formation equilibrium constant and 4 additional binary interaction terms were adjusted on CO_2-MEA-H_2O VLE data reported Lee et al. (1976a).

While the Guggenheim equation is known accurately represent activity coefficients only to ionic strengths of 0.1 mol/kg, Deshmukh and Mather were able to achieve fair representation of experimental VLE data for the MEA-acid gas-H_2O systems to higher ionic strengths approaching 5 mol kg^{-1} or higher in the temperature range 25 to 120°C. It appears likely that the adjustment of the carbamate formation and MEA protonation equilibrium constants were able to compensate for inadequacies of the activity coefficient equation.

Chakravarty (1985) extended the method of Deshmukh and Mather by fitting, or refitting, adjustable parameters of the Deshmukh and Mather model for the H_2S-amine-H_2O and CO_2-amine-H_2O systems (where amine represents MEA, DEA, MDEA, and DIPA) to the extensive body of acid gas solubility data reported in the literature. Chakravarty further extended the method to systems including two amines - MDEA-MEA and MDEA-DEA. However, at the time there were no experimental acid gas solubility data reported in the literature for these mixed amine systems that could be used to validate the extension for the amine mixtures of interest.

Edwards et al. (1978) extended the range of validity of their sour water model to weak electrolyte concentrations of 10 to 20 molal by adopting Pitzer's equation (1973) to represent activity coefficients. It may be recalled that Pitzer's model is an extension of Guggenheim's equation. Edwards extended Pitzer's model to also account for short-range ion-molecular solute and molecular solute-molecular solute interactions. Pitzer's equation treats both binary and ternary interactions of solute species. However, only binary parameters were used by Edwards and coworkers;

these were determined in a manner similar to that adopted in their earlier work to estimate the parameters of Guggenheim's equation.

Beutier and Renon (1978) also used Pitzer's equation with the thermodynamic framework of Edwards et al. (1975) to calculate VLE in sour water systems. These researchers accepted the binary molecule-molecule interaction parameters determined in the earlier work of Edwards or refit the parameters on binary system data. Molecule-ion parameters were estimated using Debye-McAulay's electrostatic theory (Harned and Owen, 1958). They developed a method, similar to Bromley's (1972), for estimating ion-ion binary interaction parameters. Beutier and Renon included a small number of ternary parameters for those species which they determined to be present at significant concentrations solution. They adjusted these ternary parameters on experimental data. Beutier and Renon reported that their model satisfactorily represents equilibrium partial pressures in the ternary systems H_2S-NH_3-H_2O, CO_2-NH_3-H_2O, and SO_2-NH_3-H_2O between 0 and 100°C to high ionic strengths. However, large deviations from experimental data resulted when the concentration of undissociated NH_3 was high, that is, when the solution could not be treated as a single solvent system.

Chen et al. (1979) correlated vapor-liquid equilibrium data for the CO_2-NH_3-H_2O system at 293.15°K and the K_2CO_3-CO_2-H_2O system of the Hot Potassium Carbonate Process (Kohl and Riesenfeld, 1985) in the temperature range from 343.15°K to 413.15°K. Activity coefficients were represented by their own reformulation of Pitzer's equation. Like Edwards, Chen extended the Pitzer equation to include second order virial coefficients representing molecular solute-ion and molecular solute-molecular solute short-range interactions. Statistically significant parameters in the model were identified by a preliminary order of magnitude analysis and adjusted on vapor-liquid equilibrium data. For the CO_2-NH_3-H_2O system three ion-ion and three molecule-ion binary parameters were adjusted resulting in a good fit of Van Krevelen's (1949) experimental data in the composition range 1 to 2 kmol m^{-3} NH_3, and 0.5 to 2 kmol m^{-3} CO_2 at 293.15°K. Six ion-ion binary parameters were adjusted on the experimental data of Tosh et al. (1959) for the K_2CO_3-CO_2-H_2O system. No molecule-ion interaction parameters were adjusted. The model was found to satisfactorily represent CO_2 equilibrium partial pressures in the composition range 20 to 40 wt% K_2CO_3.

While Pitzer's excess Gibbs energy model (1973) has been shown to be valid to ionic strengths representative of those encountered in industrial practice, it's application is generally limited to aqueous (single solvent) systems. The solute-solute binary interaction parameters are unknown functions of solvent composition. The amine-water system is more properly treated as a mixed solvent system of variable composition. Furthermore, Pitzer's model contains a large number of binary and ternary temperature dependent adjustable parameters. Approximating these parameters with any physical significance is difficult for a system with a large number of liquid phase solute species, ionic and molecular, such as the H_2S-CO_2-amine-H_2O system.

Dingman et al. (1983) developed a VLE model for the H_2S-CO_2-diglycolamine-H_2O system. The framework of the model is equivalent to the framework used by Edwards et al. (1975). Activity coefficients were developed from a combination of NRTL theory (Renon and Prausnitz, 1968), Bromley's correlation (1972), the method of Meissner, Kusik, and Tester (1972), and Born theory. The drawback of this approach is that the resulting activity coefficients are thermodynamically inconsistent according to the Gibbs-Duhem equation.

Chapter Four

A VLE Model for H_2S - CO_2 - Alkanolamine - H_2O Systems

4.1 Thermodynamic Framework

As suggested by the phenominological discussion in Chapter One, and so that it may be used in the context of a rate based model, the thermodynamic framework adopted for the VLE model developed in this work is based on both *chemical reaction/dissociation equilibria* and *vapor-liquid phase equilibria* for molecular species. The purpose of this chapter is to present the framework of the proposed VLE model for the acid gas - alkanolamine - water system in depth. The equations and mathematical algorithms that are used to determine equilibrium distributions of components in the liquid phase and between the liquid phase and the vapor phase are reviewed. In addition, the functions that are used to represent important thermodynamic variables are presented and adjustable parameters of these functions are discussed. Finally, the method that was used to determine the best values of the adjustable parameters is outlined.

4.1.1 Standard States

In this work, both water and alkanolamine are treated as solvents. The standard state associated with each solvent is the pure liquid at the system temperature and pressure. In view of the availability of literature data and the need for a common reference state for ionic species in various mixed solvent electrolyte systems, the standard state for ionic solutes is the ideal, infinitely dilute aqueous solution (infinitely dilute in solutes and alkanolamine) at the system temperature. Finally, in view of the unavailability of Henry's constants in pure alkanolamines, the reference state chosen for molecular solutes (H_2S and CO_2) is also the ideal, infinitely dilute aqueous solution at the system temperature and pressure. This leads to the following unsymmetric convention for normalization of activity coefficients:

$$
\begin{array}{lllll}
\text{solvents:} & \gamma_s \rightarrow 1 & \text{as} & x_s \rightarrow 1 & \\
\text{ionic and molecular solutes:} & \gamma_i^* \rightarrow 1 & \text{as} & x_i \rightarrow 0 & (4.1) \\
 & & & x_{k \neq i} = 0 & \\
 & & & x_{s \neq w} = 0 &
\end{array}
$$

where the subscript s refers to any solvent, i and k refer to ionic or molecular solutes, and w refers to water. This choice of standard states allows the use of equilibrium constants reported in the literature for all relevant reactions while the solution is treated as a solvent mixture. As noted in Chapter Two, activity coefficients are weak functions of pressure, especially when the system pressure is adopted as the reference pressure. Therefore, to simplify the calculational procedure, activity coefficients of all species are taken to be independent of pressure.

This choice of reference states was dictated largely by the standard state options and physical property models available for use with ASPEN PLUS simulation software. As will be discussed in more detail in a later section, ASPEN PLUS was used to determine best values of the adjustable parameters of the model using a nonlinear parameter estimation algorithm.

4.1.2 Chemical Equilibria

Chemical equilibria governs the distribution of an electrolyte in the liquid phase between its free molecular and chemically bound and/or ionic forms. Since it is the undissociated or molecular form of the weak electrolyte that comes to equilibrium with the same component in the vapor phase, chemical equilibria significantly affects phase equilibria and vice-versa.

In aqueous solutions, H_2S and CO_2 react in an acid-base buffer mechanism with alkanolamines. The acid base equilibrium reactions accounted for in this work are written primarily as chemical dissociation:

Water: $2\,H_2O \leftrightarrow H_3O^+ + OH^-$ (4a)

Hydrogen Sulfide: $H_2O + H_2S \leftrightarrow H_3O^+ + HS^-$ (4b)

Hydrogen Bisulfide: $H_2O + HS^- \leftrightarrow H_3O^+ + S^=$ (4c)

Carbon Dioxide: $2\,H_2O + CO_2 \leftrightarrow H_3O^+ + HCO_3^-$ (4d)

Bicarbonate: $H_2O + HCO_3^- \leftrightarrow H_3O^+ + CO_3^=$ (4e)

Protonated Alkanolamine $H_2O + RR'R''NH^+ \leftrightarrow H_3O^+ + RR'R''N$ (4f)

In these equations RR'R"N is the chemical formula for the alkanolamine. R represents an alkyl group, alkanol group, or hydrogen.

In addition to its reaction with amines through an acid-base buffer mechanism, CO_2 may also react directly with many primary and secondary amines to form stable carbamate species as discussed in section 2.6.2. The proposed mechanism for this reaction was also presented in section 2.6.2. In this work the equilibrium reversion of carbamate to bicarbonate is included as an independent reaction rather than the direct formation of carbamate. This reaction results from the proper combination of reactions (2e), (2f), and (2g):

Carbamate reversion to bicarbonate:

$$RNHCOO^- + H_2O \leftrightarrow RNH_2 + HCO_3^- \tag{4g}$$

As noted by Deshmukh and Mather (1981), additional reactions are known to occur that may affect equilibrium. The amines may react with carbon dioxide to form heterocyclic compounds at high temperatures (Kennard and Meisen, 1985). The results of kinetic measurements on these reactions by Kim and Sartori (1984) suggest that these reactions may occur fast enough to affect equilibrium measurements if a carbonated alkanolamine solution under investigation is held at an elevated temperature (exceeding 100°C) for a substantial period of time. These degradation reactions were not included in the equilibrium model because the effect of such degradation in most experimental measurements is likely to be small. Alkanolamines may also react with other acid gases that are present in lesser quantities in the source gas such as carbonyl sulfide and carbon disulfide. These reactions were also not included in the framework of the equilibrium model.

To determine the distribution of H_2S, CO_2, alkanolamine, and water between the corresponding molecular and chemically bound and/or ionic forms, the molar Gibbs free energy of the liquid phase, written in terms of mole numbers, is minimized. The resulting system of equations is ***equivalent*** to the set of equations that results from writing equation (2.42) (which represents the traditional equilibrium constant approach to determining the equilibrium composition of a chemical system) for each reaction represented above together with appropriate atomic mass balance equations. In fact, equilibrium constants are used to determine a consistent set of standard state chemical potentials. The algorithm for determining the equilibrium distribution of species in the liquid phase is described in detail in section 4.2.

4.1.3 Phase Equilibria

Phase equilibria governs the distribution of species between the vapor and liquid phases. In a closed vapor - liquid system containing both electrolytes and nonelectrolytes, the electrolyte species will partially or wholly dissociate in the liquid phase to form ionic species. However, unless the system temperature is very high, vapor phase dissociation of the electrolyte will be negligible. This suggests that, in *practice*, it is necessary to apply the equations governing phase equilibria, equations (2.57) to neutral molecular species only for the purpose of determining the equilibrium distribution of components between the vapor and liquid phases. Accordingly, because ionic species will only be present in the liquid phase for applications of interest in this work, equations (2.57) are neglected for ionic species.

The reference state for molecular solutes (CO_2 and H_2S) is the ideal infinitely dilute aqueous solution at the system pressure and temperature characterized by a Henry's constant. Henry's constants are normally measured and reported at the saturation pressure of the solvent. The effect of pressure on the Henry's constant is given by the following exact relation:

$$\left(\frac{\partial \ln H_{i,s}}{\partial P}\right)_T = \frac{\bar{v}^{\infty}_{i,s}(T,P)}{RT} \qquad (4.2)$$

where $H_{i,s}$ is the Henry's constant for solute i in solvent s and $\bar{v}^{\infty}_{i,s}(T,P)$ is the partial molar volume of solute i at infinite dilution in solvent s. Since the reference state is the ideal infinitely dilute aqueous solution, s in equation (4.2) refers to water. If $\bar{v}^{\infty}_{i,s}$ is taken to be independent of pressure, the Henry's constant for a solute at the system pressure can be related to the Henry's constant at the saturation pressure of the solvent by

$$H^{P}_{i,w} = H^{P^o}_{i,w} \exp \frac{\bar{v}^{\infty}_{i,w}\,(P - P^{o}_{w})}{RT} \qquad (4.3)$$

where $H^{P^o}_{i,w}$ is the Henry's constant of solute i in water at the system temperature and the vapor pressure of water (P^{o}_{w}), $H^{P}_{i,w}$ is the Henry's constant of solute i in water at the system temperature and system pressure (P), and $\bar{v}^{\infty}_{i,w}$ is the partial molar volume of solute i at infinite dilution in water. Using equation (2.58) for the vapor phase fugacity, equation (2.66) for the liquid phase fugacity, and equation (4.3) for the effect of pressure on the Henry's constant, the condition of equilibrium for molecular solutes is expressed as

$$y_i \hat{\varphi}_i P = x_i \gamma_i^* H_{i,w}^{P^o} \exp \frac{\bar{v}_{i,w}^{\infty} (P - P_w^o)}{RT} \tag{4.4}$$

where γ_i^* is the unsymmetrically normalized activity coefficient of the solute. As mentioned above, it is assumed to be independent of pressure.

The reference state for each solvent species, water or alkanolamine, is the pure solvent at the system temperature and pressure. The fugacity of the pure solvent at the system temperature under its own vapor pressure is given by equation (2.63)

$$f_s^{oL}(T) = P_s^o(T) \, \varphi_s^o(T) \tag{2.63}$$

The effect of pressure on the fugacity of the pure solvent is given by

$$\left(\frac{\partial \ln f_s}{\partial P}\right)_T = \frac{v_s(T, P)}{RT} \tag{4.5}$$

where $v_s(T,P)$ is the molar volume of the pure solvent. If v_s is taken to be independent of pressure, the fugacity of the pure solvent at the system temperature and pressure can be expressed as

$$f_s^{oL}(T) = P_s^o(T) \, \varphi_s^o(T) \exp \frac{v_s(T) \, (P - P_s^o)}{RT} \tag{4.6}$$

where v_s is the molar volume of the pure solvent at the system temperature and the saturation pressure of the solvent. Using equation (2.58) for the vapor phase fugacity of each solvent, equation (2.64) for the liquid phase fugacities, and equation (4.6) for the effect of pressure on the pure solvent fugacity, the condition of phase equilibrium for solvent species is expressed by

$$y_s \hat{\varphi}_s P = x_s \gamma_s P_s^o \varphi_s^o \exp \frac{v_s(T)(P - P_s^o)}{RT} \tag{4.7}$$

4.1.4 Equilibrium Constants, Henry's Constants, and Vapor Pressures - Units and Temperature Dependence

In this work, equilibrium constants are expressed on the mole fraction scale; they are dimensionless. Equilibrium constants for reactions (4a) through (4f) are available in the literature, but are based on the molality concentration scale. The temperature dependence of the equilibrium constants is represented in this work by

$$\ln K = C_1 + C_2/T + C_3 \ln T + C_4 T \tag{4.8}$$

Coefficients C_1 through C_4 are summarized in Table 4.1 for all reactions together with literature sources. Note that the coefficients of the first dissociation constant of H_2S, the first and second dissociation constant of CO_2, and the dissociation constants of protonated MEA and DEA differ in coefficient C_1 from the original sources. It was necessary to convert these equilibrium constants from a molality basis to a mole fraction basis in accordance with the procedure outlined in section 2.6.3. It should be noted that an additional correction was applied to equilibrium constants for reaction (4f). In the measurement of the dissociation constants of protonated alkanolamines, the amines are usually treated as solutes with unsymmetrically normalized activity coefficients. Using this reference state the activity coefficient of the alkanolamine goes to unity at infinite dilution. However, the symmetrically normalized activity coefficient of the alkanolamine adopted in this model goes to a value other than unity at infinite dilution in water, unless the alkanolamine and water form an ideal pair. The correction to the equilibrium constant is, therefore, related to the infinite dilution activity coefficient of the amine in water. Infinite dilution activity coefficients for the pertinent alkanolamines in water were estimated in this work from published alkanolamine - water binary VLE data.

Henry's constants are expressed in units of Pascals (Pa). The temperature dependence is given by the same functional form as equation (4.8). Parameters C_1 through C_4 of equation (4.8) for CO_2 and H_2S Henry's constants are presented in Table 4.2 together with literature sources. Pure component vapor pressures are also expressed in units of Pascals and are represented in this work by

$$\ln P^o = D_1 + \frac{D_2}{T + D_3} + D_4 T + D_5 \ln T + D_6 T^{D_7} \tag{4.9}$$

Parameters D_1 through D_7 for water, MEA, DEA, MDEA, and DGA are presented in Table 4.2 together with literature sources.

4.1.5 Partial Molar Volumes of Solute Species

The partial molar volumes of H_2S and CO_2 at infinite dilution in water are estimated by the method of Brelvi and O'Connell (1972). The Brelvi-O'Connell

Table 4.1. Temperature dependence of equilibrium constants for reactions (4a) through (4g).

$$\ln K_x = C_1 + C_2/T + C_3 \ln T + C_4 T$$

Rxn #	Comp	C_1	C_2	C_3	C_4	Temperature Range (°C)	Source
4a	H_2O	132.899	-13445.9	-22.4773	0.0	0 - 225	a
4b	H_2S	214.582	-12995.4	-33.5471	0.0	0 - 150	a
4c	HS^-	-32.0	-3338.0	0.0	0.0	14 - 70	b,c
4d	CO_2	231.465	-12092.10	-36.7816	0.0	0 - 225	a
4e	HCO_3^-	216.049	-12431.70	-35.4819	0.0	0 - 225	a
4f	MEA	2.1211	-8189.38	0.0	-0.007484	0 - 50	d
4f	DEA	-6.7936	-5927.65	0.0	0.0	0 - 50	e
4f	MDEA	-9.4165	-4234.98	0.0	0.0	25 - 60	f
4f	DGA	1.6957	-8431.65	0.0	-0.005037	not reported	g
4g	MEA	2.8898	-3635.09	0.0	0.0	25 - 120	h
4g	DEA	4.5146	-3417.34	0.0	0.0	25 - 120	h
4g	DGA	8.8334	-5274.40	0.0	0.0	25 - 100	h

a - Edwards et al. (1978); b - Giggenbach (1971); c - Meyer et al. (1983); d - Bates and Pinching, (1951); e - Bower et al. (1962); f - Schwabe et al. (1959); g - Dingman et al. (1983); h - fitted on VLE data in this work.

Table 4.2. Temperature dependence of H_2S and CO_2 Henry's constants.

$$\ln H_i^{P0}\,(\mathrm{Pa}) = C_1 + C_2/T + C_3 \ln T + C_4 T$$

Gas	C_1	C_2	C_3	C_4	Temperature Range (°C)	Source
H_2S	358.138	-13236.8	-55.0551	0.059565	0 - 150	a
CO_2	170.7126	-8477.711	-21.9574	0.005781	0 - 100	b

a - Edwards et al. (1978); b - Chen et al., 1979.

method is a semi-empirical corresponding states correlation for the compressibility of a pure liquid and the partial molar volume of a gas at infinite dilution in a liquid. Universal functions relate the compressibility of a liquid to its density and a characteristic reducing volume and the partial molar volume of a gas at infinite dilution in a liquid to characteristic volumes of the solute and solvent and the density of the solvent. The universal functions are simple polynomials whose coefficients were determined by regression of compressiblity data and infinite dilution partial molar volume data. Most characteristic volumes were also found by reduction of compressiblity data. Brelvi and O'Connell found that the partial molar volume, calculated by their expressions, agreed with experimental volumes to within 5 percent for most solute - solvent pairs, and to within 15 percent for all solute-solvent pairs that they examined.

The characteristic volume of the Brelvi-O'Connell correlation for water was taken from the original work of Brelvi and O'Connell and the characteristic volume of CO_2 was fixed at its critical volume. Following Edwards et al. (1978) the characteristic volume for H_2S was set at 90% of its critical volume.

Table 4.3. Temperature dependence of pure component vapor pressures of H_2O, MEA, DEA, MDEA, and DGA.

$$\ln P^o (\mathrm{Pa}) = D_1 + \frac{D_2}{T + D_3} + D_4 T + D_5 \ln T + D_6 T^{D_7}$$

Solv.	D_1	D_2	D_3	D_4	D_5	D_6	D_7	Temp Range (°C)	Source
H_2O	72.55	-7206.7	0.0	0.0	-7.1385	4.0460e-6	2	0 - 374	a
MEA	172.78	-13492.0	0.0	0.0	-21.914	1.3779e-5	2	10 - 365	a
DEA	286.01	-20360.0	0.0	0.0	-40.422	3.2378e-2	1	28 - 269	a
MDEA	26.137	-7588.5	0.0	0.0	0.0	0.0	0	120 - 240	b
DGA	20.86	-3314.6	-140.83	0.0	0.0	0.0	0	not reported	c

a - Daubert and Danner, DIPPR Data Tables (1985); b - DOW Chemical Co. (1987); c - Sheu (1989).

4.1.6 Solvent Molar Volumes: Modified Rackett Equation

The molar volumes of all alkanolamine solvents are estimated by the modified Rackett equation. The molar volume of water is calculated from a polynomial that was fitted to steam table data. The modified Rackett equation is an empirical expression for calculating the saturated liquid density of pure liquids (Spencer and Danner, 1972) or bubble-point densities of mixtures (Spencer and Danner, 1973) as a function of temperature. For a mixture, the modified Rackett equation is

$$\frac{1}{\rho_m} = \left(\frac{RT_{cm}}{P_{cm}}\right) Z_{RAm}^{[1 + (1 - T_{rm})^{2/7}]} \tag{4.10}$$

where ρ_m is the mixed solvent density, T_{cm} and P_{cm} are the critical temperature and pressure of the mixture, T_{rm} is the reduced temperature of the solvent mixture, and Z_{RAm} is an empirical parameter for the mixture that can be fitted on experimental data or can be estimated from the critical compressibilities of the constituent solvents. In the original Rackett equation (Rackett, 1970), Z_{RAi} for each species was taken to be its critical compressibility. The mixing rules adopted by Spencer and Danner for mixture critical constants are as follows:

$$\frac{T_{cm}}{P_{cm}} = \sum_i x_i \frac{T_{ci}}{P_{ci}} \tag{4.11a}$$

$$v_{cm} = \sum_i x_i v_{ci} \tag{4.11b}$$

$$T_{cm} = \frac{1}{v_{cm}^2} \sum_i \sum_j x_i x_j v_{ci} v_{cj} (T_{ci} T_{cj})^{1/2} (1 - k_{ij}) \tag{4.11c}$$

$$z_{RAm} = \sum_i x_i \, z_{RAi} \qquad (4.11d)$$

$$T_{rm} = T / T_{cm} \qquad (4.11e)$$

and

$$k_{ij} = 1.0 - \left[\frac{(v_{ci}^{1/3} \, v_{cj}^{1/3})^{1/2}}{(v_{ci}^{1/3} + v_{cj}^{1/3})/2} \right]^3 \qquad (4.11f)$$

where the expression for k_{ij} was adopted from the work of Chueh and Prausnitz (1967). The molar volume of a pure species is found by substituting pure component parameters in equation (4.10). Critical constants for all relevant molecular species are reported in Table 4.3 together with literature sources.

4.2 Liquid Phase Equilibrium Composition

Molecular electrolytes dissociate and/or react in the liquid phase to produce ionic species. The extent of dissociation is governed by chemical equilibria. It was shown in Chapter Two that the problem of calculating the equilibrium composition is *traditionally* formulated as a set of nonlinear equations of the form

$$K_x = \Pi \, (a_i)^{\upsilon_i} \qquad (2.43)$$

where a_i is the activity (mole fraction based) of species i. Using $\gamma_i \, x_i = a_i$, equation (2.42) was also be expressed as

$$K_x = \Pi \, (\gamma_i \, x_i)^{\upsilon_i} \qquad (2.42)$$

where γ_i is the activity coefficient of species i. Note that the asterisk denoting unsymmetrically normalized activity coefficients has been omitted for generality. One equation of the form (2.42) must be included for each independent reaction that can be written for the system. Therefore, as was shown in section 2.5.1, to solve for the equilibrium composition of a system composed of N species and for which R independent reactions can be written, R nonlinear algebraic equations of the form (2.42) and N minus R linear algebraic equations representing mass balances must be simultaneously solved for N equilibrium values of x_i.

Table 4.4. Pure component properties used in application of Rackett equation and Redlich-Kwong-Soave equation of state.

Comp.	MW	T_c (°K)	P_c (kPa)	V_c (m^3 $kmol^{-1}$)	Z_c	ω	Source
H_2S	34.08	373.2	8936.9	0.0986	0.284	0.100	a
CO_2	44.01	304.2	7376.5	0.0939	0.274	0.225	a
H_2O	18.02	647.3	22090.0	0.0568	0.233	0.344	b
MEA	61.08	638.0	6870.0	0.2250	0.291	0.797	b
DEA	105.14	715.0	3270.0	0.3490	0.192	1.046	b
MDEA	119.16	677.8	3876.1	0.3932	0.192	1.242	c
DGA	105.14	674.6	4354.9	0.327	0.254	1.046	d

a - Reid et al., (1977); b - Daubert and Danner, DIPPR Data Tables (1985); c - Peng (1987) ; d - Texaco Chemical Company.

The traditional equilibrium constant approach to calculating the composition of a chemical system at equilibrium is sometimes classified as a stoichiometric formulation of the equilibrium problem (Smith and Missen, 1982). In such a formulation, the closed-system constraints, the elemental balance equations, are treated by means of stoichiometric equations, leading to an unconstrained minimization (of the Gibbs free energy) problem. Recall that equations (2.42) and (2.43) were developed by application of the necessary conditions for a minimum in the Gibbs free energy.

In practice, equation (2.42) can written for reactions (4a) through (4g). These equations can then be solved, together with a sufficient number of elemental or mole balance constraints, for the equilibrium concentrations of all species in the system. This represents a system of nonlinear algebraic equations implicit in the mole fractions (or mole numbers) of the components of the system. There is at least one equation for each component included in the system. In principle, this system of equations can be solved by one of the methods commonly applied to nonlinear systems (Finlayson, 1980). However, these equations are often difficult to solve because component mole fractions in aqueous electrolyte solutions vary over several orders of magnitude. This can lead to computational problems.

In the (stand-alone) algorithm to be described in section 4.5, equations (2.42) are not used directly to solve for the liquid phase equilibrium composition. Instead, the problem is reformulated in such a way that fewer equations must be solved *simultaneously* to yield the liquid phase equilibrium composition. The approach adopted in this work to solve for the equilibrium composition of the liquid phase was developed by Smith and Missen (1988). It is classified as a *nonstoichiometric* formulation of the equilibrium problem. It is based on constrained minimization of the liquid phase Gibbs free energy and has been found to be both fast and reliable in the applied context. Smith and Missen (1982) show that the stoichiometric and nonstoichiometric formulations of the chemical equilibrium problem are equivalent.

As will be discussed shortly, the model presented in this work was first used within the framework of ASPEN PLUS process simulation software. The Data Regression System of ASPEN PLUS was used to estimate adjustable parameters of the model. ASPEN PLUS employs the traditional equilibrium constant approach to determine the equilibrium composition of the liquid phase. The two methods are equivalent.

4.2.1 Nonstoichiometric Formulation

At a constant temperature and pressure, the most stable state of a system, its equilibrium state, is the state at which the Gibbs free energy is a minimum. The condition of chemical equilibria can be found by minimizing G, at constant temperature and pressure, in terms of N mole numbers and subject to M elemental balance constraints. That is, the equilibrium composition state is the solution to the following optimization problem:

$$\min G(\mathbf{n}) = \sum_{i=1}^{N} n_i \mu_i \tag{4.12}$$

subject to

$$\sum_{i=1}^{N} a_{ki} n_i = b_k \qquad k = 1, 2, ..., M \tag{4.13}$$

where N is the number of components in the system (excluding inerts), M is the number of elements in the system, a_{ki} is the subscript to the kth element in the molecular formula of species i, and b_k is some fixed amount of element k in the system. Equations (4.12) and (4.13) can also be expressed in vector notation as

$$\min G(\mathbf{n}) = \mathbf{n}^T \mu \tag{4.14}$$

subject to

$$\mathbf{A}\,\mathbf{n} = \mathbf{b} \tag{4.15}$$

where $\mathbf{n} \in E^N$, $\mathbf{A} \in E^{MN}$ $(M < N)$, and $\mathbf{b} \in E^M$. That is, **n** is a vector of length N, **A** is an M x N matrix, and **b** is a vector of length M. Normally, R = N - C, where C = rank (A). Usually C is equal to the number of elements, M, in the system.

In the Smith and Missen (1988) algorithm, which is essentially a variation of the RAND algorithm (White et al., 1958), the constrained minimization problem is transformed into an unconstrained minimization problem through the use of multipliers (for a discussion of the method of Lagrange multipliers, see Luenberger, 1984). This is done by formulating the Lagrangian from equations (4.12) and (4.13):

$$L(\mathbf{n}, \lambda) = \sum_{i=1}^{N} n_i \mu_i + \sum_{k=1}^{M} \lambda_k \left(b_k - \sum_{i=1}^{N} a_{ki} n_i \right) \tag{4.16}$$

where λ is a vector of M unknown Lagrange multipliers, $\lambda = (\lambda_1, \lambda_2, \ldots, \lambda)^T$. The necessary conditions for a minimum in $L(\mathbf{n}, \lambda)$ are

$$\left(\frac{\partial L}{\partial n_i}\right)_{n_{j\neq i}, \lambda} = \mu_i - \sum_{k=1}^{M} a_{ki} \lambda_k = 0 \qquad i = 1, 2, \ldots, N \tag{4.17}$$

$$\left(\frac{\partial L}{\partial \lambda_i}\right)_{\mathbf{n}, \lambda_{j\neq i}} = b_k - \sum_{i=1}^{N} a_{ki} n_i = 0 \qquad k = 1, 2, \ldots, M \tag{4.18}$$

Equations (4.17) and (4.18) represent a set of (N + M) nonlinear algebraic equations in (N + M) unknowns ($n_1, n_2, ...n_N, \lambda_1, \lambda_2, ..., \lambda_M$). In theory, once expressions for chemical potentials in terms of mole numbers are introduced into equations (4.17) and (4.18), the system of equations can be solved for the equilibrium composition of the solution by a method for solving nonlinear algebraic equations. However, by application of the Smith and Missen variation of the Rand algorithm, this set of equations is reduced to a smaller set (M) of *linear* algebraic equations which are solved simultaneously for the M Lagrange multipliers only. The Lagrange multipliers are used in an iterative procedure to solve for the mole numbers of all components at equilibrium.

4.2.2 Smith and Missen Algorithm

The Smith-Missen algorithm was developed in terms of ideal solution properties for a multicomponent, single-phase system. It is a simple matter to extend its application to nonideal solutions. The basic algorithm will be outlined here for an ideal solution. Extension of the algorithm for application with nonideal solutions will be shown following the general development.

The system of algebraic equations represented by equations (4.17) and (4.18) are difficult to solve due to the nonlinear dependence of the chemical potential on mole numbers (or equivalently mole fraction, see equation (2.12)). Therefore, White et al. (1958), and subsequently Smith and Missen (1988) adopted an iterative procedure whereby equations (4.17) are linearized (in mole numbers) by expansion in a Taylor series with truncation after the linear term, and used with equation (4.18) to solve for mole numbers. The procedure is repeated until the difference between mole numbers of the constituent components on consecutive iterations is less than a specified convergence criterion.

If the chemical potential is written in dimensionless form, ie., if chemical potential is divided by the thermal energy, RT, then equation (4.17) can be written as

$$\frac{\mu_i}{RT} - \sum_{k=1}^{M} a_{ki}\Psi_k = 0 \qquad i = 1, 2, ..., N \qquad (4.19)$$

where $\Psi_k = \frac{\lambda_k}{RT}$

Linearization of equation (4.19) about an estimate of the equilibrium state solution $(\mathbf{n}^{(m)}, \Psi^{(m)})$ yields, after rearrangement

$$\frac{\mu_i^{(m)}}{RT} - \sum_{k=1}^{M} a_{ki}\Psi_k^{(m)} + \frac{1}{RT}\sum_{j=1}^{N}\left(\frac{\partial\mu_i}{\partial n_j}\right)_{\mathbf{n}}^{(m)} \delta n_j^{(m)} - \sum_{k=1}^{M} a_{ki}\,\delta\Psi_k^{(m)} = 0$$

$$i = 1, 2, \ldots , N \qquad (4.20)$$

with $\delta n_j^{(m)} = n_j - n_j^{(m)}$ and $\delta\Psi_k^{(m)} = \Psi_k - \Psi_k^{(m)}$

where the superscript (m) denotes evaluation at the point $(\mathbf{n}^{(m)}, \Psi^{(m)})$. $\mathbf{n}$ is related to related to the current estimate of $\mathbf{n}^{(m)}$ through the elemental abundance constraints, equations (4.13), by

$$\sum_{j=1}^{N} a_{kj}\,\delta n_j^{(m)} = b_k - b_k^{(m)} \qquad k = 1, 2, ..., M \qquad (4.21)$$

where

$$b_k^{(m)} = \sum_{j=1}^{N} a_{kj}\, n_j^{(m)} \qquad k = 1, 2, ..., M \qquad (4.22)$$

Equations (4.20) and (4.21) are a set of (N + M) linear equations in the unknowns $\delta n_j^{(m)}$ and $\delta \Psi_k^{(m)}$. These linear equations can be solved and new estimates of (**n**, Ψ) can be obtained from

$$\Psi^{(m+1)} = \Psi^{(m)} + \omega^{(m)} \delta\Psi^{(m)} \qquad (4.23)$$

$$\mathbf{n}^{(m+1)} = \mathbf{n}^{(m)} + \omega^{(m)} \delta\mathbf{n}^{(m)} \qquad (4.24)$$

where ω is a step size parameter that varies between zero and one. However, by further algebraic rearrangement, Smith and Missen show that this system of (M + N) linear equations can be reduced to a system of M linear equations in M unknowns by combining equations (4.20) and (4.21) to yield an explicit expression for the variables $\delta\mathbf{n}^{(m)}$. It was shown in Chapter Two, section 2.3.1 that the chemical potential of an ideal solution is defined as

$$\frac{\mu_i}{RT} = \frac{\mu_i^o}{RT} + \ln x_i \qquad (4.25)$$

If x_i is written in terms of mole numbers ($x_i = n_i / n_t$) where n_t represents total moles in the phase including inerts, then

$$\frac{\mu_i}{RT} = \frac{\mu_i^o}{RT} + \ln n_i - \ln n_t \qquad (4.26)$$

The derivative of μ_i with respect to n_j is given by

$$\frac{1}{RT}\frac{\partial}{\partial n_j}(\mu_i) = \frac{\delta_{ij}}{n_j} - \frac{1}{n_t} \tag{4.27}$$

where $\delta_{ij} = 0$ for $i \neq j$ and $\delta_{ij} = 1$ for $i = j$

Combining equations (4.20) and (4.27) yields

$$\frac{\mu_j^{(m)}}{RT} = -\frac{1}{n_j^{(m)}}\delta n_j^{(m)} + \sum_{j=1}^{N}\frac{\delta n_j^{(m)}}{n_t^{(m)}} + \sum_{k=1}^{M} a_{kj}\,\Psi_k \tag{4.28}$$

Rearranging

$$\frac{1}{n_j^{(m)}}\delta n_j^{(m)} = -\frac{\mu_j^{(m)}}{RT} + u + \sum_{k=1}^{M} a_{ki}\,\Psi_k$$

$$j = 1, 2, \ldots, N \tag{4.29}$$

with

$$u = \sum_{j=1}^{N}\frac{\delta n_j^{(m)}}{n_t^{(m)}} = \frac{\delta n_t^{(m)}}{n_t^{(m)}} \tag{4.30}$$

Rearranging equation (4.29) gives

$$\delta n_j^{(m)} = n_j^{(m)}\left[-\frac{\mu_i^{(m)}}{RT} + u + \sum_{k=1}^{M} a_{ki}\,\Psi_k^{(m)}\right]$$

$$j = 1, 2, \ldots, N \tag{4.31}$$

Introducing equation (4.31) into the modified element abundance constraints, equations (4.21), and rearranging yields

$$\sum_{i=1}^{M}\sum_{j=1}^{N}(a_{kj}\,a_{ij}\,n_j^{(m)})\Psi_i + b_k^{(m)}u$$

$$= \frac{1}{RT}\sum_{j=1}^{N} a_{kj}\,n_j^{(m)}\,\mu_j^{(m)} + (\,b_k - b_k^{(m)}\,)$$

$$k = 1, 2, ..., M \qquad (4.32)$$

Using equation (4.30), equations (4.31) can be summed over j, the number of components excluding inerts, to yield

$$\sum_{i=1}^{M} b_i^{(m)}\Psi_i - n_z u = \sum_{k=1}^{N} n_k^{(m)}\frac{\mu_k^{(m)}}{RT} \qquad (4.31b)$$

where n_z is the number of moles of inert components. Equation (4.32) together with equation (4.31b) represents a system of (M+1) equations in (M + 1) unknowns, the M Lagrange multipliers, Ψ_i, and u. During each iteration of the RAND algorithm (White et al., 1958), equations (4.32) and (4.31b) are solved for all M values of Ψ_i and u. $\delta\mathbf{n}$ is then calculated from equation (4.31) and a new estimate of the mole number vector is calculated using equation (4.24). A suitable value of the step size parameters, $\omega^{(m)}$, can be determined by a line search for a minimum in G(**n**). In this work $\omega^{(m)}$ is fixed at unity. The Smith and Missen variation of the RAND algorithm, applied in this work, results by dropping u from the calculation (ie. setting u to zero) leading to a system of M equations (1 fewer) in M unknowns - Ψ_i. Smith and Missen (1988) prove that this procedure still leads to a descent algorithm. Iterations are repeated until the the single phase composition does not change significantly on consecutive iterations. In this work, iterations are repeated until the following convergence criterion is met:

$$\max_{\text{all species, } i} \left| \delta n_i^{(m)} / n_i^{(m)} \right| \leq \varepsilon$$

ε is an input variable that takes on a value determined by the user.

4.2.3 Nonstoichiometric Algorithm for Nonideal Solutions

The nonstoichiometric algorithms presented in Section 4.2.2 were developed for ideal solutions for which the chemical potential of each species is expressed as

$$\mu_i = \mu_i^o + RT \ln x_i \tag{2.12}$$

Thus, the chemical potential of a component of an ideal solution depends in a simple way on its own mole fraction. The ideal solution assumption made it possible to express $\partial\mu_i/\partial n_j$ analytically, which, in turn, was instrumental in the construction of the RAND algorithm and the Smith and Missen variation. In Chapter Two, section 2.3.1, the chemical potential for a nonideal solution was expressed as

$$\mu_i = \mu_i^o + RT \ln x_i + RT \ln \gamma_i \tag{4.33}$$

Equation (4.33) is a definition of the activity coefficient, γ, which is seen as a correction to the ideal solution chemical potential for the effects of nonideal solution behavior. In general, γ_i, is a complex function of solution composition. Therefore, for a real solution, μ_i is also a complex function of solution composition and a *simple* analytical expression for $\partial\mu_i/\partial n_i$ is not, in general, possible.

In order to utilize algorithms for real solutions that were developed for the ideal solution, Smith and Missen (1982) suggest an indirect approach. Equation (4.33) is rewritten by combining the standard state chemical potential with the activity coefficient term so that

$$\mu_i = \mu_i^o(T, P, \mathbf{n}) + RT \ln x_i \tag{4.34}$$

where

$$\mu_i^o(T, P, \mathbf{n}) = \mu_i^o(T, P) + RT \ln \gamma_i(T, P, \mathbf{n}) \tag{4.35}$$

Equation (4.34) is employed in the algorithm in place of the equation (4.25) for the chemical potential of component i. The calculation procedure is iterative. On the first iteration the equilibrium composition is calculated assuming that all γ_i are unity and $\mu_i^o(T, P, \mathbf{n}) = \mu_i^o(T, P)$. Using the composition of the system on the first iteration, activity coefficients are calculated for all species using the adopted excess Gibbs energy function. On the next iteration, a new value of $\mu_i^o(T, P, \mathbf{n})$ is computed by equation (4.35) such that

$$\mu_i^{o(1)} = \mu_i^o + RT \ln \gamma(T, P, \mathbf{n}^{(1)}) \tag{4.36}$$

Note that in applying the algorithm developed for an ideal system, $\mu_i^{o(m)}$ is not treated as function of composition. That is, $\partial\mu_i^{o(m)}/\partial n_j$ is assumed to be zero. The procedure is repeated until the composition does not change significantly on consecutive iterations. Equation (4.36) becomes

$$\mu_i^{o(m+1)} = \mu_i^o + RT \ln \gamma(T, P, \mathbf{n}^{(m)}) \tag{4.37}$$

4.2.4 Standard State Chemical Potentials from Equilibrium Constants

The Smith and Missen algorithm adopted in this work for calculating the equilibrium composition of the system utilizes standard state chemical potentials, μ_i^o, for all species participating in the independent set of chemical reactions. However, for several of the components of the system H_2S - CO_2 - amine - H_2O, standard state chemical potentials are not available in the literature. Fortunately, equilibrium constants for all participating reactions (reactions 4a - 4g) are available. Equilibrium constants for reactions (4a) through (4f) were taken from the literature and the equilibrium constant for reaction (4g), reversion of carbamate to bicarbonate, for MEA, DEA, and DGA were determined by data regression in this work. Equation (2.41) provides a connection between standard state chemical potentials for the components participating in a reaction and the equilibrium constant for that reaction:

$$RT \ln K_x = - \sum_{i=1}^{N} \upsilon_i \mu_i^o = \Delta G_T^o \tag{4.38}$$

The problem is to determine a suitable vector μ^o from K_x. Consideration of equation (2.42) suggests that any vector μ^o which yields the correct value of K_x through equation (2.41) will give rise to the correct equilibrium composition of the system. Therefore, any vector μ^o which satisfies equation (2.41) can be used to determine the equilibrium composition of the system by the nonstoichiometric algorithm (because the nonstoichiometric formulation is equivalent to the traditional equilibrium constant approach represented by equation 2.42). Such a vector, μ^o, is said to be consistent with the equilibrium constant K_x.

For a system consisting of N species and for which R independent chemical reactions can be written, the problem is to find μ^o that satisfies

$$RT \ln K_{x_j} = - \sum_{i=1}^{N} \upsilon_{ij} \mu_i^o \qquad j = 1, 2, ..., R \tag{4.39}$$

Equation (4.39) represents a system of R equations in N unknowns. Since N is generally greater than R, there are an infinite number of vectors μ^o that are consistent with the j values of K_x. One such vector results from setting N minus R values of μ_i^o to zero and using equations (4.39) to solve for the remaining R values. In vector notation, this can be written as

$$\binom{\mathbf{N}^T}{\mathbf{I}} \mu^o = -RT \binom{\mathbf{K}'}{\mathbf{0}} \tag{4.40}$$

where μ^o is a N x 1 column vector, **N** is a N x R matrix with elements υ_{ij}, **I** is a (N-R) x N identity matrix, $\mathbf{K}'$, is an R x 1 column vector composed of the elements ln K_{x_j}, and **0** is an (N-R) x 1 zero vector. This method has been adopted in this work for determining a consistent set of μ_i^o.

4.3 Thermodynamic Functions

4.3.1 Vapor Phase Fugacity Coefficient: The Redlich - Kwong - Soave Equation of State

Soave's (1972) modification of the Redlich-Kwong (Redlich-Kwong, 1949) equation of state (EOS) is used to represent the equilibrium behavior of the vapor phase. Fugacity coefficients for all species in the vapor phase are calculated from the Redlich-Kwong-Soave (RKS) using equation (2.60).

The original Redlich-Kwong EOS in pressure explicit form is

$$P = \frac{RT}{v-b} - \frac{a}{T^{0.5} v (v + b)} \tag{4.41}$$

where a and b are parameters that reflect the strength of attraction between molecules and the size of the molecules respectively. Values of the parameters a and b can be determined by forcing the Redlich-Kwong EOS to satisfy the condition of criticality:

$$\left(\frac{\partial P}{\partial v}\right)_T = \left(\frac{\partial^2 P}{\partial v^2}\right)_T = 0 \tag{4.42}$$

Application of the criticality conditions yields the following equations for a and b in terms of the critical properties:

$$a = 0.427480 \frac{R^2 T_c^2}{P_c} \tag{4.43}$$

$$b = 0.086640 \frac{R\,T_c}{P_c} \tag{4.44}$$

Soave (1972) modified the Redlich-Kwong equation by replacing the temperature-dependent term $\frac{a}{T^{0.5}}$ by a function $a(T, \omega)$ involving temperature and the acentric factor. In pressure explicit form, Soave's modified Redlich-Kwong (referred to hereafter as the Redlich-Kwong-Soave or RKS) equation of state is

$$P = \frac{RT}{v-b} - \frac{a(T,\omega)}{v (v + b)} \tag{4.45}$$

where

$$a(T, \omega) = a\,\alpha(T, \omega)$$

The parameters a and b assume the same values in the RKS equation as they do in the Redlich - Kwong equation. The function $\alpha(T, \omega)$ was formulated to make the EOS fit pure fluid vapor pressure data, with the following result:

$$\alpha(T, \omega) = [1 + f_\omega(1 - T_r^{0.5})]^2 \tag{4.46}$$

where T_r is the reduced temperature and f_ω is a quadratic equation in the acentric factor, ω. The parameters in this equation were determined empirically by Soave. The parameter values were improved by Graboski and Daubert (1978a,b) using a large data set:

$$f_\omega = 0.48508 + 1.55171\omega - 0.15613\omega^2 \tag{4.47}$$

Using this function, the RKS equation of state predicts the vapor pressure of nonpolar and slightly polar fluids with a high degree of accuracy.

Mixing rules must be adopted to determine the parameters a_m and b_m for the gas mixtures. In this work, the original combining rules applied by Redlich and Kwong (1949) were adopted:

$$a_m = \sum_i \sum_j x_i x_j (a_i \alpha_i a_j \alpha_j)^{0.5} \tag{4.48}$$

$$b_m = \sum_i x_i b_i \tag{4.49}$$

By proper rearrangement, the RKS equation of state can also be written as a cubic equation in volume:

$$v^3 - \frac{RT}{P} v^2 + \frac{1}{P}(a\alpha - bRT - Pb^2)\, v - \frac{a\alpha\, b}{P} = 0 \tag{4.50}$$

As discussed in Chapter Two, section 2.7.1, the fugacity coefficient of any component in a gas mixture can be computed from an equation of state using mixing rules for the equation of state parameters and the definition of the partial molar volume through application of equation (2.60):

$$\ln \hat{\varphi}_i = \frac{-1}{RT} \int_0^P \left(\frac{RT}{P} - \bar{v}_i \right) dP \qquad (2.60)$$

The partial molar volume, $\bar{v}_i$, of any molecular component is calculated from equation (4.50) and the mixing rules, equations (4.48) and (4.49). From equations (2.60), (4.48), (4.49), and (4.50) the fugacity coefficient based on the RKS equation of state is

$$\ln \hat{\varphi}_i = \frac{b_i}{b_m}(z-1) - \ln\left[z\left(1 - \frac{b_m}{v}\right)\right] + \frac{(a\alpha)_m}{b_m RT}\left[\frac{b_i}{b_m} - \frac{2}{(a\alpha)_m}\sum_j y_j (a\alpha)_{ij}\right] \ln\left(1 + \frac{b_m}{v}\right) \qquad (4.51)$$

where

$$z = PV/RT$$

$$(a\alpha)_{ij} = \left[(a_i\alpha_i)(a_j\alpha_j) \right]^{1/2}$$

$$(a\alpha)_m = \sum_i \sum_j y_i y_j (a\alpha)_{ij}$$

$$b_m = \sum_i y_i b_i$$

In order to calculate $\hat{\varphi}_i$ it is first necessary to calculate v of the mixture. In this work, this is accomplished by solving for the vapor phase root of equation (4.50) using a Newton-Raphson procedure. The initial guess of the vapor phase root is obtained by solving for v^{ideal} from the ideal gas law. Equation (4.51) is then used to calculate the fugacity coefficient of all components in the vapor phase.

4.3.2 Liquid Phase Activity Coefficient: Electrolyte - NRTL Equation

The Electrolyte - NRTL equation (Chen and Evans, 1986), modified for mixed solvent electrolyte solutions (Scauflaire et al., 1989) is used to represent liquid phase activity coefficients. This is a generalized excess Gibbs energy model that accounts for molecular/ionic interactions between all true liquid phase species. The basic postulate of the model is that the excess Gibbs energy of a mixed solvent electrolyte system can be written as the sum of two contributions, one related to the local or short-range (van der Waals type) interactions that exist in the immediate neighborhood of any component (ion or neutral molecule), and the other related to the long-range (LR) ion-ion interactions that exist beyond the immediate neighborhood of a central ionic species:

$$g^{ex*} = g^{ex*}_{LR} + g^{ex*}_{local} \qquad (4.52)$$

For the long-range ion-ion interaction contribution Chen and Evans adopted Pitzer's reformulation of the Debye-Hückel equation (Pitzer, 1980):

$$g^{ex*}_{PDH} = -RT\,(\sum_{k} x_k)\,(1000/M_m)^{1/2}\,(4\,A_\phi\,I_x/\rho)\,\ln\,(1 + \rho\,I_x^{1/2}) \qquad (4.53)$$

where A_ϕ is a function of the mixed solvent dielectric constant and mixed solvent density. M_m is the mole fraction averaged mixed solvent molecular weight (ie., average molecular weight of water plus nonaqueous solvents). Since A_ϕ is a function of mixed solvent properties, the reference state for ionic solutes implied by equation (4.53) is the ideal infinitely dilute state of the solute in the mixed solvent. However, because much of the reported thermodynamic data pertains to electrolytes (including equilibrium constants for the dissociation of weak electrolytes) in water, Scauflaire et al. (1989) adopted the ideal infinitely dilute state in water as the standard state for ionic species. Therefore, the standard state chosen for ionic species in this work, discussed in section 4.1.1, is consistent with the standard state adopted for ions within the framework of the Electrolyte-NRTL equation.

To make the Pitzer-Debye-Hückel contribution consistent with the adopted reference state for ions (the infinitely dilute aqueous solution), Scauflaire and coworkers included an additional term in the long range contribution to the excess Gibbs energy. That is, the Born equation (Harned and Owen, 1958) was introduced into the long-range contribution to account for the excess Gibbs energy of transferring an ion at infinite dilution in the mixed solvent to infinite dilution in the aqueous phase. The Born equation is

$$\ln \gamma^{\infty}_{i\ \mathrm{BORN}} = -\left(\frac{e^2}{2kT}\right)\left(\frac{z_i^2}{r_i}\right)\left(\frac{1}{D_m} - \frac{1}{D_w}\right) \tag{4.54}$$

In equation (4.54) D_m represents the dielectric constant of the mixed solvent and D_w represents the dielectric constant of pure water, e is the electronic charge, z_i is the valence of ionic species i, and r_i is the radius of ionic species i. The Born equation presented above is derived from consideration of the work required to transfer an ion from a solvent of dielectric constant D_m to dielectric constant D_w at extreme dilution (Harned and Owen, 1958).

As noted in section 4.1.1, the reference state for molecular solutes is also the ideal, infinitely dilute aqueous solution. The contribution of the Pitzer-Debye-Hückel term to the activity coefficients of molecular solutes is assumed to be the same as that for solvents. Furthermore, it is assumed that no contribution to the excess free energy is required to transfer (neutral) molecular solutes at infinite dilution from the mixed solvent to infinite dilution in the aqueous phase. That is, there is no contribution to the excess Gibbs energy for neutral solutes analogous to equation (4.54).

Applying equation (2.96) in principle, the long-range contribution to the excess Gibbs energy is expressed as

$$g_{LR}^{ex*} = g_{PDH}^{ex*} - RT \sum_i x_i \ln \gamma_{i\,BORN}^{\infty} \tag{4.55}$$

Therefore, the Born contribution to the excess Gibbs energy, equation (4.52), is

$$g_{BORN}^{ex} = RT \left(\frac{e^2}{2kT}\right) \left(\sum_i \frac{x_i z_i^2}{r_i}\right) \left(\frac{1}{D_m} - \frac{1}{D_w}\right) \tag{4.56}$$

The local interaction contribution to the excess Gibbs energy was derived from the local composition concept of the nonrandom two-liquid (NRTL) hypothesis (Renon and Prausnitz, 1968). In a straightforward extension of the original NRTL theory, Chen adopted an electrolyte solution structure consisting of three types of cells. One type consists of a central neutral molecule surrounded by other molecules and by anions and cations. To this type of cell he applied the assumption of *local electroneutrality*. That is, he assumed that the distribution of cations and anions around a central solvent molecule is such that the net local ionic charge is zero. The other two types of cells, Chen postulated, have either a cation or an anion at the center and are surrounded by molecules and oppositely charged ions, but not by ions of the same charge type. This assumption, *like-ion repulsion*, implies that the local concentration of cations (anions) around cations (anions) is zero. The NRTL contribution to the excess Gibbs energy is expressed as

$$\frac{g^{ex}_{NRTL}}{RT} = \sum_m X_m \frac{\sum_j X_j G_{jm} \tau_{jm}}{\sum_k X_k G_{km}}$$

$$+ \sum_c X_c \sum_{a'} \frac{X_{a'} \sum_j G_{jc.a'c} \tau_{jc.a'c}}{\sum_{a''} X_{a''} \sum_k X_k G_{kc.a'c}}$$

$$+ \sum_a X_a \sum_{c'} \frac{X_{c'} \sum_j G_{ja.c'a} \tau_{ja.ca}}{\sum_{c''} X_{c''} \sum_k X_k G_{ka.c'a}} \qquad (4.57)$$

with

$$G_{cm} = \frac{\Sigma_a X_a G_{ca.m}}{\Sigma_{a'} X_{a'}} \qquad G_{am} = \frac{\Sigma_c X_c G_{ca.m}}{\Sigma_c X_{c'}}$$

$$\alpha_{cm} = \frac{\Sigma_a X_a \alpha_{ca.m}}{\Sigma_{a'} X_{a'}} \qquad \alpha_{am} = \frac{\Sigma_c X_c \alpha_{ca.m}}{\Sigma_c X_{c'}}$$

where $X_j = x_j C_j$ ($C_j = Z_j$ for ions and C_j = unity for molecules)

α = nonrandomness parameter

τ = binary energy interaction parameter

and

$$G_{jc,a'c} = \exp(-\alpha_{jc,a'c} \tau_{jc,a'c}) \qquad G_{ja,c'a} = \exp(-\alpha_{ja,c'a} \tau_{ja,c'a})$$

$$G_{im} = \exp(-\alpha_{im} \tau_{im}) \qquad G_{ca,m} = \exp(-\alpha_{ca,m} \tau_{ca,m})$$

$$\tau_{ma,ca} = \tau_{am} - \tau_{ca,m} + \tau_{m,ca} \qquad \tau_{mc,ac} = \tau_{cm} - \tau_{ca,m} + \tau_{m,ca}$$

Equation (4.57) reduces to the NRTL equation (Renon and Prausnitz, 1968) when no ionic species are present in the solution. Therefore, binary parameters for nonionic pairs can be obtained from analysis of the corresponding nonelectrolyte mixtures.

Note that g^{ex}_{NRTL} must be normalized to the desired reference states, expressed by equations (4.1), using equation (2.96) and infinite dilution activity coefficients of molecular solutes, cations, and anions. Infinite dilution activity coefficients can be obtained from equation (4.57) by application of equation (2.85) to obtain activity coefficient expressions and subsequently calculating activity coefficients at the proper concentration limits. For the ideal infinitely dilute aqueous reference state, infinite dilution activity coefficients are given by

$$\ln \gamma^{\infty}_{m} = \tau_{wm} + G_{mw} \tau_{mw} \tag{4.58}$$

$$\ln \gamma^{\infty}_{c} = Z_c \left\{ G_{cw} \tau_{cw} + \frac{\sum_{a'} x_{a'} \tau_{wc.a'c}}{\sum_{a''} x_{a''}} \right\} \tag{4.59}$$

$$\ln \gamma^{\infty}_{a} = Z_a \left\{ G_{aw} \tau_{aw} + \frac{\sum_{c'} x_{c'} \tau_{wa.c'a}}{\sum_{c''} x_{c''}} \right\} \tag{4.60}$$

In equations (4.57), (4.58), (4.59), and (4.60), the subscripts m, c, and a refer to molecular solute, cation, and anion respectively. The subscript w refers to water. By equation (2.96), the NRTL contribution to the unsymmetric excess Gibbs free energy becomes

$$g^{ex*}_{NRTL} = g^{ex}_{NRTL} - RT \sum_{m \neq w} x_m \ln \gamma^{\infty}_{m} - RT \sum_{c} x_c \ln \gamma^{\infty}_{c} - RT \sum_{a} x_a \ln \gamma^{\infty}_{a} \tag{4.61}$$

The sum of equations (4.53), (4.56), and (4.61) constitute the Electrolyte-NRTL equation for mixed solvent electrolyte systems:

$$g^{ex*} = \{ g^{ex*}_{PDH} + g^{ex}_{BORN} \} + g^{ex*}_{NRTL} \tag{4.62}$$

The activity coefficient for any species, ionic or molecular, solute or solvent, is derived from the partial derivative of the excess Gibbs energy with respect to mole number:

$$\ln \gamma_i = \left[\frac{\partial(n_t \cdot g^{ex*}/RT)}{\partial n_i}\right]_{T,P,n_{j\neq i}} \tag{2.79}$$

Activity coefficients derived by the use of equation (2.79) are presented in Appendix A. Note that although the Born term in equation (4.62) is a function of the solvent composition, Scauflaire and coworkers keep it constant when differentiating with respect to solvent mole number. This, they imply, follows from the fact that the symmetric solvent activity coefficients should not be affected by the reference state chosen for the ionic solutes. The Born term is a used to adjust the Pitzer-Debye-Hückel contribution to the adopted reference state for ions only. However, it is not clear that the resulting activity coefficients obey the Gibbs-Duhem equation.

Note that equation (4.58) was used to estimate alkanolamine activity coefficients at infinite dilution in water. These infinite dilution activity coefficients were then used to modify published equilibrium constants for the dissociation of protonated amines (ie. the K_a's of the alkanolamines) so that the reference state of an amine was taken to be the state of the pure liquid at the system temperature as discussed in section 4.1.4 and expressed by equation (2.56).

4.3.3 Debye-Hückel Coefficient

As applied in the framework of the Electrolyte-NRTL equation, the Debye-Hückel coefficient, A_ϕ, is a function of solvent density and solvent dielectric constant:

$$A_\phi = \left(\frac{1}{3}\right)\left(\frac{2\,\pi\,N_o\,d_m}{1000}\right)^{1/2}\left(\frac{e^2}{D_m\,k\,T}\right)^{3/2} \tag{4.63}$$

Here d_m and D_m are the mixed solvent density and mixed solvent dielectric constant respectively. N_o is Avogadro's number, e is the charge of an electron, and k is Boltzmann's constant. Scauflaire et al. (1989) adopted the following approximation for the mixed solvent density of an aqueous - nonaqueous mixture:

$$\frac{1}{d_m} = x^{sf}_{H_2O}\,v_{H_2O} + x^{sf}_{nonaq}\,v_{nonaq} \tag{4.64}$$

In this work, v_{H_2O} is taken to be the molar volume of saturated water interpolated using a polynomial fitted on steam table data. v_{nonaq} is the saturation molar volume of the nonaqueous solvent fraction (alkanolamine or mixture of amines in this work) estimated by the modified Rackett equation (Spencer and Danner, 1973). $x^{sf}_{H_2O}$ and x^{sf}_{nonaq} are the solute-free mole fractions of water and total nonaqueous solvent respectively.

Note that while A_ϕ is a function of solvent composition, Scauflaire et al. (1989) do not differentiate it with respect to solvent mole number in deriving activity coefficients from equation (4.53) or equation (4.62). They assume that the contribution to the natural logarithm of the activity coefficient that results from differentiating A_ϕ is negligibly small.

4.3.4 Mixed Solvent Dielectric Constant

Scauflaire and coworkers adopted a simple linear mass fraction average mixing rule to calculate the mixed solvent dielectric constant:

$$D_m = \sum_i x_{m_i}^{sf} D_i \tag{4.65}$$

In equation (4.65), $x_{m_i}^{sf}$ is the solute-free mass fraction of solvent i, and D_i is the dielectric constant of solvent i. The dielectric constant of saturated water is calculated using the empirical correlation of Helgeson and Kirkham (1974). Dielectric constants for MEA and DEA were taken from Ikada et al. (1968). The dielectric constant of purified MDEA was measured in this work over the temperature range from 25 to 50°C at atmospheric pressure using the experimental technique described by Middleton* (1988). Measured values of the dielectric constant for MDEA are reported in Table 4.5. Values of A and B for all alkanolamines are reported in Table 4 6. The dielectric constant of DGA was set equal to the value adopted for DEA. For all alkanolamines, the dielectric constant was fitted to the following function of temperature:

$$D_i = A + B\left[\frac{1}{T} - \frac{1}{273.15}\right] \tag{4.66}$$

---

* M. Middleton kindly made these measurements for the author.

Table 4.5. Dielectric Constant of pure MDEA at 1 atmosphere total pressure.

Temperature (°C) (±0.1)	Dielectric Constant (±0.2)
25.0	22.0
35.1	21.0
49.6	19.7

Table 4.6. Dielectric constants for pure MEA, DEA, and MDEA as a function of temperature by equation (4.66).

Amine	Dielectric constant by equation (4.66)
MEA:	$D = 36.76 + 14836\ [1/T - 1/273.15]$
DEA:	$D = 28.01 + 9277.0\ [1/T - 1/273.15]$
MDEA:	$D = 24.74 + 8989.3\ [1/T - 1/273.15]$
DGA*:	$D = 28.01 + 9277.0\ [1/T - 1/273.15]$

* Dielectric constant of DGA fixed at same value as DEA.

4.3.5 Parameters of the Electrolyte - NRTL Equation

The parameters required by the Electrolyte-NRTL equation for the H_2S-CO_2-alkanolamine-H_2O system include the distance of closest approach, ρ, in the Pitzer-Debye-Hückel term, and pure component dielectric constants, D, and ionic radii, r, in the Born term. The parameters of the NRTL term are the nonrandomness factors, α_{ij}, and the binary interaction energy parameters, τ_{ij}. In this work, the distance of closest approach term was fixed at 14.9 as suggested by Pitzer (1980). Ionic radii were assigned default values of 3 angstroms. Following Chen and Evans (1986), the nonrandomness factor was fixed at 0.2 for molecule-molecule interactions ($\alpha_{mm'}$) and for water-ion pair interactions ($\alpha_{w,ca}$ or $\alpha_{ca,w}$). Nonrandomness factors for alkanolamine-ion pair and acid gas-ion pair interactions were fixed at a value of 0.1 as suggested by the results of Mock et al. (1986) for nonaqueous solutions of electrolytes.

Therefore, the only adjustable parameters of the Electrolyte-NRTL model are the short-range binary interaction parameters ($\tau_{mm'}$, $\tau_{m'm}$, $\tau_{ca,m}$, $\tau_{m,ca}$, $\tau_{ca,ca'}$, $\tau_{ca',ca}$, $\tau_{ca,c'a}$, $\tau_{c'a,ca}$) representing energies of interaction between liquid phase species. These are characteristic of pair interactions of components of the solution and are independent of solution composition. Further, these are empirical parameters with little absolute physical significance, although relative values of the interaction parameters are important. For example, Chen (1980) notes that $\tau_{m,ca}$ is always positive while $\tau_{ca,m}$ is always negative. Moreover, Chen and Evans (1986) found that ion pair-ion pair parameters ($\tau_{ca,ca'}$, $\tau_{ca',ca}$, $\tau_{ca,c'a}$, $\tau_{c'a,ca}$) could usually be set to zero without significantly affecting representation of VLE data.

As noted by Chen (1980) the assumption of *local electroneutrality* results in the treatment of molecule-ion pair parameters ($\tau_{ca,m}$, $\tau_{m,ca}$) as adjustable parameters in the Electrolyte-NRTL equation rather than molecule-ion parameters. However, molecule-ion parameters are functionally related to the molecule-ion pair parameters as can be seen in equation (4.57).

An advantage of local composition models such as the NRTL equation is that binary parameters of a multicomponent system and of its constituent binary systems are the same and no higher-order parameters are required. Best values of these binary parameters for the systems under consideration in this study were, therefore, determined by data regression using binary and ternary system VLE data (TPx).

4.4 Data Regression

4.4.1 Adjustable Parameters: Binary Energy Interaction Parameters

There are three types of binary interaction parameters in the NRTL contribution to the excess Gibbs energy or activity coefficient: molecule-molecule ($\tau_{m,m'}$ and $\tau_{m',m}$), molecule-ion pair ($\tau_{m,ca}$ and $\tau_{ca,m}$), and ion pair-ion pair (with a common cation or anion) ($\tau_{ca,ca'}$ and $\tau_{ca',ca}$ or $\tau_{ca,c'a}$ and $\tau_{c'a,ca}$). Acid gas-water interaction parameters were fitted in the earlier work of Chen and Evans (1986). Amine-water binary parameters were adjusted in this work on experimental binary system (amine - water) data. Using the best values of the molecule-molecule binary interaction parameters fitted on binary system VLE data, statistically significant molecule - ion pair parameters were then fitted on ternary system (i.e. alkanolamine-H_2S-H_2O and alkanolamine-CO_2-H_2O) VLE (Tpx) data reported in the literature. There is a large body of experimental H_2S and CO_2 solubility data reported in the literature for the single acid gas - MEA - water or single acid gas - DEA - water systems. To make the job of parameter estimation tractable, data regression was arbitrarily restricted to VLE data published after 1956. Literature sources used in fitting all parameters are summarized in Chapter Six.

Following Chen and Evans (1986) all ion pair-ion pair parameters were fixed at zero. Parameters fitted on the binary and ternary systems were used to represent experimental data for the corresponding quaternary systems (H_2S-CO_2-alkanolamine-water) without adjusting additional parameters on these systems.

Much of the solubility data reported for single amine-single acid gas systems represent experimental measurements at moderate to high liquid phase acid gas loadings. There is little data reported in the low acid gas loading (less than 0.1 or 0.2 moles acid gas per mole amine), low acid gas partial pressure range, especially at low temperatures. This is because equilibrium acid gas partial pressures are often too low to measure accurately at low temperatures unless the liquid phase concentration of acid gas is high (Mather, 1988). For example, at low temperatures and low acid gas loadings, gas chromatography, which is often used to determine the acid gas content of the vapor phase, may not provide the precision necessary to determine acid gas vapor phase concentration. In addition, at low temperatures and low acid gas loadings, the equilibrium partial pressure of water can be greater than the acid gas partial pressure. Since most acid gas solubility measurement techniques require that the partial pressure of water be subtracted from the total pressure to obtain the acid gas partial pressure, an error in estimating the water partial pressure can translate into a large relative error in the measured acid gas equilibrium partial pressure.

Therefore, the best values of the adjustable binary interaction parameters were determined by data regression using the available solubility data, most of which was measured at moderate to high loadings. Since the adjustable binary interaction parameters are characteristic of pair interactions of components of the solution and are independent of solution composition, the fitted parameters are valid outside the range of concentrations over which they were fitted. Hence, the VLE model itself is valid at low acid gas partial pressures even though the parameters of the activity coefficient model were not fitted on data in this range.

At high temperatures, there are relatively more equilibrium partial pressure measurements reported at low loadings presumably because absolute acid gas equilibrium partial pressures are greater. However, high temperature acid gas partial pressure measurements at low loadings are still often believed to be of questionable accuracy because the partial pressure of water can be of the same relative magnitude as the acid gas partial pressure (Moore, 1989). Again, an error in estimating the water partial pressure can translate into an relatively large error in the measured acid gas equilibrium partial pressure.

In the alkanolamine-H_2S-CO_2-H_2O system, where the alkanolamine is MEA, DEA, or DGA, there are 8 ionic species and 4 molecular species present in the liquid phase (Am, H_2S, CO_2, H_2O, AmH^+, H_3O^+, $AmCOO^-$, HS^-, S^{-2}, HCO_3^-, CO_3^{-2}, OH^-). Tertiary alkanolamines, like MDEA, do not form stable carbamates, so there is one less component in the MDEA-H_2S-CO_2-H_2O system. In either case there are a large number of binary parameters, molecule-molecule, molecule-ion pair, and ion pair-ion pair can, in principle, be formulated for this system. However, because many of these species are present in the liquid phase at low or negligible concentrations, parameters associated with them do not significantly affect representation of VLE. Important parameters in the system were identified by the statistical significance with which they could be fitted on experimental VLE data. **All** water-ion pair and ion pair-water parameters that could **not** be fitted with statistical significance were fixed at default values of 8.0 and -4.0 respectively. **All** alkanolamine-ion pair and ion pair-alkanolamine binary parameters, and all acid gas-ion pair and ion pair-acid gas binary parameters were fixed at values of 15.0 and -8.0, respectively. These default values represent approximate average values of a large number of water-ion pair and organic solvent-ion pair parameters reported by Chen and Evans (1986) and Mock et al. (1986) respectively. **All** molecule-molecule parameters and ion pair-ion pair parameters not fitted were fixed default values of zero.

Binary interaction parameters were assumed to be temperature dependent and were fitted to the following function of temperature:

$$\tau = a + b/T \tag{4.67}$$

4.4.2 Adjustable Parameters: Carbamate Stability Constant

There is very limited data reported in the literature for the carbamate stability constant (Reaction 4g) of MEA, DEA, or DGA. Jensen et al. (1954) report a value of the carbamate stability constant for both MEA and DEA, but only at 18°C. Chan and Dankwerts (1981) measured the same constants in sodium bicarbonate solutions at 25° and 40°C, but apparently they did not correct for affects of ionic strength. Likewise, Mahajani and Dankwerts (1982) measured the MEA and DEA carbamate stability constants in a 30% potash solution at 100°C. Again no correction was made for ionic strength. Hence, the carbamate stability constant was treated as an additional adjustable parameter of the VLE model. The coefficients of equation (4.8) for the carbamate stability constant were fitted, simultaneously with the appropriate interaction parameters, on CO_2-alkanolamine-H_2O ternary system VLE data.

4.4.3 Parameter Estimation with the Data Regression System of ASPEN PLUS

The best values of a and b in equation (4.67) and the coefficients of equation (4.8) for the carbamate stability constants were determined using the Data Regression System (DRS) of ASPEN PLUS process simulator (Aspen Technology, 1985). The DRS of ASPEN PLUS is based on the maximum likelihood principle for the estimation of parameters in nonlinear implicit algebraic models. It has been developed specifically for physical property models including vapor-liquid equilibrium models. DRS accepts data measurements such as temperature, pressure, and mole fraction of either pure component or multicomponent systems and calculates maximum likelihood estimates of adjustable parameters and state variables for a set of user-selected physical property models.

DRS employs two algorithms for estimating parameters - an algorithm based on the work of Deming (1943) yielding an approximate estimate of physical property model parameters and the Britt-Luecke algorithm (Britt and Luecke, 1973) which yields true maximum likelihood estimates of the parameters and is a refinement of the Deming algorithm. Both methods were originally implemented as computer algorithms by Britt and Luecke (1973). The attractive feature of these algorithms is that they take into account error in all measured variables resulting in a method that does not, in general, distinguish between dependent and independent variables.

The maximum likelihood algorithms employed by DRS of ASPEN PLUS for estimating parameters in physical property models leads to an equality constrained minimization problem. Minimization is achieved through the use of Lagrange multipliers.

For the estimation of the adjustable parameters (ie. binary energy interaction parameters and carbamate stability constants) of the model presented here, it was found that the Deming algorithm was more stable than the Britt-Luecke algorithm. While the Deming algorithm is approximate in the sense that it does not lead to true maximum likelihood estimates of the parameters, best values of the adjustable parameters of other physical property models have been found, by this algorithm, to be in good agreement with values of the same parameters estimated by the Britt-Luecke algorithm (Britt and Luecke, 1973). In this work, the Deming algorithm was used exclusively to estimate parameter values.

4.4.4 Minimization Algorithms - Theoretical Development

The problem considered here is that of estimating parameters in nonlinear algebraic (ie. physical property) models by fitting the models to experimental data. The number of data points must equal or exceed the number of parameters to be estimated. Consider a model in which an n-vector of unknown parameters θ_0 and a q-vector of observable variables with *true* values $\mathbf{z_0}$ at the time of measurement are related through a k-vector of functions, $\mathbf{f(z, \theta)}$ such that

$$\mathbf{f}(\mathbf{z}_0, \theta_0) = \mathbf{0} \tag{4.68}$$

Note that $q \geq k > n$. Since dependent and independent variables are not distinguished there is only a single vector of observable variables **z**. The important feature of this approach is that all experimental data is used. In the Deming and Britt-Luecke algorithms, the measured values of $\mathbf{z_o}$ are assumed to contain random experimental errors so that

$$\mathbf{z_m} = \mathbf{z_o} + \mathbf{e} \qquad (4.69)$$

where $\mathbf{z_m}$ is the q-vector of all measurements (ie., a vector containing values of T, P, and x for all solubility measurements) and **e** is a q-vector of measurement errors. $\mathbf{z_o}$ is treated as a vector of unknown parameters since it represents the ***true*** or error free values of the measured variables. Therefore, maximum likelihood estimates of θ_o and $\mathbf{z_o}$ are made simultaneously.

An implicit assumption of maximum likelihood methods is that the error **e** is a normally distributed random vector having zero mean and that the covariance between different measured variables is zero, and that the variances of the variables are known (through replicate measurements) or can be estimated. This yields a positive definite variance-covariance q x q matrix, **R**, whose diagonal elements are the variable variances. For a normal distribution of measurements errors, the joint probability density function for the measurement vector $\mathbf{z_m}$ is given by

$$g(\mathbf{z_m}) = (2\pi)^{-q/2} |R|^{-1/2} \exp\{-0.5\,(\mathbf{z_m} - \mathbf{z_o})^T R^{-1} (\mathbf{z_m} - \mathbf{z_o})\} \qquad (4.70)$$

In effect, the maximum likelihood method requires that the unknown parameters be chosen is such a way as to make the experimentally measured values, $\mathbf{z_m}$, appear most probable when taken as a whole (Anderson et al., 1978). The function $g(\mathbf{z_m})$ gives the probability of obtaining the observed values $\mathbf{z_m}$ given the estimated true values $\mathbf{z_o}$.

The likelihood function is obtained from the joint probability density function by treating $\mathbf{z_o}$ and θ_o as the variables $(\mathbf{z}, \theta)$ giving

$$L(\mathbf{z}, \theta) = (2\pi)^{-q/2} |R|^{-1/2} \exp\{-0.5\,(\mathbf{z_m} - \mathbf{z})^T R^{-1} (\mathbf{z_m} - \mathbf{z})\} \qquad (4.71)$$

where $(\mathbf{z}, \theta)$ are constrained to those points which satisfy the equation

$$\mathbf{f}(\mathbf{z}, \theta) = \mathbf{0} \qquad (4.72)$$

Equation (4.72) represents physical constraints such as thermodynamic conditions for phase equilibrium (isofugacity). DRS is capable of handling multiple such constraints.

The best estimates of the model parameters and *true* values of the measured variables are those which maximize $L(\mathbf{z}, \theta)$ subject to the model constraints, equations (4.72). That is, any solution of the constraint equations (4.72) that maximizes the likelihood function is a maximum likelihood *estimate* of $(\mathbf{z_o}, \theta_o)$. Maximizing $L(\mathbf{z}, \theta)$ is equivalent to minimizing the function

$$F(\mathbf{z}, \theta) = \frac{1}{2}(\mathbf{z_m} - \mathbf{z})^T \mathbf{R}^{-1} (\mathbf{z_m} - \mathbf{z}) \qquad (4.73)$$

subject to the constraints

$$\mathbf{f}(\mathbf{z},\theta) = \mathbf{0} \qquad (4.72)$$

This is an equality constrained minimization problem. The Deming and Britt-Luecke algorithms minimize $F(\mathbf{z}, \theta)$ subject to equations (4.72) through the use of Lagrange multipliers.

4.4.5 Application of the Data Regression System

In this work, the Deming algorithm was found to be significantly more stable than the Britt-Luecke algorithm. For this reason, the Deming algorithm was used solely to determine interaction parameters. To stabilize the regression algorithm further, the DRS of ASPEN PLUS makes several state variable and property variable transformations. Of relevance in this work are transformations of pressure, mole fraction, and fugacity. Pressure is transformed by the function

$$P' = \ln P$$

To prevent concentrations from taking on unrealistic values, apparent mole fractions, x_a, are transformed by the function

$$x'_{ai} = \ln\left(\frac{x_{ai}}{1 - x_{ai}}\right)$$

where the bounds for x_{ai} are zero and one, exclusive. Thus x'_{ai} varies from $-\infty$ to ∞ as x_i varies from zero to one. Finally, like pressure, fugacity is also transformed by the function

$$f'_i = \ln f_i$$

The minimization objective function for the vapor-liquid equilibrium model used in this work is expressed as

$$F = \sum_{i=1}^{M} \frac{(P'^{t}_{i} - P'^{e}_{i})^2}{\sigma^2_{P'_i}} + \frac{(T^t_i - T^e_i)^2}{\sigma^2_{T_i}} + \frac{(x'^{t}_{ai} - x'^{e}_{ai})^2}{\sigma^2_{x'_{ai}}} \qquad (4.74)$$

where the summation is over all M experimental measurements. In this application, x_{ai} (which is transformed to x'_{ai})is the apparent mole fraction of the acid gas. The apparent mole fraction of any component is calculated assuming that the electrolytes do not dissociate. Therefore, the apparent mole fractions of all ions are zero. The actual liquid phase mole fractions of all species are determined by solving the equations of chemical equilibrium.

T^e, P'^e, and $x_a^{'e}$ are the experimentally measured values of the acid gas partial pressure (transformed), system temperature, and liquid phase apparent mole fractions (transformed). T^t, P'^t, and $x_t^{'e}$ are the estimated *true* values (ie. maximum likelihood estimates) of the respective state variables corresponding to each measured data point. Each term in the summation is normalized by the estimated experimental variance, $\sigma_{U_k}^2$ of each of the measured variables, ie. temperature, pressure, and apparent liquid phase mole fractions. The objective function is minimized by the adjustment of the *true* variables and the model parameters, τ, subject to the following constraints and bounds:

1. Vapor-liquid equilibrium constraints on acid gases, equation (4.4).

$$f(z, \theta) = \ln f_i^v - \ln f_i^l = 0$$

2. Chemical equilibrium constraints for all relevant reactions. This is an implicit constraint

3. Parameter bounds:

$$\tau_{lb} < \tau < \tau_{ub}$$

The equilibrium constraints represent, in effect, the VLE model. In this work, iterations were repeated until $|| \theta_{i+1} - \theta_i ||$ was less than 0.01.

It is clear from equation (4.74) that it is not necessary to know the actual values of the variable variances, $\sigma_{U_k}^2$, but rather the relative values. This is fortunate because this information is often not reported with experimental acid gas solubility data published in the literature. Nor are replicate measurements often reported so that measurement errors can be estimated. It should be recalled that in the development of Britt-Luecke and Deming maximum likelihood algorithms, it was assumed that measurement errors are randomly and normally distributed. However, the results to be presented in the Chapter Six suggest that errors in data from some data sources may not be randomly distributed. That is, data from a number of literature sources appears to be skewed especially at very low acid gas partial pressures and low acid gas liquid phase loadings. As noted previously, this may be due to limitations in the precision with which acid gas concentrations can be measured by gas chromatography (Mather, 1988). Data sets which obviously contained nonrandom errors were weighted less heavily in parameter estimation than other data sets.

4.4.6 Parameter Variance and Correlation

One of the primary goals of a modeling effort of this nature is to provide a means to confidently interpolate between and extrapolate beyond reported experimental data. The latter is particularly important in view of the relative lack of experimental data at low acid gas partial pressures. The confidence that is placed in interpolation and extrapolation (prediction) with the model is dependent on both correct model formulation and the quality of the data used to fit parameters of the model. This is partly reflected in the variances of the estimated parameters.

The DRS system provides an estimate of the parameter estimation errors, based on the assumption that the linearized form of the model is valid in a region about the *estimated* maximum likelihood values of $(\hat{z},\hat{\theta})$ that includes the *true* values of the variables and parameters (z_0,θ_0). Parameter estimation errors are reported in the parameter variance-covariance matrix. A discussion of the variance-covariance matrix can be found in the text by Beck and Arnold (1977). The diagonal elements of this matrix are the estimated variances of the various parameter values. The square roots of these variances are estimates of the standard deviations of the parameter values. They are, in effect, measures of the uncertainties in the estimated parameter values. The off-diagonal elements of this matrix are the covariances between various adjustable parameters. These are a measure of the correlation between corresponding parameters. The correlation coefficient, ρ, between two parameters - θ_i and θ_j - is defined as

$$\rho(\theta_i, \theta_j) = \frac{\mathrm{cov}(\theta_i, \theta_j)}{\sigma_{\theta_i}\sigma_{\theta_j}} \tag{4.75}$$

where $\mathrm{cov}(\theta_i, \theta_j)$ is the covariance between the two parameters θ_i and θ_j, and σ_{θ_i} and σ_{θ_j} are the estimated standard deviations of the estimates of θ_i and θ_j. Parameters that are completely independent have a correlation coefficient of zero. Parameters that are perfectly correlated have a correlation coefficient of ± 1. If two parameters are highly correlated, it is difficult to determine them uniquely. ASPEN PLUS DRS also provides the matrix of correlation coefficients corresponding to the parameter variance-covariance matrix.

It is well known that the parameters of the NRTL equation are often highly correlated (Renon 1985). Results of the work conducted by Chen and Evans (1986) and results of this work, presented in Chapter Six, suggest that corresponding pairs of water - ion pair interaction parameters of the Electrolyte - NRTL equation are also highly correlated. A high level of correlation between parameters suggests that it might be possible to reduce the number of adjustable parameters by formulating a single parameter that is some combination of the highly correlated parameters. No such attempt was made in this work. However, for several binary interaction parameters, the elements a and b of equation (4.67) were also found to be highly correlated. In such cases, the value of either a or b was often fixed at some arbitrary value and the best value of the other parameter was determined by data regression.

4.5 VLE Model Algorithm

4.5.1 Stand-Alone Model

The model described in the previous sections was first used to represent VLE data for the acid gas - alkanolamine - water system within the framework of the Data Regression System of Aspen Plus. The model has also been developed as a stand-alone algorithm for use in applications outside the framework of ASPEN PLUS. The ASPEN version of the model and the stand-alone model are virtually identical with respect to the functions used to represent thermodynamic variables. However, application of the model within ASPEN must, of necessity, be more general to facilitate its use in a variety of flash (including bubble point and dew point) routines. The stand-alone algorithm has been developed as a bubble point type routine only; at a specified temperature and liquid phase composition, the total pressure and vapor phase composition are calculated.

The purpose of this section is to briefly describe the stand-alone algorithm which was coded in Fortran and implemented on a VAX 11/780 computer. The thermodynamic variables which must be evaluated during execution are summarized in Table 4.7 together with the functional dependence of each and with the parameters required by each.

Table 4.7 Thermodynamic variables evaluated during execution of VLE model.

Thermodynamic Variables	Functional Dependence	Parameters required for Evaluation
$K\ (\mu_i^o)$	T	Coefficients of Eq. (4.8).
P_i^o (solvents)	T	Coefficients of Eq. (4.9).
H_i^o (acid gases)	T	Coefficients of Eq. (4.8).
d_m	T, x	T_{ci}, P_{ci}, V_{ci}, Z_{RAi} of Eqs. (4.10), (4.11).
D_m	T, x_w*	A, B of Eq. (4.66).
γ_i	T, x	ρ, M_m of Eq. (4.53); r_i of Eq. (4.56); Z_i of Eqs. (4.56), (4.57); a of Eq. (4.57); $\tau_{mm'}$, $\tau_{m'm}$, for all mm' pairs, Eq. (4.57); $\tau_{ca,m}$, $\tau_{m,ca}$, for all ca,m pairs, Eq. (4.57); (note all ion pair - ion pair parameters are fixed at values of zero).
$\bar{v}_i^{\infty}$ (acid gases)	T	Brelvi-O'Connell characteristic volumes of acid gases and water.
v_i (solvents)	T	T_{ci}, P_{ci}, V_{ci}, Z_{RAi} of Eqs. (4.10), (4.11).
φ_s^o	T, P	P_i^o; T_{ci}, P_{ci} of Eqs. (4.43), (4.44); ω_i of Eq. (4.47).
$\hat{\varphi}_i$	T, P, y	T_{ci}, P_{ci} of Eqs. (4.43), (4.44); ω_i of Eq. (4.47).

*x_w is the vector of mass fractions of all species.

The algorithm was developed so that one could calculate total pressure and vapor phase partial pressures of all molecular components given temperature, T, the vector of liquid phase apparent mole fractions of water and all alkanolamines on an acid gas free basis, x_a^{agf}, and the vector of loadings, α, of H_2S and/or CO_2, in moles of acid gas per mole total alkanolamine. The subscript 'agf' designates an acid gas-free-basis. Recall that the apparent mole fraction of any component is its mole fraction calculated assuming no reaction occurs in the liquid phase; apparent mole fractions of all ions are zero. x_a^{agf} is the vector of solvent mole fractions corresponding to the alkanolamine concentration of interest. For example, if the user were interested in the solubility of H_2S or CO_2 in a 2.5 molar MEA solution, then the vector x_a^{agf} would be composed of the elements $x_a^{agf}(H_2O)=0.95$ and $x_a^{agf}(MEA)=0.05$.

The algorithm can be viewed as consisting of two separate sub-algorithms. The first algorithm is responsible for determining the actual or true composition of the liquid phase at equilibrium given temperature and the apparent composition of the liquid phase. In this context, true composition refers to the composition of the liquid phase corresponding to the *equilibrium distribution of species*. It should not be confused with estimates of the *true* (maximum likelihood estimates) measured state variables generated during parameter estimation. The true composition is determined from the apparent composition by minimizing the Gibbs free energy of the liquid phase.

Once the equilibrium distribution of components in the liquid phase has been determined, the second algorithm is used to calculate total pressure, P, and the vapor phase composition, **y**. Both algorithms are iterative. The first, hereafter referred to as the chemical equilibrium algorithm, is illustrated in block diagram form in Figure 4.1.

The second algorithm, hereafter referred to as the phase equilibrium algorithm, is illustrated in block diagram form in Figure 4.2.

4.5.2 The Chemical Equilibrium Algorithm

Given the temperature, T, apparent mole fractions of all solvents on an acid gas free basis, x_a^{agf}, the acid gas loadings, α_{H_2S} and α_{CO_2}, the indexing vectors, the element abundance matrix, A, and the stoichiometric coefficient matrix, N, for a set of independent chemical reactions, and the parameters listed in Table 4.5, the chemical equilibrium algorithm determines the true liquid phase composition. All thermodynamic variables in Table 4.7 that depend on temperature only (K, H_i, P_i^0) are calculated on the first iteration of each bubble point calculation only. From the equilibrium constants a consistent set of standard state chemical potentials are calculated by the procedure outlined in section 4.2.4. Apparent mole fractions of the acid gases are then determined from the acid gas free apparent mole fractions of alkanolamines and the acid gas loadings (in moles acid gas per mole total amine). Apparent mole fractions are renormalized to unity.

Assuming a total of one mole of the liquid phase on an apparent basis, the apparent mole fractions are mapped into the true mole number vector. All other mole numbers (ie., mole numbers of all ionic species) are set to an arbitrarily small number. In effect, the apparent mole fraction vector serves as an initial estimate of the true mole numbers. In addition, apparent mole numbers of water, all alkanolamines, and all acid gases are used to calculate the total mole numbers of all elements by equations (4.13). In this work the elements are taken to be H, O, C, S, and amine (rather than N).

Treating the amines as elements simplifies the element abundance matrix, A, but it also leads to a negative entry for element a_{ij}, where i = H and j = carbamate.

From the initial guess of the true mole number vector, the chemical potentials of all species are calculated by equation (4.25). Given the initial estimates of all mole numbers and all chemical potentials, and the element abundance and stoichiometric coefficient matrices, A and N, the Smith - Missen algorithm, section 4.2.2, is executed to update the mole number vector. An updated vector of chemical potentials is calculated from the new mole number vector and the Smith - Missen algorithm is re-executed. The mole fractions of all liquid phase species are renormalized on each iteration so that $\sum_i x_i = 1$. Iterations of this kind continue until true mole numbers do not change significantly on consecutive iterations. Convergence is achieved when

$$\max_i \; | \delta n_i^{(m)} / n_i^{(m)} | \leq \varepsilon$$

where n_i is the true mole number of component i, $\delta n_i^{(m)}$ is given by equation (4.31) and ε input by the user.

The iterations described above constitute the inner loop of the chemical equilibrium algorithm. The converged mole number vector, together with temperature, are used to calculate a new estimate of the activity coefficients of all species using the Electrolyte-NRTL equation, section 4.3.2. Recall that activity coefficients are assumed to be independent of pressure. The new estimate of the activity coefficient vector is passed to the inner loop which is re-executed yielding a new estimate of the true mole fraction vector. The outer loop is repeated until the mole numbers of all species do not change significantly on consecutive iterations. Convergence is achieved when

$$\max_i \left| \left(n_i^{m+1} - n_i^{m} \right) / n_i^{m} \right| < \varepsilon$$

where ε is input by the user. When ε is set to 1×10^{-5}, 4 to 9 iterations of the outer loop of the chemical equilibrium algorithm are executed before convergence is achieved.

4.5.3 Phase Equilibrium Algorithm

The output of the chemical equilibrium algorithm are the true mole fraction vector and activity coefficient vector. Together with temperature, this information is used by the phase equilibrium algorithm to calculate the vapor phase composition by equations (4.4) and (4.7). The algorithm is iterative because the total pressure, which is needed for determination of the fugacity coefficients of all vapor phase species, and which is a variable needed for evaluation of the Poynting pressure correction factors of equations (4.4) and (4.7), is unknown. However, convergence is generally rapid.

Initially, the vapor phase fugacity coefficients and Poynting factors of all molecular components are set to unity and the total pressure is set to zero. The first operation of the phase equilibrium algorithm is calculation of an initial estimate of the vapor phase partial pressures, p_i, of all molecular components by equations (4.4) and (4.7). An estimate of the total pressure, P_T, is then calculated as the sum of the partial pressures and vapor phase mole fractions are calculated from $y_i = p_i / P_T$ so that the y_i's automatically satisfy $\sum_i y_i = 1$. Using this estimate of P_T, the Poynting pressure correction terms of equations (4.4) and (4.7) are evaluated and the liquid phase standard state fugacities are adjusted for the affect of pressure. The partial pressures of all molecular species are then recalculated and a new estimate of the total pressure is made. Iterations continue until the following convergence criterion is achieved:

$$(P_T^{m+1} - P_T^{m}) / P_T^{m} < 1 \times 10^{-3}$$

The iterations described above constitute the inner loop of the phase equilibrium algorithm. From the converged estimates of P_T and y, the fugacity coefficients of all species are (re)estimated using the Redlich-Kwong-Soave equation of state, section 4.3.1. The updated vector of fugacity coefficients is passed back to the inner loop which is re-executed yielding new estimates of P_T and y. Iterations of the outer loop continue until

$$\max_i | (y_i^{m+1} - y_i^{m}) / y_i^{m} | < \varepsilon$$

where ε is input by the user. When ε is 1×10^{-5}, the phase equilibrium algorithm generally requires 2 to 3 iterations of the outer loop to achieve convergence.

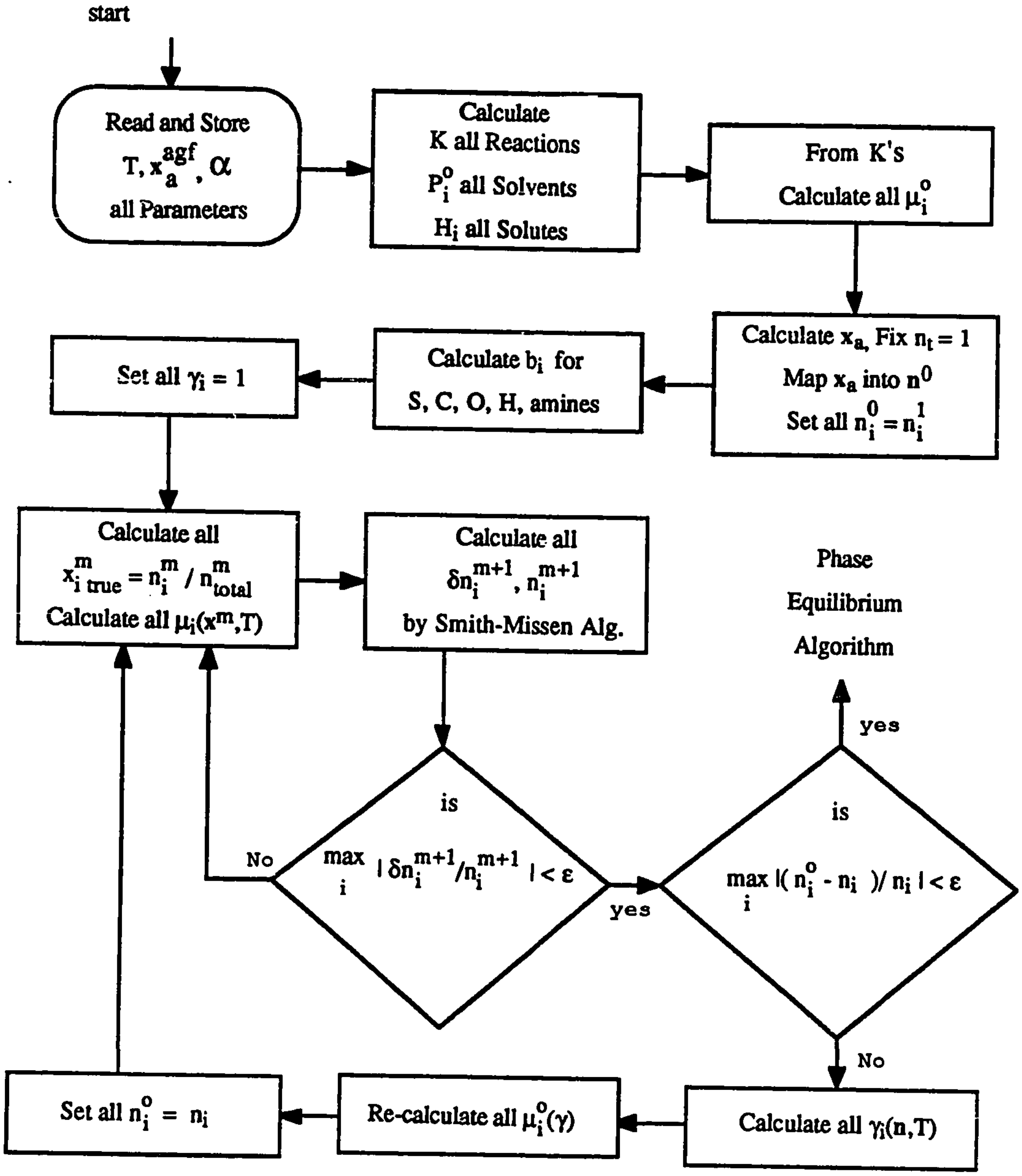
start
Read and Store
T, x_a^{agf}, α
all Parameters
Calculate
K all Reactions
P_i^o all Solvents
H_i all Solutes
From K's
Calculate all μ_i^o
Calculate x_a, Fix $n_t = 1$
Map x_a into n^0
Set all $n_i^0 = n_i^1$
Calculate b_i for
S, C, O, H, amines
Set all $\gamma_i = 1$
Calculate all
$x_{i\,true}^m = n_i^m / n_{total}^m$
Calculate all $\mu_i(x^m,T)$
Calculate all
δn_i^{m+1}, n_i^{m+1}
by Smith-Missen Alg.
Phase
Equilibrium
Algorithm
yes
is
$\max_i |\delta n_i^{m+1}/n_i^{m+1}| < \varepsilon$
No
yes
is
$\max_i |(n_i^o - n_i)/n_i| < \varepsilon$
No
Calculate all $\gamma_i(n,T)$
Re-calculate all $\mu_i^o(\gamma)$
Set all $n_i^o = n_i$

Figure 4.1 Block diagram of chemical equilibrium algorithm, stand-alone model.

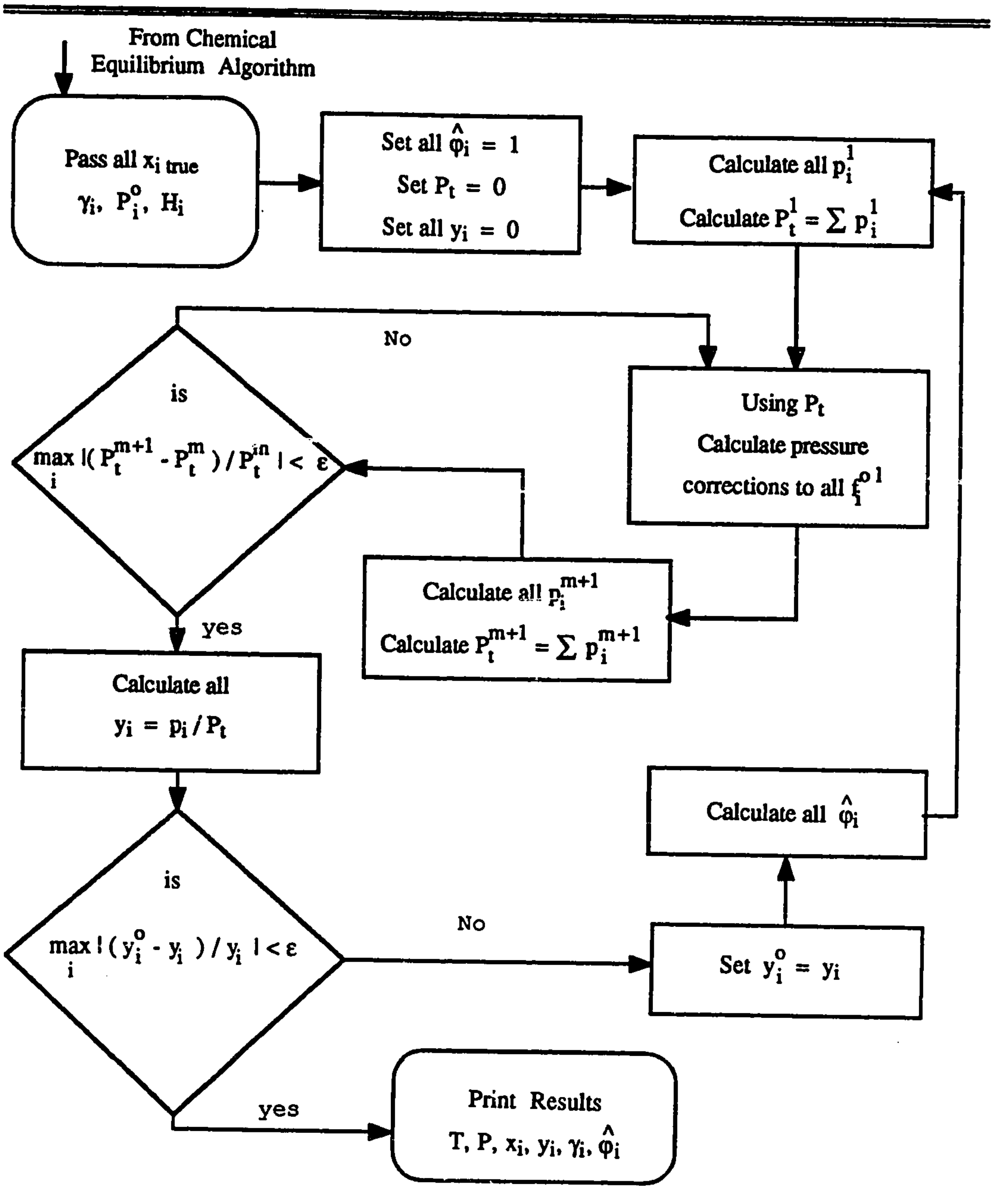
From Chemical Equilibrium Algorithm
Pass all x_i true γ_i, P_i^o, H_i
Set all $\hat{\varphi}_i = 1$
Set $P_t = 0$
Set all $y_i = 0$
Calculate all p_i^1
Calculate $P_t^1 = \sum p_i^1$
No
is
max $|(P_t^{m+1} - P_t^m)/P_t^{in}| < \varepsilon$
i
Using P_t
Calculate pressure corrections to all $f_i^{o\,l}$
Calculate all p_i^{m+1}
Calculate $P_t^{m+1} = \sum p_i^{m+1}$
yes
Calculate all $y_i = p_i/P_t$
Calculate all $\hat{\varphi}_i$
is
max $|(y_i^o - y_i)/y_i| < \varepsilon$
i
No
Set $y_i^o = y_i$
yes
Print Results
T, P, x_i, y_i, γ_i, $\hat{\varphi}_i$

Figure 4.2. Block diagram of phase equilibrium algorithm, stand-alone model.

Chapter Five

Measurement of CO_2 Solubility in Mixtures of MDEA with MEA and DEA

5.1 Experimental

Best values of the adjustable parameters of the Electrolyte - NRTL must be determined by fitting the VLE model to experimental data. There are experimental H_2S and CO_2 solubility data reported in the literature for aqueous solutions of MEA, DEA, MDEA, and DGA. However, there are no data reported for CO_2 solubility in mixtures of MDEA with MEA or DEA. Therefore, as part of this work it was necessary to measure the CO_2 solubility in these aqueous mixtures. This data was used both to validate the extended model for the mixed amine systems and to determine the best values of unique parameters of the Electrolyte-NRTL equation for the mixed amine systems.

5.1.1 Reagents

Commercial grade methyldiethanolamine (MDEA) was supplied by the DOW Chemical Co. with a reported purity of not less than 99 weight percent. The stock MDEA was analyzed by Texaco Chemical Co. (Moore, 1988) by gas chromatography (GC) using a thermal conductivity detector. The GC column, 0.125 inches in diameter and 4 feet long, was packed with 10 percent silicon OV101 and 10 percent Carbowax 20M on Chromsorb W support. Sample size was 1 microliter. Analysis by GC showed less than 0.1 weight percent impurities on a water free basis. The impurities appeared to be primarily diethanolamine. To remove primary and secondary amine contaminants that might react with CO_2 to form carbamates, and thereby affect equilibrium measurements, the pure MDEA was vacuum distilled at approximately 110°C. Analysis of the distillate by GC indicated that the purified MDEA contained less than 0.01 weight percent impurities on a water-free basis. Purified grade MEA was obtained from Fischer Scientific Co. Reported purity was not less than 99 weight percent MEA. Commercial grade DEA was obtained from Union Carbide Corp. Reported purity was not less than 98.5 weight percent DEA with up to 1 weight percent MEA and/or 1 weight percent triethanolamine (TEA) impurities. Both MEA and DEA were used without further purification. Aqueous solutions of the alkanolamines were prepared with distilled water.

Pure CO_2 and three CO_2/N_2 mixtures were obtained from Big Three Industrial Gas, Inc. The mixtures were 0.142, 0.995, and 9.60 mole percent CO_2 respectively. The 0.995 mole percent CO_2 standard was prepared gravimetrically with NBS traceable (S) series weights. All other CO_2 concentrations were substantiated by GC or using calibrated continuous flow infared CO_2 analyzers. Reported impurities in the mixtures were less than 0.2 mole percent, the primary contaminant being Argon.

5.1.2 Apparatus and Procedure

The experimental equilibrium apparatus is shown in Figure 5.1. This was a continuous flow apparatus. The system consisted of two 300 ml stainless steel cylinders mounted vertically in a thermostated water bath. Each cylinder had a nominal

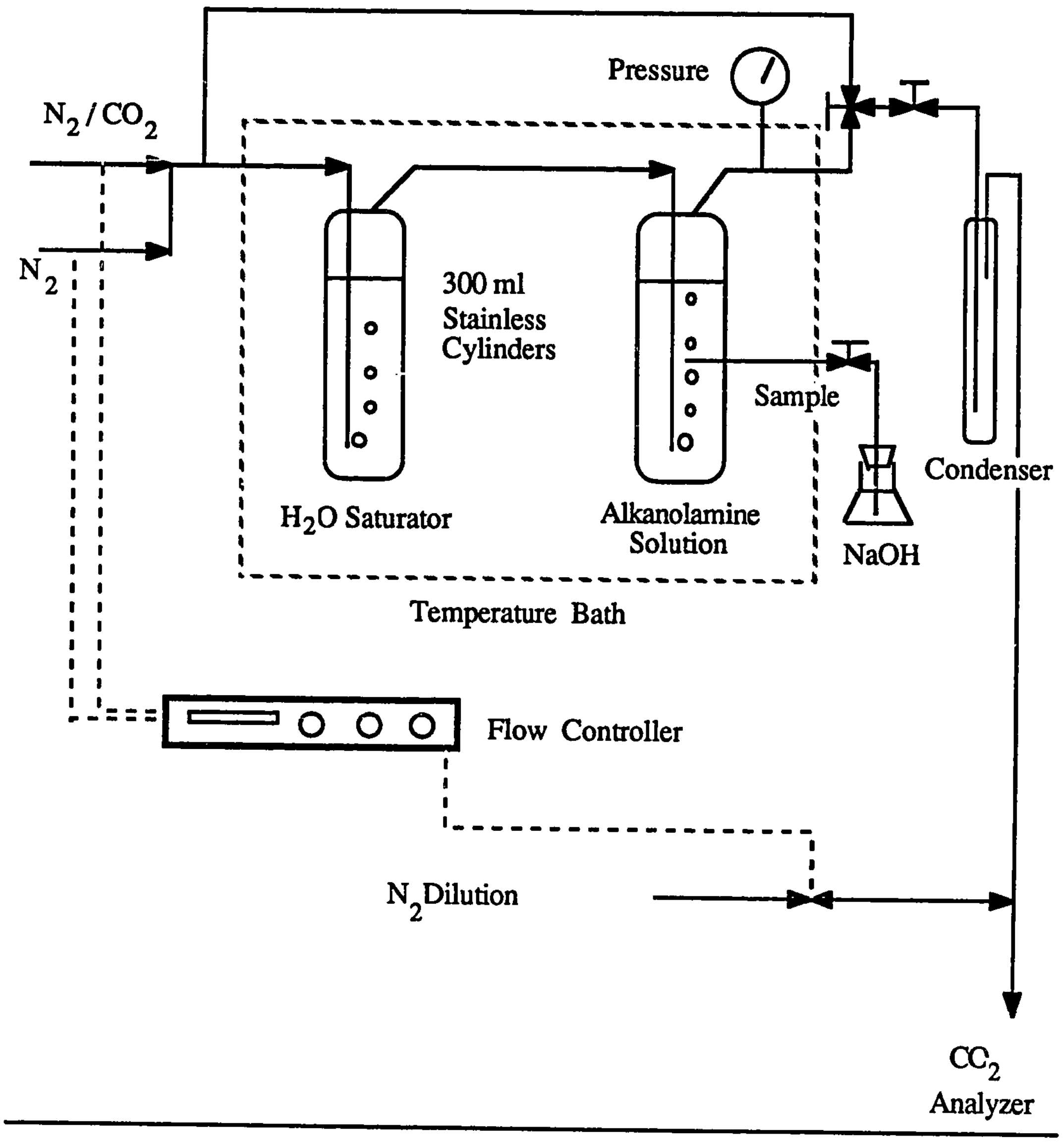
N_2/CO_2
N_2
Pressure
300 ml
Stainless
Cylinders
Sample
Condenser
H_2O Saturator
Alkanolamine
Solution
NaOH
Temperature Bath
Flow Controller
N_2Dilution
CO_2
Analyzer

Figure 5.1 Experimental apparatus for the determination of CO_2 solubility in aqueous alkanolamine solutions.

height of 17 cm and diameter of 5 cm. Temperature was controlled to within ± 0.2 °C at 40°C and ± 0.4 °C at 80°C. The first cylinder served as a water saturator. The second cylinder served as the equilibrium cell and contained the alkanolamine solution. Inserted through the top of each cell was a 0.25 inch stainless steel tube around which a gas-tight seal was made with compression fittings. Inside each cylinder a #12C gas dispersion tube was connected to the 0.25 inch stainless tube. The dispersion tubes extended to the bottom of each cell, approximately 13 cm below the liquid surface; approximately 230 ml of solution was placed into each cell. The dispersion tubes produced finely divided gas bubbles that provided a high contact area between the bubbling gas and the liquid.

Precisely calibrated Brooks Mass Flow Controllers, Series 5850, powered and controlled by a Brooks Controller, Model 5878, were used to deliver N_2 and CO_2/N_2 mixtures to the equilibrium apparatus. Total flow rate was maintained at 60 to 100 ml min^{-1}. Several flow controllers were used with ranges of 0-10, 0-20, and 0-100 ml min^{-1} allowing very precise adjustment of the CO_2 content of the feed gas. The flow controllers have a reported reproducibility of ± 0.20 percent of full scale.

The effluent gas from the equilibrium cell passed through a condenser operating at 0 - 10 °C to remove water and then to one of two infared CO_2 analyzers: a Horiba Model PIR-2000 with three ranges - 0.0 to 0.2 mole percent, 0.0 to 0.6 mole percent, and 0.0 to 1.0 mole percent CO_2, or an Infared Industries, Inc. Model IR702 with two higher ranges - 0 to 3 mole percent and 0 to 10 mole percent. The analyzers were calibrated daily with the appropriate CO_2/N_2 gas mixtures.

As shown in Figure 5.1, the feed gas could also be delivered directly to one of the infared CO_2 analyzers. During a solubility measurement, the CO_2 content of the feed gas was adjusted using the mass flow controllers until the CO_2 concentration in the feed gas was equal to the CO_2 concentration in the effluent from the equilibrium cell. When the feed and effluent CO_2 concentrations were equal, the CO_2 partial pressure of the feed gas was taken to be the CO_2 partial pressure in equilibrium with the alkanolamine solution. The system was operated at total pressures from 100 to 300 kPa. CO_2 solubility measurements could, therefore, be made over an effective CO_2 partial pressure range from 0.01 to 300 kPa. Atmospheric pressure was measured daily with a calibrated barometer.

Samples of the alkanolamine solution were drawn from the side of the equilibrium cell into 10 to 20 ml of a 0.5 or 1.0 kmol m^{-3} NaOH. Duplicate samples were taken at each CO_2 partial pressure. The NaOH solution served to chemically fix the solubilized CO_2 as $CO_3^=$ so that none would escape by flashing. The apparent CO_2 content of the solution was then measured using an Oceanography International model 525 carbon analyzer. A flow schematic of the carbon analyzer is shown in Figure 5.2.

Using this apparatus, a 5 to 10 μl sample of the carbonated NaOH solution was injected into a 25 weight percent H_3PO_4 solution. The H_3PO_4 served to revert the $CO_3^=$ to CO_2 which was swept with N_2 to a dedicated Horiba CO_2 infared analyzer. The Horiba analyzer had an effective measurement range of 0.00 to 0.05 mole percent CO_2. A zero to five volt output signal, representing CO_2 concentration, was sent from the Horiba analyzer to a digital integrator. Injection of the carbonated NaOH solution was repeated at least twice so that results could be averaged. Immediately prior to, and immediately following analysis of each liquid sample, the liquid analyzer was calibrated with 0.010 or 0.100 kmol m^{-3} aqueous solutions of Na_2CO_3, prepared from certified grade anhydrous sodium carbonate and boiled, deionized water. Using the weights of

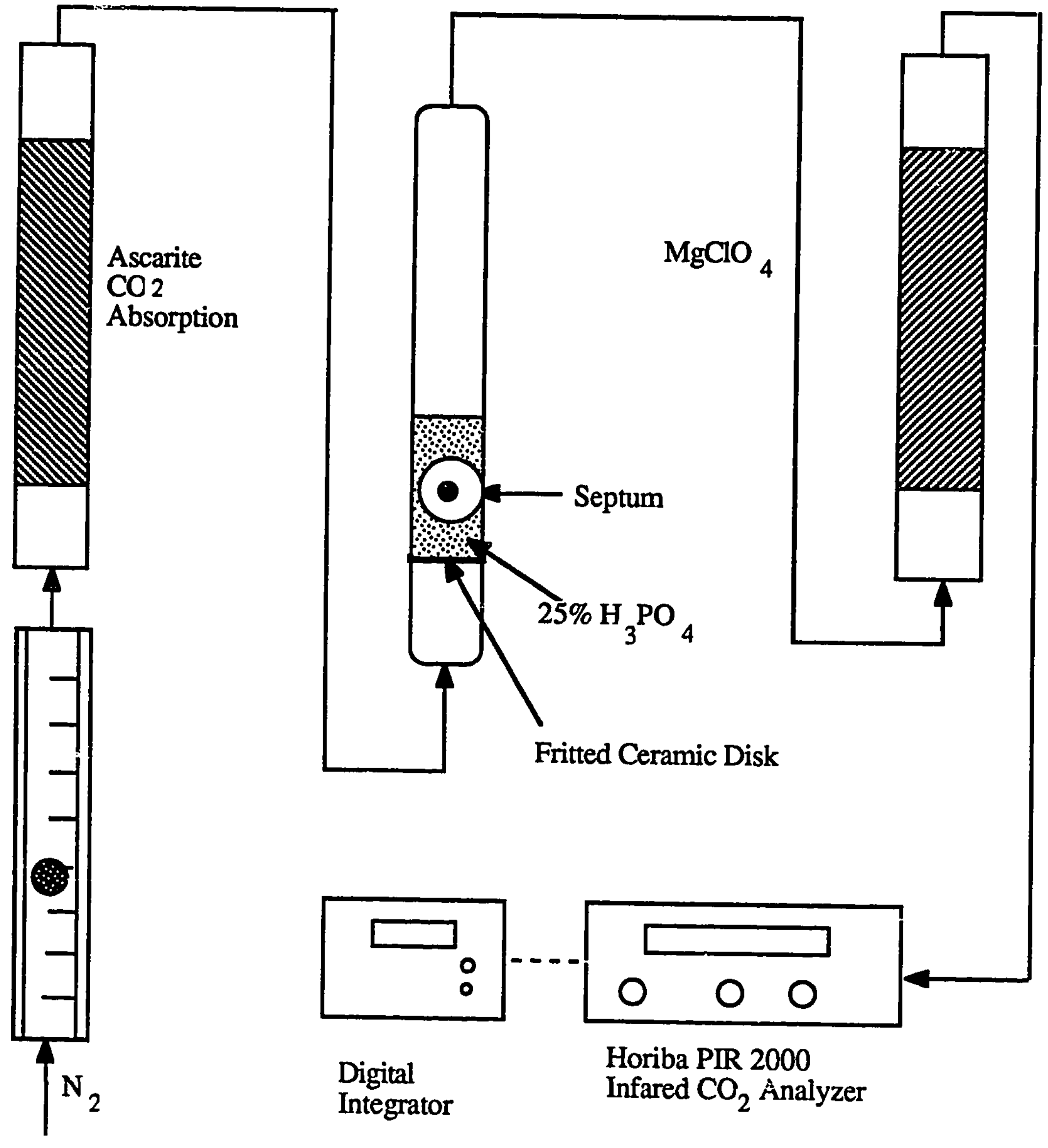
Ascarite
CO 2
Absorption
MgClO 4
Septum
25% H3PO4
Fritted Ceramic Disk
N2
Digital
Integrator
Horiba PIR 2000
Infared CO2 Analyzer

Figure 5.2 Flow schematic for Oceanography International model 525 carbon analyzer used to measure apparent CO_2 concentration in liquid phase.

the undoped NaOH solution and the alkanolamine sample drawn into it, the densities of each solution, the volume of carbonated NaOH injected into the phosphoric acid, and the moles of CO_2 liberated, the apparent concentration of CO_2 in the alkanolamine solution was calculated.

The NaOH solution into which the alkanolamine sample was drawn was prepared from boiled, distilled water and stored in an airtight bottle. As NaOH solution was drawn from its storage bottle, air was admitted through a glass tube containing ascarite to remove the CO_2 present in the air. A blank sample of the NaOH solution was analyzed for total CO_2 content at the same time that each carbonated NaOH sample was analyzed. CO_2 content in the NaOH solution varied from approximately 2×10^{-4} to 3×10^{-4} kmol m^{-3}. Hence, the CO_2 content of the stock NaOH solution could be subtracted from the value measured for the NaOH solution doped with the carbonated alkanolamine solution.

A third sample of the alkanolamine solution was taken from the equilibrium cell at each CO_2 partial pressure so that apparent alkanolamine concentration could be determined by titration with 1.00 kmol m^{-3} HCl. This procedure is accurate even when the solution is partially loaded with CO_2 (a weak acid) because HCl is a stronger acid (lower pKa) than CO_2. As it is added to a loaded amine solution it preferentially displaces CO_2 as the amine protonating species. Molecular CO_2 is thereby liberated from the solution. The titration equivalence point, the point at which the amine was fully neutralized (protonated) by the HCl, was determined by pH measurement. The equivalence point was characterized by a pH of 3.5 to 4.0. From the weight of the alkanolamine sample and its density and the volume of 1.00 kmol m^{-3} HCl required to reach the equivalence point, the concentration of alkanolamine was calculated.

Each solubility measurement took approximately 6 to 8 hours to complete. A series of measurements was conducted over a several day period; usually one measurement was made each day. A series of measurements was begun with a very CO_2 lean solution of alkanolamine in the equilibrium cell. Following completion of each measurement, after samples were withdrawn from the equilibrium cell for determination of CO_2 loading and amine concentration, 20 to 70 additional milliliters of alkanolamine solution were removed from the cell. The total volume of alkanolamine removed was replaced with a corresponding volume of the alkanolamine solution presaturated with CO_2 at atmospheric pressure.

During a period of several days, it was found that the apparent alkanolamine concentration (on an acid gas free basis) would decrease slightly. This, of course, was due to the fact that the activity of water in the equilibrium cell was lower than the activity of water in the water saturator (where the activity was unity). As a result, there was a net transfer of water from the saturator to the equilibrium cell. The drop in alkanolamine concentration was, to some extent, offset by the addition of CO_2 rich alkanolamine solution following each measurement. Over the course of several days, the alkanolamine concentration usually did not decrease more that one percent.

5.1.3 Solution Density

In order to determine the liquid phase apparent CO_2 concentration, it was necessary to know the density of the loaded aqueous amine mixtures. Solution densities of carbonated single amine solutions (MEA, DEA, and MDEA) were taken from the work of Licht and Weiland (1989). Densities of CO_2 loaded 2 kmol m^{-3} MEA

- 2 kmol m^{-3} MDEA mixtures and CO_2 loaded 2 kmol m^{-3} DEA - 2 kmol m^{-3} MDEA mixtures (amine concentrations are reported on a CO_2 free basis) were measured using a Paar DMA 46 density meter. Measurements were made at room temperature (23°C). The density meter was calibrated with distilled water.

Amine mixtures containing various levels of CO_2 were prepared in the following way for density measurement. Approximately 200 ml of the stock aqueous amine mixture were saturated with CO_2 at atmospheric pressure. The density of the saturated mixture was measured using the Paar density meter and the CO_2 concentration (and loading) was determined using the Oceanography International carbon analyzer. Care was exercised to prevent excessive exposure of the saturated amine mixture to air to prevent loss of the CO_2 by flashing. The CO_2 rich amine mixture was then mixed with appropriate weights of the corresponding CO_2 free amine mixture in 25 ml erlenmeyer flasks to obtain additional amine mixtures at lower CO_2 loadings. The CO_2 concentration in each mixture was determined by mass balance. The densities of each of these mixtures was then measured with the Paar density meter.

Results of the solution density measurements for carbonated 2 kmol m^{-3} MDEA - 2 kmol m^{-3} MEA and 2 kmol m^{-3} MDEA - 2 kmol m^{-3} DEA are summarized in Table 5.1 and presented graphically in Figure 5.3. The results of this work, as well as those of Licht and Weiland (1989), indicate that the density of an aqueous solution of MEA, DEA, or MDEA, or a mixture of MDEA with MEA or DEA, increases as the loading of CO_2 increases. In fact, the results suggest that the density increases in such a way that the total volume of a solution of alkanolamine changes little as it is loaded with CO_2. This suggests that, as an approximation, the density of a carbonated alkanolamine solution can be calculated using only a knowledge of the density of the CO_2 free solution and the total CO_2 loading.

The linearity and consistency of the results presented in Figure 5.3 also suggest that density measurement may be a more precise means of measuring CO_2 content of alkanolamine solutions.

Table 5.1. Density of CO_2 loaded 2.0 kmol m^{-3} MDEA - 2.0 kmol m^{-3} MEA and CO_2 loaded 2.0 kmol m^{-3} MDEA - 2.0 kmol m^{-3} DEA at 23 °C. Amine concentrations are CO_2 free.

2 kmol m^{-3} MDEA - 2 kmol m^{-3} MEA		2 kmol m^{-3} MDEA - 2 kmol m^{-3} DEA	
α_{CO_2} (mol/mol)	ρ (g/ml)	α_{CO_2} (mol/mol)	ρ (g/ml)
0.0000	1.0250	0.0000	1.0440
0.0791	1.0395	0.0488	1.0647
0.180	1.0568	0.195	1.0769
0.256	1.0691	0.267	1.0884
0.338	1.0787	0.362	1.1029
0.436	1.0954	0.439	1.1138
0.523	1.1063	0.539	1.1274

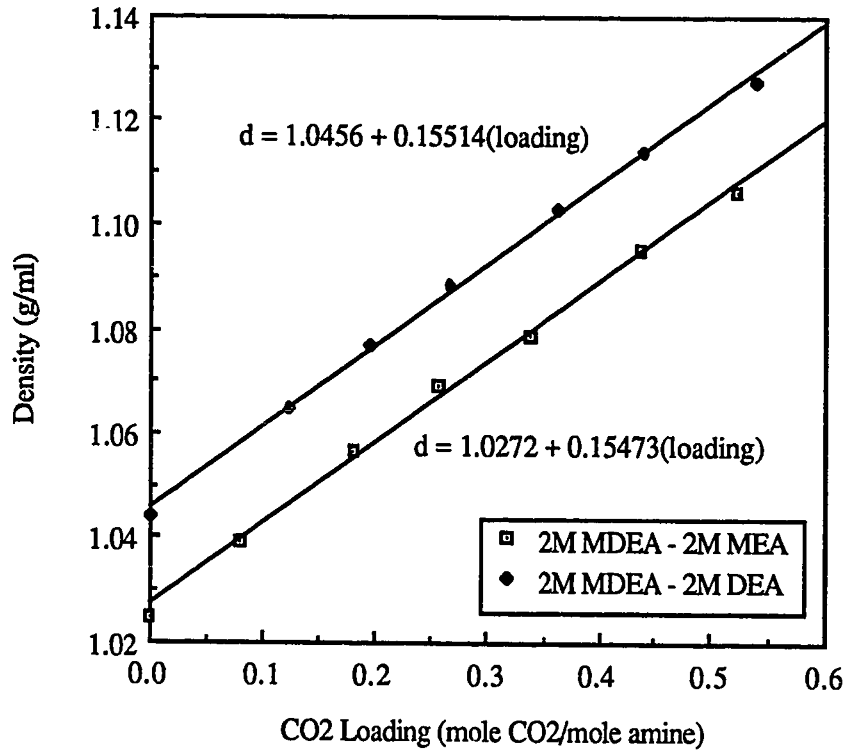

Figure 5.3 Densities of carbonated 2 kmol m^{-3} MDEA - 2 kmol m^{-3} MEA and 2 kmol m^{-3} MDEA - 2 kmol m^{-3} DEA aqueous mixtures at 23°C.

5.2 Solubility Measurement Results

The experimental method used in this work was tested by measuring the CO_2 solubility in 2.5 kmol m^{-3} MEA at 40 and 80°C and in 2.0 and 4.28 kmol m^{-3} MDEA solutions at 40°C. Results of CO_2 solubility measurements in 2.5 kmol m^{-3} aqueous MEA are summarized in Table 5.2 and presented graphically in Figure 5.4 together with data taken from the literature. As can be seen in Figure 5.4, measurements made in this work for CO_2 solubility in aqueous MEA are in good agreement with data of Jones et al. (1959) and in good agreement with data of Lee et al. (1976a) except at the lower temperature and at low CO_2 loadings.

Results of CO_2 solubility measurements in aqueous MDEA solutions are summarized in Table 5.3 and are presented graphically in Figures 5.5 and 5.6 together with data taken from the literature. Figure 5.5 shows that the CO_2 solubility measurements made in this work are in good agreement with corresponding measurements made by Jou et al. (1982) for a 2.0 kmol m^{-3} aqueous MDEA solution at 40°C. Figure 5.6 reveals that there is slightly less agreement between CO_2 solubility measurements made in this work with those of Jou et al. (1982) for a 4.28 kmol m^{-3} aqueous solution at 40°C at moderate loadings between 0.01 and 0.1 moles CO_2 per mole MDEA. However, agreement appears to be satisfactory at a CO_2 loading of 0.003 moles CO_2 per mole MDEA and at higher loadings.

Table 5.2. Solubility of CO_2 in 2.5 kmol m^{-3} MEA solution at 40 and 80°C. Amine concentration is CO_2 free. α_{CO_2} = CO_2 loading in mole CO_2 / mole MEA.

T	P_{CO_2}	α_{CO_2}		T	P_{CO_2}	α_{CO_2}	
(°C)	(kPa)	S 1	S 2	(°C)	(kPa)	S 1	S 2
40.0	0.0934	0.354	0.351	80.0	1.01	0.267	0.266
	0.298	0.419	0.415		7.04	0.405	0.403
	2.48	0.500	0.502		155.6	0.591	0.592
	92.6	0.676	0.698		228.7	0.620	0.620

S = Sample number.

Table 5.3. Solubility of CO_2 in 2.0 and 4.28 kmol m^{-3} MDEA solution at 40°C. Amine concentrations are CO_2 free. α_{CO_2} = CO_2 loading in mole CO_2 / mole MDEA.

[MDEA]	P_{CO_2}	α_{CO_2}		[MDEA]	P_{CO_2}	α_{CO_2}	
(kmol m^{-3})	(kPa)	S 1	S 2	(kmol m^{-3})	(kPa)	S 1	S 2
2.0	0.0056	0.00603	0.00600	4.28	0.0102	0.00314	0.00331
	0.0151	0.0117	0.0118		0.118	0.0140	0.0141
	0.0452	0.0215	0.0216		0.585	0.0367	0.0360
	0.177	0.0444	0.0470		3.04	0.105	0.105
	0.419	0.0740	0.0740		93.6	0.671	0.663
	0.887	0.113	0.113		93.6	0.652	
	6.95	0.362	0.351				
	92.8	0.842	0.838				

S = Sample number

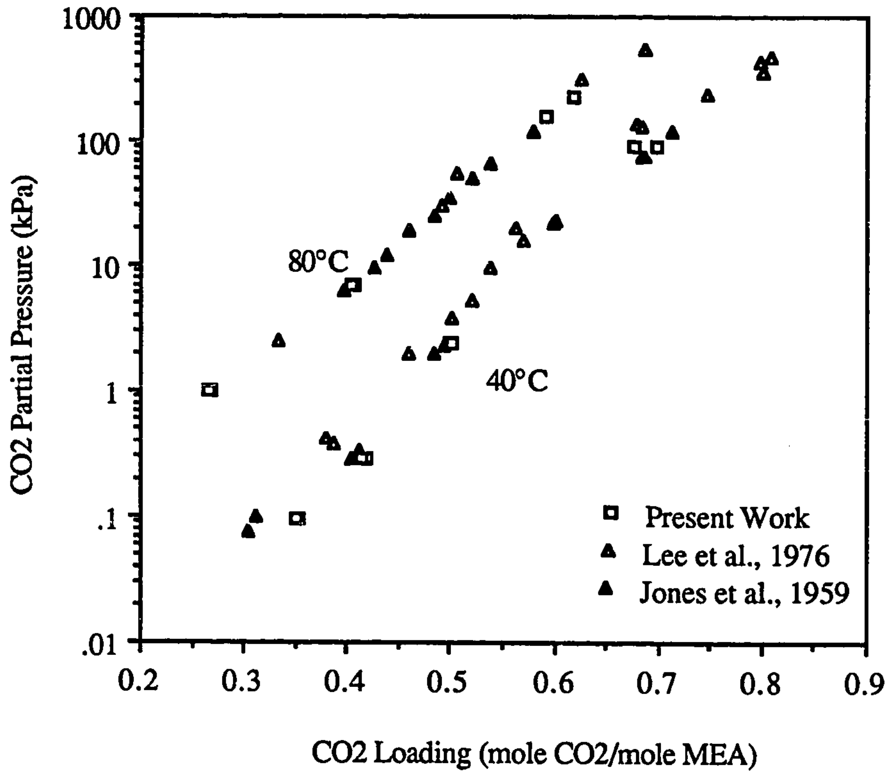

Figure 5.4 Solubility of CO_2 in 2.5 kmol m^{-3} MEA aqueous solution at 40 and 80°C. Amine concentration is based on a CO_2 free solution.

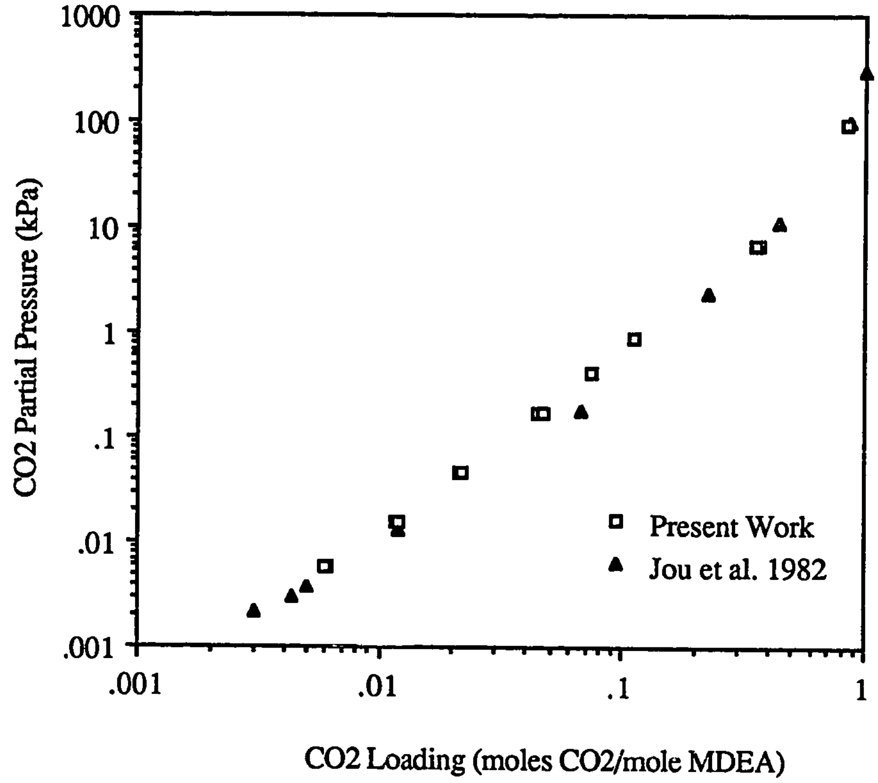

Figure 5.5 Solubility of CO_2 in 2.0 kmol m^{-3} MDEA aqueous solution at 40°C. Amine concentration is based on a CO_2 free solution.

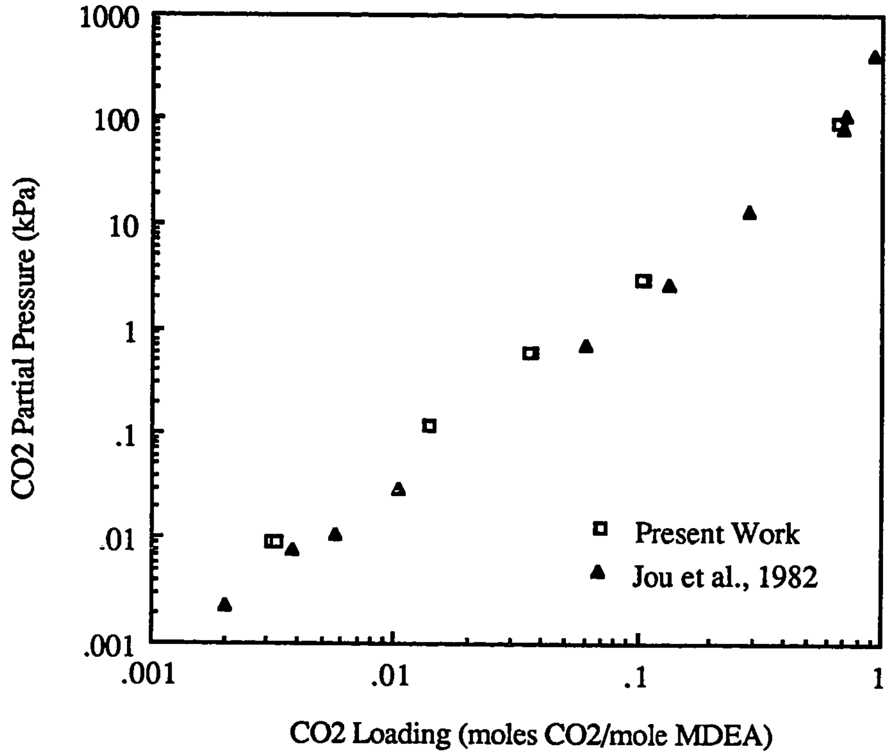

Figure 5.6 Solubility of CO_2 in a 4.28 kmol m^{-3} MDEA aqueous solution at 40°C. Amine concentration is based on a CO_2 free solution.

The agreement of the CO_2 solubility measurements in the aqueous MEA and MDEA solutions made in this work with literature data suggested that the experimental method employed here was valid. Therefore, CO_2 solubility measurements were made in aqueous mixtures containing 2 kmol m^{-3} MDEA plus 2 kmol m^{-3} MEA or 2 kmol m^{-3} DEA. An amine mixture such as this, equimolar in MDEA with a primary or secondary amine, would not normally be used in an industrial gas treating application for bulk CO_2 removal. The presence of such a high concentration of MEA or DEA in an MDEA based solvent would negate the energy advantages of using MDEA for CO_2 removal. MEA or DEA would be used at lower concentrations primarily to enhance the CO_2 absorption rate. However, one objective of this work was to test the validity of the extended VLE model for the mixed amine/CO_2 systems. It was felt that the model would be most rigorously tested by comparing model representation with experimental CO_2 solubility measurements in a mixture containing relatively high concentrations of both MDEA and MEA or DEA. Furthermore, the only additional/unique adjustable parameters that arise for the mixed amine systems are related to the protonated MDEA cation and the MEA or DEA carbamate anions. It was, therefore, desirable to have high concentrations of both MDEA and MEA or DEA simultaneously in the solution so that the model calculations would be sensitive to the additional parameters.

Measurements of CO_2 solubility in the mixed amine solutions were made at 40 and 80°C over the CO_2 pressure range from 0.05 to approximately 300 kPa. Most measurements at 40°C were made at total pressures equal to atmospheric pressure. Solubility measurements at 80°C were made at total pressures from 200 to 300 kPa.

Results of the CO_2 solubility measurements in the amine mixtures are summarized in Tables 5.4 and 5.5. These results are examined in relation to CO_2 solubility in 4 kmol m^{-3} MDEA, 4 kmol m^{-3} MEA, and 4 kmol m^{-3} DEA solutions with results of the modeling work in Chapter Seven.

Table 5.4. Solubility of CO_2 in 2.0 kmol m^{-3} MDEA , 2.0 kmol m^{-3} MEA aqueous solution at 40 and 80°C. Amine concentration is CO_2 free. α_{CO_2} = CO_2 loading in mole CO_2 / mole amine.

T	P_{CO_2}	α_{CO_2}		T	P_{CO_2}	α_{CO_2}	
(°C)	(kPa)	S 1	S 2	(°C)	(kPa)	S 1	S 2
40.0	0.0506	0.156	0.157	80.0	0.304	0.0756	0.0759
	0.122	0.199	0.198		1.65	0.151	0.152
	0.323	0.243	0.245		9.54	0.257	0.256
	0.724	0.289	0.286		111.8	0.439	0.440
	2.48	0.358	0.354		168.5	0.486	0.482
	8.99	0.446	0.449		258.2	0.524	0.526
	51.7	0.601	0.594				
	93.1	0.649	0.649				
	203.7	0.710	0.726				
	312.9	0.781	0.777				

S = Sample number.

Table 5.5. Solubility of CO_2 in 2.0 kmol m^{-3} MDEA , 2.0 kmol m^{-3} DEA Aqueous Solution at 40 and 80°C. Amine concentration is CO_2 free. α_{CO_2} = CO_2 loading in mole CO_2 / mole amine.

T	P_{CO_2}	α_{CO_2}		T	P_{CO_2}	α_{CO_2}	
(°C)	(kPa)	S 1	S 2	(°C)	(kPa)	S 1	S 2
40.0	0.136	0.0748	0.0750	80.0	0.455	0.0240	0.0242
	0.276	0.107	0.107		1.42	0.0471	0.0469
	0.769	0.171	0.171		9.06	0.132	0.130
	2.24	0.257	0.256		120.0	0.373	0.379
	5.92	0.341	0.340		178.4	0.440	0.432
	24.2	0.492	0.486		259.1	0.495	0.494
	93.2	0.655	0.650				
	205.2	0.741	0.745				
	203.4	0.746	0.753				
	309.3	0.802	0.793				

S = Sample number

Chapter Six

Representation of Equilibria in H_2S-CO_2-Alkanolamine-Water Systems

6.1 Introduction

To achieve good representation of acid gas solubility in aqueous solutions of alkanolamines it was necessary to fit the VLE model described in Chapter Four to reported acid gas - alkanolamine - water VLE data. As discussed in Chapter Four, the adjustable parameters of the model are the carbamate stability constants for MEA, DEA, and DGA and binary energy interaction parameters of the Electrolyte - NRTL equation. Best values of the carbamate stability constants and the adjustable NRTL binary interaction parameters were determined by fitting the model to reported solubility data using the Data Regression System (DRS) of ASPEN PLUS process simulator.

It is the purpose of this chapter to present a critical analysis of the quality of representation of acid gas solubility in aqueous solutions of a *single* amine with the VLE model presented in Chapter Four and to provide a summary and analysis of adjusted parameter values. Prausnitz et al. (1980) suggest plotting residuals, the difference between the estimated *true* values and the measured values of the state variables, to evaluate representation of experimental VLE data. The *true* values of each measured state variable are the maximum likelihood estimates of the state variables that are found during the course of data regression using the maximum likelihood method. Good agreement between maximum likelihood estimates of state variables and experimentally measured values of state variables indicate good representation of the data. Hence, residual plots provide a visual means of assessing quality of data representation. They can also reveal random experimental error, consistent or systematic experimental error, or a 'lack of fit' of the data by the model.

For the systems of interest in this work, reported values of the experimentally measured state variables - partial pressure and acid gas apparent mole fraction - vary over several orders of magnitude. Therefore, to provide scaling, the *ratios* of the *true* to measured values of equilibrium acid gas pressure and apparent mole fraction in the liquid phase were plotted rather than the residuals in order to evaluate representation.

6.1.1 Adjustable Parameters and Data Regession: A Review

There are three types of binary interaction parameters in the NRTL contribution to the excess Gibbs energy or activity coefficient: **molecule-molecule** ($\tau_{m,m'}$ and $\tau_{m',m}$), **molecule-ion pair** ($\tau_{m,ca}$ and $\tau_{ca,m}$), and **ion pair-ion pair** (with a common cation or anion) ($\tau_{ca,ca'}$ and $\tau_{ca',ca}$ or $\tau_{ca,c'a}$ and $\tau_{c'a,ca}$). An advantage of local composition models such as the NRTL equation is that binary parameters of a multicomponent system and of its constituent binary systems are the same and no higher-order parameters are required. Best values of these binary parameters for the systems under consideration in this study were, therefore, determined by data regression using binary and ternary system VLE data (TPx).

Using the DRS of ASPEN PLUS, **molecule-molecule** binary parameters were first adjusted on experimental binary system (molecule-molecule, ie. amine-water) data reported in the literature or provided by Texaco Chemical Company. Best values of **molecule-ion pair** and **ion pair-molecule** interaction parameters were then determined by fixing molecule-molecule parameters at previously estimated values and fitting molecule-ion pair parameters on ternary system (i.e. H_2S-amine-H_2O and CO_2-amine-H_2O) VLE (Tpx) data reported in the literature. Best values of the carbamate stability constants for MEA, DEA, and DGA were determined simultaneously with the corresponding Electrolyte-NRTL parameters on CO_2-amine-water data. Following Chen and Evans (1986) all **ion pair-ion pair** parameters were fixed at zero. Recall that binary interaction parameters were assumed to be temperature dependent and were fitted to the following function of temperature:

$$\tau = a + b/T \tag{4.67}$$

In the H_2S-CO_2-alkanolamine-H_2O system there are up to 8 ionic species and 4 molecular species present in the liquid phase (Am, H_2S, CO_2, H_2O, AmH^+, H_3O^+, $AmCOO^-$, HS^-, S^{-2}, HCO_3^-, CO_3^{-2}, OH^-). Therefore, a large number of binary parameters, molecule-molecule, molecule-ion pair, and ion pair-ion pair can, in principle, be formulated for this system. However, as discussed earlier, many of these species are present in the liquid phase at low or negligible concentrations. Hence, parameters associated with them do not significantly affect representation of VLE. Important parameters of the system, those that affected representation of alkanolamine-acid gas-water VLE data, were identified by the statistical significance with which they could be fitted on experimental VLE data as measured by estimates of the standard deviations of the parameter values.

For all ternary systems (acid gas-alkanolamine-water), the only molecule-ion pair and ion pair-molecule interaction parameters that could be estimated with statistical significance were those for which the molecule was water. This was not unexpected; for VLE data reported in the literature, the other molecular species in the system, alkanolamines and acid gases, are generally present at concentrations below 10 and 3 mole percent; water is usually present in excess of 90 mole percent.

All molecule-molecule parameters that could not be adjusted with statistical significance were fixed at default values of zero. All water-ion pair and ion pair-water parameters that could not be adjusted with statistical significance were fixed at default values of 8.0 and -4.0 respectively. All alkanolamine-ion pair and ion pair-alkanolamine binary parameters and all acid gas-ion pair and ion pair-acid gas binary parameters that could not be adjusted with statistical significance were fixed at values of 15.0 and -8.0, respectively. These molecule-ion pair and ion pair-molecule default values represent approximate average values of a large number of water-ion pair and organic solvent-ion pair parameters reported by Chen et al. (1982) and Mock et al. (1986), respectively, for strong electrolyte systems.

The only additional Electrolyte-NRTL parameters that arise for the corresponding single amine quaternary systems including both H_2S and CO_2 (H_2S-CO_2-amine-H_2O) are acid gas-ion pair and ion pair-ion pair parameters. Following the approach adopted for ternary systems, these were fixed at default values. No additional parameters were adjusted on quaternary system data. To test representation of reported quaternary system data, parameters fitted on the binary and ternary systems were fixed at best adjusted values or default values and maximum likelihood estimates were made of reported experimental data (temperature, acid gas pressure, acid gas apparent mole fractions in the liquid phase).

6.2 Binary (Nonelectrolyte) System VLE Representation

Three constituent binary mixtures can, in principle, be formed from the acid gas-alkanolamine-water system. These are the alkanolamine-water, acid gas-water, and acid gas-alkanolamine mixtures. Since the first two (alkanolamine-water and acid gas-water) are aqueous *single* weak electrolyte systems, and the degree of dissociation of electrolyte in each is negligible except at high dilutions, chemical equilibria can be ignored. Hence, the VLE model for these systems reduces to equations (4.4) and (4.7) (isofugacity conditions).

It is not necessary to model VLE behavior of the acid gas-alkanolamine system for the purposes of fitting the corresponding binary interaction parameters because there are no data reported for these systems. Moreover, as suggested earlier, the binary parameters associated with the acid gas-alkanolamine pair were found not to affect representation of VLE data in aqueous solutions; because of chemical reaction, these species are never simultaneously present in aqueous solution at significant concentrations. Indeed, it was found that the corresponding binary interaction parameters could not be adjusted with physical significance nor could values other than zero lead to a substantially reduced objective function when they were adjusted on ternary system (acid gas-alkanolamine-water) data.

It was noted earlier that the Electrolyte-NRTL equation reduces to the NRTL equation (Renon and Prausnitz, 1968) when no ionic species are present in solution. As suggested above, it is a valid to assume that no ionic species are present in aqueous solutions of either an alkanolamine or an acid gas for the purpose of modeling the VLE behavior of these binary systems. Hence, the NRTL equation was used to represent activity coefficients in the relevant binary systems. The NRTL binary interaction (**molecule-molecule**) parameters fitted on the binary system data are entirely consistent with corresponding parameters of the Electrolyte-NRTL equation. The NRTL equation also contains a single nonrandomness parameter corresponding to each pair of interaction parameters (see equation 4.57). To be consistent with the approach adopted for acid gas-alkanolamine-water systems, nonrandomness parameters for binary molecular pairs were fixed at a value of 0.2.

6.2.1 Data Sources

Acid gas-water interaction parameters were fitted in the earlier work of Chen and Evans (1986). Water-alkanolamine interaction parameters were fitted on experimental VLE data reported in the literature or in-house VLE data provided by Texaco Chemical Co. The data provided by Texaco Chemical have not been published. They were employed in this work because there are very few reliable VLE measurements for the DEA-water, MDEA-water, and DGA-water systems reported in the literature.

As noted in section 4.4.5, the maximum likelihood method requires estimates of the standard deviations of all measured state variables. These standard deviations are used in the maximum likelihood objective function in a manner similar to the use of weighting coefficients (for example, see equation 4.79). Standard deviations of experimental data for the systems of interest in this work are rarely reported and few replicate measurements are reported to allow estimation of standard deviations. Fortunately, as suggested by equation (4.79) only relative values of the standard deviations are important; absolute values of standard deviations are not necessary. Therefore, estimation of standard deviations for all measured variables is equivalent to implicitly assigning a weight to the respective variable; the smaller the standard deviation, the higher the weight. For binary systems, standard deviations were generally estimated as follows: $\sigma_T = 0.2$ K, $\sigma_P = 0.05$ x pressure, and $\sigma_x = 0.01$. A *relative* standard deviation was selected for pressure so that high pressure data would not be weighted more heavily than low pressure data during minimization of the objective function.

Sources of amine-water VLE data are summarized in Table 6.1 together with the ranges of temperature, pressure, and amine composition over which the data extend. The Data Regression System of ASPEN allows an explicit relative weight to be assigned to data sets as a whole. These weights are not to be confused with weights discussed above that are implicitly assigned to individual measured variables through estimation of experimental standard deviations. The relative weights assigned to each data source are also reported in Table 6.1.

6.2.2 Parameter Estimation Results

Fitted values of the NRTL binary interaction parameters (coefficients of equation 4.67) for amine-water and acid gas-water systems are reported in Table 6.2 together with the corresponding standard deviations of the estimated parameter values. Recall that the DRS system provides an estimate of the parameter estimation errors in the form of the variance-covariance matrix based on the premise that a linearized form of the VLE model is valid in a region about the maximum likelihood estimates of the

Table 6.1. Summary of literature sources of experimental VLE data used for adjusting amine-water binary interaction parameters.

Data source	Relative weight	Amine mole fraction range	Temperature range (°C)	Pressure range (mm Hg)
MEA-H_2O				
Touhara et al., 1982	1.0	0 - 1	25.0, 35.0	0.48 - 42
Nath and Bender, 1983	1.0	0 - 1	60.0, 78.0, 91.7	9.8 - 568.8
DEA-H_2O				
Texaco Chemical 1988*	1.0	0.2 - 0.8	44.4 - 183.2	49.5 - 746.8
Dow Chemical 1962	0.1	0 - 1	37.8 - 115.6	10.2 - 680.0
MDEA - H_2O				
Texaco Chemical 1988*	1.0	0.05 - 0.78	61.3 - 159.4	145.6 - 748.3
Kuwairi, 1962	0.1	0.02, 0.045	45.0 - 155.8	7.33 - 428.9
DGA - H_2O				
Texaco Chemical 1988*	1.0	0.25 - 0.76	68.9 - 154.9	89.6 - 742.9

* In-house data, not published.

Table 6.2. Fitted values of NRTL binary interaction parameters for alkanolamine - H_2O systems.

$$\tau = a + b/T$$

Molecule Pair	a	σ_a	b(°K)	σ_b
H_2O-MEA	1.674	0.24	0.00	*
MEA-H_2O	0.000	*	-649.75	38.1
H_2O-DEA	-0.965	1.64	1317.63	618.1
DEA-H_2O	-0.661	0.64	-718.08	233.9
H_2O-MDEA	3.895	0.12	0.00	**
MDEA-H_2O	-2.471	0.03	0.00	**
H_2O-DGA	1.992	0.35	0.00	*
DGA-H_2O	0.000	*	-770.41	62.2
H_2O-H_2S	-3.674	†	1155.9	†
H_2S-H_2O	-3.674	†	1155.9	†
H_2O-CO_2	10.064	†	-3268.14	†
CO_2-H_2O	10.064	†	-3268.14	†

$\alpha = 0.2$

* Parameter fixed at bound, could not be estimated with statistical significance by DRS.

** Parameter was fixed at zero in DRS input file, no standard deviation was estimated.

† Parameter was fitted in earlier work of Chen and Evans (1986), standard deviations were not reported.

measured variables and model parameters. The diagonal elements of this matrix represent the variances of the various estimated parameters. The square roots of these variances are estimates of the standard deviations in the parameters. They are, in effect, measures of the uncertainties in the parameter estimates. That is, the standard deviations reported in Table 6.2 are a measure of the statistical significance with which each of the corresponding parameters could be estimated.

As the results summarized in Table 6.2 indicate, one of the coefficients of equation (4.67) for each of the corresponding binary interaction parameters were assigned a value of zero for several of the amine-water mixtures. This occurred either because the parameter values encountered a bound during minimization of the objective function (MEA and DGA) or they were fixed at zero because it was evident that little improvement in VLE representation could be made by adjusting the parameter. For MEA, MDEA, and DGA, parameters other than those fixed at zero were determined with a high degree of confidence as implied by the low values of the parameter standard deviations relative to the absolute parameter values. The parameters corresponding to the DEA-water mixture reported in Table 6.2 have high parameter standard deviations. As will be shown shortly, the reported DEA-water parameters allow for very good representation of the data to which they were fitted even though the parameters are not well determined. It appears likely that the poor confidence in the DEA-water parameters is due to a high degree of correlation between the corresponding parameters.

Recall that the off-diagonal elements of the variance-covariance matrix represent the covariances between adjustable parameters. Covariances are a measure of the correlation between corresponding parameters. The correlation coefficient, ρ, between two parameters - θ_1 and θ_2 - is defined as

$$\rho(\theta_1, \theta_2) = \frac{\mathrm{cov}(\theta_1, \theta_2)}{\sigma_{\theta 1}\sigma_{\theta 2}} \tag{4.75}$$

where $\mathrm{cov}(\theta_1, \theta_2)$ is the covariance between the two parameters θ_1 and θ_2, and $\sigma_{\theta 1}$ and $\sigma_{\theta 2}$ are the estimated standard deviations of the parameters θ_1 and θ_2. Parameters that are completely independent have a correlation coefficient of zero. Parameters that are perfectly correlated have a correlation coefficient of ±1. If two parameters are highly correlated, it is difficult to determine them uniquely. ASPEN PLUS DRS produces the matrix of correlation coefficients corresponding to the parameter variance-covariance matrix. The elements of the correlation coefficient matrix are estimated correlation coefficients for corresponding adjustable parameters.

It is well known that the parameters of the NRTL equation are often highly correlated (Renon 1985). Correlation coefficient matrices for the relevant amine-water mixtures are reported in Appendix B. The correlation coefficient matrices in Appendix B for the amine-water systems show that the NRTL parameters for the amine-water systems of interest in this work are, indeed, highly correlated. In particular, the correlation coefficient matrix for the DEA-water system indicates that the coefficients 'a' and 'b' of equation (4.67) for each binary interaction parameter of the DEA-water system (ie., $\tau_{DEA\text{-}H_2O}$ and $\tau_{H_2O\text{-}DEA}$ parameters) are highly correlated. Moreover, 'a' coefficients of the corresponding binary interaction parameters are highly correlated as are 'b' coefficients for the DEA-water system. This high degree of correlation may be the cause of the large relative standard deviations in parameters for the DEA-water system.

6.2.3 Binary System Data Representation

Figures 6.1 through 6.8 are graphical summaries of the *ratios* of estimated *true* (maximum likelihood estimates) to experimentally measured values of equilibrium system pressure (total) and liquid phase mole fraction of amine. Because of the small standard deviation assigned to experimentally reported values of system temperature, estimated *true* values of the system temperature were always in close agreement with measured values. It was, therefore, unnecessary to examine similar plots for temperature.

Each data point on Figures 6.1 through 6.8 represents a unique state variable (either pressure or composition) measurement used in parameter estimation. For MEA-water mixtures, data at different temperatures were given different plot symbols, and for DGA-water mixtures, data at different mole fractions were given different plot symbols. Also note that for the MEA-water system, ratios of the *true* to measured state variables are plotted against MEA mole fraction while for all other systems the corresponding ratios were plotted against total system pressure. This was done simply as a matter of convenience. The TPx data supplied by Texaco for DEA, MDEA, and DGA water mixtures reported pressure and temperature measurements at three (widely ranging) amine mole fractions only. Hence, plots of the ratios of state variables for MEA-, DEA-, and MDEA-water mixtures yield more information when ratios are plotted as a function of pressure rather than as a function of mole fraction.

If all experimental data were error-free, and if the VLE model fit the data perfectly, all *ratios* of the *true* to measured equilibrium system pressures and liquid phase mole fractions in Figures 6.1 through 6.8 would assume values of unity. It can be seen in these figures that most values of the pressure and amine mole fraction ratios lie in a band within 2.5 to 5 percent of unity. These results suggest that the NRTL equation satisfactorily represents activity coefficients of amine and water in the represented amine-water mixtures.

While the absolute values of the pressure and amine mole fraction ratios suggest that the data are well represented by the model, there appears to be a slightly nonrandom distribution of ratios about a value of unity for the MEA-water and DGA-water mixtures. The nonrandom distribution is clearly seen in Figures 6.7 and 6.8 for the DGA-water mixture; the values of both the pressure and mole fraction ratios are consistently above unity for DGA mole fractions of 0.252 and 0.398, and consistently below unity for a DGA mole fraction of 0.764. Still, the proximity of the pressure and amine mole fraction ratios to unity for all pertinent amine-water mixtures suggests that the apparent lack of fit as a function of amine concentration is relatively unimportant.

As noted earlier, the nonrandomness parameters, α, corresponding to all amine-water mixtures, were fixed at a value of 0.2. To improve representation of the amine-water VLE data, the nonrandomness parameters could have been treated as adjustable, and best values of these parameters could have been estimated simultaneously with the binary interaction parameters.

It was also noted earlier that acid gas-water parameters were taken from the work of Chen and Evans (1986). Since they used the same CO_2 and H_2S Henry's constants in equation (4.4) to fit the CO_2 and H_2S NRTL binary interaction parameters as those adopted here, the use of the parameters reported by Chen and Evans in this work is valid. In estimating the H_2S-water and CO_2-water binary energy interaction parameters on H_2S and CO_2 solubility data, Chen and Evans (1986) also used a value of 0.2 for the corresponding nonrandomness parameters, α_{CO_2} and α_{H_2S}.

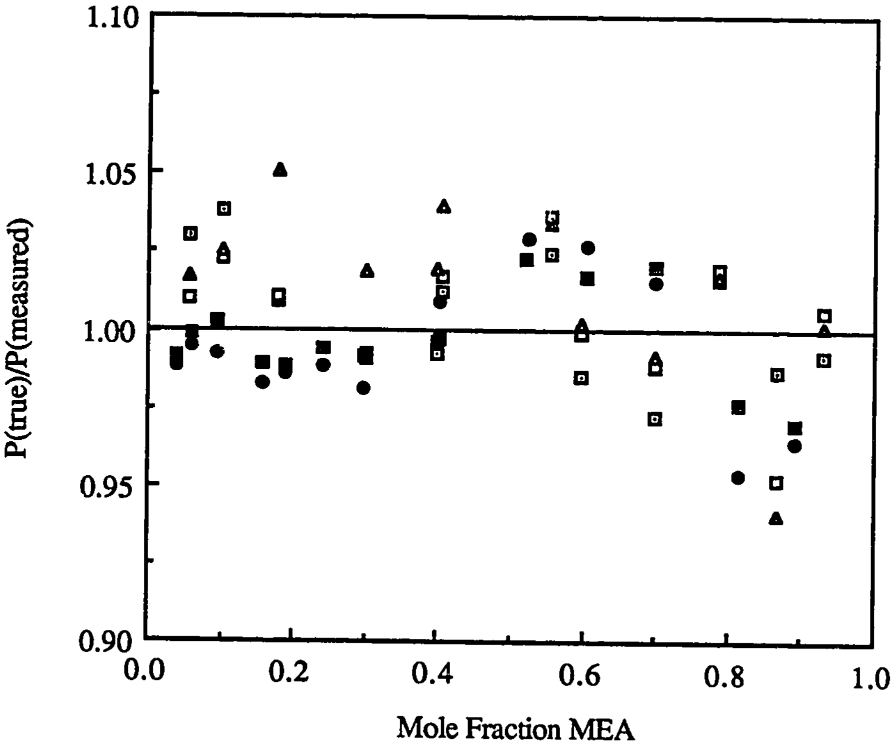

Figure 6.1 Comparison of maximum likelihood estimates and experimentally measured values of total system pressure in MEA-water mixtures. Nath and Bender, 1983: (▣) 60°C; (□) 78°C; (▲) 92°C. Touhara et al., 1982: (●) 25°C; (■) 35°C.

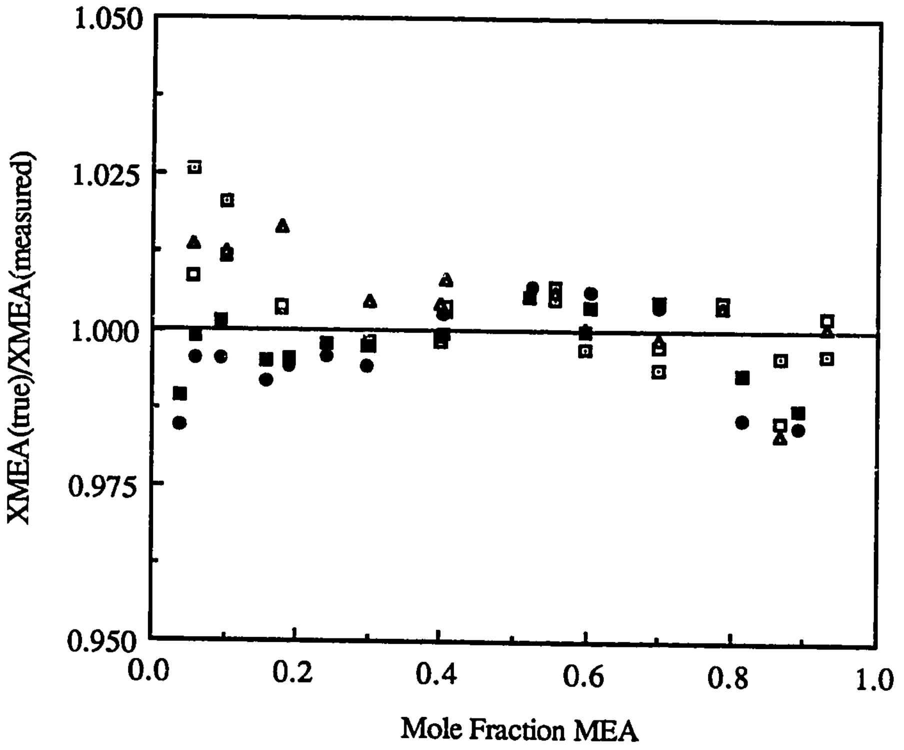

Figure 6.2 Comparison of maximum likelihood estimates and experimentally measured values of the liquid phase mole fraction of MEA in MEA-water mixtures. Nath and Bender, 1983: (▣) 60°C; (□) 78°C; (▲) 92°C. Touhara et al., 1982: (●) 25°C; (■) 35°C.

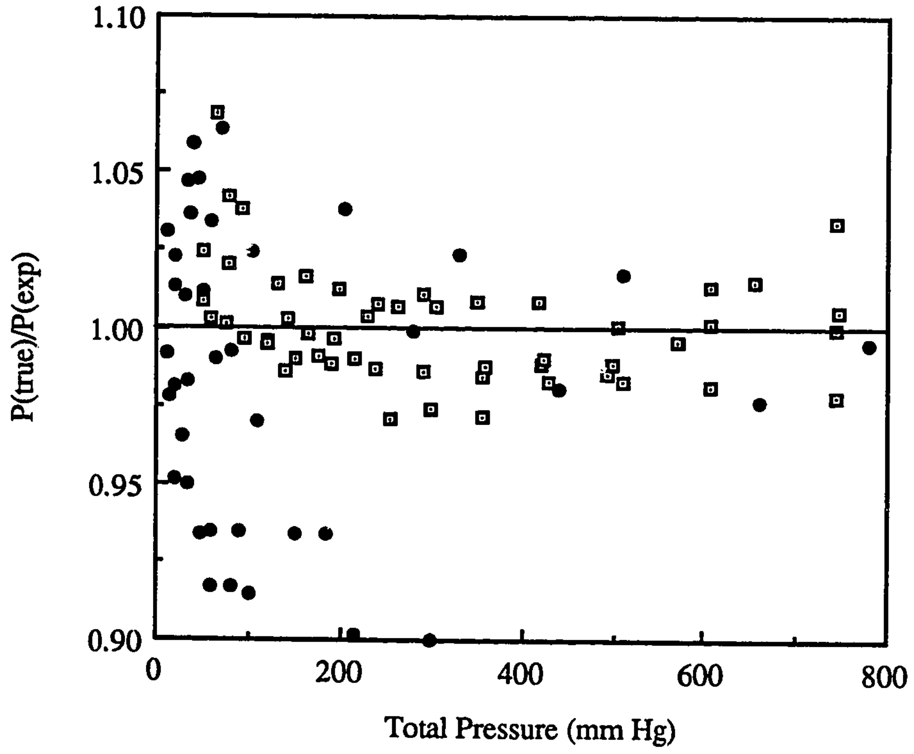

Figure 6.3 Comparison of maximum likelihood estimates and experimentally measured values of the total pressure in DEA-water mixtures. (▫) Texaco Chemical Co., 1988; (●) Dow Chemical Co., 1962 (weight = 0.1).

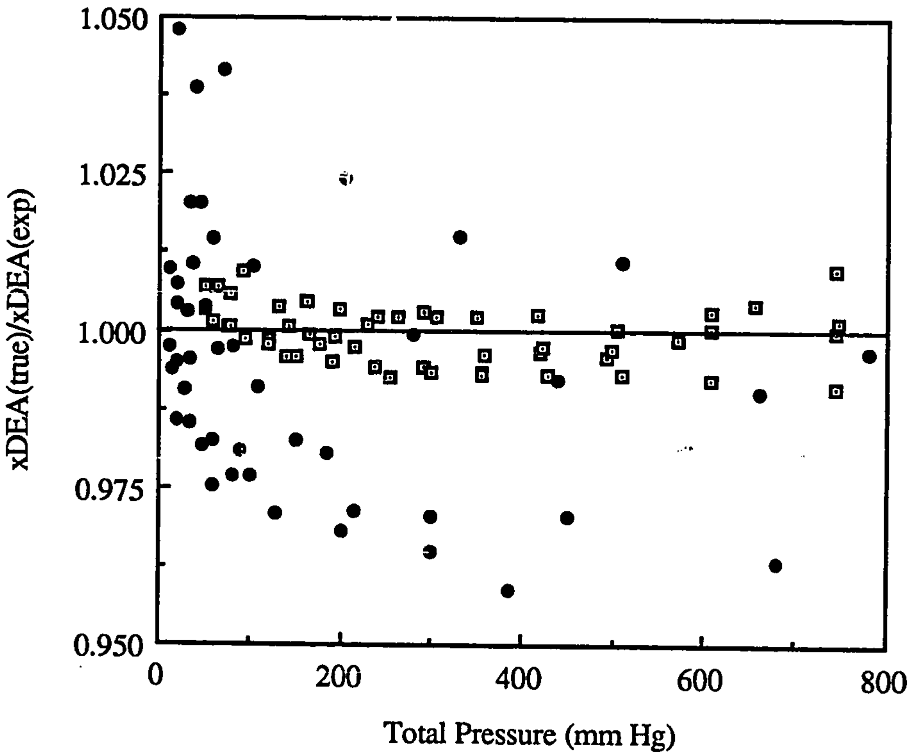

Figure 6.4 Comparison of maximum likelihood estimates and experimentally measured values of the liquid phase mole fraction of DEA in DEA-water mixtures. (◘) Texaco Chemical Co., 1988; (●) Dow Chemical Co., 1962 (weight = 0.1).

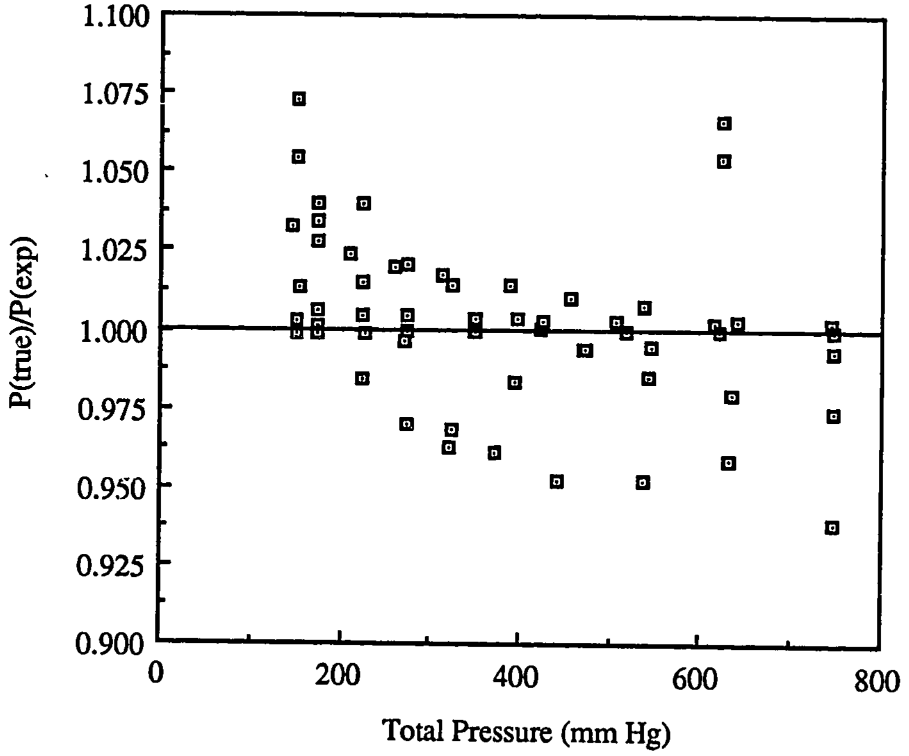

Figure 6.5 Comparison of maximum likelihood estimates and experimentally measured values of the total pressure in MDEA-water mixtures. (▫) Texaco Chemical Co., 1988.

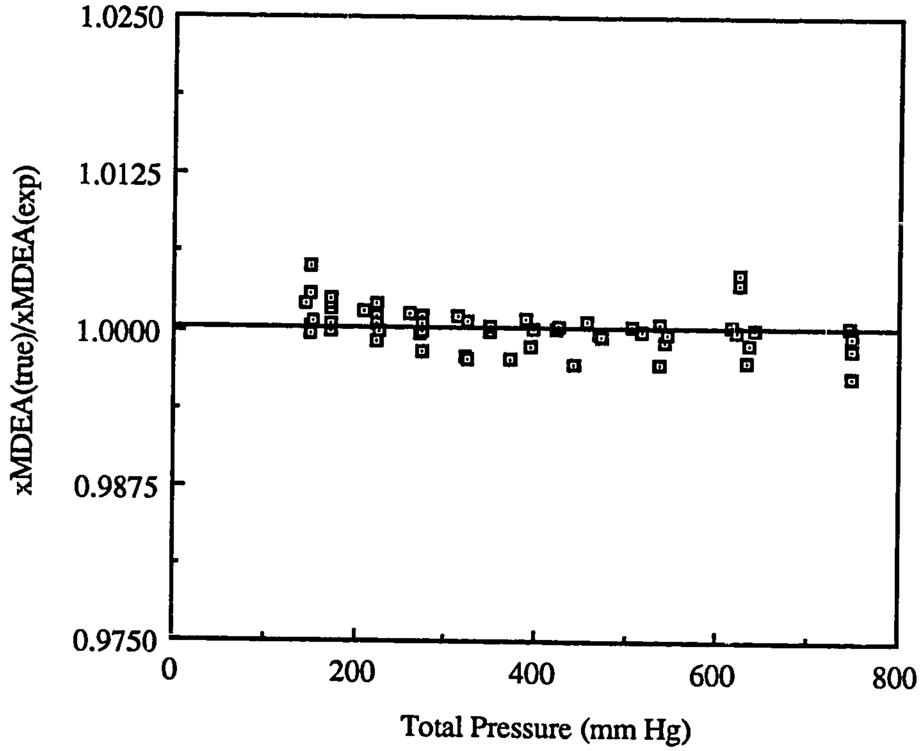

Figure 6.6 Comparison of maximum likelihood estimates and experimentally measured values of the liquid phase mole fraction of MDEA in MDEA-water mixtures. (▣) Texaco Chemical Co., 1988.

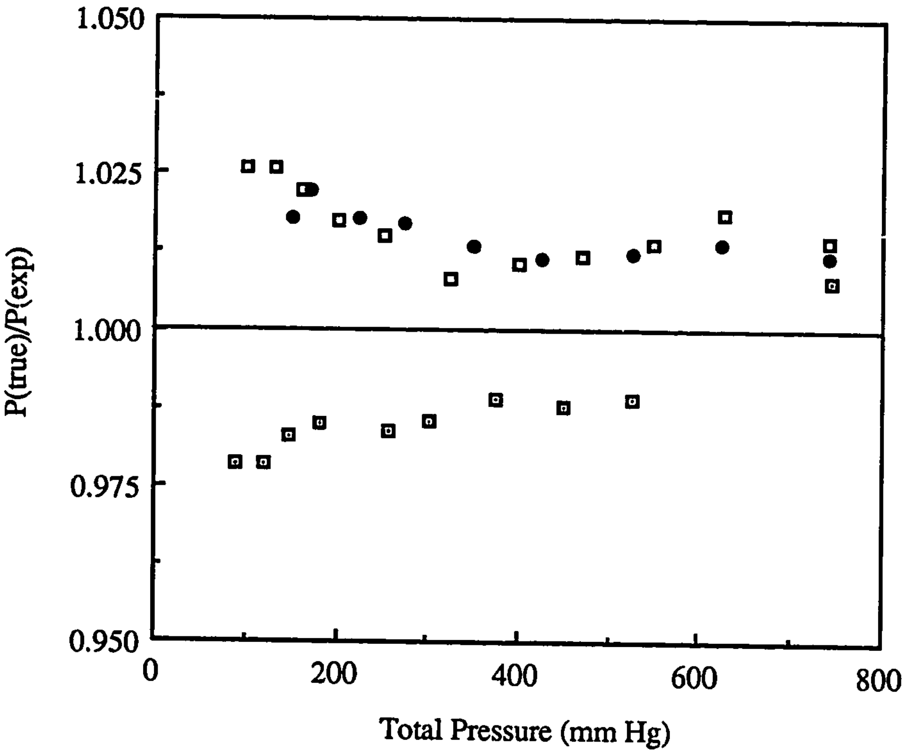

Figure 6.7 Comparison of maximum likelihood estimates and experimentally measured values of the total system pressure in DGA-water mixtures. Texaco Chemical Co. 1988: (◘) x(DGA)=0.764; (◘) x(DGA)=0.398; (●) x(DEA)=0.252.

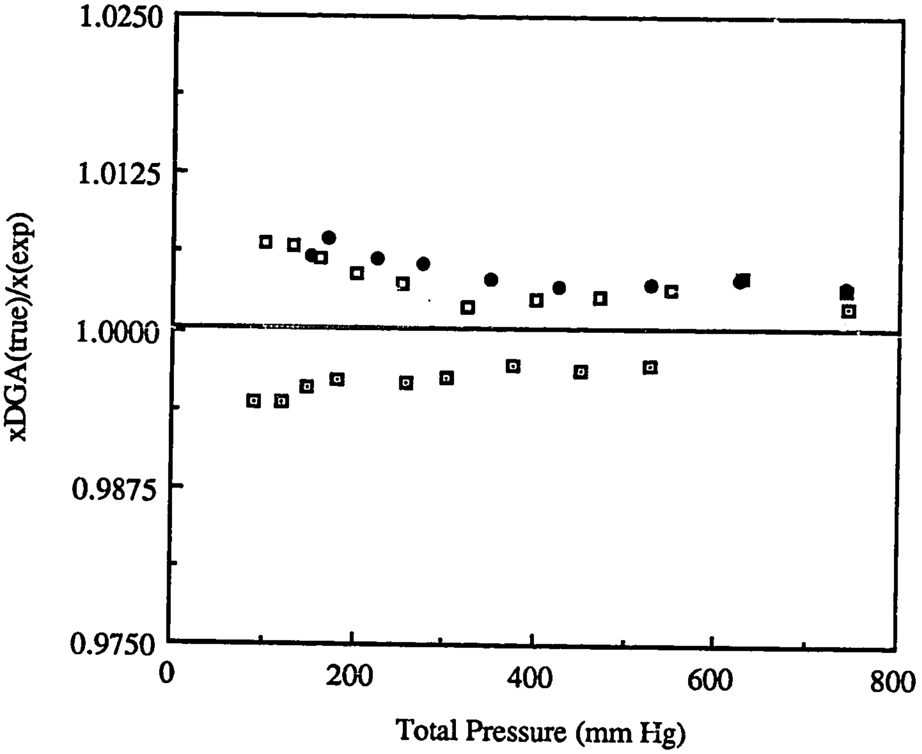

Figure 6.8 Comparison of maximum likelihood estimates and experimentally measured values of the liquid phase mole fraction of DGA in DGA-water mixtures. Texaco Chemical Co.: (▣) x(DGA)=0.764; (□) x(DGA)=0.398; (●) x(DEA)=0.252.

6.2.4 Nonideality in the Binary Systems

The results of modeling the binary alkanolamine-water VLE data suggest that the alkanolamine-water liquid mixtures of interest in this work exhibit strong negative deviations from ideality. This was ascertained by fixing the NRTL binary interaction parameters at the adjusted values and generating the excess Gibbs energy (relative to RT) and activity coefficients for each of the relevant alkanolamine-water mixtures. The excess Gibbs energies of aqueous solutions of MEA, DEA, MDEA, and DGA are plotted as functions of water concentration in Figure 6.9 at 298.15 °K. The results indicate that for the systems of interest in this work, molar excess Gibbs energy varied in the following order:

$$g^{ex}_{\text{DEA-water}} \approx g^{ex}_{\text{DGA-water}} < g^{ex}_{\text{MEA-water}} < g^{ex}_{\text{MDEA-water}}$$

This suggests that DEA-water and DGA-water mixtures exhibit the strongest deviations from ideality.

Through the measurement of vapor pressures, De Oliveira et al. (1980) also found that the MEA-water and DEA-water systems (as well as the triethanolamine-water system) exhibited strong negative deviations from ideality, which, they suggest, is due to the formation of hydrogen bonds between ethanol groups and water. Unfortunately De Oliveira and coworkers did not report the conditions of temperature or pressure at which they made vapor pressure measurements. However, they did conclude that

$$g^{ex}_{\text{DEA-water}} < g^{ex}_{\text{MEA-water}}$$

in agreement with the results shown in Figure 6.9.

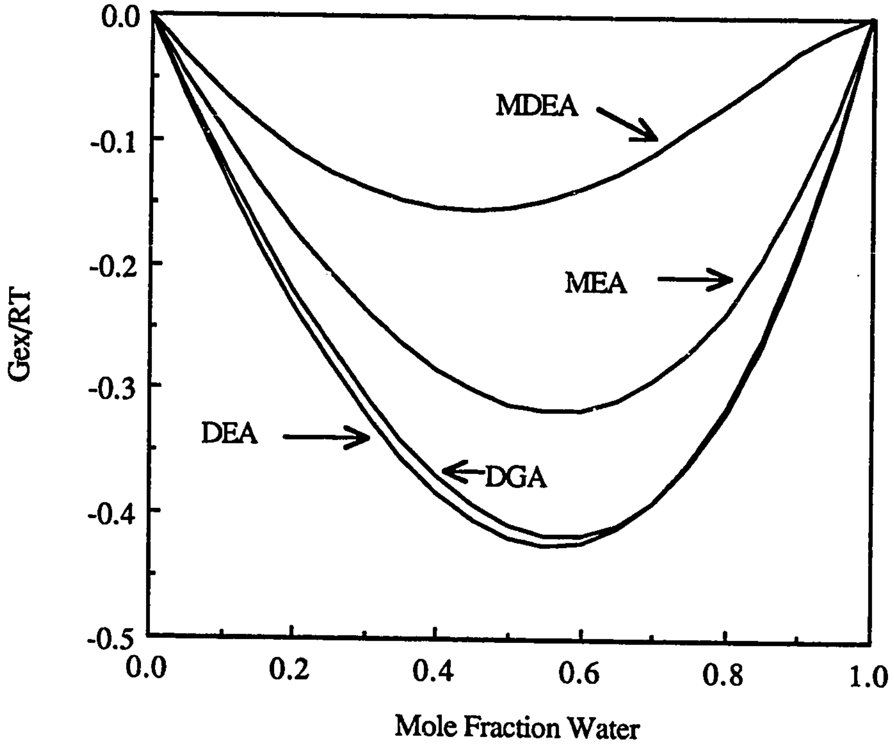

Figure 6.9 Representation of the molar excess Gibbs energy of aqueous solutions of MEA, DEA, MDEA, and DGA at 298.15 °K with the NRTL equation. Parameters of the NRTL equation for these amine-water mixtures are summarized in Table 6.2

Touhara et al. (1982) report vapor pressures, molar excess enthalpies, and densities of 2-aminoethanol (MEA) - water, N-methyl-2-aminoethanol - water, and N,N-dimethyl-2-aminoethanol - water mixtures measured at 298.15 and 308.15 °K over the entire composition range. Touhara and coworkers found that, in accordance with the general characteristics of aqueous solutions of highly hydrophilic compounds, the signs and relative magnitudes of the molar excess functions varied according to

$$0 > g^{ex} > Ts^{ex} > h^{ex}, \quad v^{ex} < 0$$

except for aminoethanol-rich solutions of N,N-dimethyl-2-aminoethanol where g^{ex} was found to be slightly positive. In addition, they found the molar excess Gibbs energy to be smallest in the MEA-water solution and to increase rapidly as methyl groups were added, so that the molar excess Gibbs energy was greatest in the N,N-dimethyl-2-aminoethanol-water solution.

Touhara and coworkers concluded that there are, in effect, opposing contributions from the molar excess entropy and enthalpy to the molar excess Gibbs energy in the systems studied. These effects are best understood by expressing the molar excess Gibbs free energy in terms of the molar excess entropy and enthalpy:

$$g^{ex} = h^{ex} - Ts^{ex} \tag{6.1}$$

Touhara indirectly measured g^{ex} (by vapor pressure measurement) and directly measured h^{ex} (by calorimetric measurements) and used equation (6.1) to calculate molar excess entropies. The negative excess entropies inferred from their results indicate that the aminoethanols which they studied are hydrophobic and that the degree of hydrophobicity increases rapidly with the addition of methyl groups to the amine. However, they also concluded that the mixing process is enthalpy controlled due to strong hydrogen bonding between water and the alkanolamine as indicated by the measured large negative excess enthalpies. In effect, the alkanolamine-water systems studied by Touhara and coworkers exhibit negative deviations from ideality because enthalpic effects are generally predominant over entropic effects.

The results of De Oliveira et al. (1980) and Touhara et al. (1982) provide an explanation for the *relative* deviations from ideality of the MEA-water, DEA-water, and MDEA-water mixtures as indicated by the positions of the molar excess Gibbs energy curves in Figure 6.9. As already noted, the results of De Oliviera et al. indicate that the DEA-water system should exhibit greater deviations from ideality than the MEA-water mixture, perhaps because DEA can potentially form a greater number of hydrogen bonds with water. The results of Touhara et al. suggest that the addition of a methyl group to the amino group in DEA leads to a higher degree of hydrophobicity, a greater negative molar excess entropy, and therefore, a larger (less negative) molar excess Gibbs energy in accordance with the relationship shown in Figure 6.1.

It is difficult to speculate about how the molar excess Gibbs energy of a DGA-water solution should behave relative to the other alkanolamine-water mixtures studied here based on the studies of De Oliveira et al. or on the studies of Touhara et al. Texaco's data, and the analysis presented here, suggest that DGA behaves like DEA in aqueous solution with respect to the excess Gibbs energy, perhaps because the additional oxygen in ethoxy group positioned between the ethanol group and the amino group (see Figure 1.2) is also capable of hydrogen bonding.

Negative deviations from ideality lead to activity coefficients that are smaller than unity. Activity coefficients for both alkanolamine and water are shown over the entire composition range for the binary mixtures MEA-water, DEA-water, MDEA-water, and DGA-water in Figures 6.10 through 6.13. These figures reveal that values of the activity coefficients of MEA, DEA, and DGA are well below unity at 298.15 °K in the dilute amine region. The relative degrees to which activity coefficients of the various amines vary from unity in Figures 6.10 - 6.13 is qualitatively consistent with the degrees to which the (normalized) molar excess Gibbs energies vary from zero in Figure 6.9. Except for MDEA, alkanolamine activity coefficients vary from unity to the greatest extent at infinite dilution.

In practice, the mole fraction of alkanolamine in an acid gas-alkanolamine-water system generally varies from near zero to 0.2. Hence, accurate representation of amine activity coefficients in this region is important, especially for determining the composition of the liquid phase at chemical equilibrium.

Figure 6.12 indicates that activity coefficients in the MDEA-water mixture do not vary from unity to as great an extent as activity coefficients in the MEA-water, DEA-water, and DGA-water mixtures. Moreover, the activity coefficient of MDEA behaves differently than the activity coefficients of MEA, DEA, and DGA in the dilute region. Interestingly, in fitting molecule-ion pair parameters to ternary system data, it was found that better representation of H_2S-MDEA-H_2O and CO_2-MDEA-H_2O data could be achieved by fixing the corresponding pair of MDEA-water interaction parameters at zero rather than at the values reported in Table 6.2. It is unclear if this was due to inaccurate binary system data, leading to incorrect MDEA-water interaction parameters, inaccurate ternary system data (acid gas-MDEA-water) that was simply better represented with MDEA-water interaction parameters fixed at zero, or some anomolous behavior of the MDEA systems that was not accounted for explicitly by the model but was better treated by fixing MDEA-water parameters at zero.

Activity coefficients of H_2S and CO_2 in aqueous solution are shown in Figures 6.14 and 6.15 at 298.15 °K to a solute mole fraction of 0.045. In practice, the concentration of unreacted acid gas rarely exceeds this concentration. Activity coefficients for the CO_2-water and H_2S-water systems were generated with the NRTL equation using values of the corresponding binary interaction parameters reported by Chen and Evans (1986). Note that the acid gas activity coefficients are unsymmetrically normalized so that

$$\ln \gamma_w \rightarrow 1 \text{ as } x_w \rightarrow 1 \quad \text{and} \quad \ln \gamma_i \rightarrow 1 \text{ as } x_i \rightarrow 0$$

Figures 6.14 and 6.15 reveal that deviations from ideality are relatively minor in both acid gas - water systems. At 298.15 °K, the activity coefficient of H_2S is slightly less than unity in aqueous solution while the activity coefficient of CO_2 is greater than unity in aqueous solution in the same concentration range. In neither system does the activity coefficient vary significantly from this value. In view of the activity coefficient normalization convention, this behavior is expected because the mole fraction of water is near unity. Figure 6.16 shows that at higher temperatures, the activity coefficients of H_2S and CO_2 reverse with respect to unity. Gibbs and Van Ness (1971) reported similar findings for the behavior of the CO_2 activity coefficient as a function of temperature in the CO_2 - water system.

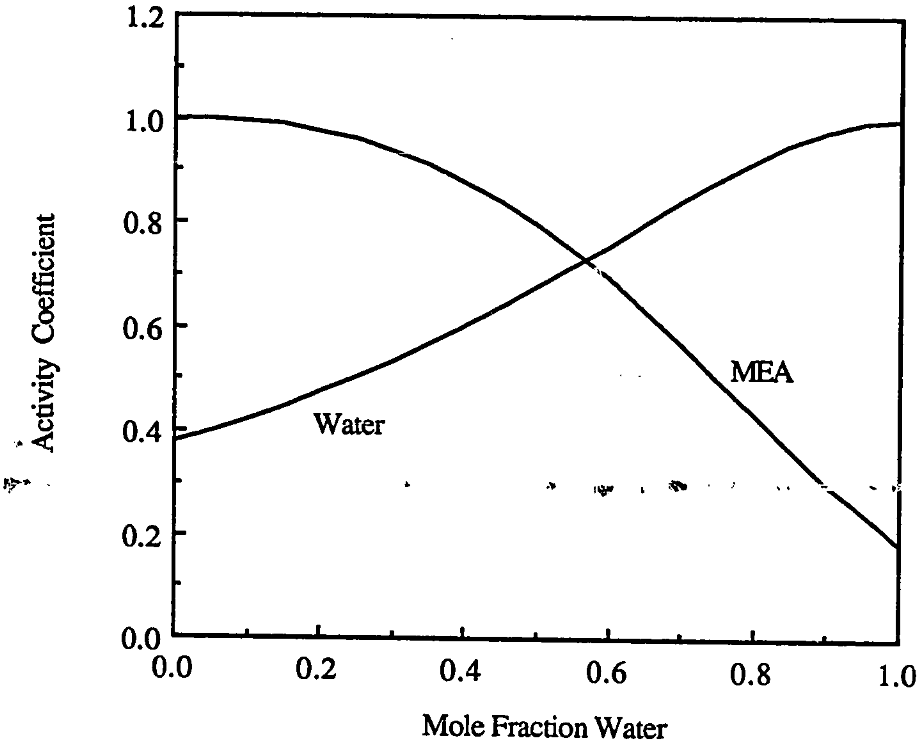

Figure 6.10 Representation of component activity coefficients in an MEA-water mixture at 298.15 °K with the NRTL equation. Parameters of the NRTL equation for the MEA-water mixture are reported in Table 6.2.

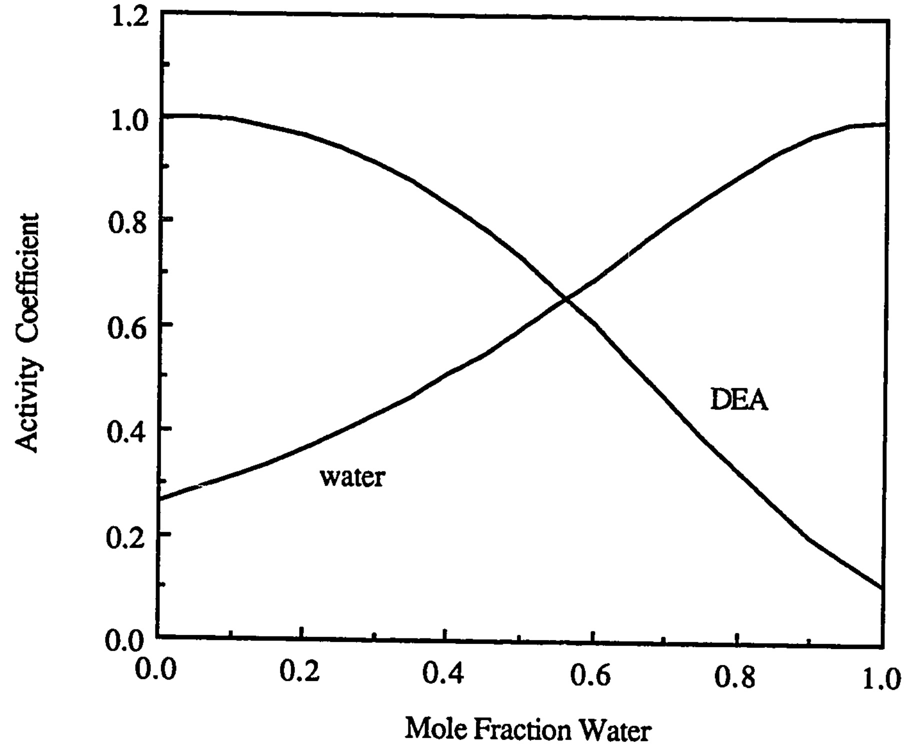

Figure 6.11 Representation of component activity coefficients in a DEA-water mixture at 298.15 °K with the NRTL equation. Parameters of the NRTL equation for the DEA-water mixture are reported in Table 6.2.

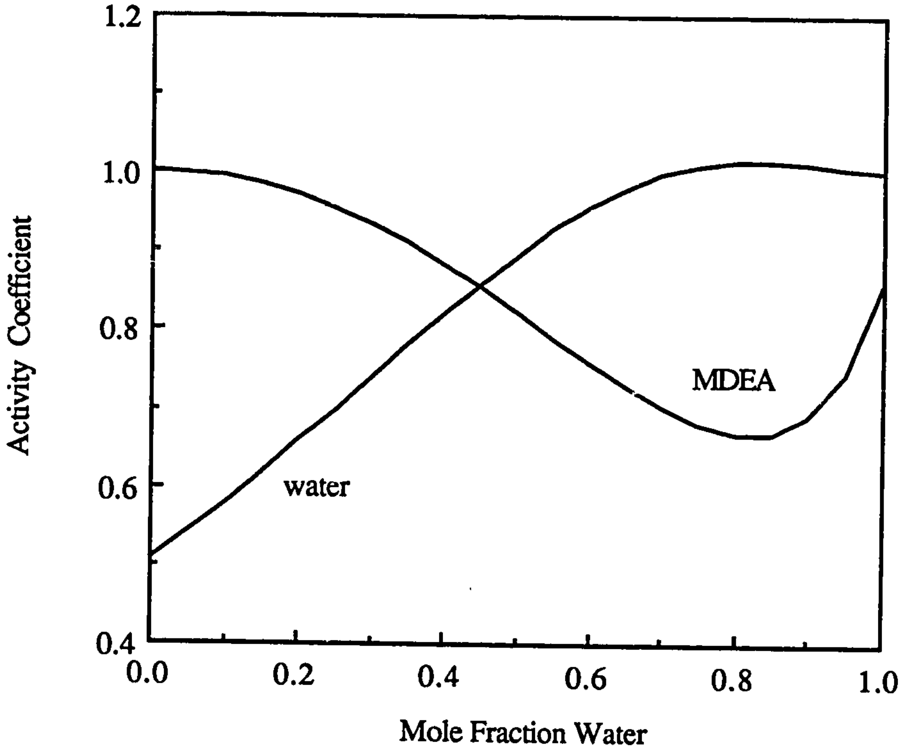

Figure 6.12 Representation of component activity coefficients in an MDEA-water mixture at 298.15 °K with the NRTL equation. Parameters of the NRTL equation for the MDEA-water mixture are reported in Table 6.2.

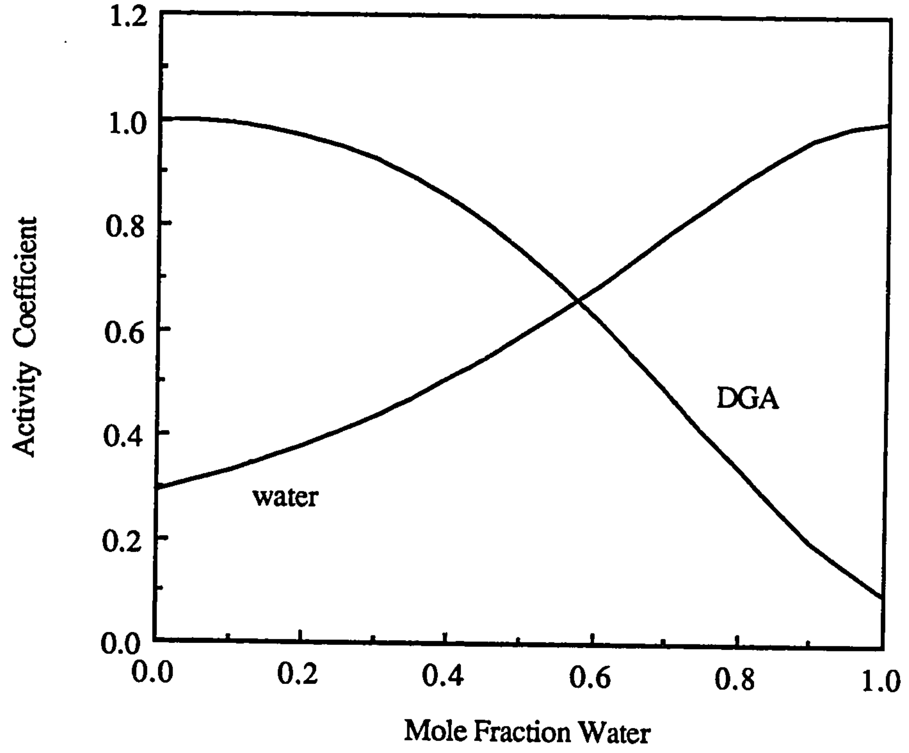

Figure 6.13 Representation of component activity coefficients in an DGA-water mixture at 298.15 °K with the NRTL equation. Parameters of the NRTL equation for the DGA-water mixture are reported in Table 6.2.

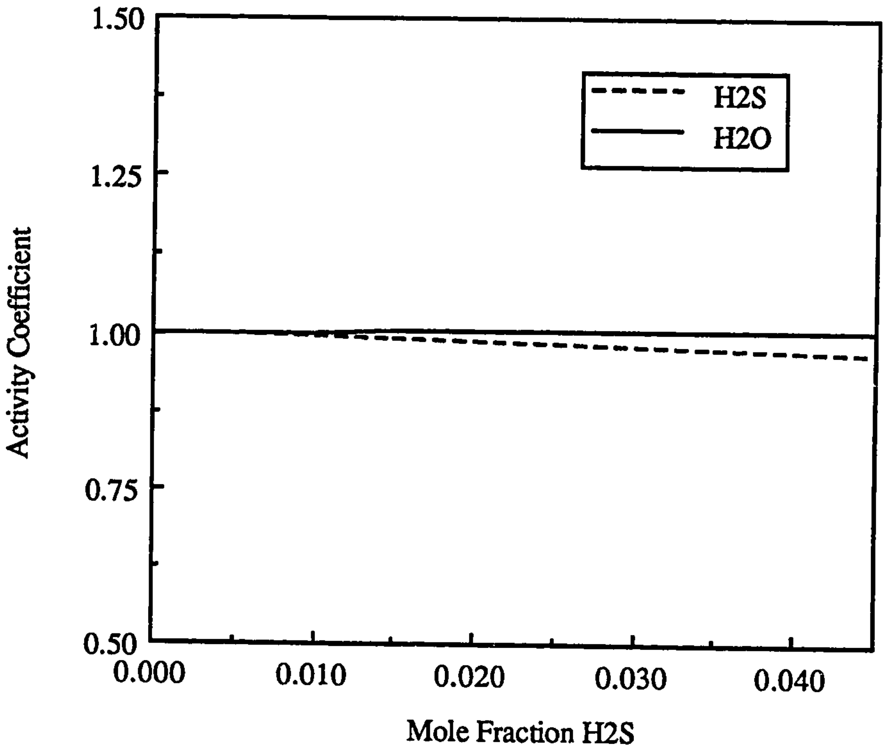

Figure 6.14 Representation of component activity coefficients in an H_2S-water mixture at 298.15 °K with the NRTL equation at low H_2S mole fractions. Parameters of the NRTL equation for the H_2S-water mixture are reported in Table 6.2. The activity coefficient of H_2S is unsymmetrically normalized.

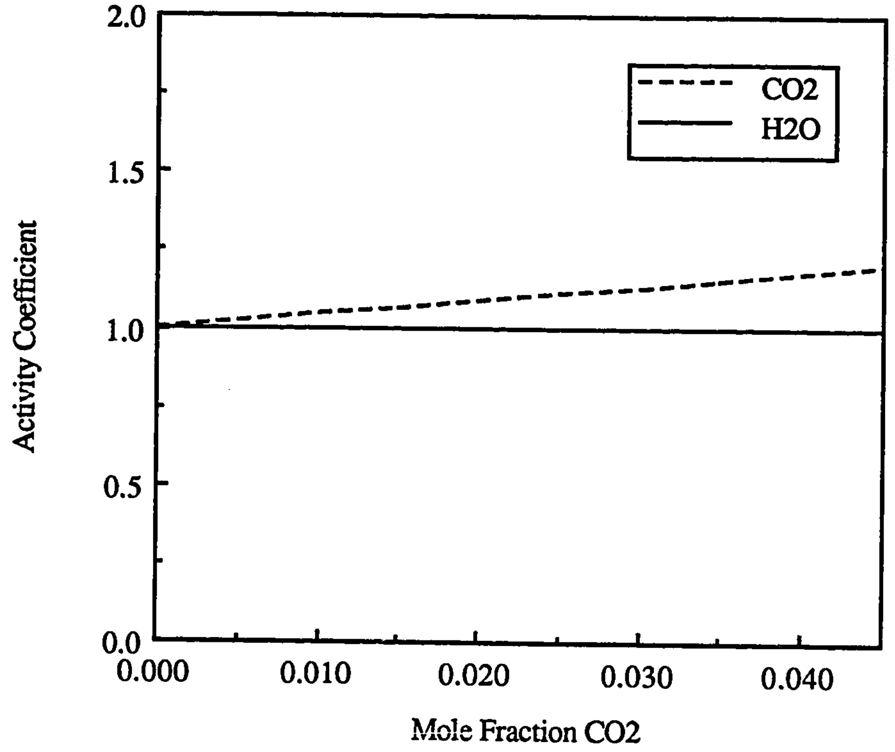

Figure 6.15 Representation of component activity coefficients in an CO_2-water mixture at 298.15 °K with the NRTL equation at low CO_2 mole fractions. Parameters of the NRTL equation for the CO_2-water mixture are reported in Table 6.2. The activity coefficient of CO_2 is unsymmetrically normalized.

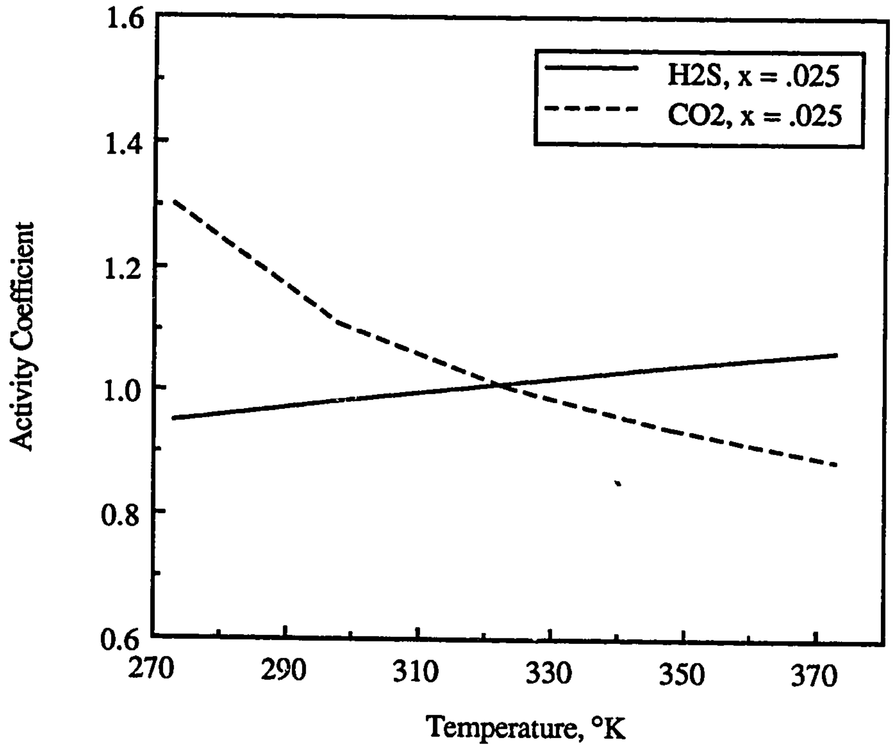

Figure 6.16 Representation of H_2S and CO_2 activity coefficients in H_2S-water and CO_2-water mixtures over the temperature range 273 to 373 °K with the NRTL equation at low acid gas mole fractions. Activity coefficients of H_2S and CO_2 are unsymmetrically normalized.

6.3 Ternary System VLE Representation

6.3.1 Data Sources

To determine best values of the **molecule-ion pair** and **ion pair-molecule** interaction parameters, the **molecule-molecule** interaction parameters were fixed at values estimated from binary system (acid gas-water and alkanolamine-water) data and the VLE model was fitted to ternary system (alkanolamine-acid gas-water) VLE data. There is a large body of experimental H_2S and CO_2 solubility data reported in the literature for aqueous alkanolamine solutions. To make the job of parameter estimation tractable, only those solubility measurements published after 1956 were used in estimating molecule-ion pair parameters.

Literature sources used in fitting all parameters are summarized in Table 6.3. There is significant scatter of experimental data both within and between the different data sources. By using several sources of experimental data for parameter estimation, the best parameter values were determined to represent the data as a whole. As a result, some data sets are better represented by the model than others. With a few exceptions at high temperatures, individual measurements within each of the data sets summarized in Table 6.3 were weighted equally (weight = 1). In the absence of information regarding the quality of the reported experimental VLE data it was felt that this was the best approach. Only when data from a specific source was clearly in poor agreement with all other sources of similar data was it weighted with a value less than unity.

Ternary system (Tpx) data are generally reported in the literature as equilibrium acid gas partial pressures and equilibrium acid gas loadings in an aqueous solution of specified amine concentration; vapor phase concentrations of the solvents - water and alkanolamine - are not reported. Therefore, the molecule-ion pair parameters were fitted on acid gas phase equilibria only and solvent phase equilibria were neglected. In addition, liquid phase concentrations of acid gas are reported as acid gas loadings (moles acid gas/mole amine) at a given total amine concentration (usually reported as acid gas free amine concentration at room temperature). The Data Regression System of ASPEN PLUS requires liquid phase concentrations in terms of mole fractions (or molalities). Hence, it was necessary to convert acid gas loadings to mole fractions for all measurements used in estimating parameters.

Like binary system data reported in the literature, standard deviations of experimental measurements for ternary systems (of interest in this work) are generally not reported and few replicate measurements are reported to allow estimation of experimental error. Therefore, estimates of experimental standard deviations for ternary system data were based partly on deviations of initial maximum likelihood estimates from reported measured values of the state variables and partly on the author's judgement based on his own experience in making acid gas solubility measurements. The following standard deviations were assigned to experimental ternary system data for MEA and DEA systems: $\sigma_T = 0.2$ K, $\sigma_P = 0.1$ x pressure, $\sigma_{x_{\text{acid gas}}} = 0.05$ x mole fraction, and $\sigma_{x_{\text{amine}}} = 0.02$ x mole fraction.

MDEA ternary system data from different sources were generally found to be in poor agreement. Therefore, acid gas partial pressures and liquid phase apparent mole fractions were assumed to have higher experimental standard deviations: $\sigma_T = 0.2$ K, $\sigma_P = 0.15$ x pressure, $\sigma_{x_{\text{acid gas}}} = 0.1$ x mole fraction, and $\sigma_{x_{\text{amine}}} = 0.02$ x mole fraction. In addition, the MDEA system data reported by Jou et al. (1982) are believed to be significantly in error at very low acid gas pressures and high acid gas loadings (Mather, 1988). Therefore, measurements at acid gas partial pressures below 0.01 kPa and acid gas loadings above 1.2 moles acid gas/mole MDEA reported by Jou et al. (1982) were not used in parameter estimation.

Finally, the following standard deviations were assigned to experimental ternary system data for DGA systems: $\sigma_T = 0.2$ K, $\sigma_P = 0.2$ x pressure, $\sigma_{x_{\text{acid gas}}} = 0.15$ x mole fraction, and $\sigma_{x_{\text{amine}}} = 0.02$ x mole fraction. DGA ternary system reported by Dingman et al. (1983) were also believed to contain error at low acid gas partial pressures (Moore, 1989). Therefore, measurements at acid gas partial pressures below 0.5 kPa reported by Dingman et al. (1983) were not used to estimate parameters.

6.3.2 Parameter Estimation Results: Electrolyte-NRTL Parameters

Fitted values of the coefficients of equation (4.67) for Electrolyte-NRTL binary **molecule-ion pair** and **ion pair-molecule** interaction parameters are reported in Table 6.4 together with the corresponding standard deviations and interaction parameter values at 298.15 °K. As was noted earlier, the only molecule-ion pair and ion pair-molecule interaction parameters that could be estimated with statistical significance for any of the ternary systems were those for which the **molecule** was **water**. Moreover, the only ions that were found to affect representation of VLE through molecule-ion pair interaction parameters were protonated amine, bisulfide, bicarbonate, and carbamate (of MEA, DEA, DGA) ions.

Table 6.3. Summary of literature sources of experimental VLE data used for estimating molecule - ion pair binary interaction parameters in the single acid gas - single alkanolamine - water systems.

Data Source	Amine † Concentrations	Temperature Range (°C)	Acid Gas Loadings
$MEA\text{-}CO_2\text{-}H_2O$:			
Lee et al. (1976a)	1.0, 2.5, 3.75, 5.0 M	25 - 120	0.09 - 2.0
Isaacs et al. (1980)	2.5 M	80, 100	0.04 - 0.32
Lawson and Garst (1976)	15.2, 30.0 wt%	40 - 140	0.11 - 1.00
Jones et al. (1959)	15.3 wt%	40 - 140	0.13 - 0.73
Muhlbauer and Monaghan (1957)	2.5 M	25, 100	0.46 - 0.74
$MEA\text{-}H_2S\text{-}H_2O$:			
Lee et al. (1974)	2.5, 5.0 M	40, 100	0.12 - 1.55
Lee et al. (1976b)	2.5, 5.0 M	25 - 120	0.21 - 1.61
Lawson and Garst (1976)	15.2, 30.0 wt%	40 - 140	0.005 - 1.63
Jones et al. (1959)	15.3 wt %	40 - 140	0.025 - 0.97
Muhlbauer and Monaghan (1957)	2.5 M	25, 100	0.20 - 0.93
$DEA\text{-}CO_2\text{-}H_2O$:			
Lee et al. (1972)	0.5, 2.0, 3.5, 5.0 M	25 - 120	0.03 - 3.32
Lal et al. (1985)	2.0 M	40, 100	0.005 - 0.37
Lawson and Garst (1976)	25, 50 wt%	38 - 120	0.32 - 1.17
$DEA\text{-}H_2S\text{-}H_2O$:			
Lee et al. (1973a)	2.0, 3.5 M	25 - 120	0.07 - 1.55
Lee et al. (1973b)††	0.5, 5.0 M	25 - 120	0.02 - 3.29
Lal et al. (1985)	2.0 M	40 - 100	0.007 - 0.22
Atwood et al. (1957)	10, 25, 50 wt%	27 - 60	0.005 - 1.00
Lawson and Garst (1976)	25, 50 wt%	38 - 150	0.004 - 1.58

Continued on following page.

Table 6.3. Continued - Summary of literature sources of experimental VLE data used for estimating molecule - ion pair binary interaction parameters in the single acid gas - single alkanolamine - water systems.

Data Source	Amine † Concentations	Temperature Range (°C)	Acid Gas Loadings
MDEA-CO_2-H_2O:			
Jou et al (1982)*	2.0, 4.28 M	25 - 120	0.001 - 3.22
Jou et al. (1986)	3.04 M	40, 100	0.002 - 0.80
Bhairi (1984)	1.0, 2.0 M, 20 wt %	25 - 116	0.16 - 1.51
MDEA-H_2S-H_2O:			
Jou et al. (1982)*	1.0, 2.0, 4.28 M	25 - 120	0.001 - 1.83
Jou et al. (1986)**	3.04 M	40 - 80	0.004 - 1.08
Bhairi (1984)	1.0 M, 20 wt %	25 - 116	0.18 - 2.17
DGA-CO_2-H_2O:			
Martin et al. (1978)	60 wt %	50, 100	0.13 - 0.80
Dingman et al. (1983)***	65 wt %	38 - 82	0.003 - 0.59
DGA-H_2S-H_2O:			
Martin et al. (1978)	60 wt %	50, 100	0.06 - 1.09
Dingman et al. (1983)***	65 wt %	38 - 82	0.003 - 0.85

† Amine concentrations are acid gas free. †† Only data points with an H_2S loading of less than 1.66 moles per mole amine were used in data regression. * Only data points with an acid gas equilibrium partial pressure greater than 0.1 kPa and a loading less than 1.2 moles per mole amine were used in data regression. ** Also reported data at 50 wt % MDEA that was not used in data regression. *** Only data points above an acid gas loading of 0.10 moles per mole amine were used in data regression.

Several trends are evident in the water-ion pair and ion pair-water parameters reported in Table 6.4. In general, values of water-ion pair and ion pair-water interaction parameters at 298.15°K are in relatively good agreement with default values of 8.0 and -4.0 respectively. Recall that these default values represent approximate average values of a large number of water-ion pair and ion pair-water parameters reported by Chen et al. (1982) for aqueous strong electrolyte systems. Note also that most of interaction parameters are well defined as indicated by the relatively small values of the associated parameter standard deviations. Standard deviation is less than 20% of the parameter value for many of the adjusted interaction parameters.

The temperature dependence of the adjusted interaction parameters also exhibits interesting trends. Most of the H_2O-RR'R"NH^+,HS^- and H_2O-RR'R"NH^+,HCO_3^- interaction parameters appear to be relatively strong functions of temperature as indicated by the relative contribution of the temperature dependent term of equation (4.67) to the interaction parameter. However, the H_2O-RR'R"NH^+,RR'$NCOO^-$ interaction parameters were found to be weak functions of temperature or completely independent of temperature. All ion pair-water interaction parameters were also found to be weak functions of temperature or independent of temperature. Finally, the H_2O-RR'NH_2^+,RR'$NCOO^-$ and the RR'NH_2^+,RR'$NCOO^-$-H_2O interaction parameters assumed the largest (absolute) values among all adjustable parameters for **all** systems (MEA, DEA, and DGA).

As noted earlier, it is known that the parameters of the NRTL equation are often highly correlated (Renon 1985). Results of the work conducted by Chen and Evans (1986) and results of this work suggest that corresponding pairs of water - ion pair interaction parameters of the Electrolyte - NRTL equation are also highly correlated.

Table 6.4 Fitted values of NRTL molecule - ion pair binary interaction parameters for CO_2-alkanolamine-H_2O and H_2S-alkanolamine-H_2O systems.

$$\tau = a + b/T$$

Parameter	a	σ_a	b(°K)	σ_b	τ(25°C)
RNH_2 = MEA					
H_2O-RNH_3^+,HS^-	6.844	0.92	501.83	312.3	8.53
RNH_3^+,HS^--H_2O	-3.560	0.38	-197.12	129.1	-4.22
H_2O-RNH_3^+,$RNHCOO^-$	10.268	0.16	0.0	†	10.27
RNH_3^+,$RNHCOO^-$-H2O	-5.098	0.08	0.0	*	-5.10
H_2O-RNH_3^+,HCO_3^-	4.550	1.00	1218.19	231.6	8.64
RNH_3^+,HCO_3^--H_2O	-4.088	0.14	0.0	*	-4.09
R_2NH = DEA					
H_2O-$R_2NH_2^+$,HS^-	5.199	1.17	1519.60	396.9	10.30
$R_2NH_2^+$,HS^--H_2O	-2.836	0.43	-636.95	145.4	-4.97
H_2O-$R_2NH_2^+$,R_2NCOO^-	11.549	0.45	102.66	36.2	11.89
$R_2NH_2^+$,R_2NCOO^--H_2O	-5.580	0.14	0.0	*	-5.58
H_2O-$R_2NH_2^+$,HCO_3^-	4.204	0.79	1588.19	196.5	9.53
$R_2NH_2^+$,HCO_3^--H_2O	-4.434	0.11	0.0	*	-4.43
R_3N = MDEA					
H_2O-R_3NH^+,HS^- **	3.735	0.64	1036.04	202.5	7.21
R_3NH^+,HS^--H_2O **	-3.225	0.06	0.0	*	-3.23
H_2O-R_3NH^+,HCO_3^- **	5.864	0.54	1147.90	151.4	9.71
R_3NH^+,HCO_3^--H_2O **	-4.511	0.06	0.0	*	-4.51
$R'NH_2$ = DGA					
H_2O-$R'NH_3^+$,HS^-	7.744	0.39	375.72	123.44	9.00
$R'NH_3^+$,HS^--H_2O	-4.337	0.03	0.0	†	-4.34
H_2O-$R'NH_3^+$,$R'NHCOO^-$	11.424	0.40	0.0	*	11.42
$R'NH_3^+$,$R'NHCOO^-$-H2O	-5.328	0.12	0.0	*	-5.33
H_2O-$R'NH_3^+$,HCO_3^-	0.0	*	2960.94	232.9	9.93
$R'NH_3^+$,HCO_3^--H_2O	-4.251	0.23	0.0	*	-4.25

† Parameter encountered a bound, standard deviation was not estimated; * Parameter value fixed at zero, normally because it could not be estimated with statistical significance; ** These parameters where determined with MDEA-H_2O and H_2O-MDEA molecule-molecule interaction parameters fixed at zero rather than values reported in Table 6.2.

That this is true can be seen easily in corresponding values of the water-ion pair and ion pair-water interaction parameters reported at 298.15 °K in Table 6.4: **Water - ion pair** interactions parameters are roughly two times greater in magnitude than the corresponding **ion pair - water** interaction parameters.

However, parameter correlation is presented in a more technically sound manner in terms of the parameter correlation matrices calculated by DRS and reported in Appendix B. Recall that the elements of these matrices are the correlation coefficients for the corresponding pairs of adjustable parameters. Parameters that are completely independent have a correlation coefficient of zero. Parameters that are perfectly correlated have a correlation coefficient of ±1.

Several trends are also apparent in the correlation coefficient matrices for the ternary systems. First, the coefficients 'a' and 'b' of equation (4.67) for any given binary interaction parameter are usually highly correlated. Moreover, the coefficients 'a' and 'b' of a **water-ion pair** interaction parameter exhibit moderate to high degrees of correlation with the coefficients 'a' and 'b' of the corresponding **ion pair-water** interaction parameter. This is consistent with the observation that water - ion pair interactions parameters are roughly two times greater in magnitude than the corresponding ion pair - water interaction parameters. For example, all fitted binary interaction parameters of the H_2S-MEA-H_2O and H_2S-DEA-H_2O systems are highly correlated. However, the coefficients 'a' and 'b' of the corresponding water-ion pair and ion pair-water parameters for the H_2S-MDEA-H_2O and H_2S-DGA-H_2O exhibit a much lower degree of correlation.

The correlation coefficient matrices for the CO_2-alkanolamine-water ternary systems indicate that the coefficients of equation (4.67) for the H_2O -

$RR'R''NH^+,HCO_3^-$ interaction parameters are only moderately correlated with the H_2O-$RR'NH_2^+,RR'NCOO^-$ parameters. Furthermore, these correlation coefficients matrices reveal that the coefficients of equation (4.8), representing the temperature dependence of the natural logarithm of the carbamate stability constants (reported in Table 6.5), are poorly or only moderately correlated with the binary interaction parameters for the CO_2-alkanolamine-water systems. These results are fortuitous as they suggests that the physical interactions involving carbamate are largely being separated from physical interactions involving bicarbonate and that all physical interactions are largely being separated from chemical interactions by the data regression process.

6.3.3 Parameter Estimation Results: Carbamate Stability Constants

Very few measurements of the carbamate stability constant (Reaction 4g) for MEA, DEA, or DGA have been reported in the literature. Jensen et al. (1954) report values of the carbamate stability constants for both MEA and DEA, but only at 18°C. Jensen and coworkers report a value of 0.0195 mol l^{-1} for the MEA carbamate stability constant and a value of 0.1514 mol l^{-1} for the DEA carbamate stability constant. Note that the smaller the constant, the more stable is the carbamate, and a more stable carbamate will resist reverting to bicarbonate. The values cited above represent measurements in solutions of finite, though low, ionic strengths. Jensen and coworkers appear not to have attempted to extrapolate their measurements to zero ionic strength.

Chan and Dankwerts (1981) measured the same constants in sodium bicarbonate solutions at 25° and 40°C. At 25°C, Chan and Dankwerts report the following values of the carbamate stability constants (each is followed in parentheses by the ionic strength at which the equilibrium constant was measured): MEA - 0.0342 mol l^{-1} (I=0.531 g ion l^{-1}); DEA - 0.2620 mol l^{-1} (I=0.531 g ion l^{-1}). Likewise, at 40°C Chan and Dankwerts report the following values of the carbamate stability constants: MEA - 0.0567 mol l^{-1} (I=0.624 g ion l^{-1}); DEA - 0.379 mol l^{-1} (I=0.531 g ion l^{-1}). Mahajani and Dankwerts (1982) measured the MEA and DEA carbamate stability constants in a 30% potash solution at 100°C. Again no correction was made for ionic strength. At 100°C, Mahajani and Dankwerts report the following values of the carbamate stability constants: MEA - 0.40 (± 8%) mol l^{-1}; DEA - 2.05 (±5%) mol l^{-1}.

Since the total number of reported carbamate stability constants measurements is small, and because few of the reported values appear to have been corrected for the affect of ionic strength, it was felt that it was best not to adopt these values to represent carbamate stability constants in the model. Instead, the coefficients of equation (4.8) for the carbamate stability constant were treated as additional adjustable parameters of the model. They were fitted, simultaneously with the appropriate interaction parameters, on CO_2-alkanolamine-H_2O ternary system VLE data.

Carbamate stability constants determined in this manner are summarized in Table 6.5. Note that the coefficients of equation (4.8) are well also well defined as indicated by the relatively small values of the standard deviations corresponding to the adjusted coefficients. Carbamate stability constants regressed in this work are compared with those determined by Kent and Eisenberg (1976) and by Chakravarty (1985) at 25°, 40° and 100°C in Table 6.6. Kent and Eisenberg fitted carbamate stability constants for MEA and DEA to equilibrium data, in essentially the same way as was done in this work, using a VLE model that was discussed in Chapter Three.

Chakravarty determined carbamate *formation* constants for MEA and DEA by data regression on *low pressure* CO_2-amine-H_2O VLE data using the model of Deshmukh and Mather (1981) (also discussed in Chapter Three). The corresponding carbamate stability constants were calculated from the carbamate formation constants and the equilibrium constants for reactions 4d and 4f used by Chakravarty.

The drawback of Chakravarty's approach is that he had to rely on low pressure solubility data that is subject to large relative errors due to limitations in the usual experimental techniques employed to the measure acid gas equilibrium partial pressures (Mather, 1988). Indeed, as will be shown shortly, the results of this study suggest that a substantial fraction of the reported low pressure CO_2 solubility data for aqueous DEA solutions appear to be of poor accuracy. In this work, the carbamate stability constant was fitted on solubility measurements over the full range of CO_2 partial pressures insuring a value more consistent with all reported data.

Equilibrium constants reported by Kent and Eisenberg and by Chakravarty are on molarity and molality basis respectively. In addition, both treat the amines as solutes with the infinite dilution reference state. In order to compare equilibrium constants on a consistent basis, it was necessary to convert the equilibrium constants fitted in this work and reported in Table 6.5 to a molality basis and to adjust the constants to the amine solute reference state.

6.3.4 Ternary system data representation

Figures 6.17 through 6.32 are graphical summaries of the *ratios* of estimated *true* (maximum likelihood estimates) to experimentally measured values of equilibrium acid gas partial pressure and liquid phase equilibrium apparent mole fraction of acid gas

Table 6.5. Fitted values of the coefficients of equation (4.8) for carbamate stability constants.

$$\ln K = C_1 + C_2/T + C_3 \ln T + C_4 T$$

Amine	C1	σ_{c_1}	C2	σ_{c_2}	C3	σ_{c_3}	C4	σ_{c_4}
MEA	2.8898	(0.506)	-3635.09	(182.8)	0.0	(0.0)	0.0	(0.0)
DEA	4.5146	(0.968)	-3417.34	(288.8)	0.0	(0.0)	0.0	(0.0)
DGA	8.8333	(0.795)	-5274.4	(279.5)	0.0	(0.0)	0.0	(0.0)

Note: K is dimensionless and based on the mole fraction scale. The standard state for amine is the state of the pure liquid at the system temperature.

for the 8 ternary systems of interest in this work: MEA-H_2S-H_2O, MEA-CO_2-H_2O, DEA-H_2S-H_2O, DEA-CO_2-H_2O, MDEA-H_2S-H_2O, MDEA-CO_2-H_2O, DGA-H_2S-H_2O, DGA-CO_2-H_2O. Each data point in Figures 6.17 through 6.32 represents a unique state variable (acid gas pressure or acid gas apparent mole fraction) measurement used in parameter estimation. Because of the small standard deviations assigned to experimentally reported values of system temperature and apparent mole fraction of alkanolamine, estimated *true* values of these state variables were always in close agreement with measured values. It was, therefore, unnecessary to examine similar plots for temperature or apparent amine mole fraction.

In the discussion to follow, data representation will be examined in terms of the *proximity to unity* of the ratios of maximum likelihood estimates (estimated *true* values) of the equilibrium acid gas partial pressures and equilibrium liquid phase apparent mole fractions to the corresponding measured values. Hereafter, these ratios

Table 6.6. Carbamate Stability Constants, K_m (mol/l), at 25°, 40°, and 100° C.

Temp (°C)	Amine	Present Work	Kent-Eisenberg*	Chakravarty	Chan Dankwerts	Mahajani Dankwerts
25	MEA	0.0277	0.0256	0.0252	0.0342	
40	MEA	0.0395	0.0420	0.0409	0.0567	
100	MEA	0.130	0.205	0.211		0.40
25	DEA	0.491	0.225	0.209	0.262	
40	DEA	0.748	0.304	0.309	0.379	
100	DEA	3.142	0.800	0.318		2.05
25	DGA	0.0822				
40	DGA	0.141				
100	DGA	0.856				

* Kent and Eisenberg report the carbamate stability constant in units of mol/liter.

will often be referred to as the partial pressure ratios and the apparent mole fraction ratios. In addition, amine concentrations at which various researchers report VLE data for the alkanolamine-acid gas systems will be frequently cited. In all cases, the cited alkanolamine concentration is on an acid gas-free basis.

As noted in the discussion of binary system results, section 6.2.3, if all data were error-free, and if the model represented the data perfectly, all acid gas partial pressure ratios and all acid gas apparent mole fraction ratios in Figures 6.17 through 6.32 would assume values of unity. It can be seen in these figures that most values of these ratios lie in a band within 10 percent of unity. Note also that *true* values of the acid gas equilibrium partial pressures vary from measured values to approximately the same extent that *true* values of the apparent acid gas mole fractions vary from measured values. Given that the represented acid gas pressures vary over four to six orders of magnitude and apparent acid gas mole fractions vary over two to three orders of magnitude, these results suggest that the model represents the data, *as a whole,* reasonably well. Closer examination of these figures reveals interesting facts concerning the quality of the data, quality of the representation, and limitations of the model.

Because a greater number of data sources were used to estimate parameters associated with the MEA and DEA ternary systems, representation of data for these ternary systems is somewhat different than data representation for the MDEA and DGA ternary systems in Figures 6.17 through 6.32. Therefore, quality of data representation will be discussed first for the MEA and DEA systems. For these systems, data sets that are well represented by the VLE model are illustrated with small black dots. Data sets that are poorly represented, either because of a 'lack of fit' or because of systematic experimental error, are represented individually by unique symbols.

Figures 6.17 through 6.20 summarize the ratios of the estimated *true* to the measured values of the equilibrium acid gas partial pressures and *true* to measured values of the apparent acid gas mole fractions for the ternary systems associated with MEA: MEA-H_2S-H_2O and MEA-CO_2-H_2O. Except for a few data points that lie above or below the ordinate ranges of these figures, all experimental measurements used in data regression up to acid gas loadings of 1.2 (moles of acid gas per mole of amine) are shown.

Figures 6.17 and 6.18 for the MEA-H_2S-H_2O system illustrates that the VLE model represents nearly all experimental data very well below 100°C. However, there appears to be a systematic deviation of the ratios from unity at high temperature. The nature of the discrepancy varies both within and between data sources. For example, at high temperature and low loading, the partial pressure ratios for the data of Lawson and Garst (1976), 15.2 wt % MEA, are generally greater than a value of unity, but for the 30 wt% data from the same source, the ratios are less than unity. In contrast to the data of Lawson and Garst (at 15.3 wt %), the partial pressure ratios for 2.5 kmol m^{-3} MEA (~15 wt %) high temperature data reported by Muhlbauer and Monaghan (1957) and Lee et al. (1974b, 1976b) generally lie below a value of unity at low loadings. These results suggest that there is systematic experimental error at high temperatures and low loadings in this system among the various data sources. The behavior of the pressure and mole fraction ratios corresponding to Lawson and Garst's data also suggest that the model may be exhibiting a weak systematic 'lack of fit' as a function of total amine concentration. However, the excellent representation of data from other sources at different amine concentrations does not support this conclusion.

Figures 6.19 and 6.20 for the MEA-CO_2-H_2O system also show systematic deviation of partial pressure and mole fraction ratios from unity at high temperature. *True* values of the CO_2 partial pressure are less than the corresponding measured values at high temperatures and at low and high loadings. Because this trend occurs across several data sets, it appears that this phenomena is due to a 'lack of fit' at these conditions and not because of systematic error in any one data source. It should be noted, however, that even at the extremes of high temperature and loading considered here, the *true* values of the CO_2 partial pressure and CO_2 apparent mole fraction generally agree with measured values within 20 percent.

It may be that the poor representation of CO_2 solubility in aqueous MEA at high temperature is a result of incorrect temperature dependence of the carbamate stability constant. As indicated in Table 6.5, only the first coefficient of the temperature dependence of the carbamate stability constant was fitted with statistical significance. It may also be that the Henry's constant for CO_2 is poorly represented above 100 °C. Chen and Evans fitted the CO_2 Henry's constant (with water as the solvent) to the tabular data of Houghton et al. (1957) which extends only to 100°C and was generated by fitting an equation-of-state to experimental data reported in the literature. It is known that the CO_2 Henry's constant passes through a maximum at approximately 150°C (Zawisza and Maleńska, 1981). Thus, the slope of the Henry's constant curve changes rapidly with temperature between 100 and 150°C.

The experimental data of Isaacs et al. (1980) are noteworthy. Isaacs and coworkers report experimental measurements of CO_2 solubility in aqueous MEA at low CO_2 loadings at 80 and 100°C (see Table 6.3). The model represents this experimental data very well at 80°C but does not agree with the experimental data at 100°C. Indeed most of the partial pressure ratios for the 100 °C data of Isaacs and coworkers lie above the range of the ordinate axis of the plot. Given that *true* values of the CO_2 equilibrium partial pressure are less than measured values for data from other sources at high temperatures and low loadings, these results suggest that the data reported by Isaacs et al. (1980) at 100°C may be of questionable accuracy.

Representation of the DEA-H_2S-H_2O system VLE data in terms of partial pressure ratios and apparent mole fraction ratios is presented in Figures 6.21 and 6.22.

These figures indicate that the experimental data are well represented by the model in the middle range of amine concentrations. For example, Lee et al (1973a,b) report H_2S equilibrium partial pressures for solutions of 0.5, 2.0, 3.5, and 5.0 M DEA. Estimated *true* values of the H_2S equilibrium partial pressure agree well with measured values for the 2.0 M DEA VLE data and reasonably well for the 3.5 M DEA data. However, the partial pressure ratios lie significantly below unity for 0.5 M DEA solutions and significantly above unity for the 5.0 M solutions. It is difficult to state with certainty whether this discrepancy which correlates with total amine concentration is due to systematic error in measurements or is a result of 'lack of fit'. There are not sufficient experimental DEA-H_2S-H_2O VLE data at high and low amine concentrations from other sources to support either conclusion. Nor do results from other ternary amine systems do not support this proposition.

Results of data representation for the DEA-CO_2-H_2O system, presented in Figures 6.23 and 6.24, also reveal a systematic 'lack of fit' at high temperature although the nature of the deviation is different than that seen for the MEA system. *True* values of CO_2 partial pressure are generally greater than corresponding measured values at high temperature and low loading and less than corresponding measured values at high temperature and high loading. Except for the very low CO_2 loading data of Lal et al. (1985) at 100 °C, the estimated *true* values of CO_2 partial pressure generally agree with measured values within 10%. The poor representation of Lal's data at 100°C while other reported data, including Lal's data at 40°C, are well represented, suggests that this particular data set may be of poor accuracy.

Figures 6.25 and 6.26 are graphical summaries of the equilibrium H_2S partial pressure ratios and the H_2S liquid phase apparent mole fraction ratios for the MDEA-

H_2S-H_2O system. Figures 6.27 and 6.28 are similar plots for the MDEA-CO_2-H_2O system. In these figures, each amine concentration from each data source, or investigator, is represented with a unique data symbol, although measurements at the same amine concentration but different temperatures from the same data source are not differentiated. Except for a few data points that lie above or below the ranges of the ordinate axes in these figures, all experimental measurements used in data regression up to acid gas loadings of 1.4 moles of acid gas per mole of amine are shown.

The wide ranging scatter in the partial pressure ratios and the apparent mole fraction ratios about a value of unity in Figures 6.25 through 6.28 reveal that the agreement of VLE data for MDEA ternary systems amongst the researchers reporting such data is poor, especially at low loadings. This made determining reasonable Electrolyte-NRTL interaction parameters from MDEA ternary system data especially difficult. Results of Chakravarty's (1985) VLE modeling reveal similar scatter and lack of representation of the data.

It can also be seen from Figures 6.25 through 6.28 that experimental data from the various data sources are best represented over limited ranges of loadings. For example, the data reported by Bhairi (1984) are represented best by the model at high loadings, and therefore, high acid gas partial pressures. The data of Jou et al. (1982) are best represented at moderate loadings. These results probably reflect the pressure and concentration ranges over which the experimental techniques used by each of the represented investigators were most accurate.

Reported acid gas solubility data for the MDEA ternary systems vary over approximately 6 orders of magnitude in acid gas partial pressure, from 0.001 to more than 1000 kPa. Equilibrium acid gas loadings vary over approximately three orders of magnitude, from 0.001 to more than 1 mole acid gas per mole amine. These wide ranges of acid gas pressures, and to a lesser extent acid gas loadings, make solubility measurements over the entire range with a single apparatus difficult, if not impossible. Indeed, Jou et al. (1982) used two separate devices to make H_2S and CO_2 solubility measurements in aqueous solutions of MDEA. They used a closed cell in which gases were circulated and bubbled through the amine solution at acid gas pressures above 100 kPa and a continuous flow apparatus was used at lower pressures.

The lower acid gas pressure limit at which solubility measurements can be made is often limited by the accuracy and precision with which the acid gas concentration of the vapor phase can be measured, usually by gas chromatography (Mather, 1988). At the high acid gas partial pressures, accuracy is often limited by the technique used to measure acid gas concentration in the liquid phase. At loadings approaching 1 mole acid gas per mole amine the acid gas tends to flash easily from the liquid phase. Bhairi (1984) attempted to circumvent this problem by applying a mass balance method to measure acid gas solubility in a closed system. However, the lower acid gas pressure limit of Bhairi's measurement technique was approximately 5 to 10 kPa preventing him from making low pressure solubility measurements.

Preliminary parameter estimation results for MDEA ternary systems suggested that the data reported by Jou et al. (1982) was of poor accuracy at very low pressures and very high pressures. Mather (1988) substantiated this suspicion. Therefore, measurements at acid gas pressures below 0.01 kPa and loadings above 1.2 moles acid gas per mole MDEA reported by Jou and coworkers (1982) were not used to estimate parameters.

Representation of one particular set of MDEA-CO_2-H_2O system VLE data reported by Bhairi (1984) is noteworthy. While most of the experimental data reported by Bhairi for this system are reasonably well represented by the model, the CO_2 solubility data for 2 kmol m^{-3} MDEA at 25°C are poorly represented. The behavior of the partial pressure ratios and apparent mole fraction ratios for this data set, seen in Figures 6.27 and 6.28 respectively, suggest that these data systematically deviate from true VLE behavior as CO_2 loading decreases. This is consistent with the fact that Bhairi's experimental technique was limited to high acid gas partial pressures.

Finally, it can be seen in Figures 6.25 through 6.28 that ratios of estimated *true* to experimentally measured values of the state variables vary more from unity at low loadings. However, the ratios are well distributed about a value of unity, suggesting that the scatter is due to experimental error in this region rather than a lack of fit by the model.

Figures 6.29 and 6.30 are graphical summaries of the equilibrium H_2S partial pressure ratios and the H_2S liquid phase apparent mole fraction ratios for the DGA-H_2S-H_2O system. Figures 6.31 and 6.32 are similar plots for the DGA-CO_2-H_2O system. Only two sources of DGA ternary system data were used to estimate the corresponding molecule-ion pair parameters. Each of these only report data at one amine concentration; Martin et al. (1978) report solubility data for a 60 wt % DGA solution and Dingman et al. (1983) report data for a 65 wt % DGA solution. As recommended by Moore (1989), data at very low acid gas loadings reported by Dingman and coworkers were not used to estimate parameters.

Figures 6.29 through 6.32 reveal that except for the DGA-H_2S-H_2O VLE data at 100°C reported by Martin et al. (1978), DGA ternary system VLE data, especially the

DGA-CO_2-H_2O data, are generally well represented by the model. Keeping in mind that the adopted standard state of all solutes in the VLE model is the ideal dilute state in water, the satisfactory representation of the DGA ternary system data is noteworthy because the solubility data are reported for solutions that are less than 50% by volume water.

In general, the model appears to represent the experimental data, as a whole, very well. This is especially true in view of the fact that the VLE data used to estimate parameters vary over extremely wide ranges of acid gas pressure and acid gas loading. Figures 6.17 through 6.32 illustrate the significant disagreement in the experimental VLE data reported in the literature for the single acid gas - single amine - water systems. Where there are differences between VLE measurements at similar experimental conditions, parameter estimation has led to parameter values that allow the model to represent, in a sense, an average of the experimental data. For the 8 ternary systems of interest, estimated *true* values of the pressure and liquid phase acid gas apparent mole fractions agree with measured values within 10% for the bulk of the experimental data.

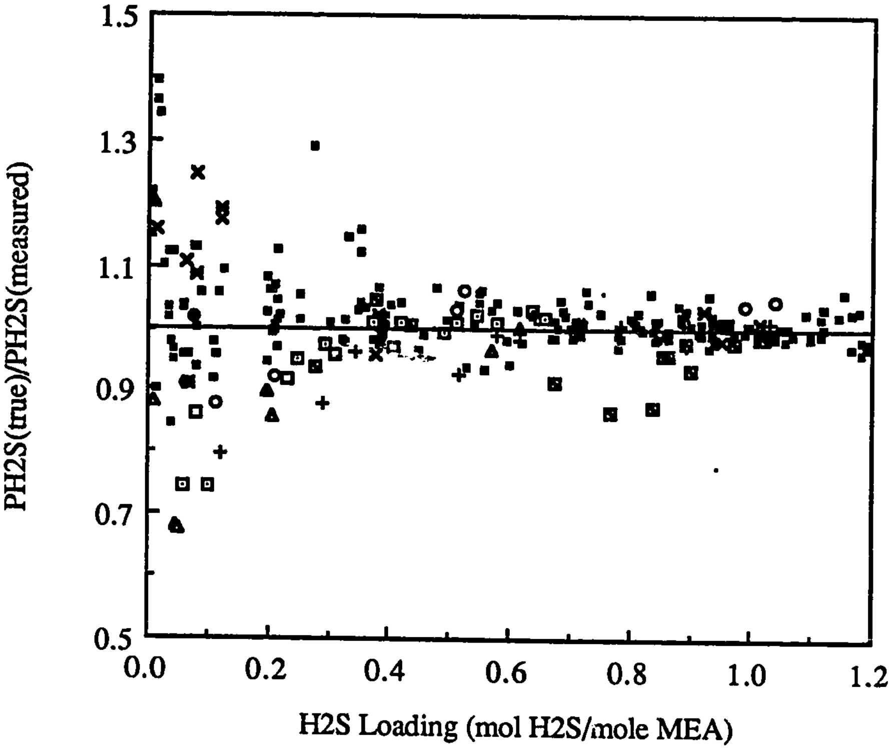

Figure 6.17 Comparison of maximum likelihood estimates and experimentally measured values of H_2S equilibrium partial pressure over aqueous MEA solutions. Lawson and Garst (1976): (×) 15.2 wt %, 100°C; (✖) 15.2 wt %, 120°C; (●) 15.2 wt %, 140°C; (□) 30 wt %, 80°F; (▲) 30 wt %, 100°F; (△) 30 wt %, 200°F. Muhlbauer and Monaghan (1957): (▣) 2.5 M, 100°C. Lee et al. (1976b): (○) 5 M, 100°C. Lee et al. (1974): ([illegible]) 5 M, 40°C; (+) 5 M, 100°C. Other, Table 6.3: (▪).

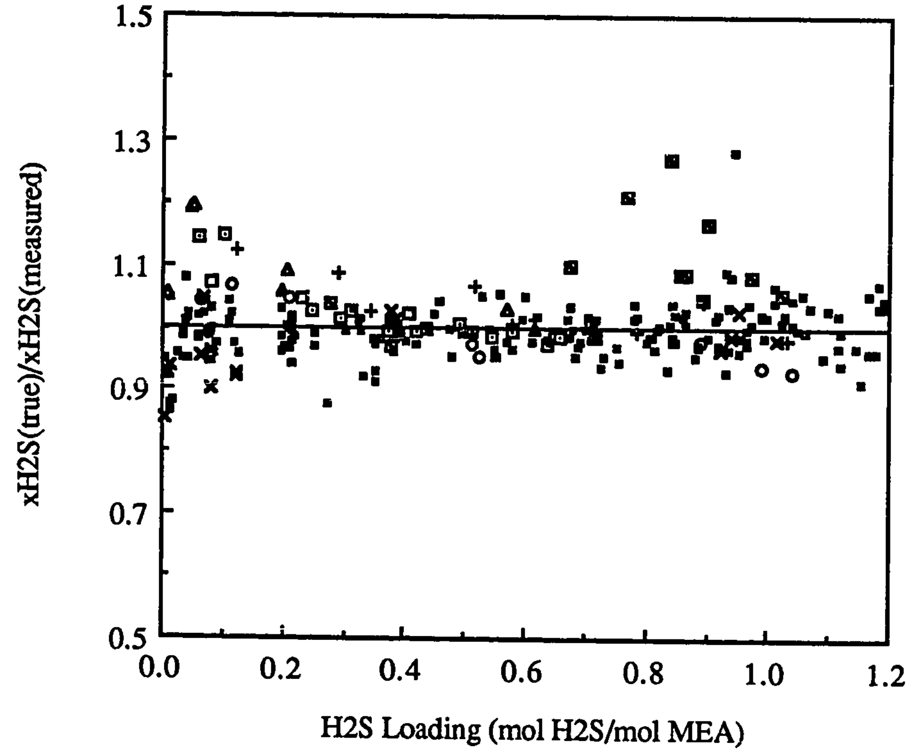

Figure 6.18 Comparison of maximum likelihood estimates and experimentally measured values of equilibrium H_2S apparent mole fraction in aqueous MEA solutions. Lawson and Garst (1976): (×) 15.2 wt %, 100°C; (✖) 15.2 wt %, 120°C; (●) 15.2 wt %, 140°C; (□) 30 wt %, 80°F; (▲) 30 wt %, 100°F; (▲) 30 wt %, 200°F. Muhlbauer and Monaghan (1957): (▣) 2.5 M, 100°C. Lee et al. (1976b): (○) 5 M, 100°C. Lee et al. (1974): (■) 5 M, 40°C; (+) 5 M, 100°C. Other, Table 6.3: (▪).

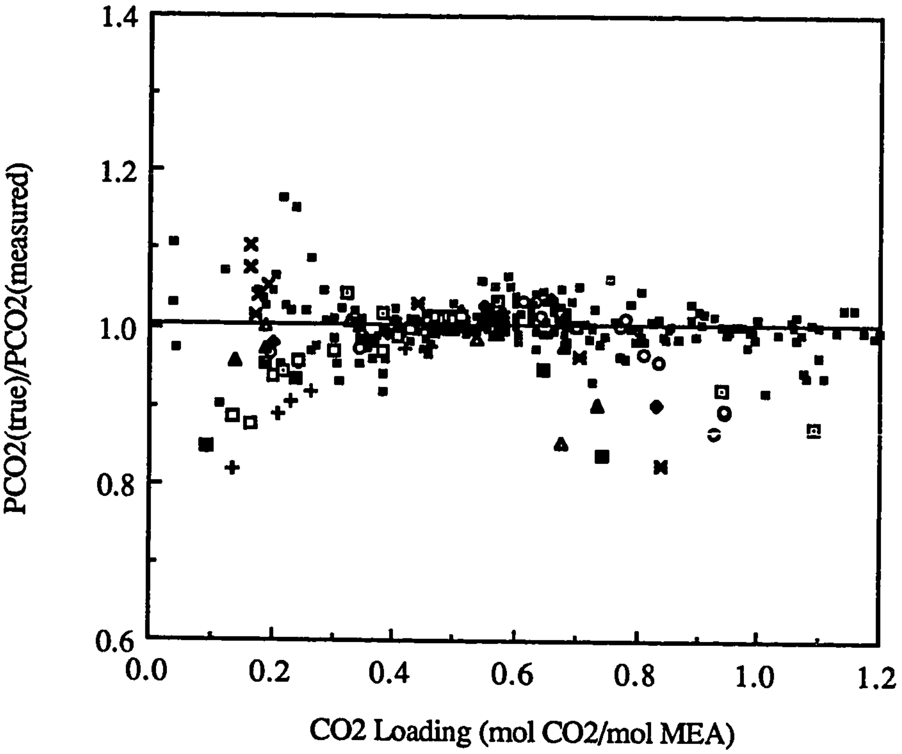

Figure 6.19 Comparison of maximum likelihood estimates and experimentally measured values of CO_2 equilibrium partial pressure over aqueous MEA solutions. Lee et al. (1976a): (◆) 1 M, 100°C; (□) 1 M, 120°C; (○) 2.5 M, 100°C; (✖) 2.5 M, 120°C; (●) 3.75 M, 100°C; (■) 3.75 M, 120°C; (▲) 5 M, 100°C; (△) 5 M, 120°C. Isaacs et al. (1980): (×) 2.5 M, 100°C. Jones et al. (1959): (+) 15.3 wt %, 140°C. Muhlbauer and Monaghan (1957): (□) 2.5 M, 100°C. Other, Table 6.3: (▪).

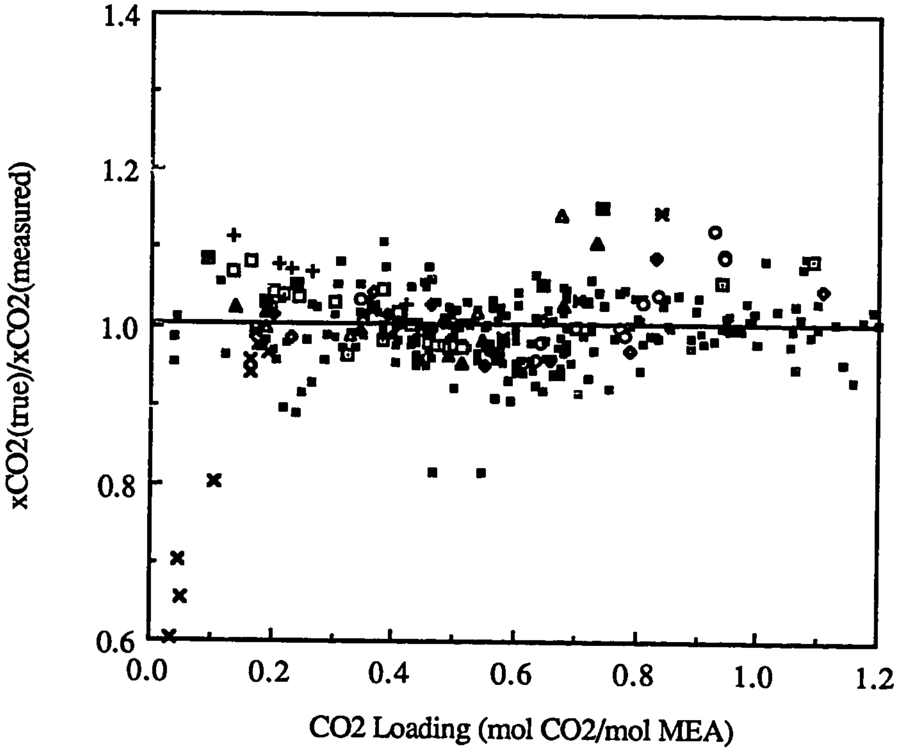

Figure 6.20 Comparison of maximum likelihood estimates and experimentally measured values of equilibrium CO_2 apparent mole fraction in aqueous MEA solutions. Lee et al. (1976a): (◆) 1 M, 100°C; (▣) 1 M, 120°C; (○) 2.5 M, 100°C; (✖) 2.5 M, 120°C; (◆) 3.75 M, 100°C; (■) 3.75 M, 120°C; (▲) 5 M, 100°C; (▲) 5 M, 120°C. Isaacs et al. (1980): (×) 2.5 M, 100°C. Jones et al. (1959): (+) 15.3 wt %, 140°C. Muhlbauer and Monaghan (1957): (□) 2.5 M, 100°C. Other, Table 6.3: (▪).

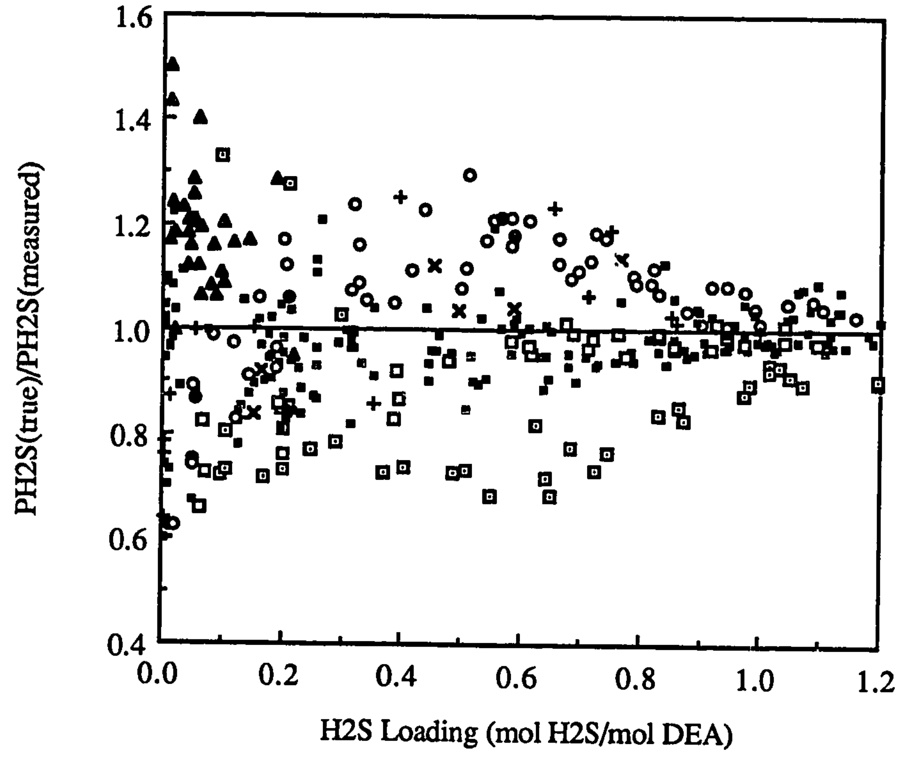

Figure 6.21 Comparison of maximum likelihood estimates and experimentally measured values of H_2S equilibrium partial pressure over aqueous DEA solutions. Lee et al. (1973a): (▣) 3.5 M, 50 to 100°C. Lee et al. (1973b): (▣) 0.5 M, 25 to 120°C; (○) 5.0 M, 25 to 120°C. Lal et al. (1985): (▲) 2.0 M, 40 and 100°C. Lawson and Garst (1976): (×) 25 wt %, 275 and 300°F; (●) 50 wt %, 200°F. Atwood et al. (1957): (+) all data. Other, Table 6.3: (▪).

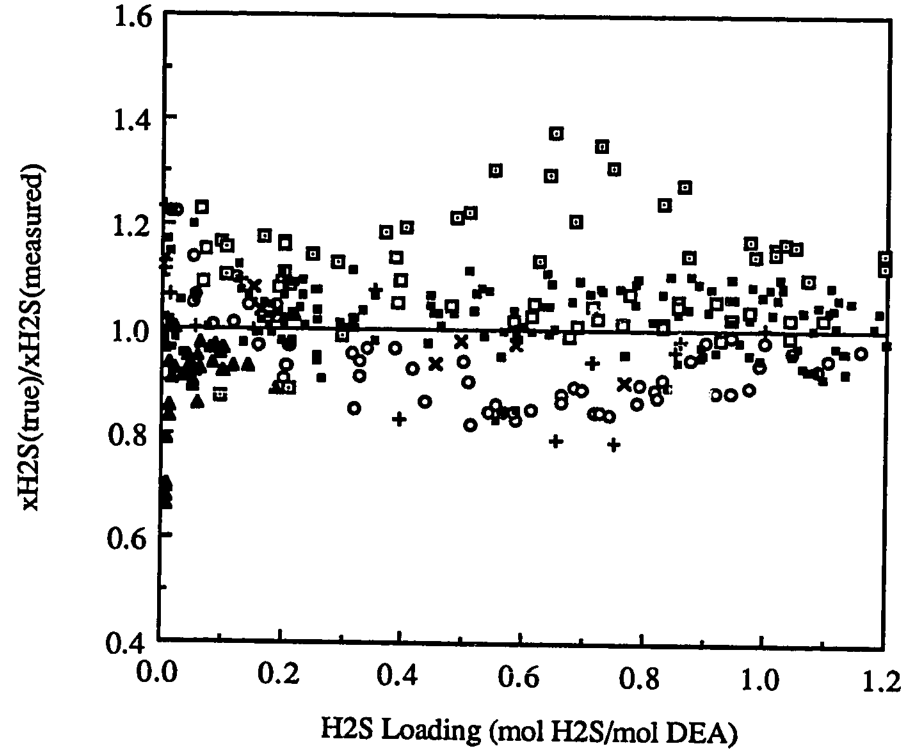

Figure 6.22 Comparison of maximum likelihood estimates and experimentally measured values of H_2S equilibrium apparent mole fraction in aqueous DEA solutions. Lee et al. (1973a): (□) 3.5 M, 50 to 100°C. Lee et al. (1973b): (⊡) 0.5 M, 25 to 120°C; (○) 5.0 M, 25 to 120°C. Lal et al. (1985): (▲) 2.0 M, 40 and 100°C. Lawson and Garst (1976): (×) 25 wt %, 275 and 300°F; (●) 50 wt %, 200°F. Atwood et al. (1957): (+) all data. Other, Table 6.3: (▪).

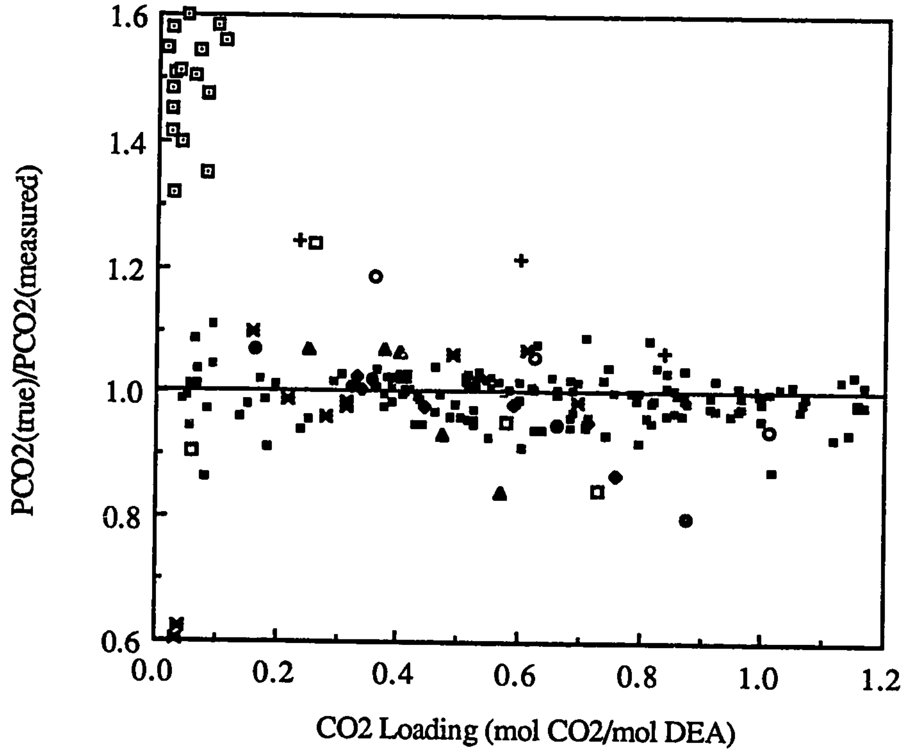

Figure 6.23 Comparison of maximum likelihood estimates and experimentally measured values of CO_2 equilibrium partial pressure over aqueous DEA solutions. Lal et al. (1985): (▣) 2.0 M, 100°C. Lee et al. (1972): (○) 0.5 M, 100°C; (+) 0.5 M, 120°C; (●) 1.98 M, 120°C; (□) 2.5 M, 120°C; (✖) 5.0 M, 100°C; (▲) 5.0 M, 120°C. Lawson and Garst (1976): (◆) 25 wt %, 250°F. Other, Table 6.3: (■).

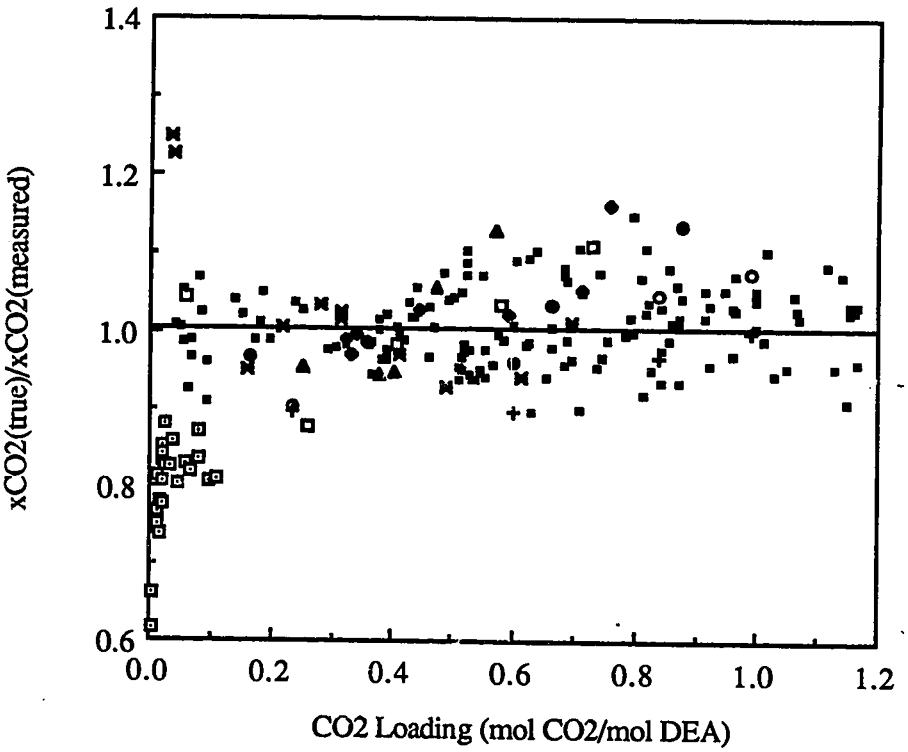

Figure 6.24 Comparison of maximum likelihood estimates and experimentally measured values of equilibrium CO_2 apparent mole fraction in aqueous DEA solutions. Lal et al. (1985): (▣) 2.0 M, 100°C. Lee et al. (1972): (○) 0.5 M, 100°C; (+) 0.5 M, 120°C; (●) 1.98 M, 120°C; (□) 2.5 M, 120°C; (✖) 5.0 M, 100°C; (▲) 5.0 M, 120°C. Lawson and Garst (1976): (◆) 25 wt %, 250°F. Other, Table 6.3: (▪).

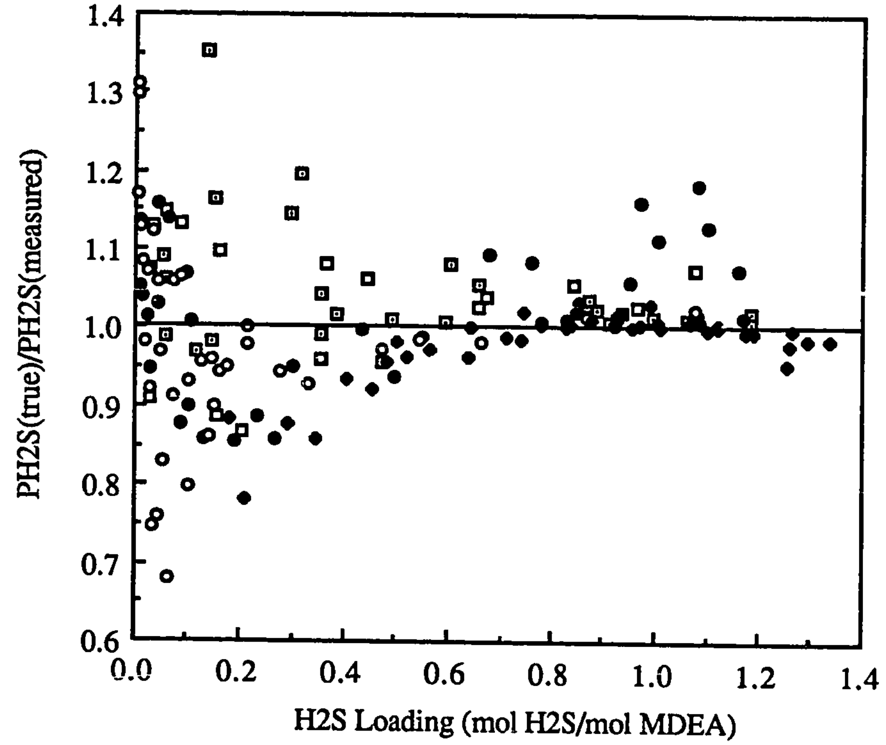

Figure 6.25 Comparison of maximum likelihood estimates and experimentally measured values of equilibrium H_2S partial pressure over aqueous MDEA solutions. Jou et al. (1982): (▣) 1.0 M, 25 to 120°C; (□) 2.0 M, 40 and 100°C; (●) 4.28 M, 25 to 120°C. Jou et al. (1976): (○) 3.04 M, 40 and 100°C. Bhairi (1984): (◆) all data.

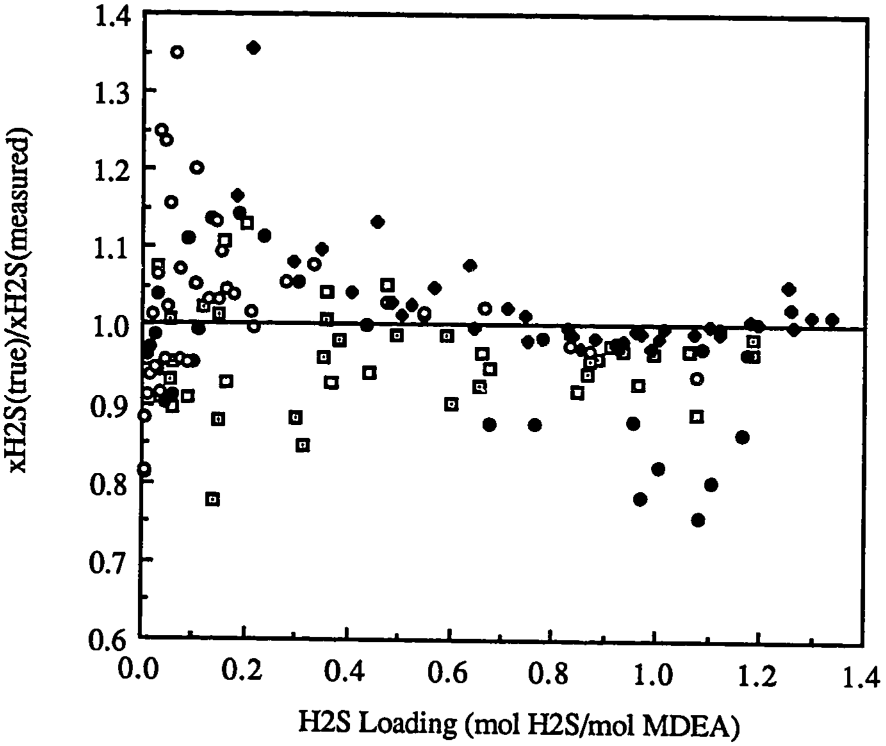

Figure 6.26 Comparison of maximum likelihood estimates and experimentally measured values of the equilibrium H_2S apparent mole fraction in aqueous MDEA solutions. Jou et al. (1982): (▣) 1.0 M, 25 to 120°C; (□) 2.0 M, 40 and 100°C; (●) 4.28 M, 25 to 120°C. Jou et al. (1976): (○) 3.04 M, 40 and 100°C. Bhairi (1984): (◆) all data.

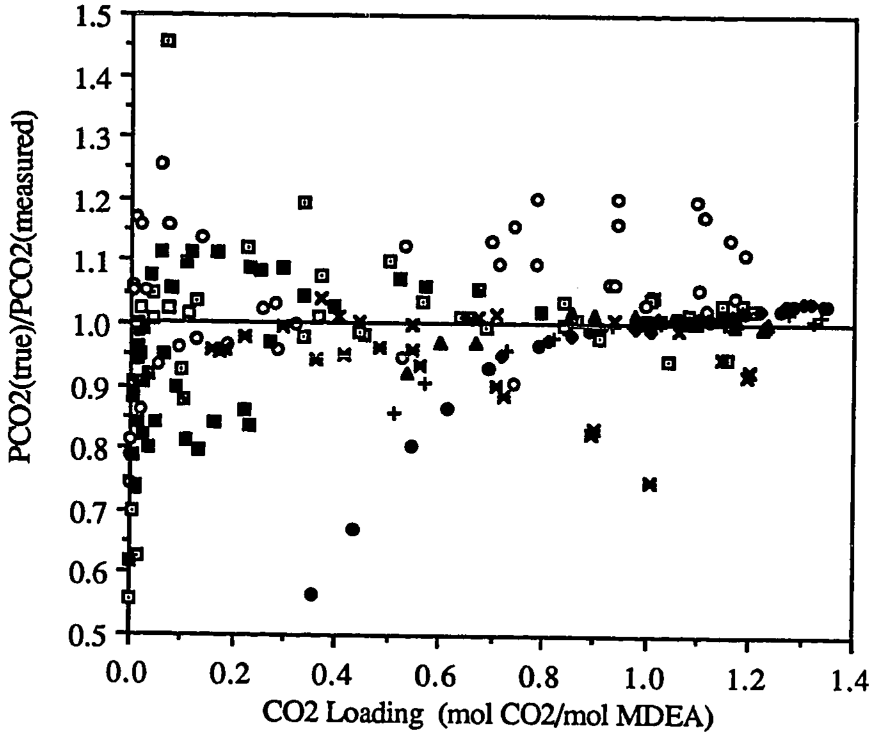

Figure 6.27 Comparison of maximum likelihood estimates and experimentally measured values of equilibrium CO_2 partial pressure over aqueous MDEA solutions. Jou et al. (1982): (⊡) 2.0 M, 25 to 120°C; (○) 4.28 M, 25 to 120°C. Jou et al. (1986): (■) 3.04 M, 40 and 100°C. Bhairi (1984): (◆) 1.0 M, 25°C; (●) 2.0 M, 25°C; (▲) 2.0 M, 50°C; (+) 20 wt %, 100°F; (×) 20 wt %, 150°F; (✖) 20 wt %, 240°F. This work, Table 5.3: (□) 2.0 M, 40°C; (▣) 4.28 M, 40°C.

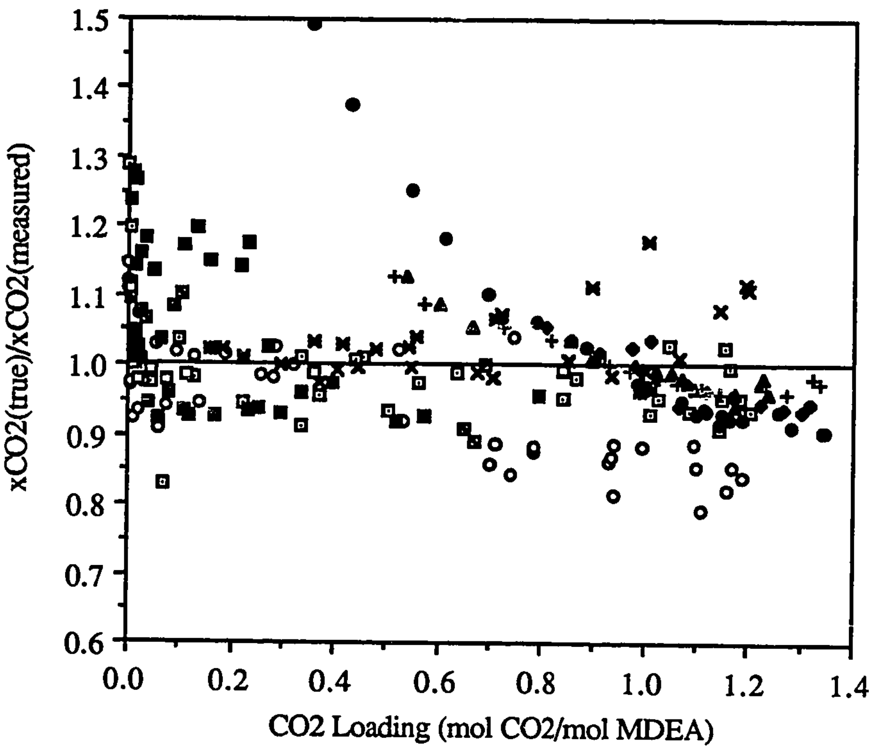

Figure 6.28 Comparison of maximum likelihood estimates and experimentally measured values of equilibrium CO_2 apparent mole fraction in aqueous MDEA solutions. Jou et al. (1982): (▣) 2.0 M, 25 to 120°C; (○) 4.28 M, 25 to 120°C. Jou et al. (1986): (■) 3.04 M, 40 and 100°C. Bhairi (1984): (●) 1.0 M, 25°C; (●) 2.0 M, 25°C; (▲) 2.0 M, 50°C; (+) 20 wt %, 100°F; (×) 20 wt %, 150°F; (✱) 20 wt %, 240°F. This work, Table 5.3: (□) 2.0 M, 40°C; (▣) 4.28 M, 40°C.

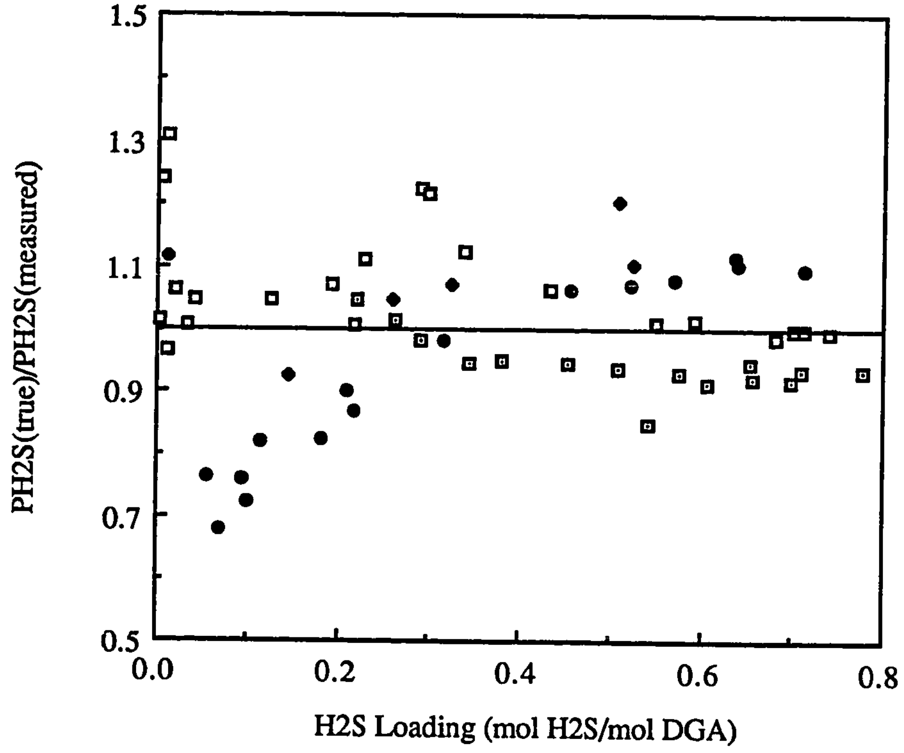

Figure 6.29 Comparison of maximum likelihood estimates and experimentally measured values of equilibrium H_2S partial pressure over aqueous DGA solutions. Martin et al. (1978): (▫) 60 wt %, 50°C; (•) 60 wt %, 100°C. Dingman et al. (1983): ▫) 65 wt %, 100°F; (•) 65 wt %, 180°F.

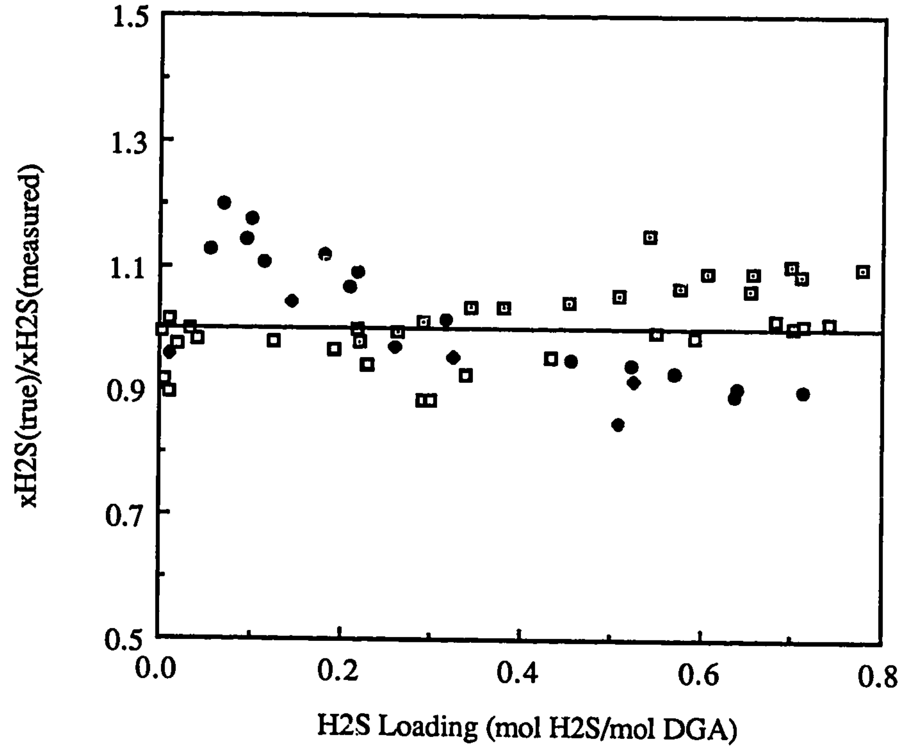

Figure 6.30 Comparison of maximum likelihood estimates and experimentally measured values of equilibrium H_2S apparent mole fraction in aqueous DGA solutions. Martin et al. (1978): (▫) 60 wt %, 50°C; (●) 60 wt %, 100°C. Dingman et al. (1983): (▫) 65 wt %, 100°F; (◆) 65 wt %, 180°F.

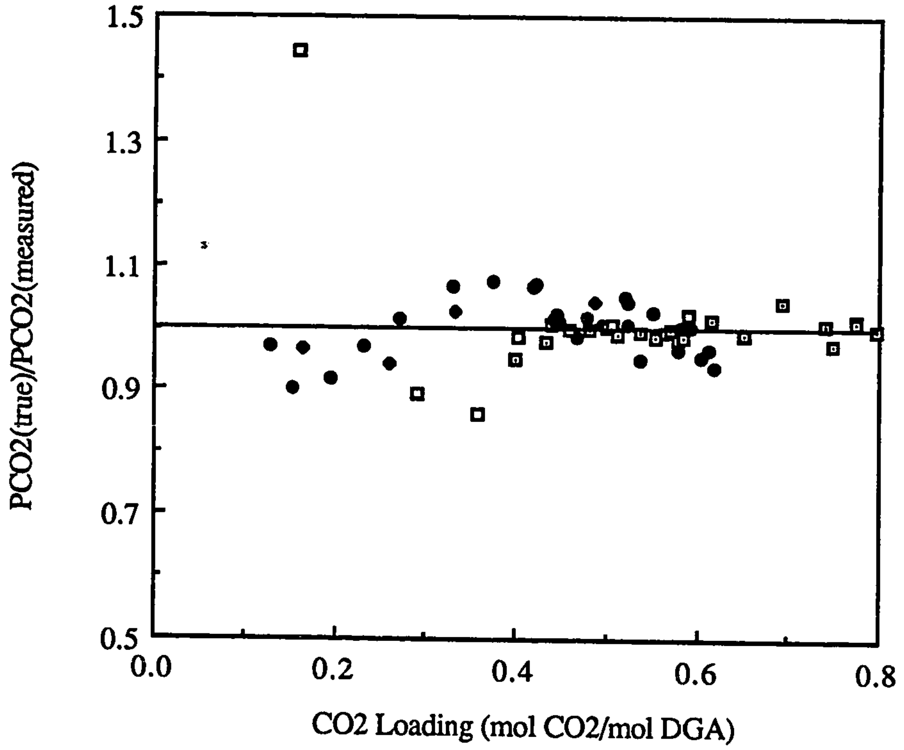

Figure 6.31 Comparison of maximum likelihood estimates and experimentally measured values of equilibrium CO_2 partial pressure over aqueous DGA solutions. Martin et al. (1978): (▫) 60 wt %, 50°C; (•) 60 wt %, 100°C. Dingman et al. (1983): (▫) 65 wt %, 100°F; (•) 65 wt %, 180°F.

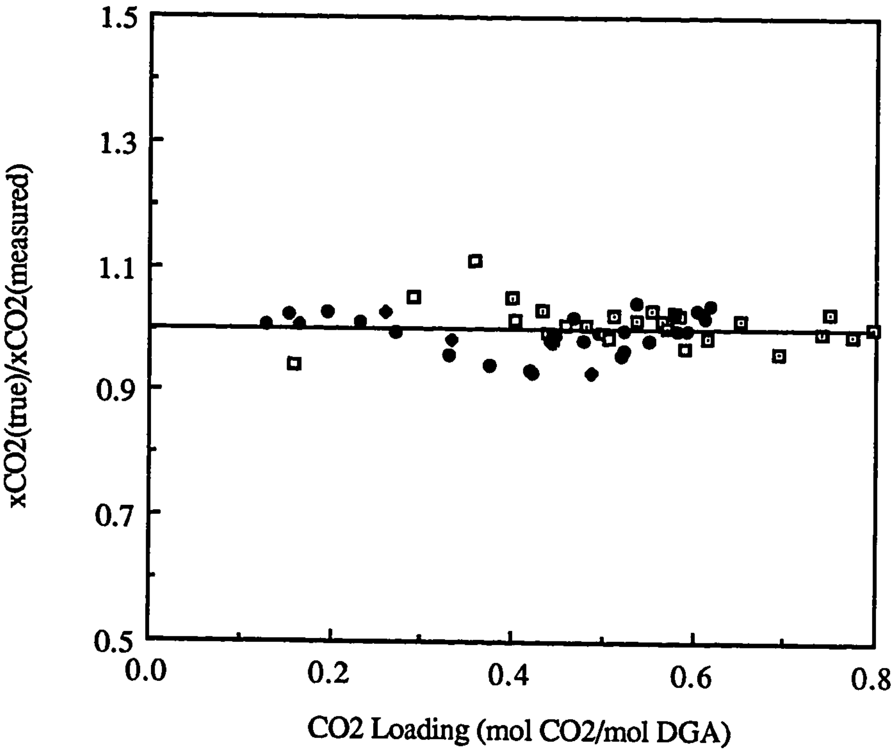

Figure 6.32 Comparison of maximum likelihood estimates and experimentally measured values of equilibrium CO_2 apparent mole fraction in aqueous DGA solutions. Martin et al. (1978): (▫) 60 wt %, 50°C; (●) 60 wt %, 100°C. Dingman et al. (1983): (▫) 65 wt %, 100°F; (◆) 65 wt %, 180°F.

6.4 Ternary Systems: Interpolation and Extrapolation and VLE Behavior

The primary goal of any modeling effort of this nature is to provide a means to confidently interpolate between and extrapolate beyond reported experimental data. The latter is particularly important in view of the relative lack of experimental data at low acid gas partial pressures. It is in the low acid gas loading, low acid gas partial pressure range where VLE is perhaps most important. VLE data in this region provides the thermodynamic partial pressure limit to which a sour gas stream may be purified.

Figures 6.33 through 6.44 present H_2S or CO_2 equilibrium partial pressures over MEA, DEA, or MDEA aqueous solutions as functions of acid gas loading in the liquid phase. These figures were generated using the model for the six ternary systems. Amine concentrations were chosen to be representative of industrial applications. In order to provide graphical representation of the model that can be utilized over the entire range of acid gas loadings, plots are presented in two formats - semi-log and log-log. The first can be utilized over the acid gas loading range from 0.1 to 1.0 (moles acid gas per mole amine). The second manner of representation is useful in the acid gas loading range below 0.1 (moles of acid gas per mole amine).

In examining the equilibrium behavior of acid gas-alkanolamine-water systems it is useful to first consider a simplified thermodynamic analysis of the chemical and physical equilibria. Such an analysis serves as an aid in understanding qualitative behavior of the equilibrium curves. In the discussion to follow the amine-H_2S-water systems are treated first followed by treatment of the amine-CO_2-water systems.

If liquid phase activity coefficients and vapor phase fugacity coefficients are all taken to be unity and if the second dissociation of H_2S to $S^=$ (reaction 4c) is neglected, it can be shown that the equilibrium partial pressure of H_2S above a solution of H_2S-amine-water is given by the following explicit algebraic equation

$$p_{H_2S} = \frac{H\, K_A\, [\mathrm{amine}]_t}{K_{H_2S}} \, \frac{\alpha_{H_2S}^2}{(1 - \alpha_{H_2S})} \tag{6.1}$$

where H represents the Henry's constant for H_2S, K_A and K_{H_2S} are equilibrium constants for reactions (4f) and (4b) respectively, $[\mathrm{amine}]_t$ is the total amine concentration (ie. the total concentration of amine in all possible forms, molecular and ionic) and α_{H_2S} is the H_2S loading in moles H_2S/mole amine. Equation (6.1) does not hold in the very low loading, high pH range where the affect of hydroxide concentration on equilibrium is important. The functional form of equation (6.1) suggests that at a constant value of H_2S loading the equilibrium partial pressure of H_2S increases as total amine concentration increases. It also suggests that over the acid gas loading range for which $\alpha << 1$ the slope of the partial pressure curve on a log-log scale should be two.

Figures 6.33 and 6.34 clearly illustrate the first point. The H_2S equilibrium partial pressure is greater for a 5.0 M MEA (5.0 M DEA) solution than for a 2.5 M MEA (2.0 M DEA) solution at all temperatures. Figures 6.36 and 6.37 show that the slope of the equilibrium curve on the log-log scale in the H_2S loading range from 0.01 to 0.10 where $\alpha << 1$ is indeed close to 2.

A similar analysis is more complicated for the CO_2-alkanolamine-water systems. In addition to the dissociation of CO_2, one must also consider the formation of carbamate for MEA and DEA. MDEA, as noted earlier, does not form a carbamate. Therefore, the equilibrium behavior of CO_2-MEA-water and CO_2-DEA-water solutions will be examined first, followed by consideration of the equilibrium behavior of the CO_2-MDEA-water system.

Because the formation of carbamate is known to dominate chemical equilibria below loadings of 0.5 (moles CO_2/mole amine) and that reversion of carbamate to bicarbonate dominates equilibria above a loading of 0.5, the two loading ranges will be examined separately. Again assuming that activity coefficients and fugacity coefficients of all species are unity, and neglecting the second dissociation of CO_2 to $CO_3^=$, the following relations can be derived for the partial pressure of CO_2 above aqueous solutions of primary or secondary alkanolamines:

For $\alpha_{CO_2} < 0.5$

$$p_{CO_2} = \frac{H\,K_A\,K_C}{K_{CO_2}} \frac{\alpha_{CO_2}^2}{(1 - 2\alpha_{CO_2})^2} \tag{6.2}$$

For $\alpha_{CO_2} > 0.5$

$$p_{CO_2} = \frac{H\,K_A\,[\text{amine}]_t^2}{K_{CO_2}\,K_C} \frac{\alpha_{CO_2}\,(2\alpha_{CO_2} - 1)^2}{(1 - \alpha_{CO_2})} \tag{6.3}$$

where K_{CO_2} and K_C are the equilibrium constants for CO_2 dissociation (reaction 4d) and carbamate reversion to bicarbonate (reaction 4g) respectively. Note that equations (6.2) and (6.3) do not converge at a loading of 0.5 mol/mol.

Equation (6.2), which holds for CO_2 loadings less than 0.5 mol/mol, suggests that the CO_2 equilibrium partial pressure is not a function of total amine concentration in this range. However, equation (6.3) indicates that above a loading of 0.5 mol/mol CO_2 equilibrium partial pressure is a quadratic function of total amine concentration. This phenomenon can be clearly seen in Figures 6.39 and 6.40 where the equilibrium curves for the 2.5 M MEA (2.0 M DEA) and 5.0 M MEA (5.0 M DEA) solutions are very nearly identical at low loadings. Above a loading of 0.5 mol/mol the difference between the equilibrium curves for the high and low amine concentrations increases abruptly. Equation (6.2) also suggests that over the range for which CO_2 loading is much less than unity (α<< 1) the slope of the CO_2 equilibrium curve should also have a value of two on a log-log scale. Figures 6.42 and 6.43 support this expected behavior.

Because MDEA cannot form a carbamate species, the VLE behavior of CO_2-MDEA-water solutions is significantly different from the VLE behavior of CO_2-MEA-water and CO_2-DEA-water solutions. Indeed, the VLE behavior of the CO_2-MDEA-water system more closely resembles the VLE behavior of aqueous H_2S-amine-water solutions as can be seen by comparing Figures 6.41 and 6.44 with the corresponding figures representing H_2S equilibrium partial pressures over aqueous amine solutions. However, unlike H_2S-amine systems, the second dissociation of the weak acid, in this case CO_2, cannot be neglected. As will be shown in section 6.5 to follow, the liquid phase concentration of carbonate ($CO_3^=$) is significant relative to the concentration of bicarbonate (HCO_3^-). In virtually all amine applications, the liquid phase concentration of bisulfide, $S^=$, is negligible relative to the liquid phase concentration of bisulfide. Therefore, the simple thermodynamic analysis applied to H_2S-amine-water systems, equation (6.1), does not apply to the CO_2-MDEA-water system.

As noted previously, as the acid gas loading approaches zero, the hydroxide concentration becomes great enough to affect equilibrium behavior. The actual loading at which this occurs depends, of course, on the pKa of the alkanolamine solvent. If activity coefficients are fixed at unity and only the dominant equilibria are considered it can be shown that the slopes of both the H_2S and CO_2 equilibrium curves on log-log scales should, in theory, approach unity as the loading approaches zero, providing the pKa of the amine is great enough to result in a substantial presence of hydroxide in the solution. The transition from a slope of unity to a slope of two is apparent at a loading of approximately 0.004 mol/mol for the MEA ternary systems. The corresponding transition does not appear clearly for the DEA systems. This is because DEA has a lower pKa (is a weaker base) than MEA; the hydroxide concentration is insignificant over the range of acid gas loadings considered here. It is not clear that this transition will appear at all for MDEA solutions because the pKa of MDEA may not be high enough to result in the formation of a substantial amount of hydroxide.

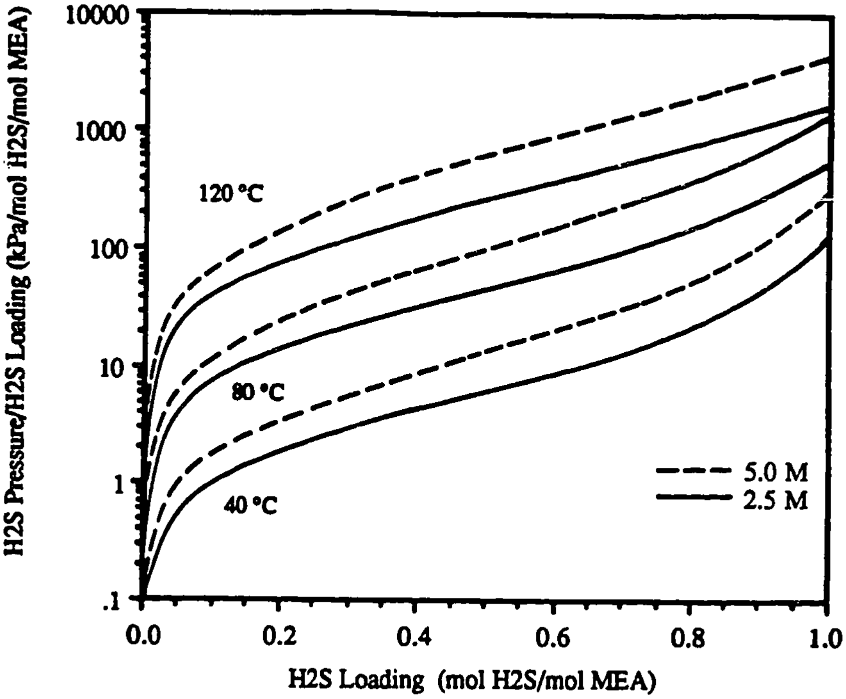

Figure 6.33 Model representation of H_2S equilibrium partial pressure over 2.5 and 5.0 kmol m^{-3} MEA solutions from 40 to 120 °C.

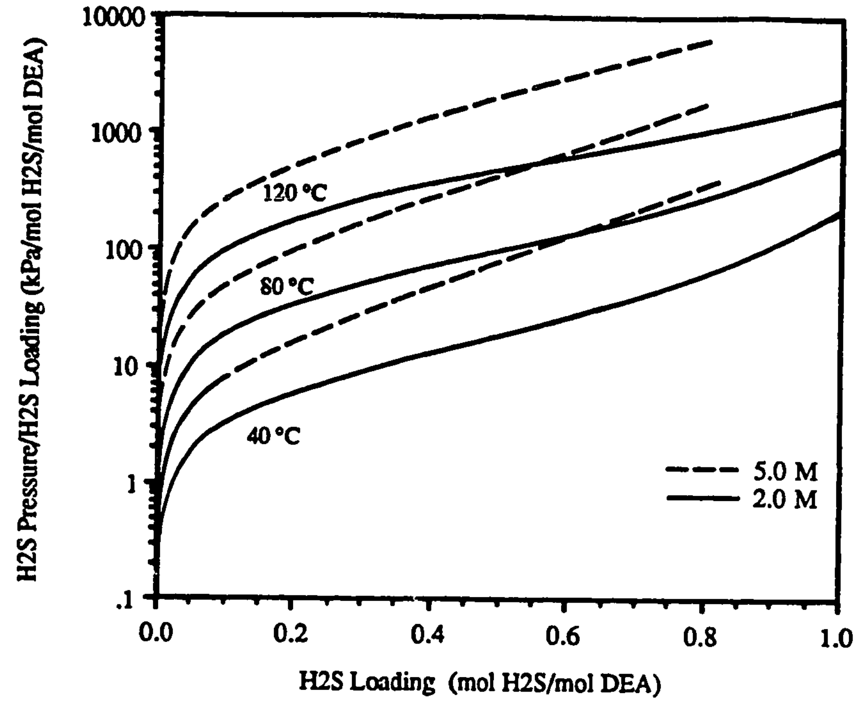

Figure 6.34 Model representation of H_2S equilibrium partial pressure over 2.0 and 5.0 kmol m^{-3} DEA solutions from 40 to 120 °C.

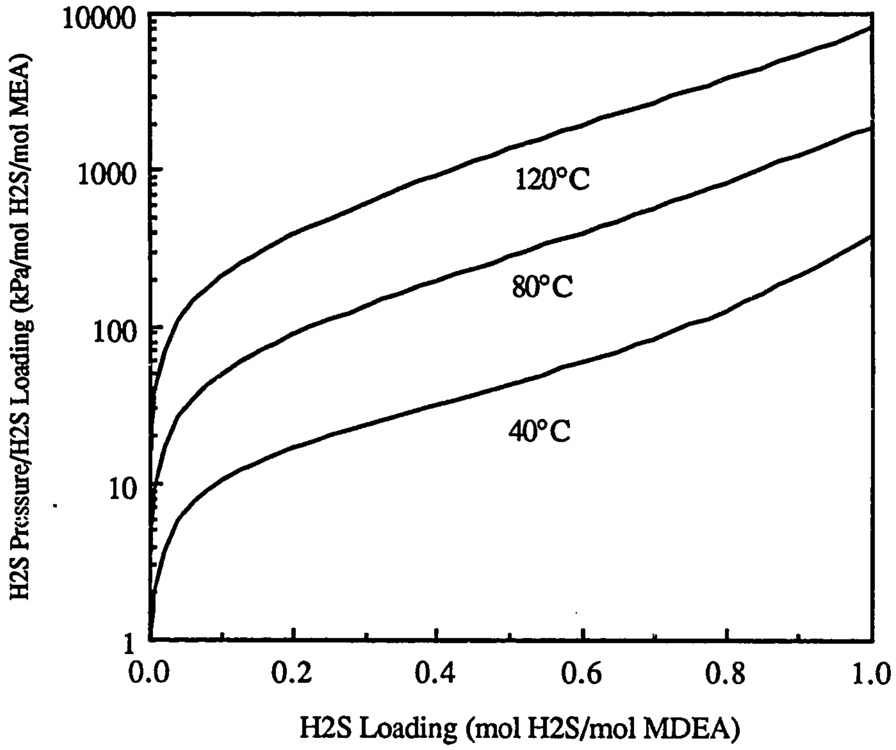

Figure 6.35 Model representation of H_2S equilibrium partial pressure over a 4.0 kmol m^{-3} MDEA solution from 40 to 120 °C.

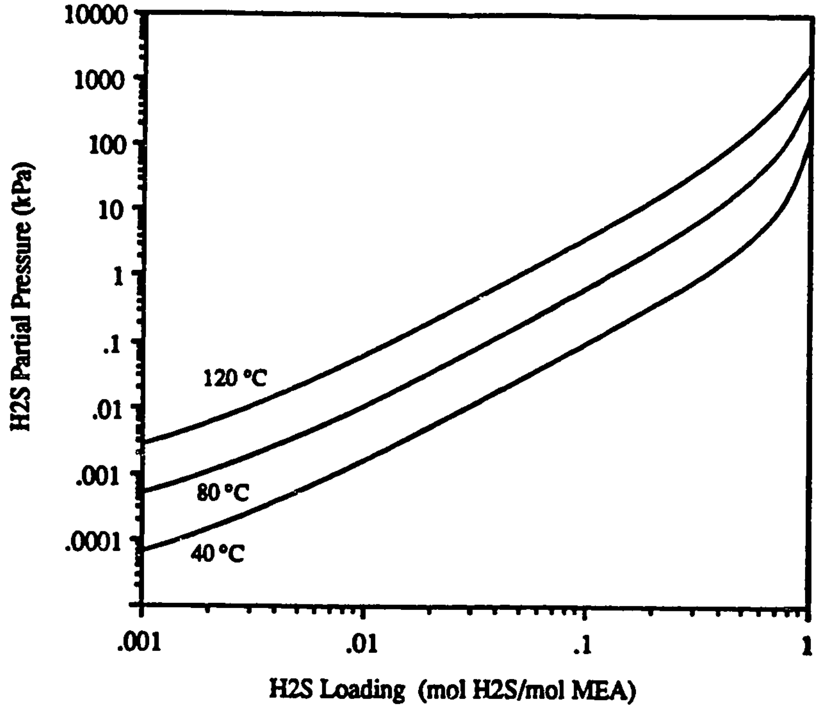

Figure 6.36 Model representation of H_2S equilibrium partial pressure over a 2.5 kmol m^{-3} MEA solution from 40 to 120 °C.

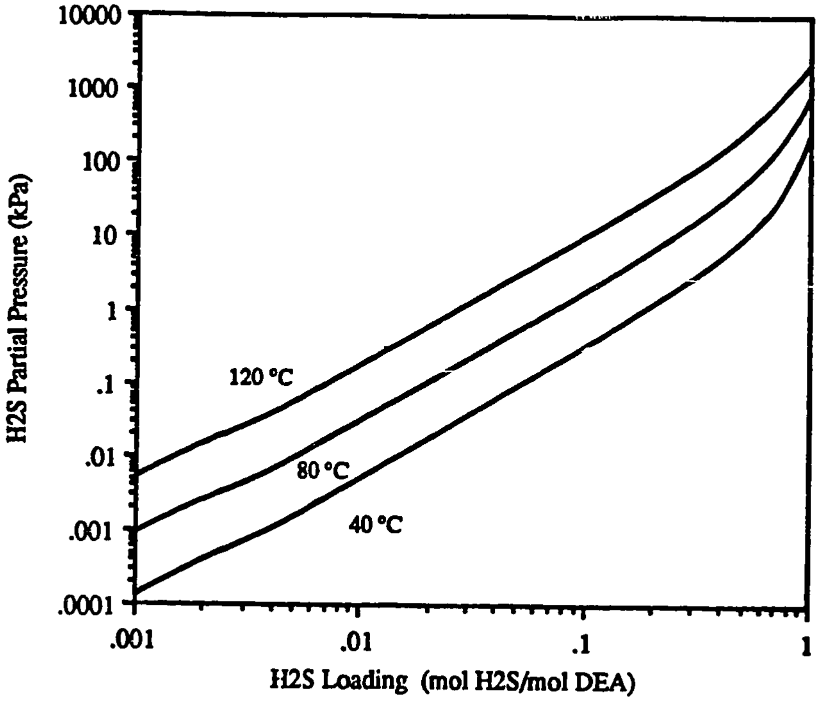

Figure 6.37 Model representation of H_2S equilibrium partial pressure over a 2.0 kmol m^{-3} DEA solution from 40 to 120 °C.

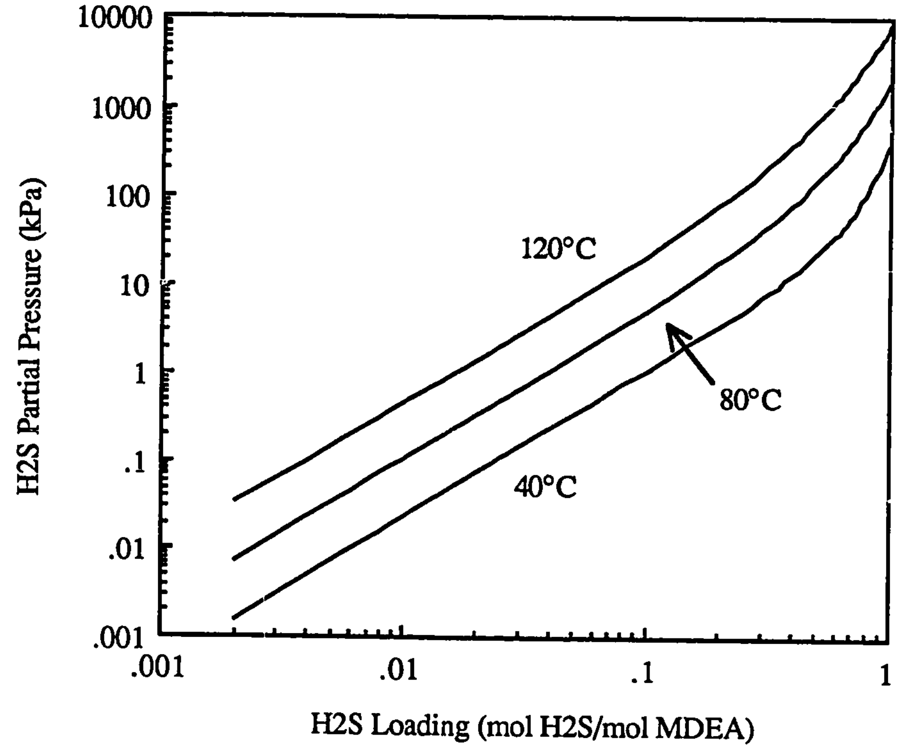

Figure 6.38 Model representation of H_2S equilibrium partial pressure over a 4.0 kmol m^{-3} MDEA solution from 40 to 120 °C.

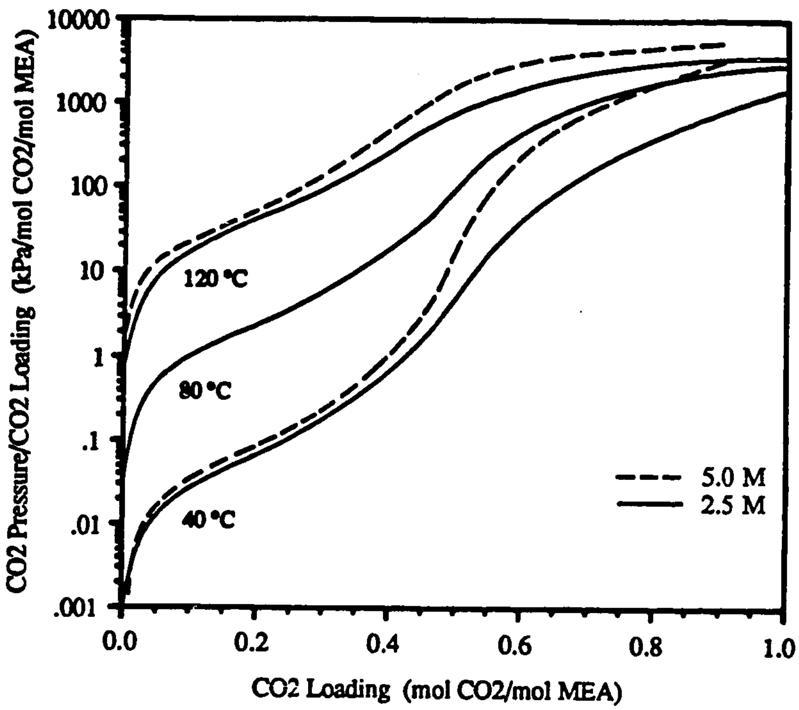

Figure 6.39 Model representation of CO_2 equilibrium partial pressure over 2.5 and 5.0 kmol m^{-3} MEA solutions from 40 to 120 °C.

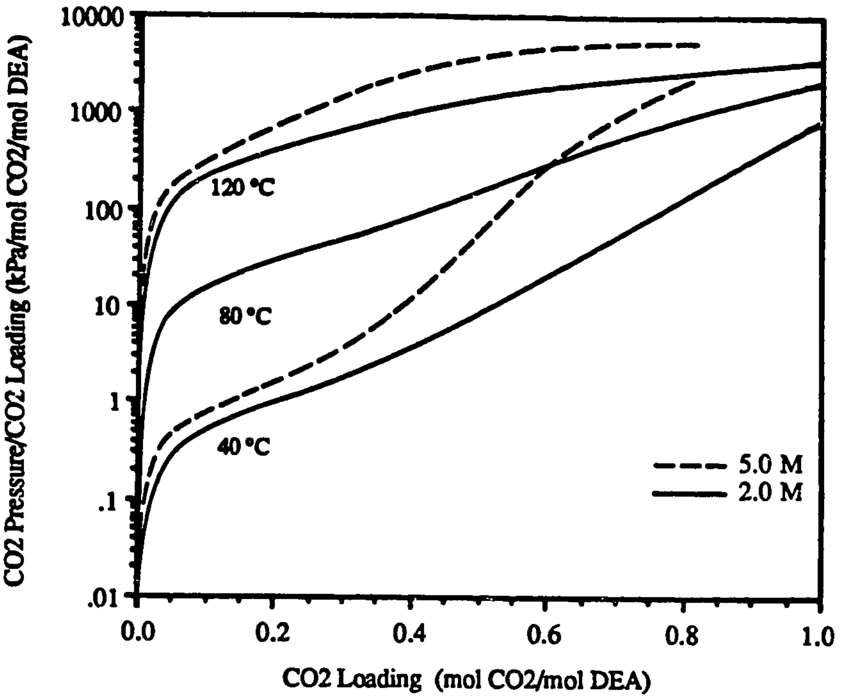

Figure 6.40 Model representation of CO_2 equilibrium partial pressure over 2.0 and 5.0 kmol m^{-3} DEA solutions from 40 to 120 °C.

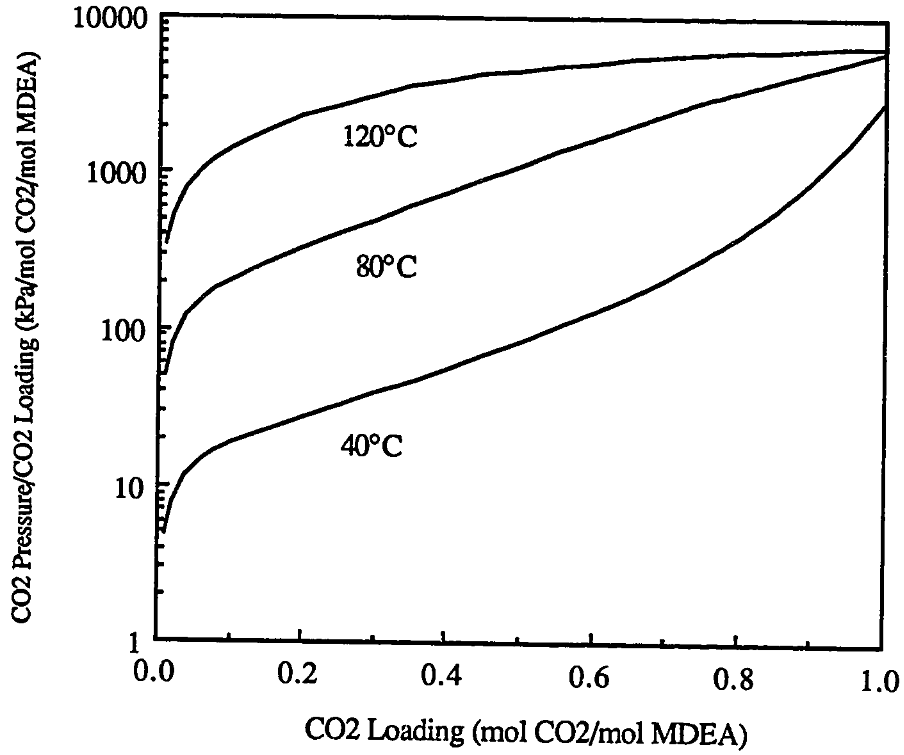

Figure 6.41 Model representation of CO_2 equilibrium partial pressure over a 4.0 kmol m^{-3} MDEA solution from 40 to 120 °C.

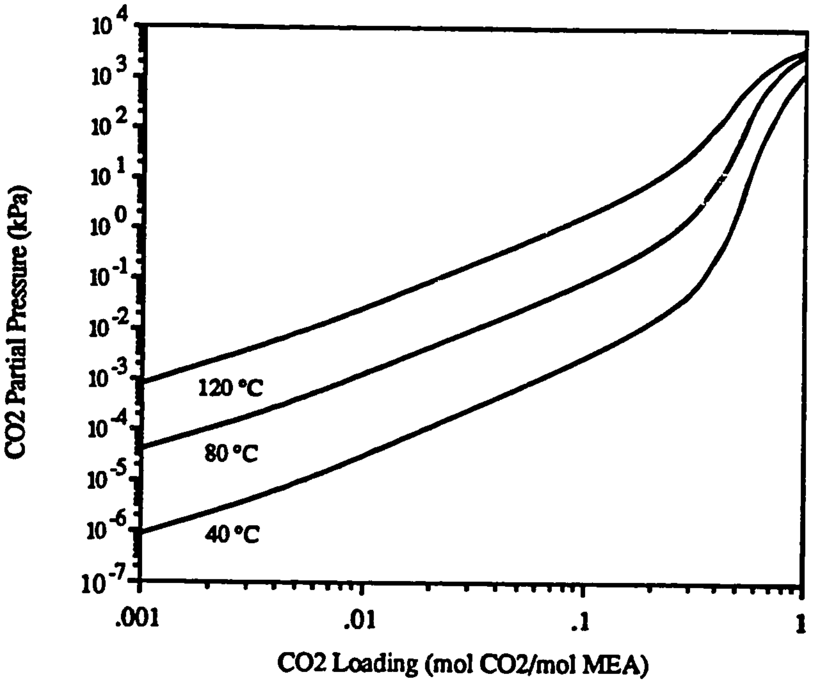

Figure 6.42 Model representation of CO_2 equilibrium partial pressure over a 2.5 kmol m^{-3} MEA solution from 40 to 120 °C.

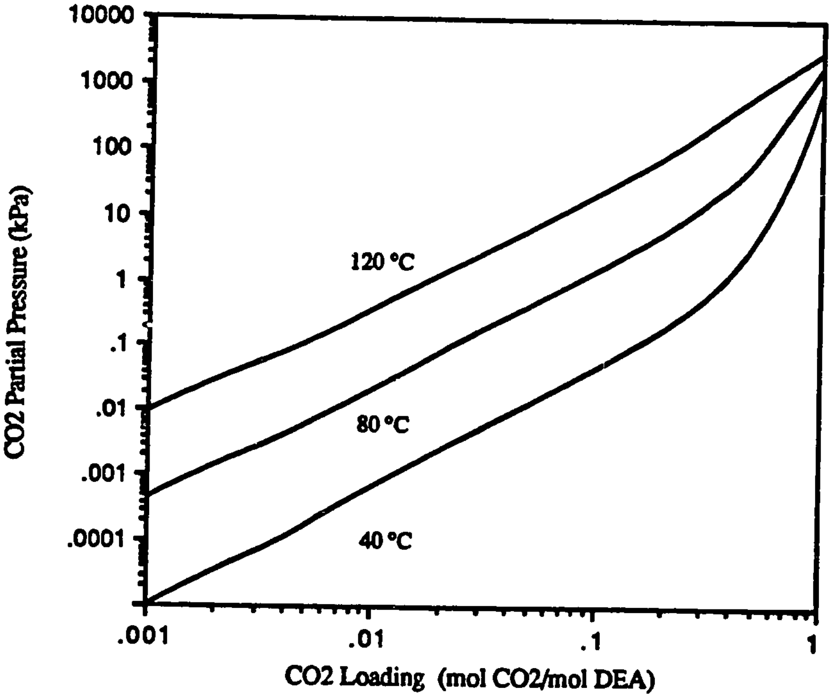

Figure 6.43 Model representation of CO_2 equilibrium partial pressure over a 2.0 kmol m^{-3} DEA solution from 40 to 120 °C.

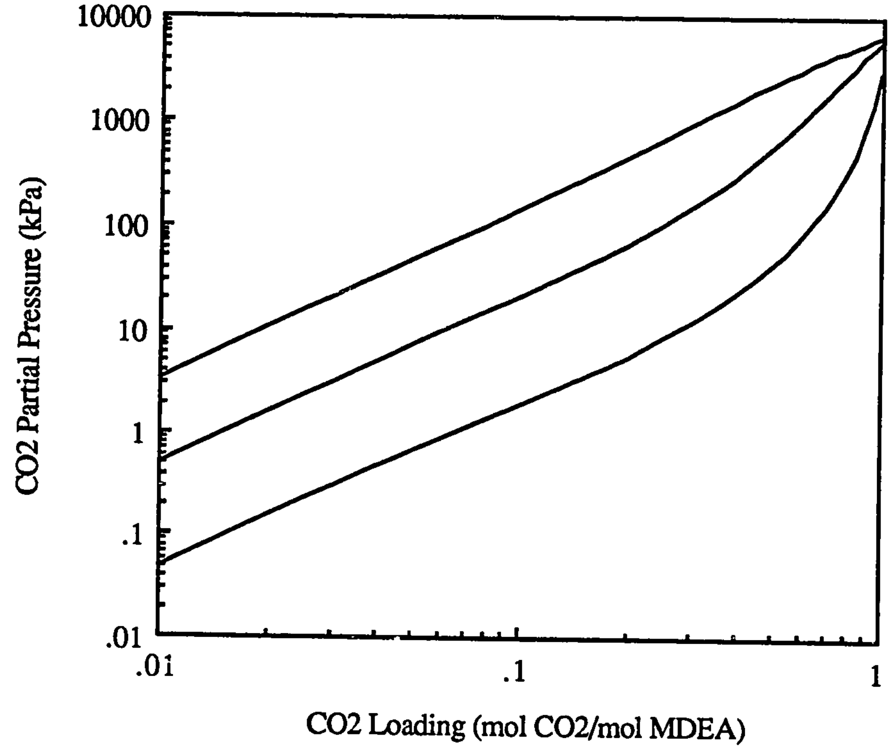

Figure 6.44 Model representation of CO_2 equilibrium partial pressure over a 4.0 kmol m^{-3} MDEA solution from 40 to 120 °C.

6.5 Quaternary Systems: Experimental Data Representation

The only additional/unique Electrolyte-NRTL binary interaction parameters that arise in modeling of single amine quaternary systems (amine-H_2S-CO_2-H_2O) are **acid gas-ion pair** parameters and **ion pair-ion pair** parameters. For ternary systems, acid gas-ion pair parameters were fixed at default values and ion pair-ion pair parameters were set to zero. The same procedure was adopted for quaternary systems. No new parameters were adjusted on the quaternary system experimental data. Instead, the model was used in a predictive manner to evaluate representation of experimental quaternary system data. That is, the Electrolyte-NRTL binary interaction parameters fitted on binary and ternary system data were fixed at adjusted values and the Data Regression system of ASPEN PLUS was used to calculate maximum likelihood estimates, or estimated *true* values, of equilibrium acid gas partial pressures and estimated *true* values of liquid phase acid gas apparent mole fractions.

To evaluate representation of quaternary system data, *true* values of acid gas partial pressures and *true* values of liquid phase apparent mole fractions are compared to measured values as was done with binary and ternary systems. The quaternary systems of interest in this work include MEA-H_2S-CO_2-H_2O, DEA-H_2S-CO_2-H_2O, MDEA-H_2S-CO_2-H_2O, and DGA-H_2S-CO_2-H_2O.

It was noted earlier that H_2O and amine partial pressures are generally not reported with equilibrium acid gas partial pressures. In reducing ternary system data this was not a handicap because the Data Regression System allows parameters to be fitted on acid gas VLE data only. In practice, this was done by equating the total system pressure, required as input by the Data Regression System, to the equilibrium acid gas partial pressure. This is a valid procedure if solvent equilibria are not used in estimating parameters. However, H_2O and amine VLE could not neglected in estimating maximum likelihood values of the state variables for quaternary systems. Still, the total system pressure was equated to the sum of acid gas partial pressures even though this is not valid at low acid gas loadings where the vapor pressure of water is of the same relative magnitude as acid gas partial pressures. Hence, maximum likelihood estimates of quaternary system state variables can not be expected to agree with experimentally measured values at low acid gas loadings.

There is an abundance of solubility data reported in the literature for the quaternary systems. It would be impossible to compare model representation with all reported experimental solubility measurements due to space limitations. Therefore, 'representative' data sources were selected for this purpose. Results of this comparison for the four systems of interest are presented in Tables 6.7 through 6.10.

Again, if the experimental measurements were error-free, and if the model represented the experimental data perfectly, the H_2S and CO_2 partial pressure ratios and apparent mole fractions ratios would all assume values of unity. As indicated in Tables 6.7 through 6.10, estimated *true* values of acid gas partial pressure and liquid phase mole fraction are generally in good agreement with experimental measurements except at very low acid gas loadings.

Only moderately good agreement was achieved between the estimated *true* values and measured values of the equilibrium CO_2 partial pressure in Table 6.9 for the MDEA quaternary system. This is not surprising in view of the poor agreement between and within different sources of ternary system MDEA-CO_2-H_2O VLE data to which Electrolyte-NRTL parameters were fitted. However, it should also be noted that many of the quaternary system VLE measurements reported by Jou et al. (1986) (to which estimated *true* values are compared) were made at very low CO_2 loadings. Therefore, poor agreement between estimated *true* and experimentally measured CO_2 partial pressures and liquid phase apparent mole fractions is expected.

Only moderately good agreement between estimated *true* values and measured values of DGA quaternary system VLE data was achieved for several of the measurements reported by Dingman et al. (1983). The disagreement is most frequent at low acid gas partial pressures, but agreement is poor for several data points with moderate or high acid gas loadings also. Moreover, disagreement between *true* and measured state variables seems to be most prevalent in the data reported at 100°F. Agreement is better at 140°F and 180°F. For the bulk of the data reported by Dingman and coworkers agreement between estimated *true* and measured values of the state variables appears to be good suggesting that the disagreement may be due to experimental problems at the lowest temperature and/or random experimental errors.

On the whole, the model satisfactorily represents quaternary system experimental data. Most ratios of estimated *true* to measured values of acid gas partial pressure and estimated *true* to measured values of liquid phase apparent mole fraction are within 10 to 15 % of unity. These results support the implicit proposition that it is not necessary to fit additional parameters on quaternary system VLE.

Table 6.7. Comparison of estimated *true* values and experimentally measured values of H_2S and CO_2 equilibrium partial pressures, P_{H_2S} and P_{CO_2}, and liquid phase mole fractions (apparent), x_{H_2S} and x_{CO_2}, for the quaternary system H_2S-CO_2-MEA-H_2O. Data are from Muhlbauer and Monaghan (1957) for a 2.5 kmol m^{-3} (acid gas free) MEA solution. α = acid gas loading = mole acid gas / mole MEA.

α_{H_2S} (mole/mole MEA)	α_{CO_2} (mole/mole MEA)	$p^e_{H_2S}$ (kPa)	$p^e_{CO_2}$ (kPa)	$\frac{x^t_{H2S}}{x^e_{H2S}}$	$\frac{x^t_{CO2}}{x^e_{CO2}}$	$\frac{p^t_{H2S}}{p^e_{H2S}}$	$\frac{p^t_{CO2}}{p^e_{CO2}}$
Temperature = 40°C:							
0.820	0.108	94.79	2.72	1.03	1.00	0.97	0.97
0.614	0.167	45.60	2.61	1.08	1.11	1.08	0.97
0.488	0.172	6.96	0.15	1.05	1.15	1.05	0.92
0.384	0.165	2.32	0.04	1.01	1.21	1.01	0.84
0.284	0.172	1.04	0.05	0.90	1.56	1.06	0.68
0.403	0.280	44.00	8.32	1.10	1.16	0.97	0.84
0.364	0.286	18.93	2.65	1.05	1.16	1.03	0.89
0.336	0.292	12.51	1.52	1.04	1.16	1.04	0.89
0.256	0.290	3.89	0.30	1.03	1.19	1.00	0.84
0.185	0.296	1.45	0.10	0.99	1.18	1.02	0.87
0.120	0.302	0.55	0.06	0.91	1.22	1.16	0.95
0.074	0.304	0.24	0.05	0.86	1.26	1.30	1.03
0.038	0.309	0.11	0.03	0.88	1.20	1.24	1.03
0.155	0.286	0.80	0.08	0.91	1.28	1.17	0.91
0.134	0.346	1.85	0.35	0.99	1.22	1.01	0.83
0.112	0.352	1.11	0.23	0.95	1.20	1.10	0.92
0.090	0.356	0.64	0.14	0.93	1.17	1.17	1.01
0.066	0.348	0.25	0.09	0.82	1.22	1.58	1.30
0.043	0.347	0.17	0.05	0.90	1.14	1.24	1.08
0.022	0.333	0.06	0.07	0.78	1.31	1.65	1.25
0.142	0.410	7.93	4.55	1.02	1.16	0.98	0.85
0.098	0.430	6.35	6.33	1.02	1.18	0.95	0.81
0.075	0.447	3.73	4.47	0.99	1.14	1.02	0.89
0.057	0.445	2.31	3.25	0.98	1.16	1.04	0.89
0.036	0.472	1.24	2.60	0.97	1.10	1.08	0.99
0.019	0.487	0.45	1.73	0.92	1.07	1.24	1.17
0.289	0.307	9.15	1.15	1.04	1.17	1.00	0.86
0.266	0.357	22.16	7.39	1.05	1.15	0.98	0.85
0.234	0.364	12.36	4.32	1.00	1.17	1.09	0.93
0.214	0.358	7.41	1.84	1.00	1.16	1.05	0.91
0.171	0.357	4.05	1.00	0.99	1.21	1.06	0.88

Table 6.7. Continued

α_{H_2S}	α_{CO_2}	$p^e_{H_2S}$	$p^e_{CO_2}$	$\frac{x^t_{H2S}}{x^e_{H2S}}$	$\frac{x^t_{CO2}}{x^e_{CO2}}$	$\frac{p^t_{H2S}}{p^e_{H2S}}$	$\frac{p^t_{CO2}}{p^e_{CO2}}$
(mole/mole MEA)		(kPa)	(kPa)				
0.383	0.317	45.33	12.56	1.04	1.13	1.04	0.92
0.300	0.350	30.66	11.17	1.04	1.15	1.02	0.89
0.170	0.456	22.93	20.93	1.03	1.12	0.95	0.85
0.138	0.460	14.59	13.87	1.03	1.11	0.94	0.85
0.117	0.471	8.69	8.91	0.99	1.09	1.03	0.94
0.092	0.464	5.16	6.56	0.96	1.11	1.12	1.00
0.556	0.181	21.73	1.24	1.04	1.18	1.18	1.00
0.451	0.180	4.80	0.14	1.00	1.24	1.14	0.92
0.220	0.175	0.56	0.03	0.84	1.60	1.04	0.65
0.146	0.174	0.26	0.03	0.75	1.80	1.05	0.58
0.114	0.174	0.16	0.01	0.77	1.55	1.09	0.70
0.742	0.104	59.06	2.13	1.07	1.11	1.16	1.05
0.684	0.112	18.67	0.37	1.04	1.12	1.17	1.04

Temperature = 100°C:

0.549	0.076	126.26	10.27	1.00	1.10	1.09	0.97
0.489	0.083	84.26	7.61	0.99	1.12	1.11	0.96
0.453	0.082	71.99	7.01	1.00	1.15	1.08	0.91
0.412	0.081	53.73	5.65	0.99	1.19	1.08	0.88
0.532	0.073	98.93	8.40	0.98	1.14	1.15	0.97
0.381	0.073	42.13	3.81	0.98	1.19	1.05	0.85
0.299	0.075	29.86	3.27	1.01	1.24	0.92	0.73
0.224	0.084	15.73	2.41	0.97	1.25	0.93	0.72
0.177	0.167	17.20	6.56	0.98	1.18	0.97	0.83
0.236	0.168	30.40	9.99	1.00	1.18	0.98	0.84
0.286	0.171	42.53	11.27	1.00	1.11	1.01	0.91
0.326	0.172	54.66	14.53	0.99	1.11	1.06	0.94
0.375	0.169	75.19	20.67	0.98	1.13	1.10	0.96
0.422	0.156	101.32	22.53	1.00	1.10	1.07	0.96
0.444	0.146	111.06	22.40	1.01	1.10	1.07	0.96
0.342	0.241	128.52	73.46	1.02	1.12	1.03	0.94
0.306	0.239	85.06	41.60	1.01	1.09	1.01	0.95
0.308	0.246	93.33	51.33	1.01	1.10	1.02	0.95
0.275	0.234	62.13	31.60	1.00	1.11	1.03	0.94
0.252	0.229	48.00	23.86	0.99	1.11	1.03	0.94
0.187	0.230	29.20	16.67	1.00	1.13	0.97	0.89
0.141	0.244	18.13	13.93	0.98	1.12	1.01	0.92
0.093	0.251	10.04	12.09	0.96	1.15	1.04	0.91

Table 6.8. Comparison of estimated *true* values and experimentally measured values of H_2S and CO_2 equilibrium partial pressures, P_{H_2S} and P_{CO_2}, and liquid phase mole fractions (apparent), x_{H_2S} and x_{CO_2}, for the quaternary system H_2S-CO_2-DEA-H_2O. Data are from Lee et al. (1974a) for a 2.0 kmol m^{-3} (acid gas free) DEA solution at 50°C. α = acid gas loading = mole acid gas / mole DEA.

α_{H_2S}	α_{CO_2}	$p^e_{H_2S}$	$p^e_{CO_2}$	$\frac{x^t_{H2S}}{x^e_{H2S}}$	$\frac{x^t_{CO2}}{x^e_{CO2}}$	$\frac{p^t_{H2S}}{p^e_{H2S}}$	$\frac{p^t_{CO2}}{p^e_{CO2}}$
(mole/mole DEA)		(kPa)	(kPa)				
1.006	0.106	1505.81	144.52	1.08	0.97	0.90	1.00
0.447	0.693	1081.11	2800.64	0.97	1.17	1.00	0.86
0.570	0.433	732.91	843.24	1.02	1.17	1.01	0.87
0.381	0.719	703.96	2149.78	0.96	1.13	1.03	0.90
0.703	0.308	682.58	404.04	1.03	1.12	1.02	0.90
0.188	0.994	675.69	5135.21	0.99	1.11	0.96	0.91
0.784	0.239	632.25	274.41	1.01	1.13	1.06	0.90
0.989	0.048	629.49	33.58	1.03	1.04	1.02	0.96
0.826	0.170	600.54	167.54	1.04	1.12	1.06	0.91
0.881	0.094	508.14	67.57	1.05	1.10	1.06	0.93
0.173	0.977	488.85	3433.57	1.03	1.06	0.92	0.94
0.125	1.140	415.76	5343.44	0.97	1.05	1.02	0.95
0.294	0.704	399.89	1292.77	1.00	1.11	0.98	0.93
0.851	0.063	359.91	29.16	1.09	1.08	1.03	0.93
0.785	0.125	340.60	71.02	1.07	1.14	1.08	0.91
0.176	0.902	299.93	1974.65	1.00	1.05	0.99	0.96
0.604	0.285	298.54	152.37	1.06	1.10	0.98	0.92
0.831	0.053	289.23	18.13	1.10	1.07	1.01	0.92
0.515	0.447	274.41	384.73	0.92	1.15	1.15	0.92
0.634	0.250	242.70	92.39	1.06	1.06	0.98	0.94
0.361	0.477	194.43	277.17	1.06	1.12	0.92	0.90
0.108	0.962	178.58	1951.21	1.00	1.03	0.98	0.97
0.154	0.856	158.58	1067.99	0.98	1.02	1.02	0.99
0.189	0.742	151.68	658.45	1.01	1.05	0.96	0.97
0.133	0.812	142.72	880.46	1.06	1.04	0.89	0.96
0.041	1.221	129.62	5764.71	0.94	1.04	1.07	0.93
0.653	0.074	93.08	7.22	1.14	1.09	0.91	0.83
0.557	0.146	91.36	17.93	1.16	1.14	0.87	0.79
0.256	0.521	88.25	144.79	1.09	1.06	0.85	0.91
0.385	0.352	80.81	71.15	1.05	1.15	0.95	0.88
0.129	0.742	80.67	422.65	1.06	1.03	0.89	0.96
0.332	0.424	79.63	82.94	1.07	1.08	0.90	0.91
0.434	0.277	72.40	33.23	1.10	1.09	0.87	0.87

Table 6.8. Continued

α_{H_2S}	α_{CO_2}	$p^e_{H_2S}$	$p^e_{CO_2}$	$\frac{x^t_{H2S}}{x^e_{H2S}}$	$\frac{x^t_{CO2}}{x^e_{CO2}}$	$\frac{p^t_{H2S}}{p^e_{H2S}}$	$\frac{p^t_{CO2}}{p^e_{CO2}}$
(mole/mole DEA)		(kPa)	(kPa)				
0.380	0.345	65.71	47.02	1.06	1.09	0.91	0.90
0.512	0.120	49.16	5.24	1.15	1.04	0.79	0.83
0.525	0.094	47.57	5.52	1.14	1.17	0.85	0.73
0.331	0.328	39.71	26.41	1.07	1.09	0.88	0.88
0.564	0.040	38.20	1.48	1.12	1.12	0.87	0.76
0.129	0.628	36.82	152.03	1.04	1.06	0.90	0.94
0.367	0.238	36.27	16.82	1.09	1.19	0.86	0.78
0.213	0.475	34.54	59.36	1.04	1.08	0.90	0.91
0.045	0.785	24.75	423.34	1.03	1.06	0.91	0.95
0.236	0.323	21.72	14.89	1.12	1.09	0.75	0.81
0.012	0.865	14.41	704.64	1.20	1.04	0.68	0.84
0.197	0.318	12.69	11.31	1.06	1.12	0.82	0.82
0.382	0.078	10.79	0.85	1.01	1.06	0.96	0.89
0.199	0.273	10.14	9.43	1.02	1.23	0.87	0.75
0.370	0.067	10.07	0.90	1.00	1.16	0.93	0.77
0.092	0.490	7.38	27.10	1.00	1.07	0.96	0.94
0.305	0.079	6.62	0.55	1.01	1.03	0.97	0.94
0.029	0.662	6.41	109.63	1.06	1.06	0.85	0.92
0.208	0.158	4.52	1.39	0.99	1.09	0.96	0.87
0.092	0.400	4.14	9.38	1.01	1.05	0.94	0.93
0.210	0.155	3.85	1.12	0.96	1.07	1.05	0.95
0.123	0.296	3.06	3.47	0.96	1.06	1.06	0.98
0.178	0.086	1.57	0.31	0.88	1.09	1.29	1.08
0.117	0.077	0.88	0.22	0.89	1.10	1.22	1.02

Table 6.9. Comparison of estimated *true* values and experimentally measured values of H_2S and CO_2 equilibrium partial pressures, P_{H_2S} and P_{CO_2}, and liquid phase mole fractions (apparent), x_{H_2S} and x_{CO_2}, for the quaternary system H_2S-CO_2-MDEA-H_2O. Data are from Jou et al. (1986) for a 3.04 kmol m^{-3} (acid gas free) MDEA solution. α = acid gas loading = mole acid gas / mole MDEA.

α_{H2S}	α_{CO_2} (mole/mole MDEA)	$p^e_{H_2S}$ (kPa)	$p^e_{CO_2}$ (kPa)	$\frac{x^t_{H2S}}{x^e_{H2S}}$	$\frac{x^t_{CO2}}{x^e_{CO2}}$	$\frac{p^t_{H2S}}{p^e_{H2S}}$	$\frac{p^t_{CO2}}{p^e_{CO2}}$
Temperature = 40°C							
0.077	0.523	3.70	23.90	1.04	0.93	0.99	1.06
0.068	0.399	2.45	15.10	1.02	0.99	0.95	0.98
0.078	0.316	2.51	11.00	1.02	1.03	0.90	0.90
0.036	0.073	0.26	0.92	0.88	1.08	1.30	0.97
0.448	0.001	8.38	0.04	0.77	1.28	0.97	0.75
0.146	0.001	2.07	0.01	0.96	1.18	0.75	0.64
0.215	0.000	4.30	0.01	1.00	1.00	0.43	0.98
0.143	0.001	1.61	0.02	0.89	1.21	0.82	0.68
0.104	0.001	1.06	0.02	0.87	1.35	0.70	0.52
0.085	0.001	0.73	0.02	0.92	1.21	0.78	0.65
0.060	0.001	0.44	0.01	0.85	1.44	0.65	0.45
0.054	0.007	0.35	0.07	0.92	1.20	0.86	0.68
0.064	0.008	0.41	0.08	0.92	1.14	0.97	0.80
0.103	0.007	1.24	0.12	0.97	1.19	0.75	0.61
0.108	0.003	1.15	0.05	0.91	1.26	0.74	0.58
0.360	0.007	10.40	0.23	0.98	1.11	0.83	0.74
0.490	0.007	12.90	0.19	0.92	1.03	1.09	1.05
0.699	0.002	48.90	0.14	0.97	1.09	0.93	0.85
0.811	0.003	76.60	0.26	0.96	1.08	0.97	0.90
0.873	0.005	97.10	0.66	0.93	1.16	0.96	0.83
0.873	0.011	98.00	2.50	0.90	1.39	0.89	0.64
0.266	0.047	5.12	1.05	0.96	1.06	0.99	0.91
0.746	0.013	59.10	1.02	0.97	1.05	0.99	0.94
0.815	0.049	86.60	9.40	0.91	1.30	0.94	0.70
0.650	0.194	68.80	33.80	0.92	1.19	1.05	0.82
0.304	0.516	31.80	70.20	0.96	1.02	1.06	0.99
0.127	0.649	13.90	88.80	1.00	1.02	1.00	0.99
0.086	0.758	6.34	97.40	0.93	0.92	1.22	0.84
0.049	0.588	1.21	33.70	0.91	0.86	1.49	0.63
0.041	0.455	0.64	18.10	0.90	0.87	1.64	0.63
0.055	0.375	0.59	9.08	0.84	0.89	2.00	1.01

Table 6.9. Continued

α_{H_2S} (mole/mole MDEA)	α_{CO_2}	$p^e_{H_2S}$ (kPa)	$p^e_{CO_2}$ (kPa)	$\frac{x^t_{H2S}}{x^e_{H2S}}$	$\frac{x^t_{CO2}}{x^e_{CO2}}$	$\frac{p^t_{H2S}}{p^e_{H2S}}$	$\frac{p^t_{CO2}}{p^e_{CO2}}$
0.160	0.154	2.09	3.43	0.85	1.10	1.30	1.00
0.341	0.096	7.88	2.16	0.96	0.98	1.12	1.12
0.715	0.020	53.40	1.65	0.97	1.08	0.96	0.88
0.194	0.001	1.96	0.03	0.78	1.32	0.90	0.68
0.047	0.001	0.23	0.01	0.84	1.36	0.77	0.56
0.024	0.001	0.06	0.01	0.85	1.26	0.95	0.74
0.017	0.006	0.03	0.02	0.79	1.23	1.33	0.90
0.017	0.021	0.04	0.11	0.79	1.10	1.76	1.13
0.010	0.788	0.74	101.00	0.98	0.91	1.13	0.45
0.366	0.021	10.19	0.72	0.96	1.12	0.87	0.76
0.353	0.031	9.70	1.10	0.96	1.13	0.87	0.74
0.355	0.032	10.46	1.21	0.97	1.13	0.84	0.72
0.352	0.039	10.42	1.62	0.96	1.17	0.83	0.68
0.339	0.078	10.92	3.27	0.98	1.14	0.85	0.71
0.358	0.067	11.56	2.82	0.98	1.13	0.86	0.73
0.343	0.084	10.85	3.42	0.98	1.13	0.87	0.74
0.341	0.102	11.25	4.21	0.98	1.12	0.88	0.77
0.355	0.249	16.97	14.53	0.98	1.07	0.98	0.89
0.331	0.291	18.72	19.09	1.00	1.07	0.94	0.89
0.310	0.310	17.46	20.46	1.00	1.07	0.95	0.89
0.321	0.260	15.33	14.88	0.99	1.08	0.95	0.88
0.346	0.226	16.68	13.17	1.00	1.09	0.93	0.84
0.338	0.168	13.23	8.70	0.98	1.13	0.90	0.77
0.200	0.027	2.71	0.46	0.94	1.06	1.04	0.94
0.197	0.032	3.16	0.72	0.94	1.12	0.91	0.77
0.204	0.053	3.85	1.35	0.96	1.12	0.88	0.75
0.236	0.076	5.00	2.16	0.95	1.12	0.90	0.77
0.230	0.091	5.14	2.67	0.96	1.11	0.90	0.77
0.214	0.112	4.50	3.19	0.95	1.11	0.94	0.81
0.219	0.127	5.19	3.95	0.96	1.11	0.92	0.79
0.209	0.164	5.47	5.44	0.97	1.10	0.92	0.81
0.193	0.178	4.41	5.45	0.95	1.09	1.00	0.87
0.209	0.218	5.84	7.81	0.96	1.08	0.98	0.88
0.208	0.252	6.01	9.34	0.95	1.06	1.02	0.92
0.177	0.270	4.90	9.42	0.96	1.05	1.04	0.95
0.222	0.242	6.50	9.51	0.95	1.08	1.02	0.89
0.192	0.237	4.91	7.65	0.95	1.05	1.05	0.95
0.149	0.199	3.32	4.61	1.00	1.00	1.01	1.00
0.161	0.184	3.91	4.17	1.03	0.99	0.95	0.99

Table 6.9. Continued

α_{H_2S} (mole/mole MDEA)	α_{CO_2} (mole/mole MDEA)	$p^e_{H_2S}$ (kPa)	$p^e_{CO_2}$ (kPa)	$\frac{x^t_{H2S}}{x^e_{H2S}}$	$\frac{x^t_{CO2}}{x^e_{CO2}}$	$\frac{p^t_{H2S}}{p^e_{H2S}}$	$\frac{p^t_{CO2}}{p^e_{CO2}}$
0.003	0.594	0.14	28.70	0.97	0.95	1.16	1.12
0.012	0.591	0.61	28.90	1.06	0.92	0.96	1.02
0.062	0.612	4.49	39.00	1.09	0.93	0.89	1.00
0.084	0.506	4.17	21.70	1.07	0.92	0.94	1.05
0.076	0.420	2.81	14.30	1.05	0.94	0.97	1.05
0.117	0.539	8.12	31.90	1.09	0.93	0.88	1.01
0.095	0.537	4.99	24.10	1.07	0.90	0.96	1.08
0.075	0.498	2.92	16.90	1.04	0.89	1.05	1.15
0.047	0.342	1.06	7.55	1.00	0.93	1.14	1.17
0.058	0.349	1.52	9.43	1.00	0.97	1.06	1.08
0.086	0.599	3.46	20.30	1.02	0.83	1.18	1.28
0.070	0.709	7.68	91.50	1.01	0.99	0.98	1.01
0.053	0.679	5.92	89.70	1.04	1.03	0.91	0.96
0.044	0.658	3.28	53.30	1.03	0.96	0.97	1.01
0.037	0.556	2.00	33.70	1.02	0.99	0.96	0.99
Temperature = 100°C							
0.147	0.008	20.30	3.84	1.02	1.07	0.84	0.78
0.105	0.016	12.20	5.54	1.05	1.01	0.85	0.87
0.268	0.006	60.20	6.00	0.97	1.17	0.81	0.67
0.118	0.020	15.80	6.65	1.08	0.96	0.86	0.97
0.386	0.004	126.00	7.13	0.90	1.33	0.71	0.53
0.075	0.098	12.40	72.80	1.00	1.11	0.82	0.68
0.193	0.077	50.40	76.10	1.04	1.11	0.77	0.69
0.213	0.111	61.80	125.00	1.02	1.10	0.82	0.74
0.079	0.172	16.90	196.00	1.00	1.07	0.88	0.60
0.060	0.191	14.00	225.00	1.02	1.06	0.85	0.60
0.178	0.172	67.00	257.00	1.04	1.12	0.74	0.67
0.367	0.150	196.00	281.00	1.03	1.08	0.86	0.80
0.365	0.161	200.00	306.00	1.03	1.07	0.86	0.81
0.071	0.235	22.90	367.00	1.04	1.08	0.78	0.58
0.210	0.244	118.00	529.00	1.06	1.13	0.74	0.68

Table 6.10. Comparison of estimated *true* values and experimentally measured values of H_2S and CO_2 equilibrium partial pressures, P_{H_2S} and P_{CO_2}, and liquid phase mole fractions (apparent), x_{H_2S} and x_{CO_2}, for the quaternary system H_2S-CO_2-DGA-H_2O. Data are from Dingman et al. (1983) for a 65 wt % (acid gas free) DGA solution. α = acid gas loading = mole acid gas / mole DGA.

α_{H2S} (mole/mole DGA)	α_{CO_2} (mole/mole DGA)	$p^e_{H_2S}$ (kPa)	$p^e_{CO_2}$ (kPa)	x^t_{H2S} / x^e_{H2S}	x^t_{CO2} / x^e_{CO2}	p^t_{H2S} / p^e_{H2S}	p^t_{CO2} / p^e_{CO2}
Temperature = 100°F							
0.011	0.061	0.029	0.007	0.73	1.27	1.23	0.77
0.002	0.093	0.005	0.007	0.84	1.06	1.48	1.11
0.011	0.092	0.044	0.005	0.97	0.97	1.20	1.19
0.003	0.100	0.014	0.038	0.64	1.61	0.93	0.20
0.023	0.095	0.082	0.006	0.89	1.03	1.26	1.10
0.005	0.125	0.027	0.004	1.15	0.81	1.09	1.69
0.002	0.135	0.013	0.008	1.06	0.92	1.04	1.21
0.001	0.154	0.006	0.008	1.03	0.90	1.21	1.34
0.001	0.165	0.004	0.010	0.83	0.98	1.76	1.33
0.003	0.168	0.022	0.014	1.06	0.97	0.90	1.01
0.002	0.225	0.024	0.021	1.05	0.95	0.96	1.06
0.001	0.228	0.006	0.023	0.86	0.99	1.42	1.09
0.138	0.093	1.276	0.012	1.00	1.08	0.89	0.83
0.001	0.266	0.013	0.019	1.10	0.85	0.99	1.20
0.010	0.259	0.102	0.036	0.91	0.99	1.22	1.07
0.002	0.270	0.026	0.044	0.96	1.01	1.09	1.00
0.005	0.279	0.056	0.019	1.11	0.83	0.95	1.22
0.001	0.291	0.020	0.052	1.04	0.99	0.93	1.00
0.121	0.187	1.179	0.067	0.76	1.31	1.14	0.82
0.001	0.312	0.018	0.075	0.98	1.01	1.05	1.00
0.042	0.282	0.323	0.104	0.64	1.16	1.93	1.09
0.168	0.184	1.841	0.080	0.77	1.31	1.19	0.87
0.000	0.362	0.010	0.144	0.98	0.99	1.06	1.02
0.088	0.275	1.496	0.147	0.79	1.16	1.36	1.02
0.224	0.174	3.468	0.096	0.83	1.27	1.15	0.90
0.136	0.267	3.840	0.237	0.85	1.19	1.22	0.98
0.011	0.394	0.347	0.320	0.84	1.00	1.51	1.15
0.034	0.390	1.158	0.560	0.77	1.04	1.78	1.23
0.061	0.373	2.799	0.862	0.78	1.10	1.67	1.19
0.168	0.272	5.081	0.580	0.74	1.35	1.54	1.05
0.358	0.087	7.308	0.416	0.88	2.42	0.91	0.40

Table 6.10. Continued

α_{H_2S}	α_{CO_2}	$p^e_{H_2S}$	$p^e_{CO_2}$	$\frac{x^t_{H2S}}{x^e_{H2S}}$	$\frac{x^t_{CO2}}{x^e_{CO2}}$	$\frac{p^t_{H2S}}{p^e_{H2S}}$	$\frac{p^t_{CO2}}{p^e_{CO2}}$
(mole/mole DGA)		(kPa)	(kPa)				
0.200	0.267	8.412	0.400	0.87	1.16	1.23	1.04
0.026	0.445	3.068	4.109	0.81	1.03	1.72	1.25
0.116	0.376	11.307	2.841	0.80	1.12	1.62	1.22
0.008	0.499	1.600	13.996	0.80	0.98	1.95	1.28
0.142	0.367	20.546	5.226	0.82	1.16	1.56	1.19
0.027	0.485	8.205	25.855	0.82	1.01	1.77	1.29
0.016	0.500	3.096	16.272	0.77	0.97	2.13	1.38
0.258	0.264	17.306	1.000	0.87	1.21	1.31	1.07
0.092	0.431	57.020	78.600	0.84	1.14	1.62	1.22
0.069	0.460	32.819	54.813	0.83	1.06	1.69	1.27
0.178	0.361	46.953	13.996	0.85	1.19	1.52	1.17
0.196	0.352	78.600	28.544	0.87	1.24	1.50	1.15
0.392	0.163	22.822	0.580	0.95	1.33	1.18	0.94
0.326	0.249	63.983	5.709	0.95	1.34	1.29	1.02
0.416	0.168	31.716	0.560	1.00	1.16	1.09	0.98
0.242	0.348	121.348	46.401	0.87	1.20	1.54	1.19
0.357	0.251	98.595	9.929	0.96	1.30	1.30	1.06
0.450	0.162	46.815	0.903	1.02	1.18	1.09	0.97
0.368	0.251	124.795	14.272	0.97	1.30	1.31	1.06
0.506	0.154	131.001	4.943	1.10	1.30	1.16	0.96
0.583	0.087	45.988	0.296	1.02	1.09	1.07	0.99

Temperature = 140°F

α_{H_2S}	α_{CO_2}	$p^e_{H_2S}$	$p^e_{CO_2}$	$\frac{x^t_{H2S}}{x^e_{H2S}}$	$\frac{x^t_{CO2}}{x^e_{CO2}}$	$\frac{p^t_{H2S}}{p^e_{H2S}}$	$\frac{p^t_{CO2}}{p^e_{CO2}}$
0.047	0.044	0.520	0.016	0.97	0.98	1.15	1.15
0.009	0.120	0.081	0.073	0.74	1.09	1.90	1.20
0.009	0.163	0.181	0.174	0.84	1.12	1.28	0.92
0.009	0.203	0.274	0.228	0.91	1.04	1.18	1.01
0.213	0.044	6.591	0.044	0.96	0.99	1.07	1.07
0.008	0.260	0.311	0.384	0.92	0.99	1.23	1.08
0.195	0.099	7.998	0.173	0.94	1.08	1.04	0.95
0.241	0.094	12.411	0.270	0.93	1.15	1.01	0.88
0.086	0.250	4.282	0.623	0.87	1.01	1.32	1.12
0.211	0.142	11.928	0.301	0.95	0.99	1.10	1.07
0.285	0.107	19.305	0.323	0.95	1.03	1.08	1.03
0.194	0.233	21.856	1.869	0.90	1.09	1.21	1.04
0.041	0.398	8.619	9.170	0.85	1.02	1.49	1.17
0.082	0.365	16.341	8.343	0.85	1.05	1.47	1.16
0.417	0.037	30.406	0.130	0.94	1.02	1.09	1.06

Table 6.10. Continued

α_{H_2S} (mole/mole DGA)	α_{CO_2}	$p^e_{H_2S}$ (kPa)	$p^e_{CO_2}$ (kPa)	$\frac{x^t_{H2S}}{x^e_{H2S}}$	$\frac{x^t_{CO2}}{x^e_{CO2}}$	$\frac{p^t_{H2S}}{p^e_{H2S}}$	$\frac{p^t_{CO2}}{p^e_{CO2}}$
0.200	0.291	47.987	7.791	0.90	1.09	1.27	1.09
0.475	0.023	39.990	0.085	0.93	0.97	1.06	1.11
0.007	0.502	4.937	83.426	0.88	0.96	1.48	1.15
0.033	0.490	29.095	158.580	0.84	0.98	1.63	1.24
0.405	0.121	56.399	1.062	0.95	1.02	1.09	1.05
0.520	0.016	58.674	0.119	0.97	1.05	1.06	1.01
0.270	0.283	133.758	25.580	0.93	1.13	1.24	1.07
0.368	0.204	134.447	10.067	0.98	1.12	1.14	1.02
0.519	0.108	121.348	2.213	0.96	1.02	1.08	1.04
0.536	0.103	184.780	4.323	1.02	1.07	1.07	0.99
Temperature = 180°F							
0.041	0.042	2.041	0.172	0.98	1.08	0.87	0.80
0.015	0.098	0.862	0.618	0.89	1.14	1.03	0.81
0.086	0.037	5.681	0.228	0.98	1.14	0.82	0.71
0.011	0.118	0.620	0.605	0.90	1.06	1.20	1.00
0.085	0.087	7.377	0.703	0.95	1.13	0.93	0.81
0.115	0.091	13.307	0.800	1.00	1.06	0.93	0.88
0.176	0.040	21.236	0.310	1.03	1.00	0.93	0.96
0.070	0.148	8.136	1.586	0.94	1.09	1.03	0.91
0.015	0.223	1.758	2.882	0.88	1.07	1.27	1.02
0.042	0.226	6.081	3.840	0.89	1.08	1.24	1.02
0.209	0.093	35.990	1.283	0.98	1.01	1.04	1.02
0.157	0.166	36.267	3.682	0.97	1.04	1.04	0.98
0.289	0.037	51.987	0.592	0.97	1.03	1.04	1.00
0.248	0.088	40.817	1.282	0.93	0.99	1.14	1.10
0.125	0.216	31.233	6.509	0.93	1.06	1.15	1.02
0.135	0.209	36.266	6.564	0.94	1.06	1.11	1.00
0.042	0.325	10.549	13.169	0.85	0.99	1.48	1.18
0.015	0.355	4.082	17.582	0.84	0.99	1.59	1.18
0.353	0.102	113.074	4.351	0.93	1.03	1.14	1.07
0.116	0.352	105.489	84.117	0.91	1.02	1.26	1.10
0.059	0.414	49.643	100.663	0.87	0.97	1.44	1.18
0.321	0.155	161.338	14.410	0.95	1.08	1.14	1.02
0.260	0.217	153.064	23.442	0.94	1.04	1.15	1.05
0.401	0.097	170.991	5.563	0.94	1.00	1.10	1.07
0.461	0.054	182.711	2.696	0.93	0.99	1.09	1.09

6.6 Speciation

The model proposed this work satisfactorily represents experimental acid gas solubility data. It could, therefore, be used in equilibrium stage design calculations. However, recent research (Hermes and Rochelle, 1987; Sivasubramanian et al. 1985; Katti and Langfitt, 1986) suggests that mass and heat transfer **rate-based** (nonequilibrium) models rather than equilibrium models are better suited to simulate absorber/stripper operations in which mass transfer is enhanced by chemical reaction. These models account explicitly for finite rates of mass and heat transfer and chemical reaction. However, phase and chemical equilibria continue to play an important role in rate based modeling. For example, physical equilibrium is usually assumed to exist at a gas-liquid interface and a bulk liquid solution is assumed to be in a state of chemical equilibrium. Indeed, these assumptions define the boundary conditions for the partial differential equations describing mass transfer with chemical reaction. Physical and chemical equilibria models, therefore, constitute necessary components of a rate based model.

Application of the Electrolyte-NRTL equation to represent activity coefficients in the alkanolamine-H_2S-CO_2-H_2O system allows the equilibrium model to be more confidently used to speciate the liquid phase through the equations of chemical equilibrium. Because the adjustable binary interaction parameters and carbamate stability constants have already been determined by fitting the model to experimental VLE data, the model can be readily employed in the context of mass transfer rate-based models to calculate *a priori* the composition of the liquid phase at equilibrium .

Figures 6.45 through 6.50 are speciation plots for the several of the ternary systems of interest in this work at 40 and 120 °C. In these figures, the equilibrium mole fractions of all species, other than water, are plotted against acid gas loading. They were generated by executing the VLE model at a number of acid gas loadings varying from zero to unity. Speciation plots are useful to illustrate trends in the relative concentrations of ionic and molecular species at equilibrium both as a function of temperature and acid gas loading.

The simplest speciation plot is for the amine-H_2S-H_2O ternary system. Figures 6.45 and 6.46 are speciation plots for an MEA-H_2S-H_2O system at 40 and 120°C respectively. The H_2S-free concentration of MEA is 2.5 kmol m^{-3}. It is clear from these figures that the only ionic species present in solution at appreciable levels in the MEA-H_2S-H_2O system are protonated MEA, $MEAH^+$, and bisulfide, HS^-. The equilibrium constant corresponding to the second dissociation of hydrogen sulfide to sulfide ion is so small relative to the equilibrium constant for the first dissociation of hydrogen sulfide to bisulfide ion that almost no sulfide forms. Only at extremely low loadings will the concentration of hydroxide ion, OH^-, be significant relative to bisulfide. Because H_2S is a weak acid, the concentration of hydronium ion, H_3O^+ will be negligible at all loadings. Therefore, as these figures reveal, conservation of mass requires that the concentrations of bisulfide and protonated MEA be approximately equal at all (but extremely low) H_2S loadings.

Also of note in Figures 6.45 and 6.46 is the behavior of the curve representing the concentration of molecular H_2S as a function of loading. Figure 6.45 reveals that only above an H_2S loading of about 0.85 mole H_2S per mole of MEA at 40°C does the concentration of molecular H_2S become appreciable. However, the same concentration of molecular H_2S is present in solution at a loading of approximately 0.40 moles H_2S per mole MEA at 120°C. The different behaviors of the H_2S concentration curves at 40 and 120°C seen in Figures 6.45 and 6.46 is, of course, the phenomenon that permits aqueous alkanolamine solutions to be used in *absorption/stripping* processes for gas treating. At low temperatures chemical equilibrium favors the conversion of H_2S to bisulfide. Hence, at low to moderate loadings, the liquid phase equilibrium concentration of molecular H_2S is low and the driving force for mass transfer results in absorption of H_2S from a sour gas. At high temperatures, chemical equilibrium favors molecular H_2S rather than bisulfide. Hence the equilibrium concentration of molecular H_2S in the liquid phase increases as temperature increases, reversing the driving force for mass transfer and resulting in the desorption of H_2S from an H_2S rich solution.

Figures 6.47 and 6.48 are speciation plots for a carbonated aqueous 2.5 kmol m^{-3} MEA solution at 40 and 120°C respectively. Figures 6.49 and 6.50 are similar plots for a 2 kmol m^{-3} DEA solution at 40 and 120°C. Of particular note in these figures are the various species to which CO_2 reacts in the solution. At very low loadings and low temperatures, CO_2 is mainly converted to carbamate, $RR'NCOO^-$, of MEA or DEA and little bicarbonate, HCO_3^-, forms. As the loading increases bicarbonate begins to form either through hydrolysis and dissociation of absorbed CO_2 (reaction 4d) or through reversion of carbamate to bicarbonate (reaction 4g). Note that little carbonate, $CO_3^=$, forms in either solution. For both MEA and DEA the maximum concentration of carbamate occurs at approximately 0.5 mol/mol corresponding to the nearly complete consumption of the amine. Above a loading of 0.5 mol/mol the carbamate concentration decreases as carbamate reverts and more bicarbonate forms.

The behavior of the liquid phase concentration curves in carbonated MEA and DEA solutions is quite different at 120°C. At this high temperature and low to moderate loadings, speciation with the model indicates that most of the CO_2 in an aqueous MEA solution is again present as carbamate. However, at this high temperature and all loadings, speciation with the model indicates that most of the CO_2 present in an aqueous DEA solution exists as bicarbonate. This suggests that the carbamate of DEA is not stable at high temperatures.

Finally, Figure 6.50 is a speciation plot for a carbonated 4 kmol m^{-3} aqueous solution of MDEA at 40°C. Because MDEA does not form a stable carbamate, CO_2 reacts to bicarbonate or carbonate only. Thus, the liquid phase behavior of the MDEA-CO_2-H_2O system might be expected to be much like the behavior of the MDEA-H_2S-H_2O system. However, unlike H_2S, the second dissociation constant of CO_2 (reaction 4e) is not negligible relative to its first dissociation constant (reaction 4d). Therefore, a significant amount of carbonate forms relative to bicarbonate. Hence, the concentration of bicarbonate is not, in general, equal to the concentration of protonated MDEA. Recall that in the H_2S-amine-H_2O system virtually no sulfide forms, so the concentration of bisulfide is approximately equal to the concentration of protanted amine at all loadings.

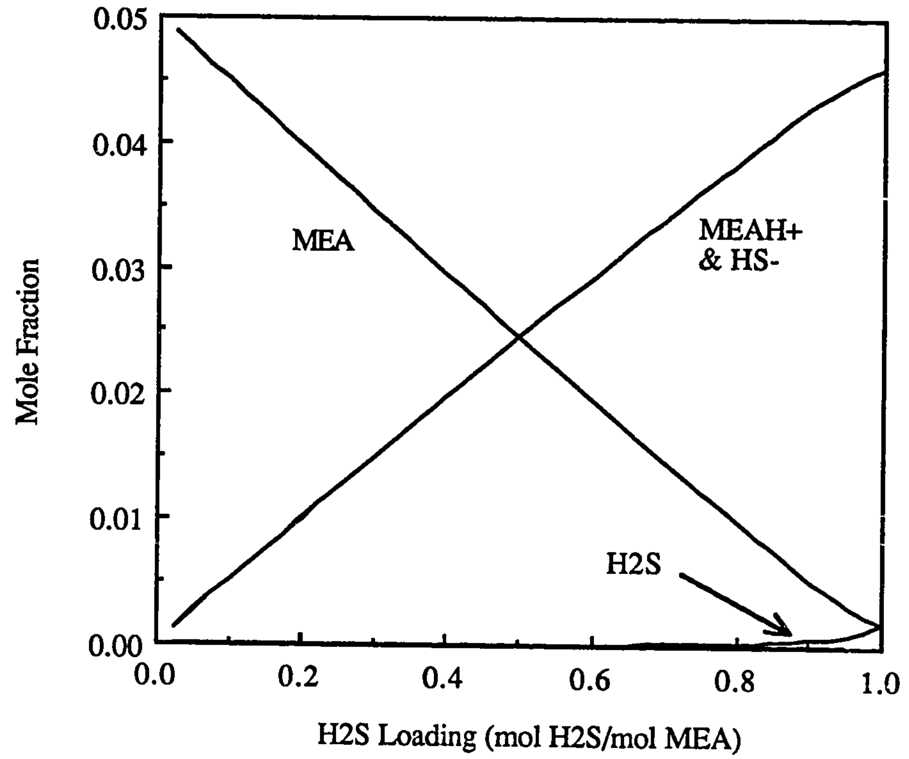

Figure 6.44 Liquid-phase composition of a 2.5 M MEA solution loaded with H_2S at 40°C. Compositions were calculated with the VLE model.

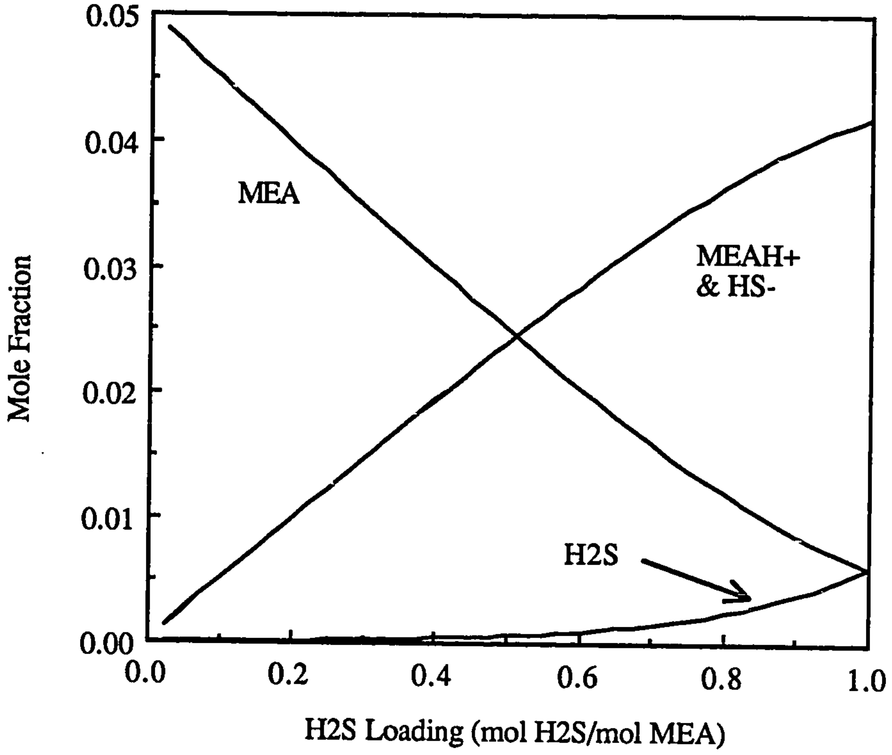

Figure 6.46 Liquid-phase composition of a 2.5 M MEA solution loaded with H_2S at 120°C. Compositions were calculated with the VLE model.

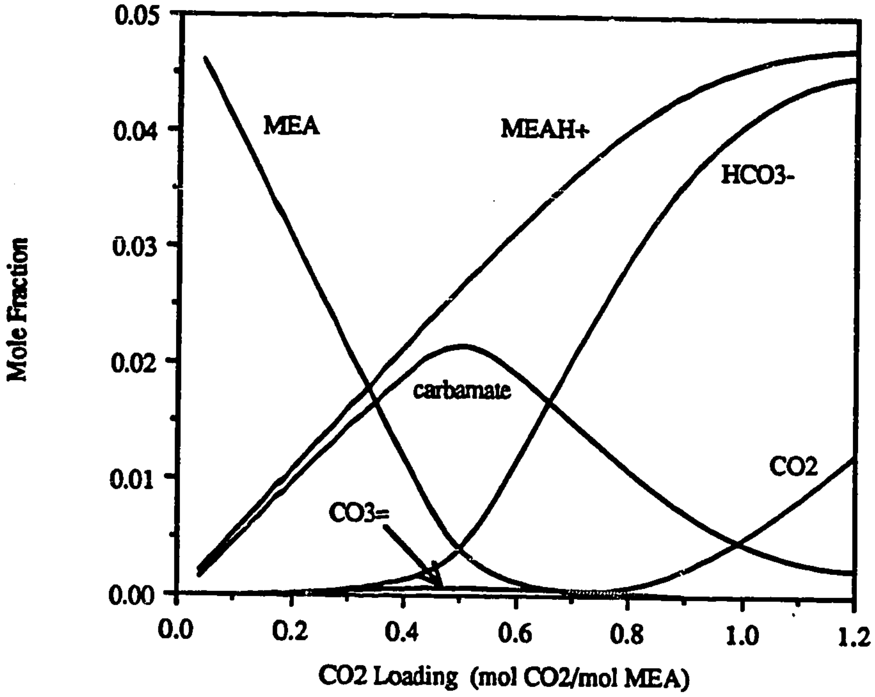

Figure 6.47 Liquid-phase composition of a 2.5 M MEA solution loaded with CO_2 at 40°C. Compositions were calculated with the VLE model.

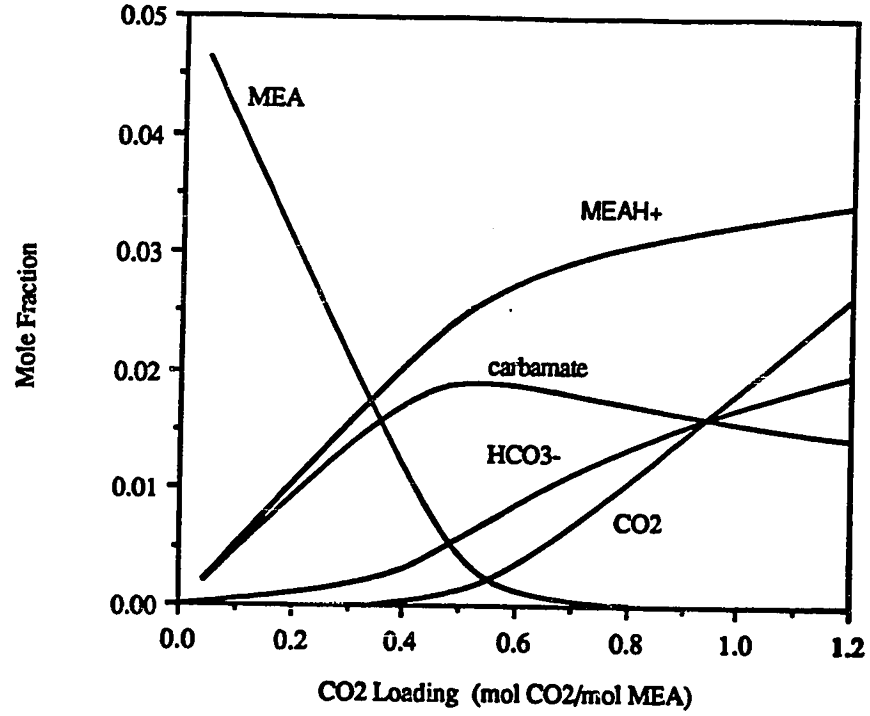

Figure 6.48 Liquid-phase composition of a 2.5 M MEA solution loaded with CO_2 at 120°C. Compositions were calculated with the VLE model.

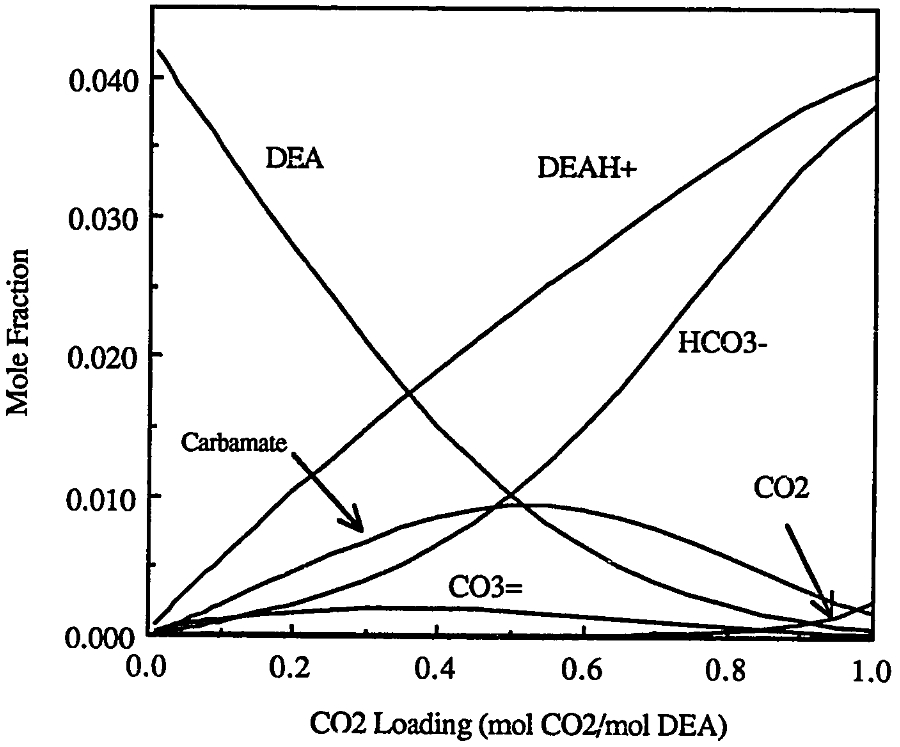

Figure 6.49 Liquid-phase composition of a 2.0 M DEA solution loaded with CO_2 at 40°C. Compositions were calculated with the VLE model.

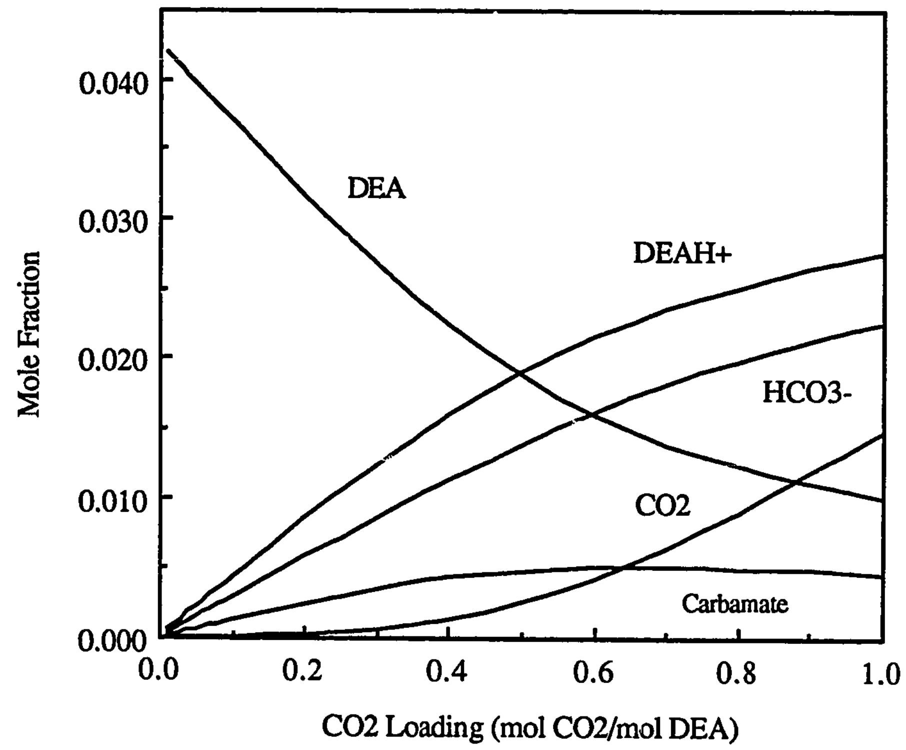

Figure 6.50 Liquid-phase composition of a 2.0 M DEA solution loaded with CO_2 at 120°C. Compositions were calculated with the VLE model.

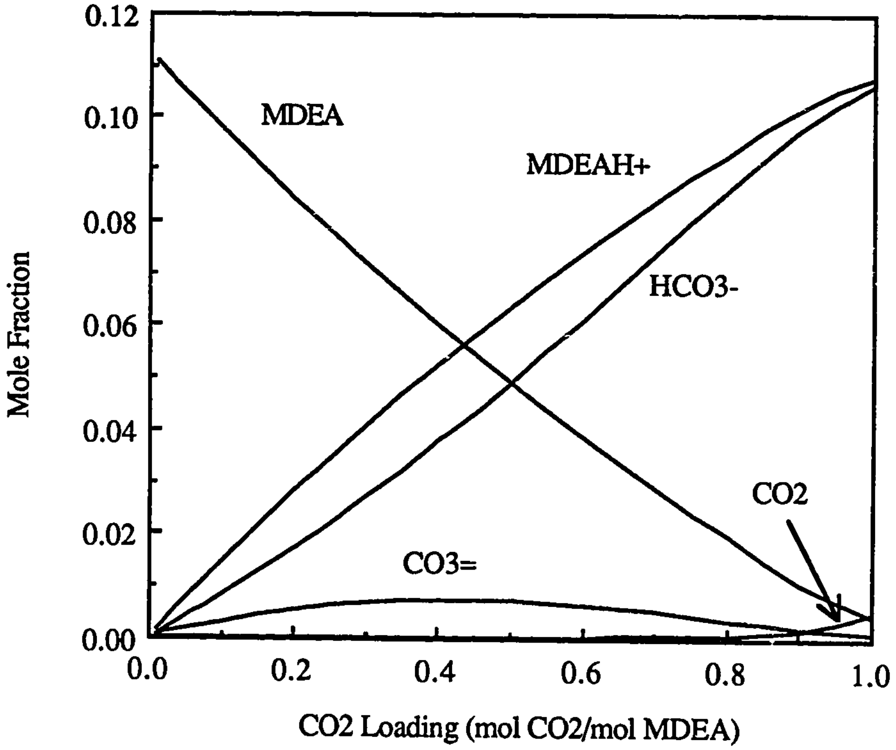

Figure 6.51 Liquid-phase composition of a 4.0 M MDEA solution loaded with CO_2 at 40°C. Compositions were calculated with the VLE model.

Chapter Seven

Modeling CO_2 Solubility in Mixtures of MDEA with MEA or DEA

7.1 Gas Treating with MDEA and Mixtures of MDEA with MEA or DEA

Monoethanolamine (MEA) and diethanolamine (DEA) have been the most widely employed gas treating alkanolamine solvents during the last several decades. In aqueous solution, both of these solvents react quickly with H_2S and CO_2. Therefore, they are normally used in gas treating applications in which complete, or nearly complete, removal of both H_2S and CO_2 is desirable.

In recent years, methyldiethanolamine (MDEA) has been used as an alternative to MEA or DEA in certain gas treating applications. MDEA reacts rapidly with H_2S. However, as a tertiary amine, it cannot react directly with CO_2 to form a carbamate anion. As noted in Chapter Four, this is the primary mechanism by which MEA, DEA, and DGA react (rapidly) with CO_2. MDEA reacts with CO_2 only through an acid-base buffer mechanism in which CO_2 is converted primarily to bicarbonate. However, CO_2 must first react with H_2O to produce carbonic acid, H_2CO_3, which subsequently dissociates to bicarbonate, HCO_3^-, or it must react directly with OH^- to form bicarbonate. By either mechanism, the net reaction rate is relatively slow in amine solutions.

Because MDEA reacts rapidly with H_2S and slowly with CO_2, it is often used for selective removal of H_2S from a gas stream containing both acid gases. However, MDEA is also useful for bulk CO_2 removal because the heat released by the reaction of CO_2 with MDEA is substantially lower than the heat released by the reaction of CO_2 with MEA, DEA, or DGA (see Table 1.1). Its use as an alternative to MEA, DEA, or DGA for bulk CO_2 removal, therefore, results in a reduction in energy required to reverse the reaction of CO_2 with MDEA and to strip it from solution. The drawback of using MDEA for bulk CO_2 removal is that, as noted above, it reacts relatively slowly with CO_2. To effect the same level of CO_2 removal, an MDEA application requires greater gas/liquid contact area than does an MEA, DEA, or DGA application.

Recent research (Chakravarty et al., 1985; Critchfield and Rochelle 1987, 1988; Katti and Wolcott, 1987) indicates that a primary or secondary amine, such as MEA or DEA, can be added to an aqueous MDEA solution to promote or enhance the absorption rate of CO_2 without significantly affecting the energy requirements for stripping. Critchfield and Rochelle (1987, 1988) discuss the interactive mass transfer and equilibrium mechanisms by which MEA and DEA promote the absorption rate of CO_2 into an MDEA based solvent mixture. The level to which MEA or DEA should be added to an MDEA solution would be determined by balancing the need to add enough promoter to sufficiently enhance the absorption rate of CO_2, with the increase in stripping costs due to the higher heat of reaction of the promoter with CO_2, and with the relative costs of the amines.

Design of gas treating operations with MDEA based aqueous solvents requires VLE data for the corresponding aqueous acid gas - alkanolamine systems. Several experimental studies reporting VLE measurements for acid gas-MDEA-water systems have been published in the literature. As discussed in Chapter One, representation of experimental data with a thermodynamically rigorous model is needed so that one can confidently and systematically interpolate between and extrapolate beyond the available data. Representation of data is especially important as the number of components, and thus the degrees of freedom, in a system increases. A thermodynamically rigorous model, employing semi-empirical thermodynamic functions, can be used to significantly reduce the experimental effort required to characterize the VLE behavior of a multicomponent system such as mixed amine - acid gas - water systems.

It was shown in Chapter Six that the model proposed in in this work satisfactorily represents VLE data for acid gas-alkanolamine-water systems. The objective of this Chapter is to show that the VLE model can be used to satisfactorily represent the solubility of CO_2 in aqueous mixtures of MDEA with MEA and DEA. Best values of the additional/unique adjustable parameters of the model for the mixed amine systems were fitted on experimental CO_2 solubility data measured in this work and reported in Chapter Five.

7.2 Representation of CO_2 Solubility in Mixed Amine Solutions

7.2.1 Data Regression

Extension of the model to represent the solubility of CO_2 in mixtures of MDEA with MEA or DEA is straightforward. To model the chemical equilibrium behavior of the liquid phase, the relevant equilibrium reactions listed in Chapter Four are included in the set of independent reactions. Thus two independent amine dissociation reactions (reaction 4f for MDEA and MEA or DEA) and one carbamate reversion reaction (reaction 4g for MEA or DEA) in addition to the first and second CO_2 dissociation reactions (reactions 4d and 4e) and the H_2O dissociation reaction (4a) are adopted as the independent set of chemical reactions.

The only additional molecule-ion pair parameters of the Electrolyte-NRTL equation that were not fitted on ternary system data, but which affect representation of CO_2 solubility in mixtures of MDEA with MEA or DEA, are those for which the molecule is water and the ion pair is formulated from protonated MDEA and the carbamate anion of MEA or DEA. These adjustable binary parameters were fitted on experimental measurements of CO_2 solubility in aqueous mixtures of MDEA with MEA and MDEA with DEA reported in Tables 5.4 and 5.5.

The data presented in Tables 5.4 and 5.5 are CO_2 solubility measurements made in aqueous mixtures containing 2 kmol m^{-3} MDEA and 2 kmol m^{-3} MEA or 2 kmol m^{-3} DEA. As discussed in Chapter Five, an amine mixture such as this, equimolar in MDEA and MEA or DEA, would not likely be used in an industrial gas treating application for bulk CO_2 removal. The presence of such a high concentration of MEA or DEA in an MDEA based solvent would negate the energy advantages gained from using MDEA. The promoters would be used at lower concentrations primarily to enhance the CO_2 absorption rate. However, the objective of this work was to test the validity of the extended VLE model for the mixed amine-CO_2-water systems. It was felt that model representation of experimental data would be most rigorously evaluated using measurements of CO_2 solubility in a mixture with relatively high concentrations of both MDEA and MEA or DEA. Furthermore, since the only additional adjustable parameters that arise for the mixed amine systems are related to the protonated MDEA cation, and the MEA or DEA carbamate anions, it was important to simultaneously have a high concentration of both ions in the solution to effect a high sensitivity of calculated CO_2 partial pressure to the relevant parameters.

Best values of the unique adjustable parameters for the mixed amine systems are reported in Table 7.1. Note that the temperature dependence of these parameters, expressed by the coefficient 'b' of equation (4.67), could not be determined and that the estimated standard deviations of fitted values of the 'a' coefficient in equation (4.67) are relatively large. This suggests that the parameters could not determined with a high degree of confidence, perhaps because they were fit on few data points.

However, because of the poor agreement of the VLE data used to fit the binary interaction parameters of the CO_2-MDEA-H_2O system, the resulting parameter values may not be consistent with the **true** equilibrium behavior of this system. Hence, they would also not be consistent with the **true** equilibrium behavior of the CO_2-MDEA-MEA-H_2O or the CO_2-MDEA-DEA-H_2O systems. If such were the case, it is possible that accurate and statistically significant binary interaction parameter values for the mixed amine systems could not be determined. Note that while the standard deviations corresponding to the parameters in Table 7.1 are high, the parameter values are in relatively good agreement with the values of the interaction parameters reported in Table 6.4 for the single amine systems and with the default values.

Table 7.1 Fitted values of NRTL molecule - ion pair binary interaction parameters for CO_2 - alkanolamine (1) - alkanolamine (2) - H_2O systems.

$$\tau = a + b/T$$

RNH_2 = MEA R_2NH = DEA R_3N = MDEA

Parameter	a	σ_a	b(°K)	σ_b	τ (25°C)
H_2O-R_3NH^+,$RHNCOO^-$	9.903	2.67	0.0	*	9.90
R_3NH^+,$RHNCOO^-$-H_2O	-4.776	1.13	0.0	*	-4.78
H_2O-R_3NH^+,R_2NCOO^-	10.387	1.65	0.0	*	10.39
R_3NH^+,R_2NCOO^--H_2O	-4.965	0.69	0.0	*	-4.97

* Parameter value fixed at zero because it could not be estimated with statistical significance;

7.2.2 Data Representation

Results of the experimental CO_2 solubility measurements in the 2 kmol m^{-3} MDEA, 2 kmol m^{-3} MEA mixtures at 40 and 80°C are shown in Figures 7.1 and 7.2. Similar results are shown for the 2 kmol m^{-3} MDEA, 2 kmol m^{-3} DEA mixtures at 40 and 80°C in Figures 7.3 and 7.4. Also shown on these figures are CO_2 solubility curves for 4 kmol m^{-3} solutions of MEA (DEA) and MDEA and for a 2 kmol m^{-3} MDEA-2 kmol m^{-3} MEA (DEA) mixture. All curves were generated using the VLE model and the parameter values reported in Tables 6.4 and 7.1.

Figures 7.1 through 7.4 show that the VLE model represents the solubility of CO_2 in the amine mixtures very well at low to moderate loadings. However, agreement between model representation and the experimental data at the higher loadings is not as good. This may be due to a poor fit of the data at higher loadings or to errors in experimental measurements at higher loadings. However, as discussed before, it may also be that the binary interaction parameters fitted on MDEA-CO_2-H_2O VLE data do not reflect the true equilibrium behavior of this ternary system.

While this discussion is centered around the solubility of CO_2 in aqueous mixtures of MDEA with MEA or DEA, examination of the relative solubilities of CO_2 in aqueous solutions of the relevant single amine solutions is useful for understanding CO_2 solubility behavior in the amine mixtures. It can be seen in Figures 7.1 through 7.4 that the CO_2 solubility curves for the 4 kmol m^{-3} solutions of MDEA and MEA (DEA) (ie. single amine solutions) cross at a loading of approximately 0.6 moles of CO_2 per mole amine. The relative positions of the CO_2 solubility curves indicate that above a certain CO_2 partial pressure, corresponding to a CO_2 loading of approximately 0.6 mol/mol, the solubility of CO_2 in a 4 kmol m^{-3} solution of MDEA is greater than the CO_2 solubility in a 4 kmol m^{-3} solution of MEA or DEA. This is primarily due to the different chemical reactions that occur in the different amine systems.

The reaction of MEA or DEA with CO_2 to form carbamate by reaction (2g) results in the conversion of two amine molecules for each CO_2 molecule reacted. Hence, for an aqueous solution of a primary or secondary amine, it is reasonable to assume (as a first order approximation) that the amine will be completely converted to products at a CO_2 loading of 0.5 moles of CO_2 per mole amine. If the carbamate is stable (small carbamate stability constant), it will resist reverting to bicarbonate (reaction 4g), and an increase in CO_2 partial pressure will result in physical absorption of CO_2 only. However, molecular CO_2 is not highly soluble in an aqueous solution.

Therefore, a substantial increase in CO_2 partial pressure would be required to effect even a small increase in the concentration of CO_2 in the liquid phase.

Chemical equilibrium behavior in a CO_2 loaded aqueous solution of an amine that forms an unstable carbamate would be different. An unstable carbamate would easily revert to bicarbonate freeing a molecule of amine which would become available to react with additionally absorbed CO_2 to form bicarbonate. Reversion of carbamate to bicarbonate would thus allow a greater loading (solubility) of CO_2 at a given CO_2 partial pressure. That is, at high partial pressures, more CO_2 can be solubilized if the carbamate is unstable and easily reverts to bicarbonate.

MDEA can be viewed as forming a very unstable carbamate. MEA can be viewed as forming a very stable carbamate. And DEA can be viewed as forming a carbamate of intermediate stability. By the argument proposed above, the CO_2-MDEA equilibrium curve crosses the CO_2-MEA and CO_2-DEA equilibrium curves largely because MEA and DEA form stable carbamate species. Therefore, at high CO_2 partial pressures, an MDEA solution can be loaded to a greater degree than can an MEA or DEA solution.

It can also be seen in Figures 7.1 through 7.4 that the CO_2 solubility curve for a 2 kmol m^{-3} MDEA, 2 kmol m^{-3} MEA (DEA) mixture approaches the CO_2 solubility curve for the 4 kmol m^{-3} MEA mixture at very low loadings. This behavior can be explained as follows. At very low loadings the primary mechanism by which CO_2 is absorbed is through reaction with MEA (DEA) to form the carbamate of MEA (DEA). This is due to the high stability of these species as reflected by the associated carbamate stability constants. As the CO_2 loading increases, the ratio of molecular MDEA to

MEA (DEA) increases. Therefore, because of the principle of mass action, both MEA (DEA) and MDEA affect the solubility of CO_2 at moderate CO_2 loadings.

At loadings approaching 1 mole CO_2 per mole of amine, the CO_2 solubility curve for the amine mixture again approaches the equilibrium curve for the 4 kmol m^{-3} MEA (DEA) solution. This behavior is probably due to the high stability of the carbamate of MEA (DEA). As will be shown shortly, the carbamate anion of MEA (DEA) is present in the mixed amine solutions even at these high loadings. The important point is that at moderate to high loadings, the reversion of carbamate of the primary or secondary amine to bicarbonate seems to play an important, if not controlling, role in determining the equilibrium behavior of CO_2 in the amine mixture.

Figures 7.1 through 7.4 indicate that the addition of MEA or DEA to an aqueous MDEA solution results in a decrease in the equilibrium CO_2 partial pressure at low to moderate loadings. Alternatively, the addition of MEA or DEA to an aqueous MDEA solution results in an increase in the solubility of CO_2 in the aqueous phase at low to moderate CO_2 partial pressures. Figures 7.5 through 7.8 more clearly illustrate the reduction (or increase) in equilibrium CO_2 partial pressures realized by adding MEA or DEA to an MDEA based solvent. These figures show the equilibrium partial pressure of CO_2 over 4 kmol m^{-3} mixtures of MDEA with MEA or DEA *relative* to the equilibrium partial pressure of CO_2 over a 4 kmol m^{-3} aqueous solution of MDEA (single amine). Note that the effect of MEA or DEA on the CO_2 equilibrium partial pressure is reduced at a higher temperature.

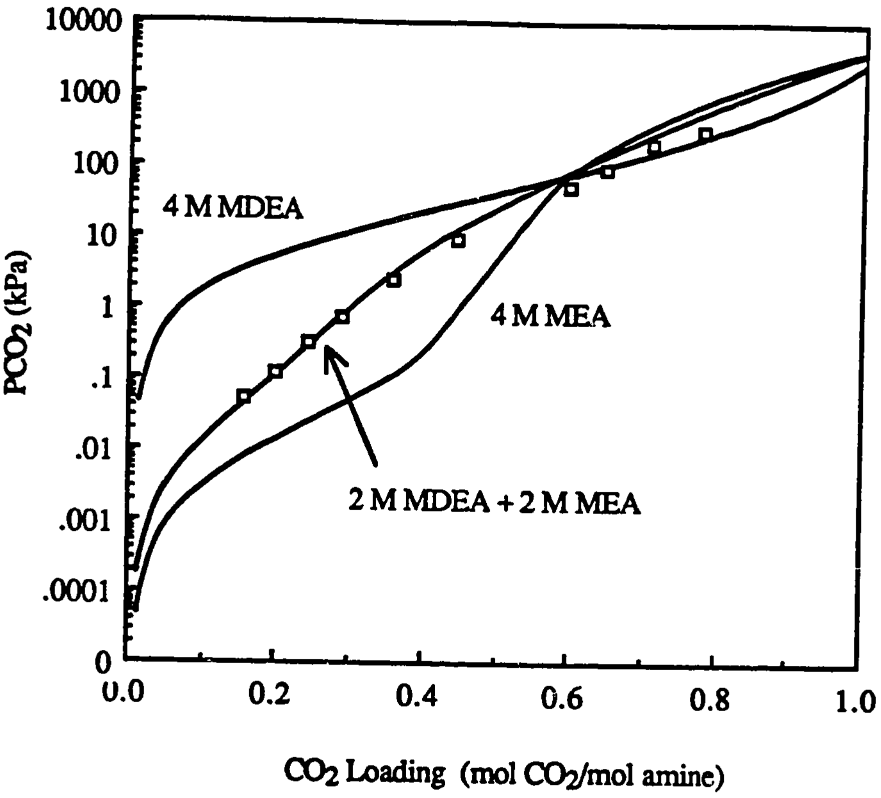

Figure 7.1 Equilibrium solubility of CO_2 in 4 kmol m^{-3} MDEA, 4 kmol m^{-3} MEA, and 2 kmol m^{-3} MDEA - 2 MEA kmol m^{-3} aqueous solutions at 40°C. Amine concentrations are CO_2 free.

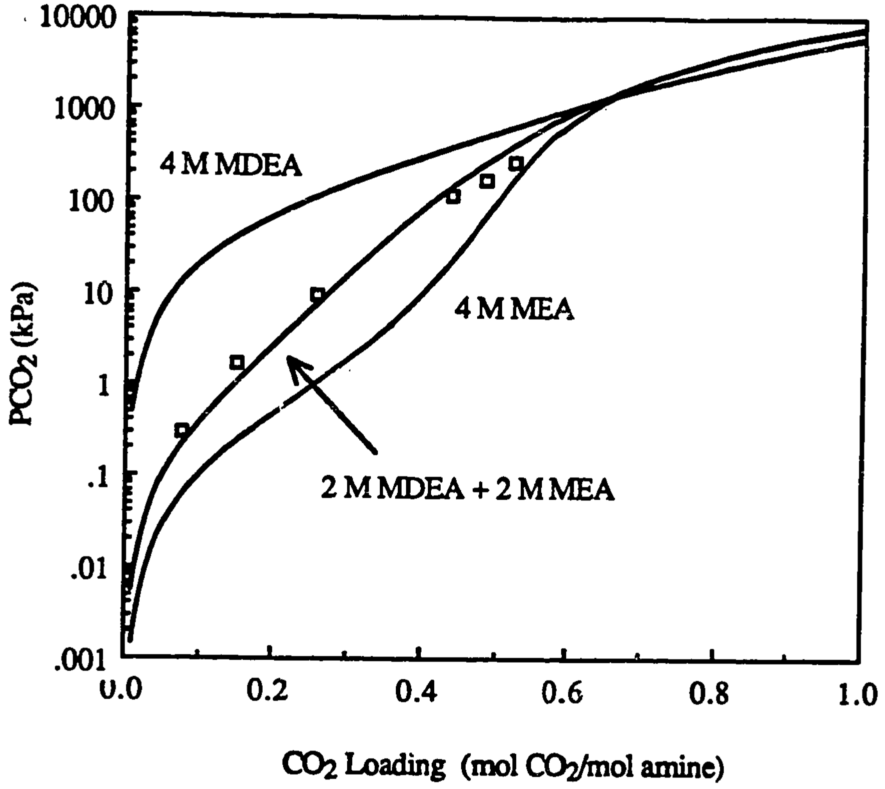

Figure 7.2 Equilibrium solubility of CO_2 in 4 kmol m^{-3} MDEA, 4 kmol m^{-3} MEA, and 2 kmol m^{-3} MDEA - 2 MEA kmol m^{-3} aqueous solutions at 80°C. Amine concentrations are CO_2 free.

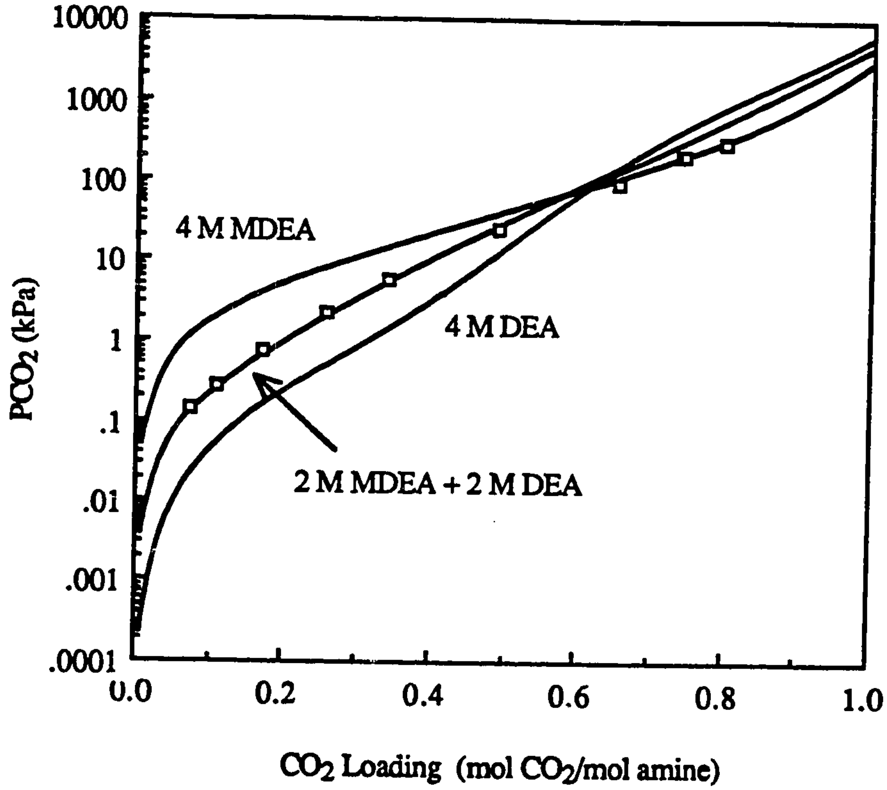

Figure 7.3 Equilibrium solubility of CO_2 in 4 kmol m^{-3} MDEA, 4 kmol m^{-3} DEA, and 2 kmol m^{-3} MDEA - 2 kmol m^{-3} DEA aqueous solutions at 40°C. Amine concentrations are CO_2 free.

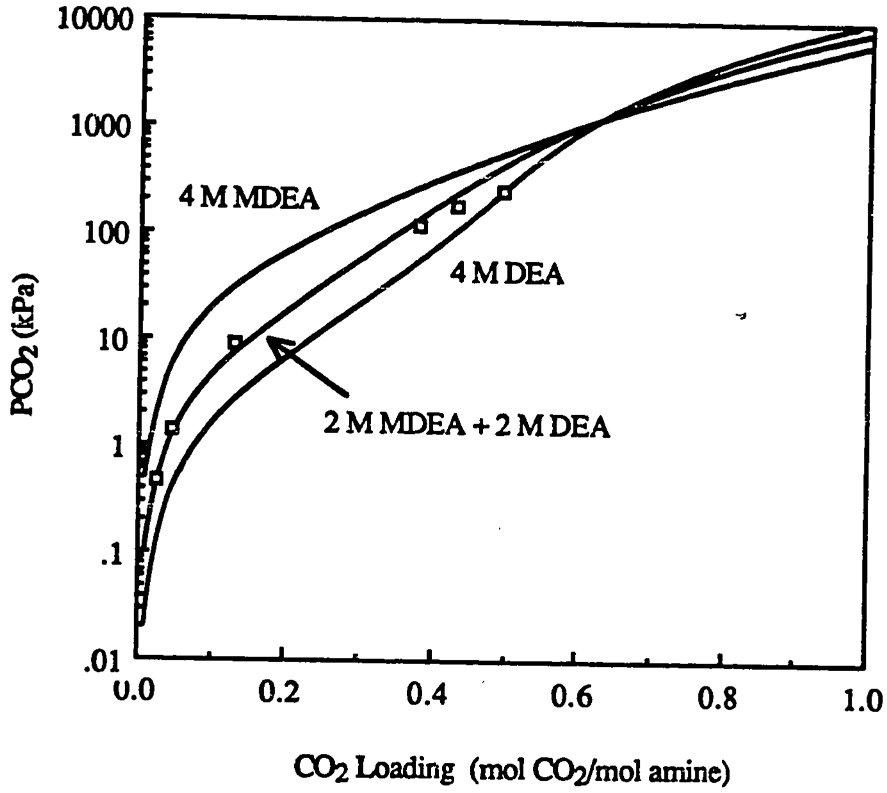

Figure 7.4 Equilibrium solubility of CO_2 in 4 kmol m^{-3} MDEA, 4 kmol m^{-3} DEA, and 2 kmol m^{-3} MDEA - 2 DEA kmol m^{-3} aqueous solutions at 80°C. Amine concentrations are CO_2 free.

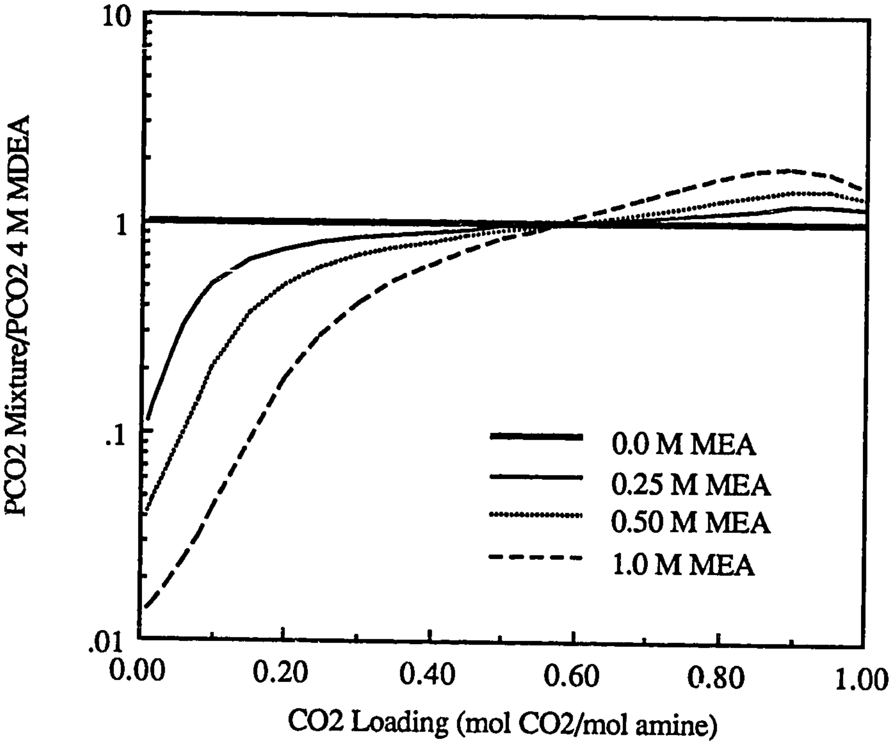

Figure 7.5 CO_2 equilibrium partial pressure over 4 kmol m^{-3} MDEA-MEA aqueous mixtures relative to the CO_2 equilibrium partial pressure over 4 kmol m^{-3} at 40°C. Amine concentrations are CO_2 free. Pressures were calculated with the VLE model.

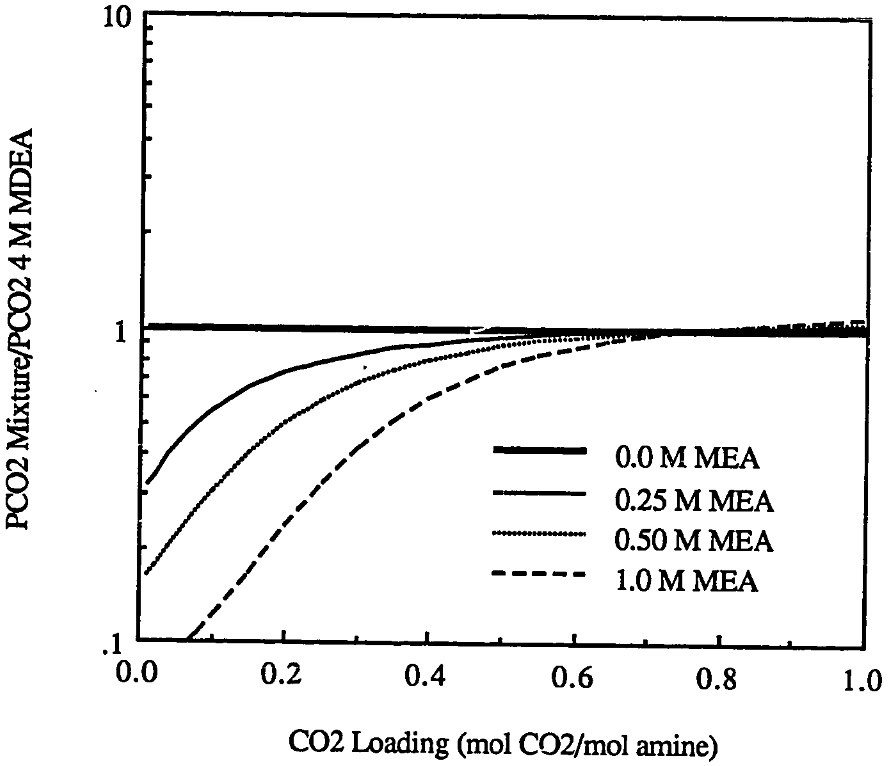

Figure 7.6 CO_2 equilibrium partial pressure over 4 kmol m^{-3} MDEA-MEA aqueous mixtures relative to the CO_2 equilibrium partial pressure over 4 kmol m^{-3} at 120°C. Amine concentrations are CO_2 free. Pressures were calculated with the VLE model.

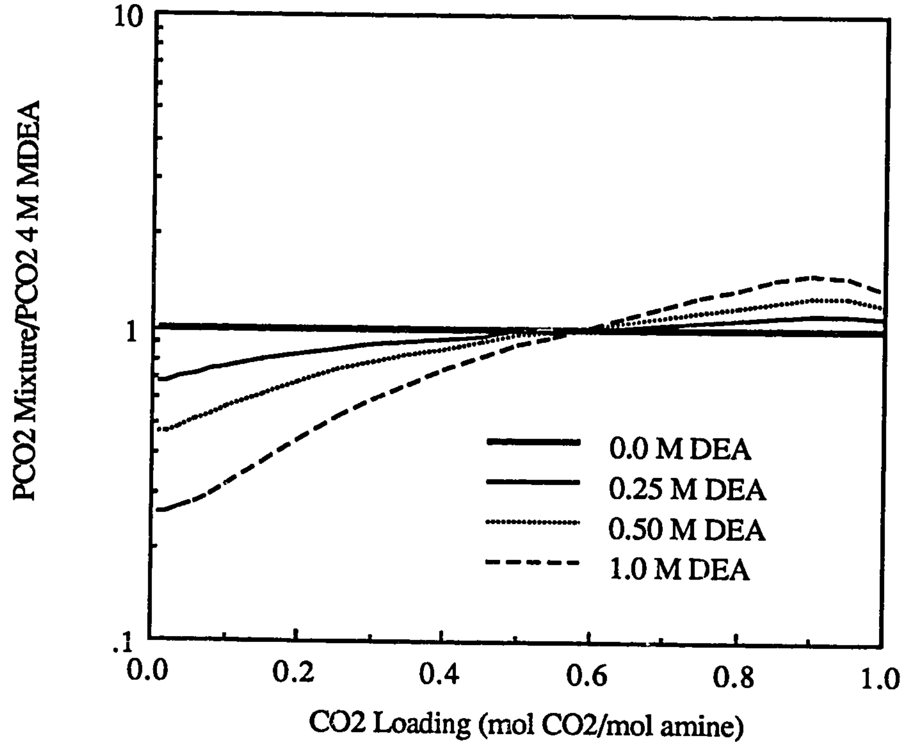

Figure 7.7 CO_2 equilibrium partial pressure over 4 kmol m^{-3} MDEA-DEA aqueous mixtures relative to the CO_2 equilibrium partial pressure over 4 kmol m^{-3} MDEA at 40°C. Amine concentrations are CO_2 free. Pressures were calculated with the VLE model.

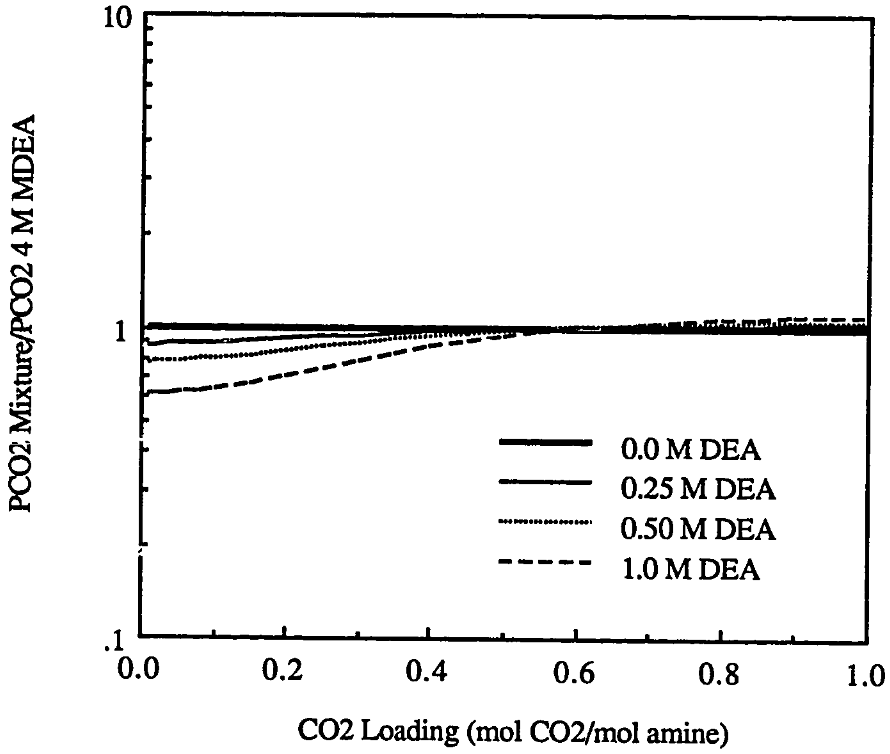

Figure 7.8 CO_2 equilibrium partial pressure over 4 kmol m^{-3} MDEA-DEA aqueous mixtures relative to the CO_2 equilibrium partial pressure over 4 kmol m^{-3} MDEA at 120°C. Amine concentrations are CO_2 free. Pressures were calculated with the VLE model.

7.3 Speciation

Speciation plots are useful in further analyzing the liquid phase chemical equilibrium behavior of carbonated aqueous mixtures of amines. Figure 7.9 is a speciation plot for a carbonated aqueous 3 kmol m^{-3} MDEA, 1 kmol m^{-3} MEA mixture at 40°C. Figure 7.10 is a similar plot for a 3 kmol m^{-3} MDEA, 1 kmol m^{-3} DEA mixture at 120°C. As shown in Chapter Six, speciation plots illustrate trends in the relative concentrations of the ionic and molecular species at equilibrium in the liquid phase as a function of acid gas concentration. They also lend insight into VLE behavior. Of particular interest in this application are the various species to which CO_2 reacts in the solution as a function of loading.

As shown in Figures 7.9 and 7.10, in an aqueous mixture of MDEA with MEA or DEA, CO_2 is mainly converted to carbamate of MEA or DEA at very low loadings. At moderate CO_2 loadings, the carbamate concentration does not vary significantly while additionally absorbed CO_2 is reacted primarily to bicarbonate. At high loadings, the carbamate reverts, and the bicarbonate concentration further increases with loading. However, even at a loading of 1.0 mol/mol, a significant fraction of CO_2 is present as carbamate in the mixed amine solution. It appears that the reversion of carbamate to bicarbonate plays an important role in determining the equilibrium behavior of CO_2 even at loadings approaching unity. This is consistent with the behavior of the CO_2 equilibrium partial pressure over MDEA-MEA or MDEA-DEA mixtures at high loadings as illustrated in Figures 7.1 through 7.4.

Also of interest in Figures 7.9 and 7.10 are the relative concentrations of MEA or DEA and MDEA. The concentrations of the unreacted alkanolamines are important in determining the rate of absorption in a rate-based simulator. In the MDEA-MEA mixture, the concentration of MDEA is essentially constant at low loadings while the concentration of MEA decreases rapidly with loading in this range. MEA preferentially reacts with CO_2 because it forms a very stable carbamate and, to a lesser extent, because of the relatively large pKa of MEA. For a 3 kmol m^{-3} MDEA, 1 kmol m^{-3} MEA mixture at 40°C, MEA is almost completely converted to protonated MEA or carbamate at a loading of 0.4 moles CO_2 per mole of amine.

Figure 7.10 indicates that DEA disappears at a slower rate as loading increases than does MEA in the corresponding amine mixtures. This is consistent with the fact that the carbamate of DEA is not as stable as the carbamate of MEA. Furthermore, while DEA disappears faster than MDEA as the CO_2 loading initially increases from zero, molecular DEA is present in the solution to a loading of 0.9 mol/mol These results suggest that DEA will continue to enhance the absorption rate of CO_2 in an MDEA based solvent mixture even when the solution is highly loaded.

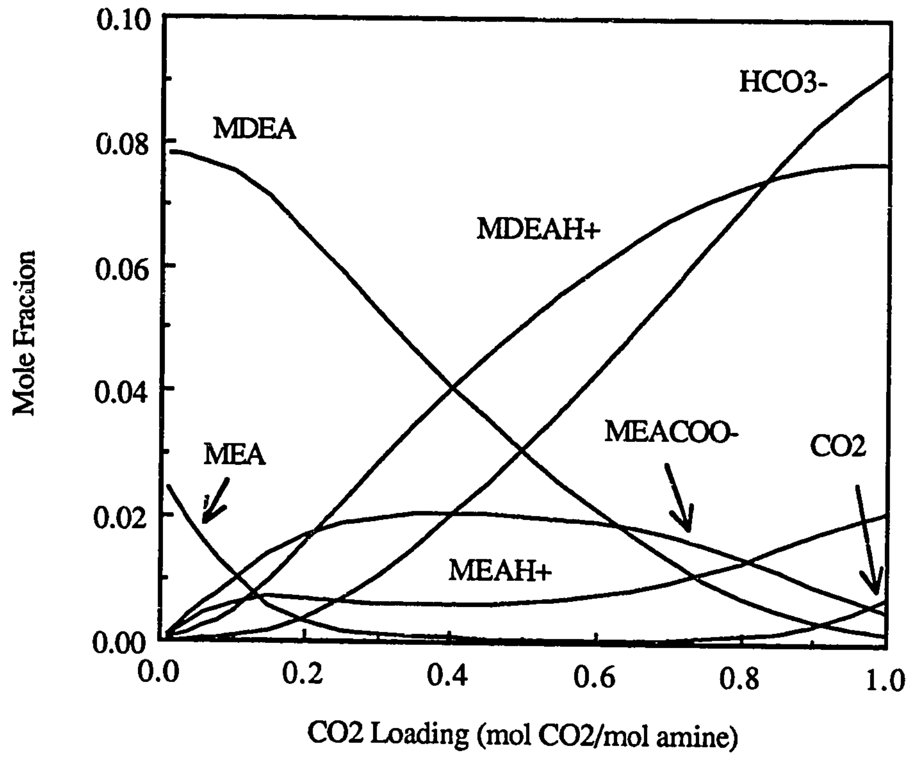

Figure 7.9 Liquid phase mole fractions of a CO_2 loaded 3 kmol m^{-3} MDEA - 1 kmol m^{-3} MEA aqueous solution at 40°C. Amine concentrations are CO_2 free. Mole fractions were calculated with the VLE model.

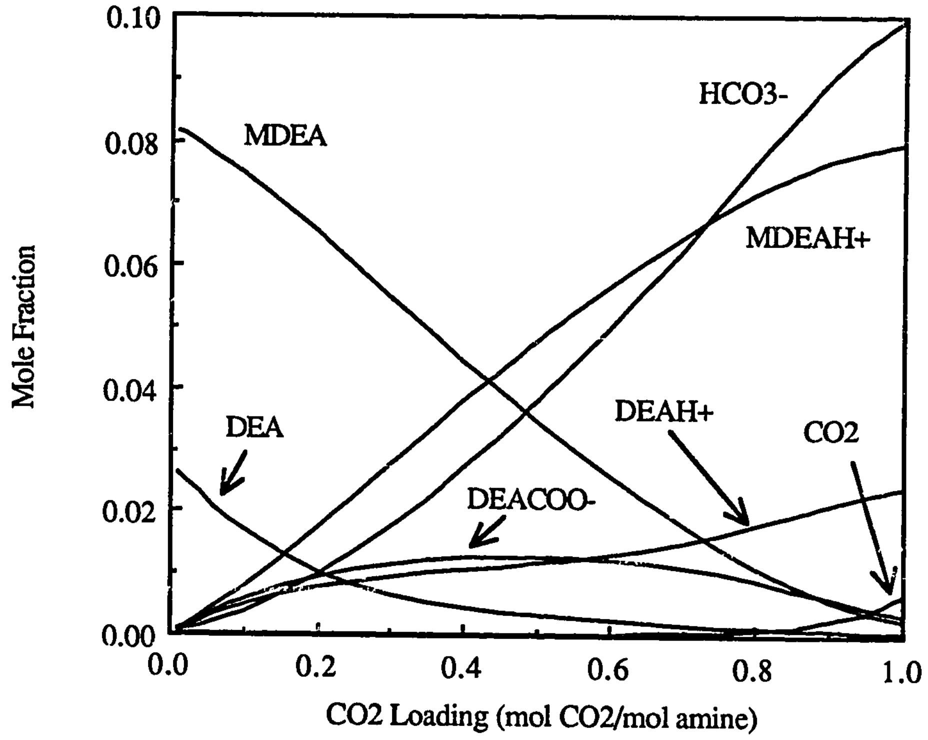

Figure 7.10 Liquid phase mole fractions of a CO_2 loaded 3 kmol m^{-3} MDEA - 1 kmol m^{-3} DEA aqueous solution at 40°C. Amine concentrations are CO_2 free. Mole fractions were calculated with the VLE model.

Chapter Eight

Summary, Conclusions and Recommendations

8.1 Summary

A physico-chemical model was developed for representing VLE in H_2S-CO_2-alkanolamine-water systems. The alkanolamines of interest in this work include monoethanolamine, MEA, diethanolamine, DEA, diglycolamine, DGA, and methyldiethanolamine, MDEA. The framework of the model is based upon both chemical equilibria, to determine the equilibrium distribution of species in the liquid phase, and phase equilibria, to determine the equilibrium distribution of molecular species between the vapor and liquid phases.

Liquid phase activity coefficients are represented with the Electrolyte-NRTL equation accounting for both long-range ion-ion interactions and local or short-range interactions between all true liquid phase species. The system is modeled as a mixed solvent (alkanolamine-water) solution. Vapor phase fugacity coefficients are calculated using the Redlich-Kwong-Soave (RKS) equation of state.

Adjustable parameters of the model, binary interaction parameters of the Electrolyte-NRTL equation and carbamate stability constants, were fitted on relevant binary system (acid gas-H_2O and alkanolamine-H_2O) and ternary system (H_2S-alkanolamine-H_2O and CO_2-alkanolamine-H_2O) VLE data reported in the literature. The ternary system VLE measurements used to estimate parameters ranged in temperature from 25 to 120°C, in alkanolamine concentration from 1 to 5 M, in liquid phase acid gas loading from 0 to 1.5 moles of acid gas per mole of amine, and in acid gas partial pressure from less than 0.1 to greater than 1000 kPa.

Best values of the adjustable parameters were determined using the Data Regression System (DRS) of ASPEN PLUS process simulator. DRS is a generalized least squares method for the estimation of parameters in physical property models including vapor-liquid equilibrium models. DRS is based upon the maximum likelihood principle. It is especially useful for estimating parameters from data for which both dependent and independent state variables are subject to error.

The model was extended to represent CO_2 solubility in aqueous mixtures of MDEA with MEA and MDEA with DEA. However, no data are reported in the literature for the solubility of CO_2 in these mixtures. Therefore, in support of this work, the solubility of CO_2 in 4 kmol m^{-3} aqueous mixtures of MDEA with MEA and MDEA with DEA was measured at 40 and 80°C over a wide range of CO_2 partial pressures. This data was used to estimate values of the additional (unique) adjustable parameters for the mixed amine systems.

A stand-alone bubble-point algorithm was developed to be used independently of ASPEN PLUS. The thermodynamic framework and thermodynamic functions used in the stand-alone algorithm are identical with those employed by ASPEN PLUS. The liquid phase equilibrium distribution of species is determined by a Gibbs free energy minimization technique in which values of the free energy are constrained by the element abundance equations. The minimum in the Gibbs free energy is found by the method of Lagrange multipliers. Because they are nonlinear in mole numbers, the necessary conditions for a minimum in the free energy are satisfied by iteratively solving a linearized set of the necessary conditions. The method has proven to be reliable and efficient.

8.2 Conclusions

Maximum likelihood estimates of H_2S or CO_2 equilibrium partial pressures and H_2S or CO_2 liquid phase apparent mole fractions were found to be in good agreement with ternary system (H_2S-amine-H_2O or CO_2-amine-H_2O) measurements for aqueous solutions of MEA, DEA, DGA, and MDEA indicating that the model successfully represents the solubility of H_2S or CO_2 in aqueous solutions of these amines. Where there is poor agreement between various sources of ternary system VLE data, maximum likelihood estimates of state variables varied somewhat more from reported measurements. Representation of CO_2 solubility was seen to be slightly skewed above 100°C for a number of the alkanolamines suggesting the model exhibits a minor systematic 'lack of fit' of CO_2 solubility at high temperatures.

Without fitting additional parameters on reported quaternary system data (H_2S-CO_2-alkanolamine-water), maximum likelihood estimates of H_2S and CO_2 equilibrium partial pressures and H_2S and CO_2 equilibrium liquid phase concentrations were found to satisfactorily agree with quaternary system measurements for all four alkanolamines. These results indicate that the model satisfactorily represents the solubility of H_2S and CO_2 mixtures in aqueous solutions of MEA, DEA, MDEA, and DGA.

Modeling of water-alkanolamine solutions revealed that these binary systems exhibit negative deviations from ideality. MEA-water, DEA-water and DGA-water systems were seen to deviate widely from ideality while the MDEA-water was seen to deviate only moderately from ideality. Alkanolamine activity coefficients were generally found to vary from unity to the greatest extent at infinite dilution. Since acid gas-alkanolamine-water systems of industrial importance are primarily water, consideration of these deviations from ideality is important if the liquid phase equilibrium concentration of free alkanolamine is to be accurately calculated. Accurate determination of liquid phase alkanolamine concentration is especially important in rate-based models wherein alkanolamine concentrations enter into kinetic expressions.

Estimated molecule-molecule and molecule-ion pair parameters were generally well determined as reflected by the relatively small standard deviations corresponding to these parameters. The only molecule-ion pair parameters that affected representation of ternary system VLE data were **water-ion pair** parameters. These were generally in good agreement with water-ion pair parameters estimated for strong electrolyte systems.

Carbamate stability constants were also well determined. Estimated values of the carbamate stability constants suggest that of the amines considered, MEA forms the most stable carbamate, DGA forms a carbamate of intermediate stability, and DEA forms the least stable carbamate.

Corresponding pairs of water-ion pair interaction parameters were generally found to be highly correlated. Fortunately, water-ion pair interaction parameters were not found to be highly correlated with other water-ion pair parameters involving different ion pairs. Nor were water-ion pair interaction parameters found to be correlated with the carbamate stability constants. This, together with the fact that most estimated parameters were well determined, suggests that the data regression process was able to separate chemical and physical interactions.

The solubility of CO_2 in MDEA - MEA and MDEA - DEA aqueous solutions containing 2 kmol m^{-3} of each alkanolamine was found to behave in a manner consistent with the solubility of CO_2 in 4 kmol m^{-3} solutions of MDEA, MEA, and DEA. The addition of MEA or DEA to an MDEA solution was seen to substantially increase the solubility of CO_2 at low acid gas loadings. Alternately, at low acid gas loadings, the addition of MEA or DEA to an MDEA solution was seen to decrease the equilibrium partial pressure of CO_2 over the solution. Both experimental results and model representation indicated that the addition of a fixed amount of MEA to an MDEA solution has a greater affect on CO_2 solubility than will a fixed amount of DEA. However, speciation with the model suggests that molecular DEA is present in solution to higher acid gas loadings, thus enhancing CO_2 absorption rates over a wider range of loadings.

Water-ion pair interaction parameters fitted on mixed amine CO_2 solubility data measured in this work were found to be in good agreement with parameters fitted on single amine ternary system VLE data. Representation of the experimental data by the model is good, especially at industrially important acid gas loadings.

8.3 Recommendations

During the course of this study, many important and interesting issues and research topics outside the scope of the work were recognized. Several are discussed here as recommendations for future work.

Perhaps the most important contribution that can be gained from this work is through the use of the model as a tool for evaluating acid gas solubility behavior in new, alkanolamine based, solvent systems. In recent years, many new solvent systems have been proposed for gas treating applications. These include hindered amines for selective H_2S removal (Sartori and Savage, 1983), and amine mixtures to which an acid has been added to effect a greater degree of H_2S removal (Union Carbide Corp., 1984). The experimental effort required to characterize the acid gas solubility behavior of these new solvent systems will be exhorbitant. However, owing to its fundamental and thermodynamically consistent basis, the model developed in this work could be used, in conjunction with experimental design, to effect a reduction in the effort required to characterize acid gas solubility behavior. Parameters of the model could adjusted on accurate solubility data measured at a minimum number of strategically selected temperatures and pressures allowing it to be confidently used for interpolation and extrapolation.

Moreover, by fixing binary parameters at default values and using only pure component data and equilibrium constants for all relevant reactions (ie. no experimental solubility data), the model could be used to calculate *first order approximations* of H_2S and CO_2 solubilities in new solvent systems.

The Electrolyte-NRTL equation is capable of representing activity coefficients to high ionic strengths. However, it is a complicated excess Gibbs energy equation; activity coefficients derived from it are also complicated. Application of the Electrolyte-NRTL equation is, therefore, computationally time-consuming. Since equilibrium models are executed often by both equilibrium-staged simulation models and rate-based simulation models, the issue of computational efficiency is important. Hence, a comparison of acid gas-alkanolamine-water VLE data representation by the model developed in this work with previously developed models (employing thermodynamically less rigorous approaches) would prove interesting.

It would also prove interesting to compare the liquid phase equilibrium compositions calculated by the model developed in this work with those calculated by earlier VLE models. Unfortunately, no data are available that can be used to judge accuracy. It has been noted that accurate calculation of liquid phase concentrations are especially important in rate-based models and in the determination of rate constants from absorption rate measurements. Of particular interest would be calculated values of the equilibrium concentration of unreacted amine in the liquid phase. It has been shown that in an aqueous system, some amines exhibit large deviations from ideal behavior. Consideration of these deviations from ideality is important if the equilibrium concentration of free alkanolamine is to be calculated accurately.

As noted in Chapter Four, the adjustable parameters of the Electrolyte-NRTL equation include molecule-**ion pair** parameters rather than molecule-**ion** parameters. This is due to Chen's assumption of *local-electroneutrality*. One of the consequences of this assumption is that in binary electrolyte-solvent systems (eg. NaCl-H_2O) cation and anion activity coefficients calculated by the Electrolyte-NRTL equation are equal. In reality, however, cation and anion activity coefficients are not generally equal. Therefore, it would be interesting to reformulate and reevaluate the Electrolyte-NRTL equation without applying the assumption of local-electroneutrality. This would, of course, be useful for applications both within and outside the scope of this work.

To date, the present VLE model is the most sophisticated developed for the acid gas-alkanolamine-water system. It has been postulated that deviations of liquid phase behavior from ideality can be more confidently represented because the Electrolyte-NRTL equation is valid to ionic strengths representative of industrial practice. It would now be useful to evaluate the equilibrium model as a component of a rate-based model. As noted earlier, the equilibrium model would be used in this context to calculate bulk liquid phase composition (the bulk liquid phase is normally assumed to be in chemical equilibrium) and the concentration of molecular CO_2 or H_2S in the liquid at the gas-liquid interface (physical equilibrium is usually assumed to exist at the gas-liquid interface).

Appendix A

Activity coefficients by the Electrolyte-NRTL Equation

Pitzer - Debye - Hückel Contribution:

Solvent:

$$\ln \gamma_s^{pdh*} = 2\left(\frac{1000}{M_m}\right)^{1/2} A_\phi \frac{I_x^{3/2}}{(1+\rho I_x^{1/2})} \qquad (A.1)$$

Ionic Species:

$$\ln \gamma_i^{pdh} = -\left(\frac{1000}{M_m}\right)^{1/2} A_\phi \Big\{ (\frac{2z_i^2}{\rho} \ln(1+\rho I_x^{1/2}) + \frac{(z_i^2 I_x^{1/2} - 2I_x^{3/2})}{(1+\rho I_x^{1/2})} \Big\} \qquad (A.2)$$

Born Contribution:

Ionic Species (only):

$$\ln \gamma_{i\,BORN}^{\infty} = -\left(\frac{e^2}{2kT}\right)\left(\frac{z_i^2}{r_i}\right)\left(\frac{1}{D_m} - \frac{1}{D_w}\right) \qquad (A.3)$$

NRTL Contribution:

Molecular Species:

$$\ln \gamma_{m\,\mathrm{NRTL}} = \frac{\sum_{j} X_j\, G_{jm}\, \tau_{jm}}{\sum_{k} X_k\, G_{km}}$$

$$+ \sum_{m'} \frac{X_{m'}\, G_{mm'}}{\sum_{k} X_k\, G_{km}} \left(\tau_{mm'} - \frac{\sum_{k} X_k\, G_{km'}\, \tau_{km'}}{\sum_{k} X_k\, G_{km'}} \right)$$

$$+ \sum_{c} \sum_{a'} \frac{X_{a'}}{\sum_{a''} X_{a''}} \frac{X_c\, G_{mc.a'c}}{\sum_{k} X_k\, G_{kc.a'c}}$$

$$\mathrm{x} \left(\tau_{mc,a'c} - \frac{\sum_{k} X_k\, G_{kc.a'c}\, \tau_{kc.a'c}}{\sum_{k} X_k\, G_{kc.a'c}} \right)$$

$$+ \sum_{a} \sum_{c'} \frac{X_{c'}}{\sum_{c''} X_{c''}} \frac{X_a\, G_{ma.c'a}}{\sum_{k} X_k\, G_{ka.c'a}}$$

$$\mathrm{x} \left(\tau_{ma,c'a} - \frac{\sum_{k} X_k\, G_{ka.c'a}\, \tau_{ka.c'a}}{\sum_{k} X_k\, G_{ka.c'a}} \right) \qquad \text{(A.4)}$$

$$\ln \gamma^{\infty}_{m\,\mathrm{NRTL}} = \tau_{wm} + G_{mw}\, \tau_{mw} \qquad \text{(A.5)}$$

Cations:

$$
\begin{aligned}
\frac{1}{Z_c} \ln \gamma_{c\,\mathrm{NRTL}} = {} & \sum_{a'} \frac{X_{a'}}{\sum_{a''} X_{a''}} \frac{\sum_k X_k G_{kc.a'c} \tau_{kc.a'c}}{\sum_k X_k G_{kc.a'c}} \\
& + \sum_m \frac{X_m G_{km}}{\sum_k X_k G_{km}} \left(\tau_{cm} - \frac{\sum_k X_k G_{km} \tau_{km}}{\sum_k X_k G_{km}} \right) \\
& + \sum_a \sum_{c'} \frac{X_{c'}}{\sum_{c''} X_{c''}} \frac{X_a G_{ca.c'a}}{\sum_k X_k G_{ca.c'a}} \\
& \times \left(\tau_{ca,c'a} - \frac{\sum_k X_k G_{ka.c'a} \tau_{ka.c'a}}{\sum_k X_k G_{ka.c'a}} \right)
\end{aligned}
\tag{A.6}
$$

$$
\ln \gamma^{\infty}_{c\,\mathrm{NRTL}} = Z_c \left\{ G_{cw} \tau_{cw} + \frac{\sum_{a'} x_{a'} \tau_{wc.a'c}}{\sum_{a''} x_{a''}} \right\}
\tag{A.7}
$$

Anions:

$$\frac{1}{Z_a}\ln\gamma_{a\,\mathrm{NRTL}} = \sum_{c'} \frac{X_{c'}}{\sum\limits_{X_{c''}} X_{c''}} \frac{\sum\limits_{k} X_k G_{ka.c'a}\tau_{ka.c'a}}{\sum\limits_{k} X_k G_{ka.c'a}}$$

$$+ \sum_{m} \frac{X_m G_{km}}{\sum\limits_{k} X_k G_{km}} \left(\tau_{am} - \frac{\sum\limits_{k} X_k G_{km}\tau_{km}}{\sum\limits_{k} X_k G_{km}}\right)$$

$$+ \sum_{c}\sum_{a'} \frac{X_{a'}}{\sum\limits_{a''} X_{a''}} \frac{X_c G_{ac.a'c}}{\sum\limits_{k} X_k G_{ac.a'c}}$$

$$\mathrm{x}\left(\tau_{ac,a'c} - \frac{\sum\limits_{k} X_k G_{kc.a'c}\tau_{kc.a'c}}{\sum\limits_{k} X_k G_{kc.a'c}}\right) \tag{A.8}$$

$$\ln\gamma^{\infty}_{a\,\mathrm{NRTL}} = Z_a\left\{G_{aw}\tau_{aw} + \frac{\sum\limits_{c'} x_{c'}\tau_{wa.c'a}}{\sum\limits_{c''} x_{c''}}\right\} \tag{A.9}$$

Activity coefficients by equations (A.4), (A.6), (A.8) are symmetrically normalized. To obtain the unsymmetrically normalized activity coefficients for which the solute (molecular and ionic) reference state is the ideal infinitely dilute aqueous solution, equations (A.5), (A.7), and (A.9) must be subtracted from the corresponding expressions for the symmetrically normalized activity coefficients.

Appendix B

Parameter Correlation Matrices

The correlation coefficient, ρ, between two parameters - θ_1 and θ_2 - is defined as

$$\rho(\theta_1, \theta_2) = \frac{\mathrm{cov}(\theta_1, \theta_2)}{\sigma_{\theta 1}\sigma_{\theta 2}} \tag{4.80}$$

where $\mathrm{cov}(\theta_1, \theta_2)$ is the covariance between the two parameters θ_1 and θ_2, and $\sigma_{\theta 1}$ and $\sigma_{\theta 2}$ are the estimated standard deviations of the estimates of θ_1 and θ_2. Parameters that are completely independent have a correlation coefficient of zero. Parameters that are perfectly correlated have a correlation coefficient of ±1. ASPEN PLUS DRS calculates the matrix of parameter correlation coefficients from the parameter variance-covariance matrix. These matrices are symmetric. Therefore, only the lower entries of the matrices are reproduced here.

Binary Systems

MEA-H_2O System

Parameters: $\tau_{H_2O\text{-}MEA} = a_{H_2O\text{-}MEA} + b_{H_2O\text{-}MEA}$

$\tau_{MEA\text{-}H_2O} = a_{MEA\text{-}H_2O} + b_{MEA\text{-}H_2O}$

	$a_{H_2O\text{-}MEA}$	$b_{H_2O\text{-}MEA}$	$a_{MEA\text{-}H_2O}$	$b_{MEA\text{-}H_2O}$
$a_{H_2O\text{-}MEA}$	1.000			
$b_{H_2O\text{-}MEA}$	0.000	0.000*		
$a_{MEA\text{-}H_2O}$	0.000	0.000	0.000*	
$b_{MEA\text{-}H_2O}$	-0.995	0.000	0.000	1.000

* Associated parameter fixed at zero, standard deviation was not estimated.

DEA-H_2O System

Parameters: $\tau_{H_2O\text{-}DEA} = a_{H_2O\text{-}DEA} + b_{H_2O\text{-}DEA}$

$\tau_{DEA\text{-}H_2O} = a_{DEA\text{-}H_2O} + b_{DEA\text{-}H_2O}$

	$a_{H_2O\text{-}DEA}$	$a_{DEA\text{-}H_2O}$	$b_{H_2O\text{-}DEA}$	$b_{DEA\text{-}H_2O}$
$a_{H_2O\text{-}DEA}$	1.000			
$a_{DEA\text{-}H_2O}$	-0.981	1.000		
$b_{H_2O\text{-}DEA}$	-0.980	0.930	1.000	
$b_{DEA\text{-}H_2O}$	0.991	-0.983	-0.978	1.000

MDEA-H_2O System

Parameters: $\tau_{H_2O\text{-}MDEA} = a_{H_2O\text{-}MDEA} + b_{H_2O\text{-}MDEA}$

$\tau_{MDEA\text{-}H_2O} = a_{MDEA\text{-}H_2O} + b_{MDEA\text{-}H_2O}$

	$a_{H_2O\text{-}MDEA}$	$a_{MDEA\text{-}H_2O}$	$b_{H_2O\text{-}MDEA}$	$b_{MDEA\text{-}H_2O}$
$a_{H_2O\text{-}MDEA}$	1.000			
$a_{MDEA\text{-}H_2O}$	-0.997	1.000		
$b_{H_2O\text{-}MDEA}$	0.000	0.000	0.000*	
$b_{MDEA\text{-}H_2O}$	0.000	0.000	0.000	0.000*

* Associated parameter fixed at zero, standard deviation was not estimated.

DGA-H_2O System

Parameters: $\tau_{H_2O\text{-}DGA} = a_{H_2O\text{-}DGA} + b_{H_2O\text{-}DGA}$

$\tau_{DGA\text{-}H_2O} = a_{DGA\text{-}H_2O} + b_{DGA\text{-}H_2O}$

	$a_{H_2O\text{-}DGA}$	$a_{DGA\text{-}H_2O}$	$b_{H_2O\text{-}DGA}$	$b_{DGA\text{-}H_2O}$
$a_{H_2O\text{-}DGA}$	1.000			
$a_{DGA\text{-}H_2O}$	0.000	0.000*		
$b_{H_2O\text{-}DGA}$	0.000	0.000	0.000*	
$b_{DGA\text{-}H_2O}$	0.998	0.000	0.000	1.000

* Associated parameter fixed at zero, standard deviation was not estimated.

Ternary Systems

H_2S-MEA-H_2O

Parameters: $\tau_{H_2O\text{-}MEAH^+,HS^-} = a_{H_2O\text{-}MEAH^+,HS^-} + b_{H_2O\text{-}MEAH^+,HS^-}$

$\tau_{MEAH^+,HS^-\text{-}H_2O} = a_{MEAH^+,HS^-\text{-}H_2O} + b_{MEAH^+,HS^-\text{-}H_2O}$

	a_1	b_1	a_2	b_2
a_1	1.000			
b_1	-0.995	1.000		
a_2	-0.980	0.977	1.000	
b_2	0.974	-0.980	-0.995	1.000

where $a_1 = a_{H_2O\text{-}MEAH^+,HS^-}$ $b_1 = b_{H_2O\text{-}MEAH^+,HS^-}$

$a_2 = a_{MEAH^+,HS^-\text{-}H_2O}$ $b_2 = b_{MEAH^+,HS^-\text{-}H_2O}$

CO_2-MEA-H_2O

Parameters:

$$\tau_{H_2O\text{-}MEAH^+,HCO_3^-} = a_{H_2O\text{-}MEAH^+,HCO_3^-} + b_{H_2O\text{-}MEAH^+,HCO_3^-}$$

$$\tau_{MEAH^+,HCO_3^-\text{-}H_2O} = a_{MEAH^+,HCO_3^-\text{-}H_2O} + b_{MEAH^+,HCO_3^-\text{-}H_2O}$$

$$\tau_{H_2O\text{-}MEAH^+,MEACOO^-} = a_{H_2O\text{-}MEAH^+,MEACOO^-} + b_{H_2O\text{-}MEAH^+,MEACOO^-}$$

$$\tau_{MEAH^+,MEACOO^-\text{-}H_2O} = a_{MEAH^+,MEACOO^-\text{-}H_2O} + b_{MEAH^+,MEACOO^-\text{-}H_2O}$$

$$\ln K_{carbamate} = C_1 + C_2/T$$

	a_1	a_2	b_1	a_3	a_4	b_3	C_1	C_2
a_1	1.000							
a_2	-0.823	1.000						
b_1	-0.952	0.616	1.000					
a_3	-0.050	0.182	-0.026	1.000				
a_4	-0.059	-0.124	0.133	-0.955	1.000			
b_3	0.000	0.000	0.000	0.000	0.000	0.000*		
C_1	-0.177	-0.065	0.318	-0.253	0.254	0.000	1.000	
C_2	0.129	0.094	-0.273	0.231	-0.199	0.000	-0.992	1.000

Note: b_2 and b_4 were fixed at zero, standard deviation was not estimated. *Associated parameter encountered a bound, standard deviation could not be estimated.

where

$a_1 = a_{H_2O\text{-}MEAH^+,HCO_3^-}$ $\quad b_1 = b_{H_2O\text{-}MEAH^+,HCO_3^-}$

$a_2 = a_{MEAH^+,HCO_3^-\text{-}H_2O}$ $\quad b_2 = b_{MEAH^+,HCO_3^-\text{-}H_2O}$

$a_3 = a_{H_2O\text{-}MEAH^+,MEACOO^-}$ $\quad b_3 = b_{H_2O\text{-}MEAH^+,MEACOO^-}$

$a_4 = a_{MEAH^+,MEACOO^-\text{-}H_2O}$ $\quad b_4 = b_{MEAH^+,MEACOO^-\text{-}H_2O}$

H_2S-DEA-H_2O

Parameters: $\tau_{H_2O\text{-}DEAH^+,HS^-} = a_{H_2O\text{-}DEAH^+,HS^-} + b_{H_2O\text{-}DEAH^+,HS^-}$

$\tau_{DEAH^+,HS^-\text{-}H_2O} = a_{DEAH^+,HS^-\text{-}H_2O} + b_{DEAH^+,HS^-\text{-}H_2O}$

	a_1	b_1	a_2	b_2
a_1	1.000			
b_1	-0.997	1.000		
a_2	-0.969	0.964	1.000	
b_2	0.967	-0.969	-0.997	1.000

where $a_1 = a_{H_2O\text{-}DEAH^+,HS^-}$ $b_1 = b_{H_2O\text{-}DEAH^+,HS^-}$

$a_2 = a_{DEAH^+,HS^-\text{-}H_2O}$ $b_2 = b_{DEAH^+,HS^-\text{-}H_2O}$

CO_2-DEA-H_2O

Parameters:

$$\tau_{H_2O\text{-}DEAH^+,HCO_3^-} = a_{H_2O\text{-}DEAH^+,HCO_3^-} + b_{H_2O\text{-}DEAH^+,HCO_3^-}$$

$$\tau_{DEAH^+,HCO_3^-\text{-}H_2O} = a_{DEAH^+,HCO_3^-\text{-}H_2O} + b_{DEAH^+,HCO_3^-\text{-}H_2O}$$

$$\tau_{H_2O\text{-}DEAH^+,DEACOO^-} = a_{H_2O\text{-}DEAH^+,DEACOO^-} + b_{H_2O\text{-}DEAH^+,DEACOO^-}$$

$$\tau_{DEAH^+,DEACOO^-\text{-}H_2O} = a_{DEAH^+,DEACOO^-\text{-}H_2O} + b_{DEAH^+,DEACOO^-\text{-}H_2O}$$

$$\ln K_{carbamate} = C_1 + C_2/T$$

	a_1	b_1	a_2	a_3	b_3	a_4	C_1	C_2
a_1	1.000							
b_1	-0.914	1.000						
a_2	-0.657	0.305	1.000					
a_3	-0.603	0.363	0.677	1.000				
b_3	0.109	0.113	0.028	-0.323	1.000			
a_4	0.555	0.304	-0.720	-0.924	0.002	1.000		
C_1	-0.243	0.129	0.303	0.459	-0.643	-0.242	1.000	
C_2	0.139	-0.078	-0.186	-0.267	0.573	0.091	-0.966	1.000

Note: b_2 and b_4 were fixed at zero, standard deviations were not estimated.

where

$a_1 = a_{H_2O\text{-}DEAH^+,HCO_3^-}$ $b_1 = b_{H_2O\text{-}DEAH^+,HCO_3^-}$

$a_2 = a_{DEAH^+,HCO_3^-\text{-}H_2O}$ $b_2 = b_{DEAH^+,HCO_3^-\text{-}H_2O}$

$a_3 = a_{H_2O\text{-}DEAH^+,DEACOO^-}$ $b_3 = b_{H_2O\text{-}DEAH^+,DEACOO^-}$

$a_4 = a_{DEAH^+,DEACOO^-\text{-}H_2O}$ $b_4 = b_{DEAH^+,DEACOO^-\text{-}H_2O}$

H_2S-MDEA-H_2O

Parameters: $\tau_{H_2O\text{-}MDEAH^+,HS^-} = a_{H_2O\text{-}MDEAH^+,HS^-} + b_{H_2O\text{-}MDEAH^+,HS^-}$

$\tau_{MDEAH^+,HS^-\text{-}H_2O} = a_{MDEAH^+,HS^-\text{-}H_2O} + b_{MDEAH^+,HS^-\text{-}H_2O}$

	a_1	a_2	b_1	b_2
a_1	1.000			
a_2	-0.339	1.000		
b_1	-0.973	0.129	1.000	
b_2	0.000	0.000	0.000	0.000*

* Note: b_2 was fixed at zero, standard deviation was not estimated.

where $a_1 = a_{H_2O\text{-}MDEAH^+,HS^-}$ $a_2 = a_{MDEAH^+,HS^-\text{-}H_2O}$

$b_1 = b_{H_2O\text{-}MDEAH^+,HS^-}$ $b_2 = b_{MDEAH^+,HS^-\text{-}H_2O}$

CO_2-MDEA-H_2O

Parameters: $\tau_{H_2O\text{-}MDEAH^+,HCO_3^-} = a_{H_2O\text{-}MDEAH^+,HCO_3^-} + b_{H_2O\text{-}MDEAH^+,HCO_3^-}$

$\tau_{MDEAH^+,HCO_3^-\text{-}H_2O} = a_{MDEAH^+,HCO_3^-\text{-}H_2O} + b_{MDEAH^+,HCO_3^-\text{-}H_2O}$

	a_1	a_2	b_1	b_2
a_1	1.000			
a_2	-0.608	1.000		
b_1	-0.966	0.391	1.000	
b_2	0.000	0.000	0.000	1.000*

Note: b_2 was fixed at zero, standard deviation was not estimated.

where $a_1 = a_{H_2O\text{-}MDEAH^+,HCO_3^-}$ $a_2 = a_{MDEAH^+,HCO_3^-\text{-}H_2O}$

$b_1 = b_{H_2O\text{-}MDEAH^+,HCO_3^-}$ $b_2 = b_{MDEAH^+,HCO_3^-\text{-}H_2O}$

H_2S-DGA-H_2O

Parameters: $\tau_{H_2O\text{-}DGAH^+,HS^-} = a_{H_2O\text{-}DGAH^+,HS^-} + b_{H_2O\text{-}DGAH^+,HS^-}$

$\tau_{DGAH^+,HS^-\text{-}H_2O} = a_{DGAH^+,HS^-\text{-}H_2O} + b_{DGAH^+,HS^-\text{-}H_2O}$

	a_1	b_1	a_2	b_2
a_1	1.000			
b_1	-0.970	1.000		
a_2	-0.266	0.035	1.000	
b_2	0.000	0.000	0.000	0.000*

* Associated parameter encountered at bound, standard deviation could not be estimated.

where

$a_1 = a_{H_2O\text{-}DGAH^+,HS^-}$

$a_2 = a_{DGAH^+,HS^-\text{-}H_2O}$

$b_1 = b_{H_2O\text{-}DGAH^+,HS^-}$

$b_2 = b_{DGAH^+,HS^-\text{-}H_2O}$

CO_2-DGA-H_2O

Parameters:

$$\tau_{H_2O\text{-}DGAH^+,HCO_3^-} = a_{H_2O\text{-}DGAH^+,HCO_3^-} + b_{H_2O\text{-}DGAH^+,HCO_3^-}$$

$$\tau_{DGAH^+,HCO_3^-\text{-}H_2O} = a_{DGAH^+,HCO_3^-\text{-}H_2O} + b_{DGAH^+,HCO_3^-\text{-}H_2O}$$

$$\tau_{H_2O\text{-}DGAH^+,DGACOO^-} = a_{H_2O\text{-}DGAH^+,MEACOO^-} + b_{H_2O\text{-}DGAH^+,DGACOO^-}$$

$$\tau_{DGAH^+,DGACOO^-\text{-}H_2O} = a_{DGAH^+,DGACOO^-\text{-}H_2O} + b_{DGAH^+,DGACOO^-\text{-}H_2O}$$

$$\ln K_{carbamate} = C_1 + C_2/T$$

	b_1	a_2	a_3	a_4	C_1	C_2
b_1	1.000					
a_2	-0.984	1.000				
a_3	-0.441	0.446	1.000			
a_4	0.381	-0.447	-0.928	1.000		
C_1	0.284	0.314	0.420	-0.398	1.000	
C_2	0.124	-0.217	-0.171	0.310	0.895	1.000

Note: a_1, b_2, b_3, and b_4 were fixed at zero, standard deviations were not estimated.

where

$a_1 = a_{H_2O\text{-}DGAH^+,HCO_3^-}$ $\quad$ $b_1 = b_{H_2O\text{-}DGAH^+,HCO_3^-}$

$a_2 = a_{DGAH^+,HCO_3^-\text{-}H_2O}$ $\quad$ $b_2 = b_{DGAH^+,HCO_3^-\text{-}H_2O}$

$a_3 = a_{H_2O\text{-}DGAH^+,DGACOO^-}$ $\quad$ $b_3 = b_{H_2O\text{-}DGAH^+,DGACOO^-}$

$a_4 = a_{DGAH^+,DGACOO^-\text{-}H_2O}$ $\quad$ $b_4 = b_{DGAH^+,DGACOO^-\text{-}H_2O}$

Nomenclature

A	coefficient of equation (4.66)
$\mathbf{A}$	element abundance matrix
A_ϕ	Debye-Hückel constant for osmotic coefficient
A_γ	Debye-Hückel constant for activity coefficient
a	activity
	parameter of Redlich-Kwong-Soave equation of state
	coefficient of equation (4.67)
B	coefficient of equation (4.66)
B_{ca}	parameter of Guggenheim equation
b	parameter of Redlich-Kwong-Soave equation of state
	coefficient of equation (4.67)
b_i	moles of element i
C_1-C_4	coefficients of equation (4.8)
C_j	parameter of Electrolyte-NRTL equation
c	concentration
D_1-D_4	coefficients of equation (4.9)
D	dielectric constant of solvent mixture
d	density
∂	partial derivative
e	charge of electron
$\mathbf{e}$	vector of errors in measured state variables
f	fugacity
	parameter of Redlich-Kwong-Soave equation of state
f'	transformed fugacity for data regression
f_i^v	vapor phase fugacity of component i
f_i^l	liquid phase fugacity of component i
G	parameter of Electrolyte-NRTL equation
	total Gibbs free energy
G^{ex}	total excess Gibbs free energy

g	molar Gibbs free energy
$\bar{g}$	partial molar Gibbs free energy
g^{ex}	molar excess Gibbs free energy
$\bar{g}^{ex}$	partial molar excess Gibbs free energy
$H_{i,s}$	Henry's law constant for solute i in solvent s
H_i^{Po}	Henry's law constant for component i in water at saturation pressure
h	molar enthalpy
I_x	ionic strength on mole fraction scale
k	Boltzmann constant
kmol	kilogram-moles
K_x	equilibrium constant, mole fraction
K_m	equilibrium constant, mole kg^{-1}
M	number of experimental measurements
	number of independent chemical reactions in system
	molarity
M_m	mixed solvent molecular weight
M_s	solvent molecular weight
M_i	solute molecular weight
m	meter
m_i	molality
N	number of components in system
$\mathbf{N}$	matrix of stoichiometric coefficients, ν_{ij}
N_o	Avogadro's number
n	moles
$\mathbf{n}$	vector of mole numbers
P	pressure, Pa or kPa as noted
P'	transformed pressure for data regression
P^{ref}	reference pressure
r	ionic radius
R	gas constant
	number of independent chemical reactions
$\mathbf{R}$	variance-covariance matrix
s	molar entropy

T	temperature, K
v	molar volume
$\bar{v}$	partial molar volume
$\bar{v}_i^{\infty}$	partial molar volume of a solute in water at infinite dilution
x	liquid phase mole fraction based on true species, molecular and ionic
x_a	liquid phase apparent mole fraction
$\mathbf{x}$	vector of mole fractions, apparent or true as indicated
x_a'	transformed liquid phase apparent mole fraction for data regression
X	effective liquid phase mole fraction ($X=x*C_j$)
y	vapor phase mole fraction
$\mathbf{y}$	vector of vapor phase mole fractions
Z	absolute value of ionic charge
Z_{RA}	parameter of Rackett equation
z	ionic charge
	compressibility factor
$\mathbf{z}$	vector of observable state variables
$\mathbf{z_o}$	vector of true values of observable state variables
$\mathbf{z_i}$	current estimate of $\mathbf{z_o}$
$\mathbf{z_m}$	vector of measured values of $\mathbf{z}$
α	NRTL nonrandomness factor
	parameter of Redlich-Kwong-Soave equation of state
	acid gas loading
$\boldsymbol{\alpha}$	vector of acid gas loadings
ε	convergence criterion parameter
δ	parameter of equation (4.20)
δ_{ij}	kronecker delta
γ	activity coefficient
$\hat{\varphi}$	vapor phase fugacity coefficient in mixture
φ^o	pure solvent vapor phase fugacity coefficient at saturation pressure
λ	Lagrange multiplier
$\boldsymbol{\lambda}$	vector of Lagrange multipliers

μ	chemical potential
ν	stoichiometric coefficient in chemical reaction
θ	adjustable parameter
$\boldsymbol{\theta}$	vector of adjustable parameters
$\boldsymbol{\theta}_o$	vector of adjustable parameters
ρ	closest approach parameter of the Pitzer-Debye-Hückel equation
	correlation coefficient
	density
σ	standard deviation of experimental measurements, parameter estimates
τ	NRTL binary interaction energy parameter
ω	acentric factor
	step size parameter
ξ	reaction extent
Ψ	λ/RT

Superscripts

agf	acid gas-free
o	standard state
*	Normalization convention II
Δ	Normalization convention III
∞	infinite dilution
e	experimental value
ex	excess property
m	iteration number
po	saturation pressure
sf	solute-free
T	transpose
t	estimated 'true' value

Subscripts

Am	amine
a,a',a"	anion
BORN	Born contribution to Electrolyte-NRTL equation
c,c',c"	cation
c	critical property
ca	ion pair
cm	critical property for mixture
i,j,k	any species
lb	lower bound
local	local contribution to excess Gibbs energy
LR	long range
SR	short range
m	molecular species
	mixture property
NRTL	nonrandom-two liquid contribution to Electrolyte-NRTL equation
nonaq	fraction of solution that is nonaqeous
PDH	Pitzer-Debye-Huckel contribution to Electrolyte-NRTL equation
r	reduced by critical value
s	solvent
T	at specified temperature
	total amount
t	total amount
ub	upper bound
w	water
z	inert components

References

Abrams, D. S., and J. M. Prausnitz, "Statistical Thermodynamics of Liquid Mixtures: A New Expression for the Excess Gibbs Energy of Partly or Completely Miscible Systems," *AIChE J.*, **21**, 1, 116 (1975).

Anderson, T. F., D. S. Abrams, and E. A. Grens II, "Evaluation of Parameters for Nonlinear Thermodynamic Models," *AIChE J.*, **24**, 1, 20 (1978).

Aspen Technology, Inc. *ASPEN PLUS™ Data Regression Manual*, Aspen Technology, Inc., Cambridge, MA (1985).

Astarita, G., D. W. Savage, and A. Bisio, *Gas Treating with Chemical Solvents*, John Wiley and Sons, New York (1983).

Astarita, G., *Mass Transfer with Chemical Reaction*, Elsevier Publishing Co. Amsterdam (1967).

Atwood, K., M. R. Arnold, and R. C. Kindrick, "Equilibria For The System, Ethanolamines - Hydrogen Sulfide - Water," *Ind. Eng. Chem.* **49**, 9, 1439 (1957).

Ball, F. X., H. Planche, W. Fürst, and H. Renon, "Representation of Deviation From Ideality in Concentrated Aqueous Solutions of Electrolytes Using a Mean Spherical Approximation Molecular Model," *AIChE J.*, **31**, 8, 1233 (1985a).

Ball, F. X., W. Furst, and H. Renon, "An NRTL Model for Representation and Prediction of Deviation from Ideality in Electrolyte Solutions Compared to the Models of Chen (1982) and Pitzer (1973)," *AIChE J.*, **31**, 3, 392 (1985b).

Bates, R. G. and G. D. Pinching, "Acidic Dissociation Constant and Related Thermodynamic Quantities for Monoethanolammonium Ion in Water From 0° to 50°C," *J. Res. Nat. Bur. Stand.*, **46**, 5, 349 (1951).

Beck, J. V. and K. J. Arnold, *Parameter Estimation in Engineering and Science*, John Wiley & Sons, New York (1977).

Beutier D. and H. Renon, "Representation of NH_3 - H_2S - H_2O, NH_3 - CO_2 - H_2O, and NH_3 - SO_2 - H_2O Vapor Liquid Equilibria," *Ind. Eng. Chem. Process Des. Dev.*, **17**, 3, 220 (1978).

Bhairi, A. M. "Experimental Equilibrium Between Acid Gases and Ethanolamine Solutions". PhD Dissertation, Oklahoma State University, OK (1984).

Bjerrum, N., *Kgl. Danske Vidensk. Selskab.*, **7**, No. 9 (1926).

Blauwhoff, P. M. M., G. F. Versteeg, and W. P. M. Van Swaaij, "A Study on the Reaction Between CO_2 and Alkanolamines in Aquous Solutions," *Chem. Eng. Sci.*, **39**, 2, 207 (1984).

Blum, L. "Mean Spherical Model for Asymmetric Electrolytes. I: Methold of Solution," *Mol. Phys.*, **30**, 1529 (1975).

Blum, L., "Primitive Electrolytes in The Mean Spherical Approximation," in *Theoretical Chemistry: Advances and Perspectives,* Volume 5, edited by H. Eyring and D. Henderson, Academic Press, New York (1980).

Bower, V. E., R. A. Robinson, and R. G. Bates, "Acidic Dissociation Constant and Related Thermodynamic Quantities for Diethanolammonium Ion in Water From 0 to 50 °C," *J. Res., Nat. Bur. Stands.-A. Physics and Chemistry*, **66A**, 1, 71 (1962).

Brelvi, S. W. and J. P. O'Connell, "Corresponding States Correlations for Liquid Compressibility and Partial Molal Volumes of Gases at Infinite Dilution in Liquids," *AIChE J.*, **18**, 1239 (1972).

Britt, H. I. and R. H. Lueke, "The Estimation of Parameters in Nonlinear, Implicit Models," *Technometrics,* **15**, 2, 233 (1973).

Bromley, L. A., "Approximate Individual Ion Values of β (or B) in Extended Debye-Huckel Theory for Uni-Univalent Aqueous Solutions at 298.15°K,". *J. Chem. Thermo.*, **4**, 669 (1972).

Bromley, L. A., "Thermodynamic Properties of Strong Electrolytes in Aqueous Solutions," *AIChE J.,* **19**, 2, 313 (1973).

Cabezas, H., and J. P. O'Connell, "A Fluctuation Theory of Strong Electrolytes," *Fluid Phase Equilibria,* **30**, 213 (1986).

Caplow, M., "Kinetics of Carbamate Formation and Breakdown," *J. Am. Chem. Soc.*, **90**, 6795 (1968).

Chakravarty, T., "Solubility Calculations For Acid Gases in Amine Blends". Ph.D. Dissertation, Clarkson College, Potsdam, NY (1985).

Chakravarty, T., U. K. Phukan, and R. H. Weiland, "Reaction of Acid Gases with Mixtures of Amines," *Chem. Eng. Prog.*, **81**, 32 (1985).

Chan, H. M. and P. V. Dankwerts, "Equilibrium of MEA and DEA with Bicarbonate and Carbamate," *Chem. Eng. Sci.*, **36**, 229 (1981).

Chen, C. C. "Computer Simulation of Chemical Processes with Electrolytes". Ph.D. Dissertation, Massachusetts Institute of Technology, Cambridge, MA (1980).

Chen, C. C., H. I. Britt, J. F. Boston, and L. B. Evans, "Extension and Application of the Pitzer Equation for Vapor-Liquid Equilibrium of Aqueous Electrolyte Systems with Molecular Solutes," *AIChE J.*, **25**, 5, 820 (1979).

Chen, C. C., H. I. Britt, J. F. Boston, and L. B. Evans, "Local Composition Model for Excess Gibbs Energy of Electrolytes Systems, Part I: Single Solvent, Single Completely Dissociated Electrolyte Systems," *AIChE J.*, **28**, 4, 588 (1982).

Chen, C. C. and L. B. Evans, "A Local Composition Model for the Excess Gibbs Energy of Aqueous Electrolyte Systems," *AIChE J.*, **32**, 3, 444 (1986).

Christensen, C., B. Sander, A. Fredenslund, and P. Rasmussen, "Towards the Extension of Unifac to Mixtures with Electrolytes," *Fluid Phase Equilibria*, **13**, 297 (1983).

Chueh, P. L. and J. M. Prausnitz, "Vapor-Liquid Equilibria at High Pressures: Calculation of Partial Molar Volumes in Nonpolar Liquid Mixtures," *AIChE J.*, **13**, 6, 1099 (1967).

Critchfield, J. E. and G. T. Rochelle, "CO_2 Absorption into Aqueous MDEA and MDEA/MEA Solutions," Presented at the AIChE National Meeting, Paper No. 43e, Houston, TX (March 29 - April 2, 1987).

Critchfield, J. E. and G. T. Rochelle "CO_2 Desorption from DEA and DEA-Promoted MDEA Solutions," Presented at the AIChE National Meeting, Paper No. 68b, New Orleans, LA (March 6 - 10, 1988).

Cruz, J. and H. Renon, "A New Thermodynamic Representation of Binary Electrolyte Solutions Nonideality in the Whole Range of Concentrations," *AIChE J.*, **24**, 5, 817 (1978).

Dankwerts, G. C. and K. M. McNeil, "The Absorption of Carbon Dioxide Into Aqueous Amine Solutions and The Effects of Catalysis," *Trans. Inst. Chem. Eng.*, **45**, T32 (1967).

Daubert, T. E. and R. P. Danner, *Data Compilation Tables of Properties of Pure Compounds;* Design Institute for Physical Property Data; American Institute of Chemical Engineers, New York, NY (1985).

Debye, P. and E. Hückel, "Zur Theorie der Elektrolyte," *Physik. Z.*, **24**, 9, 185 (1923).

Deming, W. E., *Statistical Adjustment of Data*, Wiley, New York (1943).

Denbigh, K., *The Principles of Chemical Equilibrium*, 4th Ed., Cambridge University Press, Cambridge (1981).

De Oliveira, W. A., A. F. Marconsin, A. P. Chagas, and P. L. O. Volpe, "Molar Excess Gibbs Gree Energies of Mixtures of Ethanolamines and Water," *Thermochimica Acta*, **42**, 387 (1980).

Deshmukh, R. D. and A. E. Mather, "A Mathematical Model For Equilibrium Solubility of Hydrogen Sulfide and Carbon Dioxide in Aqueous Alkanolamine Solutions," *Chem. Eng. Sci.*, **36**, 355 (1981).

Dingman, J. C., J. L. Jackson, T. F. Moore, and J. A. Branson, "Equilibrium Data For The H_2S-CO_2 - Diglycolamine Agent - Water System," Presented at the 62nd Annual Gas Processors Association Convention, San Francisco, CA (March 14-16, 1983).

Dickerson, R. E., *Molecular Thermodynamics*, The Benjamin/Cummings Publishing Company, Menlo Park (1969).

Dow Chemical Co. *Gas Conditioning Fact Book*, The Dow Chemical Co., Midland, MI (1962).

Dow Chemical Co. *Gas Treating Handbook*, Gas/Spec Technology Group, The Dow Chemical Co., Houston (1987).

Edwards, T. J., J. Newman, and J. M. Prausnitz, "Thermodynamics of Aqueous Solutions Containing Volatile Weak Electrolytes," *AIChE J.*, **21**, 2, 248 (1975).

Edwards, T. J., G. Maurer, J. Newman, and J. M. Prausnitz, "Vapor-Liquid Equilibria in Multicomponent Aqueous Solutions of Volatile Weak Electrolytes," *AIChE J.*, **24**, 6, 966 (1978).

Finlayson, B. A., *Nonlinear Analysis in Chemical Engineering*, McGraw-Hill Inc., New York (1980).

Gautam R., and W. D. Seider, "Computation of Phase and Chemical Equilibrium: Part I. Local and Constrained Minima in Gibbs Free Energy," *AIChE J.*, **25**, 6, 991 (1979a).

Gautam R., and W. D. Seider, "Computation of Phase and Chemical Equilibrium: Part III. Electrolytic Solutions," *AIChE J.*, **25**, 6, 1006 (1979b).

Gibbs, J. W., *The Scientific Papers of J. Willard Gibbs*, Vol. I., Dover Publications, Inc., New York (1961).

Gibbs, R. E., and H. C. Van Ness, "Solubility of Gases in Liquids in Relation to the Partial Molar Volumes of the Solute. Carbon Dioxide-Water," *Ind. Eng. Chem. Fundam.*, **10**, 2, 312 (1971).

Giggenbach, W., Optical Spectra of Highly Alkanaline Sulfide Solutions and the Second Dissociation Constant of Hydrogen Sulfide," *Inorg. Chem.*, **10**, 7, 1333 (1971).

Gordon, J. E., *The Organic Chemistry of Electrolyte Solutions*, John Wiley and Sons, New York (1975).

Graboski, M. S., and T. E. Daubert, "A Modified Soave Equation of State for Phase Equilibrium Calculations. 1. Hydrocarbon Systems," *Ind. Eng. Chem. Process Des. Dev.*, **17**, 4, 443 (1978a).

Graboski, M. S., and T. E. Daubert, "A Modified Soave Equation of State for Phase Equilibrium Calculations. 2: Systems Containing CO_2, H_2S, N_2, and CO," *Ind. Eng. Chem. Process Des. Dev.*, **17**, 4, 448 (1978b).

Gronwall, T. H., V. K. La Mer, and K. Sandved, "Über den Einflub der sogenar nten höheren Glieder in der Debye-Hückelschen Theorie der Lösungen starker Elektrolyte," *Physik Z.*, **29**, 358 (1928).

Guntelberg. E., "Untersuchungen über Ioneninteraktion," *Z. Physik. Chem.*, 123, 199 (1926).

Guggenheim, E. A., "The Specific Thermodynamic Properties of Aqueous Solutions of Strong Electrolytes," *Phil. Mag.*, **19**, 588 (1935).

Guggenheim, E. A., and J. C. Turgeon, "Specific Interaction of Ions," *Trans. Faraday Soc.*, 51, 747 (1955).

Harned, H. S. and B. B. Owen, *The Physical Chemistry of Electrolytic Solutions*, 3d ed.; Reinhold Publishing Corp., New York (1958).

Hasted, J. B., D. M. Ritson, and C. H. Collie, "Dielectric Properties of Aqueous Ionic Solutions. Parts I and II.," *J. Chem. Phys.*, **16**, 1, 1 (1948).

Helgeson, H. C. and D. H. Kirkham, "Theoretical Prediction of the Thermodynamic Behavior of Aqueous Electrolytes at High Pressures and Temperatures: I. Summary of the Thermodynamic/Electrostatic Properties of the Solvent," *Am. J. Science*, **274**, 1089 (1974).

Hermes, J. E. and G. T. Rochelle, "A Mass Transfer-Based Process Model of Acid Gas Absorption/Stripping Using Methyldiethanolamine," Presented at the American Chemical Society National Meeting, New Orleans, LA (Aug. 30 - Sept. 4, 1987).

Horvath, A. L., *Handbook of Aqueous Electrolyte Solutions*, Ellis Horwood Limited, Chichester, England (1985).

Houghton, G., A. M. McLean, and P. D. Ritchie, "Compressibility, Fugacity, and Water-solubility of Carbon Dioxide in the Region 0-36 atm. and 0-100°C," *Chem. Eng. Sci.*, **6**, 132 (1957).

Ikada, E., Y. Hida, H. Okamoto, J. Hagino, and N. Koizumi, "Dielectric Properties of Ethanolamines," *Bull. Inst. Chem. Res., Kyoto Univ.*, **46**, 5, 239 (1968).

Isaacs, E. E., F. D. Otto, and A. E. Mather, "Solubility of Mixtures of H_2S and CO_2 in a Monoethanolamine Solution at Low Partial Pressures," *J. Chem. Eng. Data*, **25**, 118 (1980).

Jensen, M. B., E. Jorgensen, and C. Faurholt, "Reactions Between Carbon Dioxide and Amino Alcohols I. Monoethanolamine and Diethanolamine," *Acta Chem. Scand.*, **8**, 7, 1137 (1954).

Jones, J. H., H. R. Froning, and E. E. Claytor, "Solubility of Acidic Gases in Aqueous Monoethanolamine," *J. Chem. Eng. Data*, **4**, 1, 85 (1959).

Jou, F. Y., A. E. Mather, and F. D. Otto, "Solubility of H_2S and CO_2 in Aqueous Methyldiethanolamine Solutions," *Ind. Eng. Chem. Process Des. Dev.*, **21**, 539 (1982).

Jou, F. Y., F. D. Otto, and A. E. Mather, "Solubility of Mixtures of H_2S and CO_2 in a Methyldiethanolamine Solution," Presented at the Annual Meeting of the AIChE, Paper No. 140b, Miami Beach, FL (Nov. 2-7, 1986).

Katti, S. S., and B. D. Langfitt, "Development of a Simulator for Commercial Absorbers used for Selective Chemical Absorption Based on Mass Transfer Rate Approach," Paper presented at the 65th Annual Convention, Gas Processors' Association, San Antonio, TX (March 10-12, 1986).

Katti, S. S. and R. A. Wolcott, "Fundamental Aspects of Gas Treating with Formulated Amine Mixtures," Presented at the AIChE National Meeting, Minneapolis, MN (1987).

Kennard, M. L. and A. Meisen, "Mechanisms and Kinetics of Diethanolamine Degradation," *Ind. Eng. Chem., Fundam.*, **24**, 129 (1985).

Kent, R. L. and B. Eisenberg, "Better Data for Amine Treating," *Hydrocarbon Process.*, **55**, 2, 87 (1976).

Kim, C. J., and G. Sartori, "Kinetics and Mechanism of Diethanolamine Degradation in Aqueous Solutions Containing Carbon Dioxide," *Int. J. Chem. Kinetics*, **16**, 10, 1257 (1984).

Klyamer, S. D. and T. L. Kolesnikova, "General Mathematical Description of Experimental Data for the Thermoynamic Equilibrium in Carbon Dioxide-Monoethanolamine (Diethanolamine) - Water Systems," *Russian J. Phys. Chem.*, **46**, 4, 620 (1972). See also *Zhur. Fiz. Khim.*, **46**, 1056 (1972).

Klyamer, S. D., T. L. Kolesnikova, and Rodin, Yu. A., *Gazov. Prom.*, **18**, 2, 44 (1973).

Kohl A. L. and F. C. Riesenfeld, *Gas Purification*, 4th ed. Gulf Publishing Co., Houston, TX (1985).

Kondo, K. and C. A. Eckert, "Nonideality of Single and Mixed Electrolyte Solutions Up to Moderately High Concentrations; Theory Based on Debye-Hückel Radial Distribution Function," *Ind. Eng. Chem. Fund.*, **22**, 283 (1983).

Kuwairi, B. S., *Vapor Pressures of Selected Pure Materials and Mixtures*, Ph.D. Thesis, Oklahoma State University, Stillwater, OK (1983).

La Mer, V. K., T. H. Gronwall, and L. J. Greiff, "The Influence of Higher Terms of the Debye-Hückel Theory in the case of Unsymmetric Valence Type Electrolytes," *J. Phys. Chem.*, **35**, 2245 (1931).

Lal, D., F. D. Otto, and A. E. Mather, "The Solubility of H_2S and CO_2 in a Diethanolamine Solution at Low Partial Pressures," *Can J. Chem. Eng.*, **63**, 681 (1985).

Lawson J. D. and A. W. Garst, "Gas Sweetening Data: Equilibrium Solubility of Hydrogen Sulfide and Carbon Dioxide in Aqueous Monoethanolamine and Aqueous Diethanolamine Solutions," *J. Chem. Eng. Data*, **21**, 1, 20 (1976).

Lee, J. I., F. D. Otto, and A. E. Mather, "Solubility of Carbon Dioxide in Aqueous Diethanolamine Solutions at High Pressures," *J. Chem. Eng. Data*, **17**, 4, 465 (1972).

Lee, J. I., F. D. Otto, and A. E. Mather, "Solubility of Hydrogen Sulfide in Aqueous Diethanolamine Solutions at High Pressures," *J. Chem. Eng. Data*, **18**, 1, 71 (1973a).

Lee, J. I., F. D. Otto, and A. E. Mather, "Partial Pressures of Hydrogen Sulfide over Aqueous Diethanolamine Solutions," *J. Chem. Eng. Data*, **18**, 4, 420 (1973b).

Lee, J. I., F. D. Otto, and A. E. Mather, "The Solubility of Mixtures of Carbon Dioxide and Hydrogen Sulfide in Aqueous Diethanolamine Solutions," *Can. J. Chem. Eng.*, **52**, 125 (1974a).

Lee, J. I., F. D. Otto, and A. E. Mather, "The Solubility of H_2S and CO_2 in Aqueous Monoethanolamine Solutions," *Can. J. Chem. Eng.*, **52**, 803 (1974b).

Lee, J. I., F. D. Otto, and A. E. Mather, "Equilibrium Between Carbon Dioxide and Aqueous Monoethanolamine Solutions," *J. Appl. Chem. Biotechnol.*, **26**, 541 (1976a).

Lee, J. I., F. D. Otto, and A. E. Mather, "Equilibrium in Hydrogen Sulfide - Monoethanolamine - Water System," *J. Chem. Eng. Data*, **21**, 2, 207 (1976b).

Lewis, G. N. and M. Randall, *Thermodynamics*, (revised by K. S. Pitzer and L. Brewer), McGraw-Hill Book Co., New York (1961).

Licht, S. E., and R. H. Weiland, "Density and Physical Solubility of CO_2 in Partially Loaded Solutions of MEA, DEA, and MDEA," Paper presented at the AIChE 1989 Spring National Meeting, Paper No. 57f, Houston, TX (April 2-6, 1989).

Lietzke, M. H., and R. W. Stoughton, "The Calculation of Activity Coefficients from Osmotic Coefficient Data," *J. Phys. Chem.*, **66**, 508 (1962).

Luenberger, D. G., *Linear and Nonlinear Programming*, 2nd Ed., Addison-Wesley Publishing Co., Reading, MA (1984).

Mahajani, V. V., and P. V. Dankwerts, "Carbamate-bicarbonate Equilibrium for Several Amines at 100 °C in 30% Potash," *Chem. Eng. Sci.* **37**, 6, 943 (1982).

Mather, A. E., Professor, University of Alberta, Private communication (1988).

Matin, N. B., S. M. Danov, and R. V. Efremov, "Vapor Pressures in the Systems Diethanolamine-Water and Triethanolamine-Water," *Tr. Khim. Khim. Tekhnol.*, **2**, 7 (1969).

Maurer, G., and J. M. Prausnitz, "On the Derivation and Extension of the UNIQUAC Equation," *Fluid Phase Equilibria*, **2**, 91 (1978).

Maurer, G. "On the Solubility of Volatile Weak Electrolytes in Aqueous Solutions," In *Thermodynamics of Aqueous Systems with Industrial Applications*; Newman, S. A., Ed.; ACS Symposium Series 133, pp. 139-186; American Chemical Society, Washington D.C. (1980).

McQuarrie, D. A., *Statistical Mechanics*, Harper and Row, New York (1976).

Meissner, H. P., C. L. Kusik, and J. W. Tester, "Activity Coefficients of Strong Electrolytes in Aqueous Solution-Effect of Temperature," *AIChE J.*, **18**, 3, 661 (1972).

Meissner, H. P., and J. W. Tester, "Activity Coefficients of Strong Electrolytes in Aqueous Solutions," *Ind. Eng. Chem. Process Des. Develop.*, **11**, 1, 128 (1972).

Meyer, B., K. Ward, K. Koshlap, and L. Peter, "Second Dissociation Constant of Hydrogen Sulfide," *Inorg. Chem.*, **22**, 2345 (1983).

Middleton, M. *Dielectric Properties and Structure of Oil-Continuous Microemulsions*, Ph.D. Dissertation, University of Texas, Austin (1988).

Mock, B., L. B. Evans, and C. C. Chen, "Thermodynamic Representation of Phase Equilibria of Mixed-Solvent Electrolyte Systems," *AIChE J.*, **32**, 10, 1655 (1986).

Moore, T. F., Texaco Chemical Company, Private communication (1989).

Muhlbauer, H. G., and P. R. Monaghan, "Sweetening Natural Gas With Ethanolamine Solutions," *Oil Gas J.*, **55**, 17, 139 (1957).

Nath, A., and E. Bender, "Isothermal Vapor-Liquid Equilibria of Binary and Ternary Mixtures Containing Alcohol, Alkanolamine, and Water with a New Static Device," *J. Chem. Eng. Data*, **28**, 370 (1983).

Owen, B. B., R. C. Miller, C. E. Milner, and H. L. Cogan, "The Dielectric Constant of Water as a Function of Temperature and Pressure," *J. Phys. Chem.*, **65**, 2065 (1961).

Peng, X. SINOPEC Beijing Design Institute, Private communication while Peng was visiting at ASPEN Technology, Inc. (1988).

Pitzer, K. S., "Thermodynamics of Electrolytes. I. Theoretical Basis and General Equations," *J. Phy. Chem.*, **77**, 2, 268 (1973).

Pitzer, K. S., "Electrolyte Theory - Improvements since Debye and Hückel," *Acc. Chem. Res.*, **10**, 371 (1977).

Pitzer, K. S., "Electrolytes. From Dilute Solutions to Fused Salts," *J. Am. Chem. Soc.*, **102**, 9, 2902 (1980).

Pitzer, K. S., and J. J. Kim, "Thermodynamics of Electrolytes. IV. Activity and Osmotic Coefficients for Mixed Electrolytes," *J. Am. Chem. Soc.*, **96**, 18, 5701 (1974).

Pitzer, K. S., and G. Mayorga, "Thermodynamics of Electrolytes. II. Activity and Osmotic Coefficients for Strong Electrolytes with One or Both Ions Univalent," *J. Phys. Chem.*, **77**, 19, 2300 (1973).

Pitzer, K. S., and G. Mayorga, Thermodynamics of Electrolytes. III. Activity and Osmotic Coefficients for 2-2 Electrolytes," *J. Sol. Chem.*, **3**, 7, 538 (1974).

Planche, H. and H. Renon, "Mean Spherical Approximation Applied to a Simple but Nonprimitive Model of Interaction for Electrolyte Solutions and Polar Substances," *J. Phys. Chem.*, **85**, 3924 (1981).

Prausnitz , J. M., and P. L. Chueh, *Computer Calculations for High-Pressure Equilibria*, Prentice-Hall, Inc., Englewood Cliffs, N. J. (1968).

Prausnitz, J. M., T. F. Anderson, E. A. Grens, C. A. Eckert, R. Hsieh, and J. P. O'Connell, *Computer Calculations for Multicomponent Vapor-Liquid Equilibria and Liquid- Liquid Equilibria*, Prentice Hall, Inc., Englewood Cliffs, NJ (1980).

Prausnitz, J. M., R. N. Lichtenthaler, and E. G. de Azevedo, *Molecular Thermodynamics of Fluid-Phase Equilibria*, Prentice-Hall Inc., Englewood Cliffs, N. J. (1986).

Rackett, H. G., "Equation of State for Saturated Liquids," *J. Chem. Eng. Data*, **15**, 4, 514 (1970).

Redlich, O., and J. N. S. Kwong, "On the Thermodynamics of Solutions. V An Equation of State. Fugacities of Gaseous Solutions," *Chem. Rev.*, **44**, 233 (1949).

Reid, R. C., J. M. Prausnitz, and T. K. Sherwood, *The Properties of Gases and Liquids*, 3rd Ed., McGraw-Hill Book Co., New York (1977).

Renon, H., and J. M. Prausnitz, "Local Compositions in Thermodynamic Excess Functions for Liquid Mixtures," *AIChE J.*, **14**, 1, 135 (1968).

Renon, H. "NRTL: An Empirical Equation or an Inspiring Model for Fluids Mixtures Properties," *Fluid Phase Equilibria*, **24**, 87 (1985).

Robinson, R. A., and R. H. Stokes, *Electrolyte Solutions*, 2nd ed.; Butterworth and Co.: London, 1970.

Sander, B., A. Fredenslund, and P. Rasmussen, "Calculation of Vapour-Liquid Equilibria in Mixed Solvent/Salt Systems Using An Extended Uniquac Equation," *Chem. Eng. Sci.*, **41**, 5, 1171 (1986).

Sartori, G. and D. W. Savage, "Sterically Hindered Amines for CO_2 Removal from Gases," *Ind. Eng. Chem. Fundam.*, **22**, 239 (1983).

Scatchard, G., "Concentrated Solutions of Strong Electrolytes," *Chem. Rev.*, **19**, 309 (1939).

Scatchard, G., "Osmotic Coefficients and Activity Coefficients in Mixed Electrolyte Solutions," *J. Amer. Chem. Soc.*, **83**, 2636 (1961).

Scatchard, G., R. M. Rush, and J. S. Johnson, "Osmotic and Activity Coefficients for Binary Mixtures of Sodium Chloride, Sodium Sulfate, Magnesium Sulfate, and Magnesium Chloride in Water at 25°C. III. Treatment with the Ions as Components," *J. Phys. Chem.*, **74**, 21, 3786 (1970).

Scauflaire P., D. Richards, and C. C. Chen, "Ionic Activity Coefficients of Mixed-Solvent Electrolyte Systems," *AIChE J.*, submitted (1989).

Schwabe, K., W. Graichen, and D. Spiethoff, "Physikalisch-chemische Untersuchungen an Alkanolaminen," *Z. Phys. Chem.* (Frankfurt/Main), **20**, 68 (1959).

Sheu, Y. E., Texaco Chemical Company, Private communication (1989).

Sivasubramanian, M. S., *The Heat and Mass Transfer Rate Approach for the Simulation and Design of Acid Gas Treating Units*, Ph.D. Dissertation, Clarkson College, New York (1985).

Sivasubramanian, M. S., H. Sardar, and R. H. Weiland, "Simulation of Fully-Integrated Amine Units For Acid Gas Removal," Presented at the AIChE National Meeting, paper No. 87e, Houston, TX (March 24-28, 1985).

Smith, W. R. and R. W. Missen, *Chemical Reaction Equilibrium Analysis: Theory and Algorithms*, John Wiley and Sons, New York (1982).

Smith, W. R. and R. W. Missen, "Strategies for Solving The Chemical Equilibrium Problem and an Efficient Microcomputer-Based Algorithm," *Can. J. Chem. Eng.*, **66**, 591 (1988).

Soave, G., "Equilibrium Constants from a Modified Redlich-Kwong Equation of State," *Chem. Eng. Science* , **27**, 1197 (1972).

Spencer, C. F., and R. P. Danner, "Improved Equation for Prediction of Saturated Liquid Density," *J. Chem. Eng. Data*, **17**, 2, 236 (1972).

Spencer, C. F., and R. P. Danner, "Prediction of Bubble-Point Density of Mixtures," *J. Chem. Eng. Data*, **18**, 2, 230 (1973).

Stokes, R. H., and R. A. Robinson, "Solvation Equilibria in Very Concentrated Electrolyte Solutions," *J. Sol. Chem.*, **2**, 173 (1973).

Texaco Chemical Co., In-house VLE (TPx) data for the systems diethanolamine-water, diglycolamine-water, and methyldiethanolamine-water. 1988.

Texaco Chemical Co., *Diglycolamine Agent*, Technical Publication, undated.

Tosh, J. S., J. H. Field, H. E. Benson, and W. P. Haynes, "Equilibrium Study of the System Potassium Carbonate, Potassium Bicarbonate, Carbon Dioxide and Water," *U.S. Bureau of Mines, Report of Investigations*, 5484 (1959).

Touhara, H., S. Okazaki, F. Okino, H. Tanaka, K. Ikari, and K. Nakazishi, K. "Thermodynamic Properties of Aqueous Mixtures of Hydrophilic Compounds 2. Aminoethanol and its Methyl Derivatives," *J. Chem. Thermodyn.*, **14**, 145 (1982).

Triolo, R., J. R. Grigera, and L. Blum, "Simple Electrolytes in the Mean Spherical Approximation," *J. Phys. Chem.*, **80**, 1858 (1976).

Union Carbide Corporation, European Patent Application, Application No. 84107586.4, Publication No. 0134948A2 (1984).

Van Krevelen, D. W., P. J. Hoftijzer, and F. J. Huntjens, "Composition and Vapour Pressures of Aqueous Solutions of Ammonia, Carbon Dioxide and Hydrogen Sulfide," *Recueil*, **68**, 191 (1949).

Van Ness, H. C., and M. M. Abbott, "Vapor-Liquid Equilibrium," *AIChE J.*, **25**, 4, 645 (1979).

White, W. B., S. M. Johnson, and G. B. Dantzig, "Chemical Equilibrium in Complex Mixtures," *J. Chem. Phys.*, **28**, 751 (1958).

Wilhelm, E., "Dilute Solutions of Gases in Liquids," *Fluid Phase Equilbria*, **27**, 233 (1986).

Zawisza, A., and B. Malesińska, "Solubility of Carbon Dioxide in Liquid Water and of Water in Gaseous Carbon Dioxide in the Range 0.2-5 MPa and at Temperatures to 473 K,",J. Chem. Eng. Data, **26**, 388 (1981).

VITA

David Michael Austgen Jr. was born in Merced, California, on May 12, 1959, the son of David M. and Muriel C. Austgen. After graduation from Clear Creek High School in 1977, he entered the University of Notre Dame. He earned the B.S. degree in Chemical Engineering in May, 1981. During the summers of 1980 and 1981 he was employed by Exxon Chemical Co. at the Baytown Olefins Plant, Baytown, TX. In August, 1981, he entered The Graduate School of The University of Texas. He received the M.S. degree in Chemical Engineering in August, 1983. During the following 17 months he was employed as a research engineer in Technical Service and Development at the Dow Chemical Company, Freeport, Texas. In January, 1985, he reentered The Graduated School of The University of Texas. During the summer of 1987 he was employed by Aspen Technology, Inc. Upon completion of requirements for the Ph.D. in Chemical Engineering, he will be employed by Shell Development Company, Westhollow Research Center, Houston, Texas.

Permanent address: 18503 Kingstown Ct.
Houston, TX
77058

This dissertation was typed by the author.